DTIC FILE COPY

(2)

AD-A218 787

WRDC-TR-89-1100

DTIC
ELECTE
MAR 0 6 1990
S D
D

MEGALIDAR PROOF-of-CONCEPT DEMONSTRATION

J. M. Cathcart, A. K. Garrison, G. G. Gimmestad, and D. W. Roberts

Georgia Institute of Technology
Georgia Tech Research Institute
Electromagnetics Laboratory
Electro-Optics Division
Atlanta, Georgia 30332

October 1989

Interim Report for the Period June 1988 - June 1989

Approved for Public Release; Distribution Unlimited

Avionics Laboratory
Wright Research and Development Center
Air Force Systems Command
Wright-Patterson Air Force Base, Ohio 45433-6543

90 03 05 058

NOTICE

WHEN GOVERNMENT DRAWINGS, SPECIFICATIONS, OR OTHER DATA ARE USED FOR ANY PURPOSE OTHER THAN IN CONNECTION WITH A DEFINITELY GOVERNMENT-RELATED PROCUREMENT, THE UNITED STATES GOVERNMENT INCURS NO RESPONSIBILITY OR ANY OBLIGATION WHATSOEVER. THE FACT THAT THE GOVERNMENT MAY HAVE FORMULATED OR IN ANY WAY SUPPLIED THE SAID DRAWINGS, SPECIFICATIONS, OR OTHER DATA, IS NOT TO BE REGARDED BY IMPLICATION, OR OTHERWISE IN ANY MANNER CONSTRUED, AS LICENSING THE HOLDER, OR ANY OTHER PERSON OR CORPORATION; OR AS CONVEYING ANY RIGHTS OR PERMISSION TO MANUFACTURE, USE, OR SELL ANY PATENTED INVENTION THAT MAY IN ANY WAY BE RELATED THERETO.

THIS REPORT HAS BEEN REVIEWED BY THE OFFICE OF PUBLIC AFFAIRS (ASD/PA) AND IS RELEASABLE TO THE NATIONAL TECHNICAL INFORMATION SERVICE (NTIS). AT NTIS IT WILL BE AVAILABLE TO THE GENERAL PUBLIC INCLUDING FOREIGN NATIONS.

THIS TECHNICAL REPORT HAS BEEN REVIEWED AND IS APPROVED FOR PUBLICATION.

Jan M. Servaites, AARI-4
Project Engineer
Integrated EO Sensors Group
Electro-Optics Branch

James J. Stewart, Chief, AARI-3
EO Sensors Eval/Analysis Group
Electro-Optics Branch

FOR THE COMMANDER

Gale D. Urban, Chief
Electro-Optics Branch
Mission Avionics Division

IF YOUR ADDRESS HAS CHANGED, IF YOU WISH TO BE REMOVED FROM OUR MAILING LIST, OR IF THE ADDRESSEE IS NO LONGER EMPLOYED BY YOUR ORGANIZATION PLEASE NOTIFY WRDC/AARI, WRIGHT-PATTERSON AFB, OH 45433-6543 TO HELP MAINTAIN A CURRENT MAILING LIST.

COPIES OF THIS REPORT SHOULD NOT BE RETURNED UNLESS RETURN IS REQUIRED BY SECURITY CONSIDERATIONS, CONTRACTUAL OBLIGATIONS, OR NOTICE ON A SPECIFIC DOCUMENT.

REPORT DOCUMENTATION PAGE

Form Approved
OMB No 0704-0188

1a. REPORT SECURITY CLASSIFICATION UNCLASSIFIED	1b. RESTRICTIVE MARKINGS
2a. SECURITY CLASSIFICATION AUTHORITY	3. DISTRIBUTION/AVAILABILITY OF REPORT Approved for public release; distribution is unlimited.
2b. DECLASSIFICATION/DOWNGRADING SCHEDULE	
4. PERFORMING ORGANIZATION REPORT NUMBER(S)	5. MONITORING ORGANIZATION REPORT NUMBER(S) WRDC-TR-89-1100
6a. NAME OF PERFORMING ORGANIZATION Georgia Tech Research Institute 6b. OFFICE SYMBOL (If applicable)	7a. NAME OF MONITORING ORGANIZATION Avionics Laboratories WRDC, AFSC
6c. ADDRESS (City, State, and ZIP Code) Georgia Institute of Technology Atlanta, GA 30332	7b. ADDRESS (City, State, and ZIP Code) WRDC/AARI-3 Wright-Patterson AFB, OH 45433-6543
8a. NAME OF FUNDING/SPONSORING ORGANIZATION 8b. OFFICE SYMBOL (If applicable)	9. PROCUREMENT INSTRUMENT IDENTIFICATION NUMBER Contract No. F33615-86-C-1051 Task No. 88-5-3
8c. ADDRESS (City, State, and ZIP Code)	10. SOURCE OF FUNDING NUMBERS

PROGRAM ELEMENT NO	PROJECT NO	TASK NO	WORK UNIT ACCESSION NO
62204F	2004	08	45

11. TITLE (Include Security Classification)
MEGALIDAR Proof-of-Concept Demonstration

12. PERSONAL AUTHOR(S)
Cathcart, J. M., Garrison, A. K., Gimmestad, G. G., and Roberts, D. W.

13a. TYPE OF REPORT	13b. TIME COVERED	14. DATE OF REPORT (Year, Month, Day)	15. PAGE COUNT
Interim	FROM 06/88 TO 06/89	1989 October	166

16. SUPPLEMENTARY NOTATION
This research was partially funded by the In-House Independent Research Fund.

17. COSATI CODES			18. SUBJECT TERMS (Continue on reverse if necessary and identify by block number)
FIELD	GROUP	SUB-GROUP	
04	01		Lidar, Atmospheric Density, 100-inch Collimator, Remote Sensing

19. ABSTRACT (Continue on reverse if necessary and identify by block number)

This interim report describes the MEGALIDAR proof-of-concept demonstration performed on the 100-inch collimator to demonstrate the capability of the MEGALIDAR to measure atmospheric densities to altitudes up to 80 km. The report presents a description of the lidar Nd:YAG laser transmitter, receiver and data acquisition subsystem as well as a description of the steps in adapting the collimator facility to accommodate the lidar system. The results of a series of measurements to altitudes up to 85 km are presented along with the measurement method and analyses procedures. Recommendations, based on experience during the demonstration, for improvement of the collimator facility for lidar are given.

20. DISTRIBUTION/AVAILABILITY OF ABSTRACT	21. ABSTRACT SECURITY CLASSIFICATION
☒ UNCLASSIFIED/UNLIMITED ☐ SAME AS RPT ☐ DTIC USERS	UNCLASSIFIED

22a. NAME OF RESPONSIBLE INDIVIDUAL	22b. TELEPHONE (Include Area Code)	22c. OFFICE SYMBOL
Mr. Jan M. Servaites	(513) 255-9609	WRDC/AARI-3

DD Form 1473, JUN 86 *Previous editions are obsolete.*

PREFACE

This Interim Report summarizes the efforts performed during the period from 1 June 1988 to 1 June 1989 by Georgia Tech Research Institute for WRDC/AARI-3 under contract number F33615-86-C-1051 from the Avionics Laboratory, Wright Research and Development Center.

Sponsor for the project is the EO Sensor Evaluation/Analysis Group (AARI-3) of the Avionics Laboratory, Wright Research and Development Center (WRDC). The technical monitor at WRDC is Lt. Mario Moya. He is supported by Mr. Jan Servaites.

Participants at GTRI, in addition to the authors, include S. C. Bauman, T. Boatwright, W. Brittain, R. C. DuVarney and E. M. Patterson. Mr. S. S. Steadman is project director of the GTRI EOS/ATR Sciences Development Program which is the umbrella for this task. Dr. Allen K. Garrison was the task leader. The EOS/ATR Sciences Development Program is conducted in the Electro-Optics Division, Dr. Robert S. Hyde, Chief, of the Electromagnetics Laboratory, Mr. Devon G. Crowe, Director.

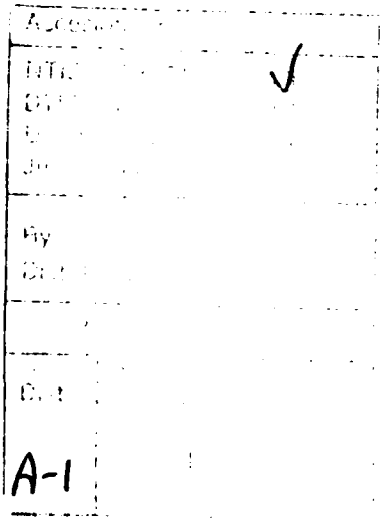

TABLE OF CONTENTS

		Page
	INTRODUCTION	1
1.	TRANSMITTER	2
2.	RECEIVER	5
3.	DATA ACQUISITION SUBSYSTEM	9
4.	ADAPTATION OF THE COLLIMATOR FOR LIDAR	11
5.	EVALUATION OF THE COLLIMATOR FACILITY	14
6.	MEASUREMENT METHOD	16
7.	METHOD OF DATA ANALYSIS	17
	7.1 Quick Look Analysis	17
	7.2 Analysis at Georgia Tech	17
8.	MEASUREMENT RESULTS	19
9.	DISCUSSION OF RESULTS AND SUMMARY	117
	REFERENCES	118
	APPENDIX A: INTERCONNECTION AND CIRCUIT DIAGRAMS	A-1
	APPENDIX B: STANDARD AND EMERGENCY OPERATIONS PROCEDURES:	B-1
	APPENDIX C: PICTURES OF THE MEGALIDAR	C-1

LIST OF FIGURES

Figure	Title	Page
1.	A Sketch of the Transmitter Optical Table. The Table is Mounted Directly on the ND:YAG Laser Case.	3
2.	A Sketch of the Transmitter Steering Mirror Mount and Mount Support The Mount Support Holds the Mirror in the Collimator Tube.	4
3.	A Schematic of the Receiver Subsystem	6
4.	The Logic Circuit for the Laser-Chopper Synchronization Interface.	8
5.	A Sketch of the Essential Parts of the Data Acquisition Subsystem.	10
6.	A Sketch of the Laser Platform Designed and Constructed at Georgia Tech The Rails are those in the Collimator Cross Tunnel Floor. The Transmitter Optical Table Shown in Figure 1 is Omitted for Clarity.	12
7.	A Top View of the Transmitter Arrangement in the Collimator Cross Tunnel.	13
8.	The Effect of the Spatial Averaging Using a 1 km Filter. (a) The Data from 4000 Consecutive Sweeps without any Corrections. (b) The Data from (a) After the Spatial Filter.	18
9.	Plot of Density Ratio Versus Altitude for 5:01:57, 12/07/88 GMT.	21
10.	Plot of Density Ratio Versus Altitude for 5:06:19, 12/07/88 GMT.	22
11.	Plot of Density Ratio Versus Altitude for 5:27:56, 12/07/88 GMT.	23
12.	Plot of Density Ratio Versus Altitude for 5:32:09, 12/07/88 GMT.	24
13.	Plot of Density Ratio Versus Altitude for 5:36:19, 12/07/88 GMT.	25
14.	Plot of Density Ratio Versus Altitude for 5:40:29, 12/07/88 GMT.	26
15.	Plot of Density Ratio Versus Altitude for 5:49:34, 12/07/88 GMT.	27
16.	Plot of Density Ratio Versus Altitude for 5:56:56, 12/07/88 GMT.	28
17.	Plot of Density Ratio Versus Altitude for 5:58:05, 12/07/88 GMT.	29
18.	Plot of Density Ratio Versus Altitude for 6:02:14, 12/07/88 GMT.	30
19.	Plot of Density Ratio Versus Altitude for 6:06:29, 12/07/88 GMT.	31
20.	Plot of Density Ratio Versus Altitude for 6:11:23, 12/07/88 GMT.	32
21.	Plot of Density Ratio Versus Altitude for 6:15:40, 12/07/88 GMT.	33
22.	Plot of Density Ratio Versus Altitude for 6:19:50, 12/07/88 GMT.	34
23.	Plot of Density Ratio Versus Altitude for 6:24:02, 12/07/88 GMT.	35
24.	Plot of Density Ratio Versus Altitude for 6:28:12, 12/07/88 GMT.	36
25.	Plot of Density Ratio Versus Altitude for 6:32:23, 12/07/88 GMT.	37
26.	Plot of Density Ratio Versus Altitude for 6:36:37, 12/07/88 GMT.	38
27.	Plot of Density Ratio Versus Altitude for 6:42:40, 12/07/88 GMT.	39
28.	Plot of Density Ratio Versus Altitude for 6:46:50, 12/07/88 GMT.	40
29.	Plot of Density Ratio Versus Altitude for 6:50:59, 12/07/88 GMT.	41
30.	Plot of Density Ratio Versus Altitude for 6:55:16, 12/07/88 GMT.	42
31.	Plot of Density Ratio Versus Altitude for 6:59:29, 12/07/88 GMT.	43
32.	Plot of Density Ratio Versus Altitude for 7:03:47, 12/07/88 GMT.	44
33.	Plot of Density Ratio Versus Altitude for 7:07:58, 12/07/88 GMT.	45
34.	Plot of Density Ratio Versus Altitude for 7:17:26, 12/07/88 GMT.	46
35.	Plot of Density Ratio Versus Altitude for 7:21:36, 12/07/88 GMT.	47
36.	Plot of Density Ratio Versus Altitude for 7:25:49, 12/07/88 GMT.	48
37.	Plot of Density Ratio Versus Altitude for 7:30:02, 12/07/88 GMT.	49
38.	Plot of Density Ratio Versus Altitude for 7:34:12, 12/07/88 GMT.	50
39.	Plot of Density Ratio Versus Altitude for 7:38:26, 12/07/88 GMT.	51
40.	Plot of Density Ratio Versus Altitude for 7:42:57, 12/07/88 GMT.	52
41.	Plot of Density Ratio Versus Altitude for 7:47:17, 12/07/88 GMT.	53
42.	Plot of Density Ratio Versus Altitude for 1:28:45, 12/10/88 GMT.	54
43.	Plot of Density Ratio Versus Altitude for 1:32:59, 12/10/88 GMT.	55
44.	Plot of Density Ratio Versus Altitude for 1:37:14, 12/10/88 GMT.	56

LIST OF FIGURES (Continued)

Figure	Title	Page
45.	Plot of Density Ratio Versus Altitude for 1:41:43, 12/10/88 GMT.	57
46.	Plot of Density Ratio Versus Altitude for 1:46:17, 12/10/88 GMT.	58
47.	Plot of Density Ratio Versus Altitude for 1:50:37, 12/10/88 GMT.	59
48.	Plot of Density Ratio Versus Altitude for 1:55:10, 12/10/88 GMT.	60
49.	Plot of Density Ratio Versus Altitude for 2:01:20, 12/10/88 GMT.	61
50.	Plot of Density Ratio Versus Altitude for 2:06:21, 12/10/88 GMT.	62
51.	Plot of Density Ratio Versus Altitude for 2:12:12, 12/10/88 GMT.	63
52.	Plot of Density Ratio Versus Altitude for 2:17:15, 12/10/88 GMT.	64
53.	Plot of Density Ratio Versus Altitude for 2:26:18, 12/10/88 GMT.	65
54.	Plot of Density Ratio Versus Altitude for 2:30:35, 12/10/88 GMT.	66
55.	Plot of Density Ratio Versus Altitude for 2:34:56, 12/10/88 GMT.	67
56.	Plot of Density Ratio Versus Altitude for 2:39:28, 12/10/88 GMT.	68
57.	Plot of Density Ratio Versus Altitude for 2:43:44, 12/10/88 GMT.	69
58.	Plot of Density Ratio Versus Altitude for 2:48:00, 12/10/88 GMT.	70
59.	Plot of Density Ratio Versus Altitude for 2:53:35, 12/10/88 GMT.	71
60.	Plot of Density Ratio Versus Altitude for 2:57:48, 12/10/88 GMT.	72
61.	Plot of Density Ratio Versus Altitude for 3:02:01, 12/10/88 GMT.	73
62.	Plot of Density Ratio Versus Altitude for 3:06:26, 12/10/88 GMT.	74
63.	Plot of Density Ratio Versus Altitude for 3:10:26, 12/10/88 GMT.	75
64.	Plot of Density Ratio Versus Altitude for 8:56:45, 12/11/88 GMT.	76
65.	Plot of Density Ratio Versus Altitude for 9:04:04, 12/11/88 GMT.	77
66.	Plot of Density Ratio Versus Altitude for 9:21:18, 12/11/88 GMT.	78
67.	Plot of Density Ratio Versus Altitude for 9:25:29, 12/11/88 GMT.	79
68.	Plot of Density Ratio Versus Altitude for 9:30:36, 12/11/88 GMT.	80
69.	Plot of Density Ratio Versus Altitude for 9:35:23, 12/11/88 GMT.	81
70.	Plot of Density Ratio Versus Altitude for 9:40:11, 12/11/88 GMT.	82
71.	Plot of Density Ratio Versus Altitude for 9:44:34, 12/11/88 GMT.	83
72.	Plot of Density Ratio Versus Altitude for 9:49:01, 12/11/88 GMT.	84
73.	Plot of Density Ratio Versus Altitude for 9:55:11, 12/11/88 GMT.	85
74.	Plot of Density Ratio Versus Altitude for 9:59:39, 12/11/88 GMT.	86
75.	Plot of Density Ratio Versus Altitude for 10:04:17, 12/11/88 GMT.	87
76.	Plot of Density Ratio Versus Altitude for 10:10:08, 12/11/88 GMT.	88
77.	Plot of Density Ratio Versus Altitude for 10:15:33, 12/11/88 GMT.	89
78.	Plot of Density Ratio Versus Altitude for 10:25:00, 12/11/88 GMT.	90
79.	Plot of Density Ratio Versus Altitude for 10:29:53, 12/11/88 GMT.	91
80.	Plot of Density Ratio Versus Altitude for 10:35:34, 12/11/88 GMT.	92
81.	Plot of Density Ratio Versus Altitude for 10:39:50, 12/11/88 GMT.	93
82.	Plot of Density Ratio Versus Altitude for 10:44:13, 12/11/88 GMT.	94
83.	Plot of Density Ratio Versus Altitude for 10:51:06, 12/11/88 GMT.	95
84.	Plot of Density Ratio Versus Altitude for 10:55:20, 12/11/88 GMT.	96
85.	Plot of Density Ratio Versus Altitude for 10:59:58, 12/11/88 GMT.	97
86.	Plot of Density Ratio Versus Altitude for 11:04:22, 12/11/88 GMT.	98
87.	Plot of Density Ratio Versus Altitude for 11:08:33, 12/11/88 GMT.	99
88.	Plot of Density Ratio Versus Altitude for 11:13:15, 12/11/88 GMT.	100
89.	Plot of Density Ratio Versus Altitude for 11:17:31, 12/11/88 GMT.	101
90.	Plot of Density Ratio Versus Altitude for 11:21:47, 12/11/88 GMT.	102
91.	Plot of Density Ratio Versus Altitude for 11:26:24, 12/11/88 GMT.	103
92.	Plot of Density Ratio Versus Altitude for 11:30:39, 12/11/88 GMT.	104
93.	Plot of Density Ratio Versus Altitude for 11:35:06, 12/11/88 GMT.	105
94.	Plot of Density Ratio Versus Altitude for 11:39:27, 12/11/88 GMT.	106

LIST OF FIGURES (CONCLUDED)

Figure	Title	Page
95.	Plot of Density Ratio Versus Altitude for 11:44:31, 12/11/88 GMT.	107
96.	Plot of Density Ratio Versus Altitude for 2:43:41, 12/12/88 GMT.	108
97.	Plot of Density Ratio Versus Altitude for 2:49:29, 12/12/88 GMT.	109
98.	Plot of Density Ratio Versus Altitude for 2:54:10, 12/12/88 GMT.	110
99.	Plot of Density Ratio Versus Altitude for 11:19:41, 12/16/88 GMT.	111
100.	Plot of Density Ratio Versus Altitude for 11:24:17, 12/16/88 GMT.	112
101.	Plot of Density Ratio Versus Altitude for 11:28:35, 12/16/88 GMT.	113
102.	Plot of Density Ratio Versus Altitude for 11:34:37, 12/16/88 GMT.	114
103.	Plot of Density Ratio Versus Altitude for 11:39:01, 12/16/88 GMT.	115
104.	Plot of Density Ratio Versus Altitude for 11:52:52, 12/16/88 GMT.	116

LIST OF TABLES

Table	Title	Page
1.	Specifications of the Transmitter Laser	2
2.	Specifications of the Receiver Subsystem	5
3.	Dates and Number of Records for Each Measurement Episode of the MEGALIDAR Proof of Concept Demonstration.	19
4.	Percent Error in the Density Ratios Shown in Figures 9-104 Corresponding to Three Standard Deviations for Selected Altitudes.	20

INTRODUCTION

This report describes the details of the MEGALIDAR Proof-of-Concept Demonstration Task which required GTRI to make essential modifications to the 100-inch collimator in the Avionics Laboratory for the installation of a laser transmitter, receiver, and data acquisition system; to install the system at the collimator; and to perform a lidar proof-of-concept demonstration. The primary objective of the proof-of-concept demonstration is to demonstrate the capability of the MEGALIDAR by measuring atmospheric densities at altitudes up to 80 km. A necessary part of this objective is a quantitative assessment of the collimator when it is operated as a lidar. A related objective is the assessment of the MEGALIDAR in terms of the operational parameters of the collimator facility. Meeting these objectives provide important data for evaluation of the collimator as a lidar and a baseline for making reliable projections of its performance in other lidar configurations.

The first three sections of the report give the specifications of the transmitter, receiver, and data acquisition subsystems that are installed on the collimator. The next section describes the modifications of the collimator facility necessary to conduct the demonstration. This is followed by an evaluation of the collimator facility suitability for lidar based on its use for the demonstration. Sections on the measurement and data analysis methods lead to a section on the results of the measurements. Finally, there is a report summary.

1. TRANSMITTER

The transmitter subsytem has three basic parts: the Quantel Nd:YAG laser with power supply and controls, the transmitter optical table and the steering mirror. This subsystem gives control over the laser pulses, expands the laser beam and measures the average power of the pulses. In addition the steering mirror controls the direction of the beam and allows for overlapping the beam with the field of view of the collimator receiver. The specifications of the laser are given in Table 1.

TABLE 1. Specifications of the Transmitter Laser

Laser	Quantel 1581C20 Nd:YAG
Wavelength	532 mn
Energy/Pulse	325 mJ
Pulse Width	10 ns
Pulse Repetition Rate	16.33 Hz *
Beam Divergence	1 mr

* The pulse rate was determined by the receiver beam chopper described below.

The basic function of the transmitter optical table is to guide the light beam from the laser to the x 4.5 beam expander which provides an exit beam divergence of about 0.2 mr. The output from a small HeNe laser that is mounted on the optical table also passes through the beam expander using an aligning mirror and beam splitter. The HeNe beam was aligned with the YAG beam by using a 1 meter focal length lens to get a burn on a paper from a single YAG pulse and then aligning the HeNe on the burn. The HeNe is used to adjust the steering mirror so that the transmitter beam is positioned correctly in the collimator. A Molectron JD 1000 Joule Meter with a pyroelectric detector head is used to measure the average power of the YAG pulses. The power meter provides an output that is recorded by the data acquisition system. Figure 1 is a sketch of the transmitter optical table layout.

The steering mirror is a 4-inch round mirror mounted on a two axes gimbal mount. Both axes are actuator driven with joy stick controllers. The controller has two drive speeds. The faster

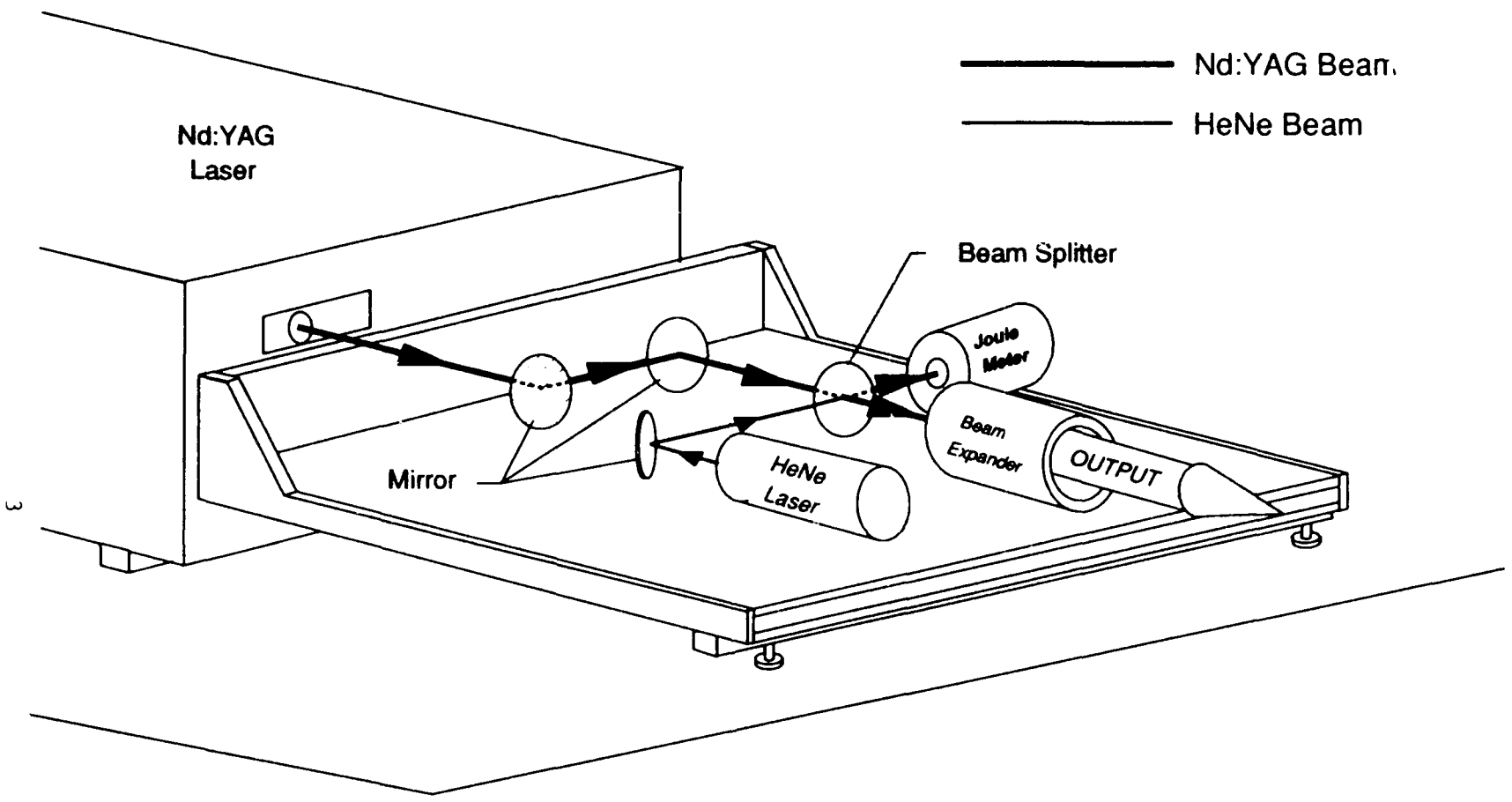

Figure 1. A sketch of the transmitter optical table.
The table is mounted directly on the Nd:YAG laser case.

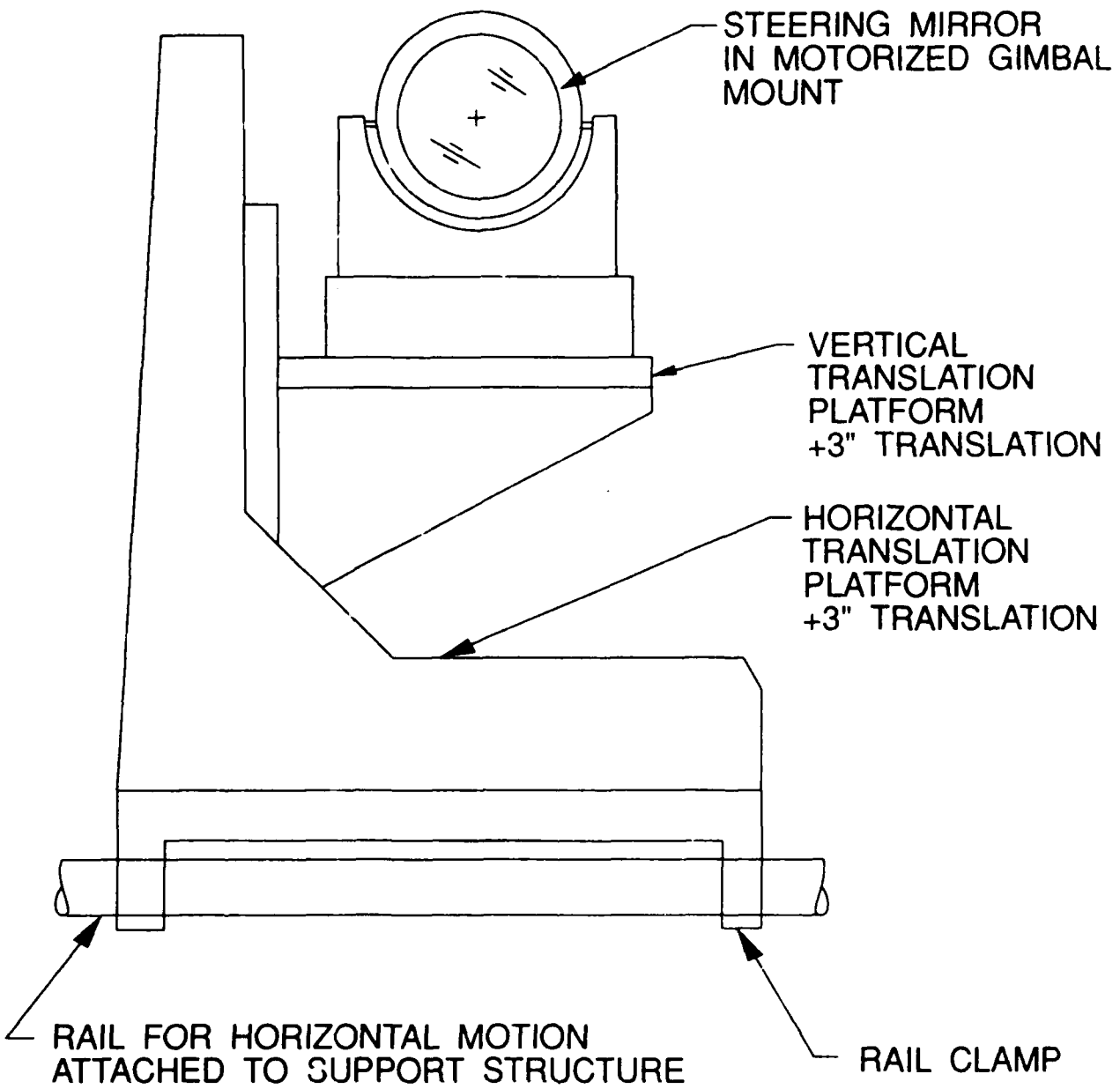

Figure 2. A sketch of the transmitter steering mirror mount and mount support. The mount support holds the mirror in the collimator tube.

2. RECEIVER

The receiver subsytem consists of a photomultiplier tube (PMT) with an internal preamplifier housed in a cooler, an optical system with a field stop wheel, narrow-band filter and light beam chopper with chopper driver and controller. The function of the receiver subsystem is to form an image of the 100-inch mirror on the PMT photosensitive surface for efficient photon-electron conversion, to limit the spectral bandwidth of the light reaching the PMT to wavelengths close to the transmitter wavelength and to shield the PMT from the near field return so it is sensitive to the low light levels returned from the higher altitudes. Table 2 lists the specifications of the receiver subsytem.

TABLE 2. Specifications of the Receiver Subsystem.

Field of View	0.2 - 0.75 mr (variable)
Detector	Photomultiplier Tube EMI 9658 52 mm, S-20 Photocathode
Filter	1.0 nm Bandpass 60% Transmission at Center 532.1 nm Center Wavelength

The details of the design considerations and alignment procedures for the optical subsytem are given in Reference 1. A schematic of the receiver subsystem is shown in Figure 3.

The light chopper wheel is driven with a 400-Hz, three-phase motor that turns at 12,000 RPM. The chopper blade is a "bow tie" type that chops the beam twice during one revolution. The three phase, 400-Hz voltage is generated from a 6 MHz crystal-controlled oscillator. The oscillator signal is divided down to 400-Hz and split into two signals shifted by 120° with respect to each other. The third signal is ground so that this is equivalent to three voltages at 120° with respect to each other. The two nonzero voltages are amplified in a two-channel audio power amplifier before going to a capacitor matching network and into the motor. A diagram for this Motor Drive Circuit is given in Appendix A.

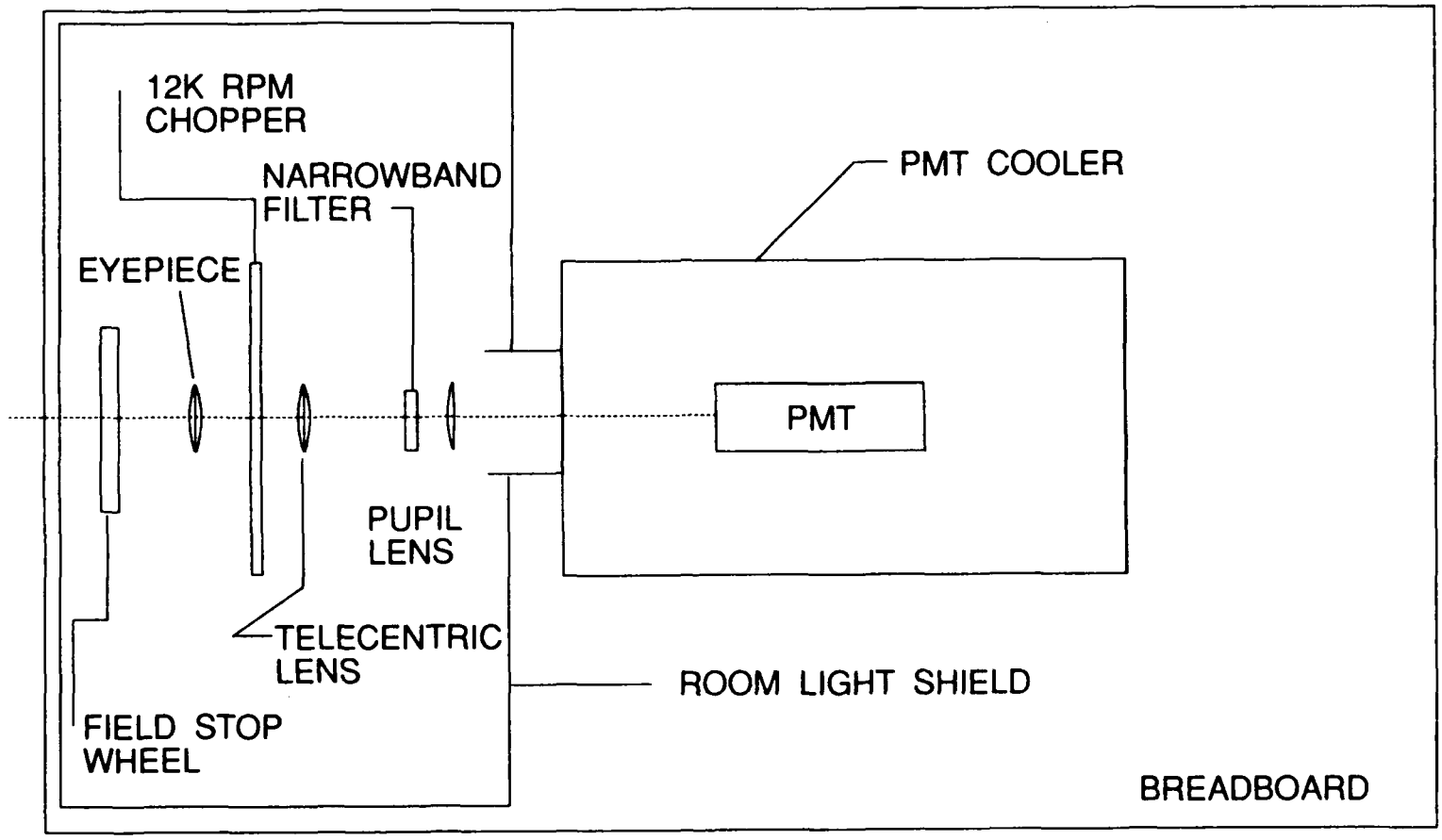

Figure 3. A schematic of the receiver subsystem.

Since the light beam chopper is the timer for the lidar pulses, the laser firing is synchronized to the chopper by using a photodiode switch on the chopper to generate a 400-Hz signal directly from the chopper. This 400-Hz signal is divided into the 20-Hz region which is the fastest rate at which the laser can be fired. However, the laser power supply must charge the firing capacitors before each pulse so there is a logical sequence of charge, charge status and fire signals which the power supply must have in order to pulse the laser from an external source. Figure 4 shows the logic circuit to accomplish the synchronization interface. One feature of the interface circuit is the digital delay which allows for adjustment of the time of firing of the laser before the PMT is uncovered. This gives a fine adjustment on the altitude at which the receiver is open. A course adjustment is made by the changing the position of the photodiode switch on the chopper wheel housing. A circuit diagram of the Laser - Chopper Interface Circuit and a Motor Interconnect Diagram are in Appendix A.

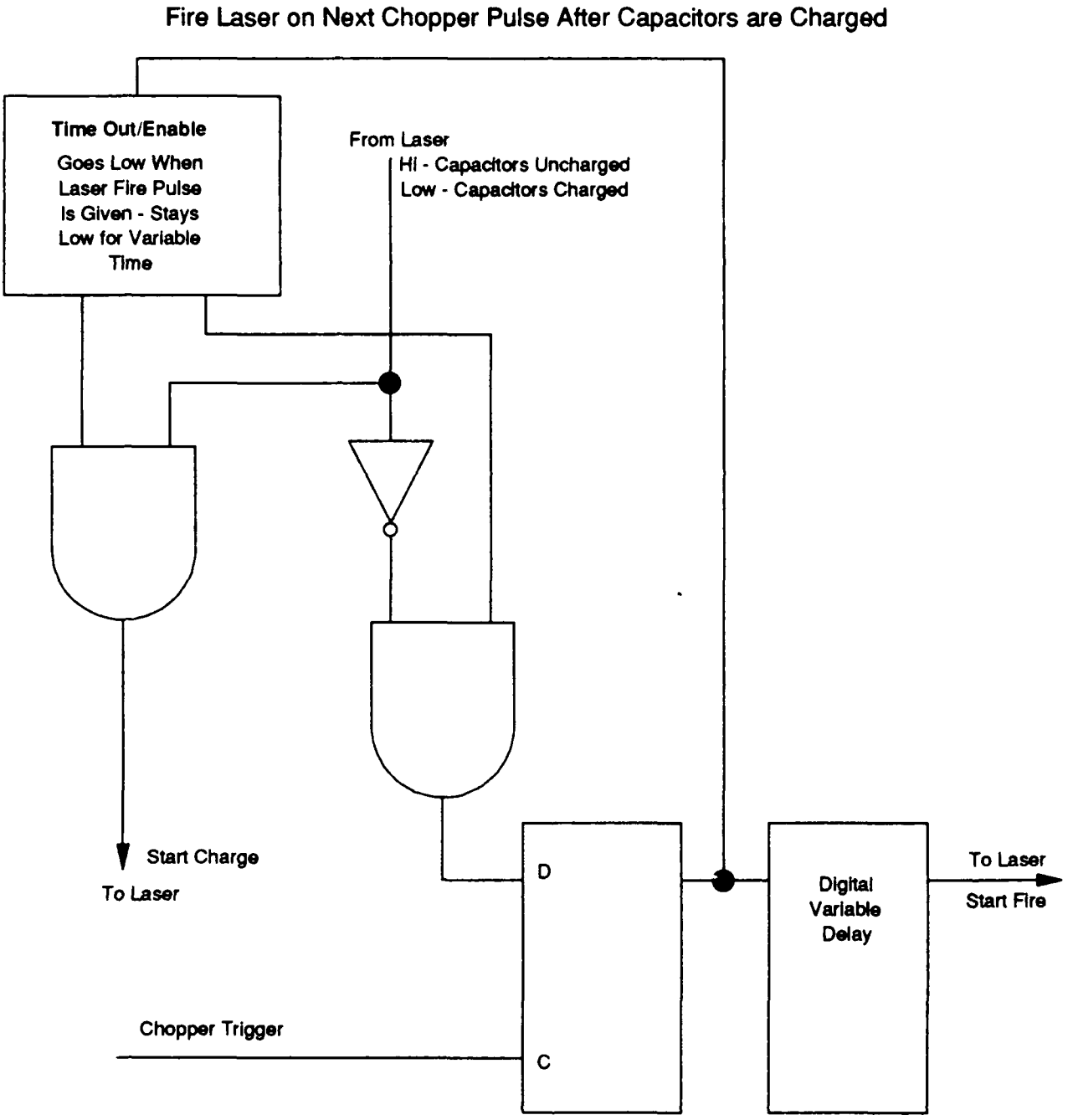

Figure 4. The logic circuit for the laser-chopper synchronization interface.

3. DATA ACQUISITION SUBSYSTEM

The primary purpose of the data acquisition subsystem is to digitize the analog electronic output of the PMT, sum the results from multiple sweeps and present it to the personal computer which displays the data and stores it on floppy disks. Figure 5 shows the essential parts of the data acquisition subsystem. The digitization is preceded by a DSP, Inc. 1020 differential amplifier that matches the output of the PMT preamplifier to the DSP 2012 10 bit/20 MHz transient recorder which feeds a DSP 4100 averaging memory. The laser power meter is monitored with a DSP ADS1612 scanning A/D converter which puts the digital value into the data track. The DSP IO612 dual I/O register manages the data track into the external PC AT. The DSP units are housed in a CAMAC power crate which is managed and monitored with the AT using the DSP 6001 mP-Camac crate controller.

The acquisition of data is menu driven from the PC except for setting the differential amplifier gain and the range bin (dwell time) of the transient recorder. The operator sets the number of sweeps to be averaged from the menu and starts the recording with the PC. The transient recorder is triggered from the Q switch of the laser and starts a sweep at every laser pulse which means the sweep has started even though the receiver beam chopper is not yet open. After the requested number of sweeps the data are transferred to the PC. The data then can be displayed in various ways using the choices in the menu which give a quick look capability. The range bin of the transient recorder was set and kept at 15 m for all the data taken during the demonstration. The averaging memory had a limit of 2^{24}-1 bits which means that the memory is close to capacity after 4000 sweeps. The laser pulse rate is 1000 pulses/min which set the maximum record time to 4 minutes. All the data were transferred to floppy disks and a log kept of the data files for each measurement episode. Copies of the data floppy disks and log were presented to the technical monitor at the completion of the demonstration. Another set of copies resides with the contractor.

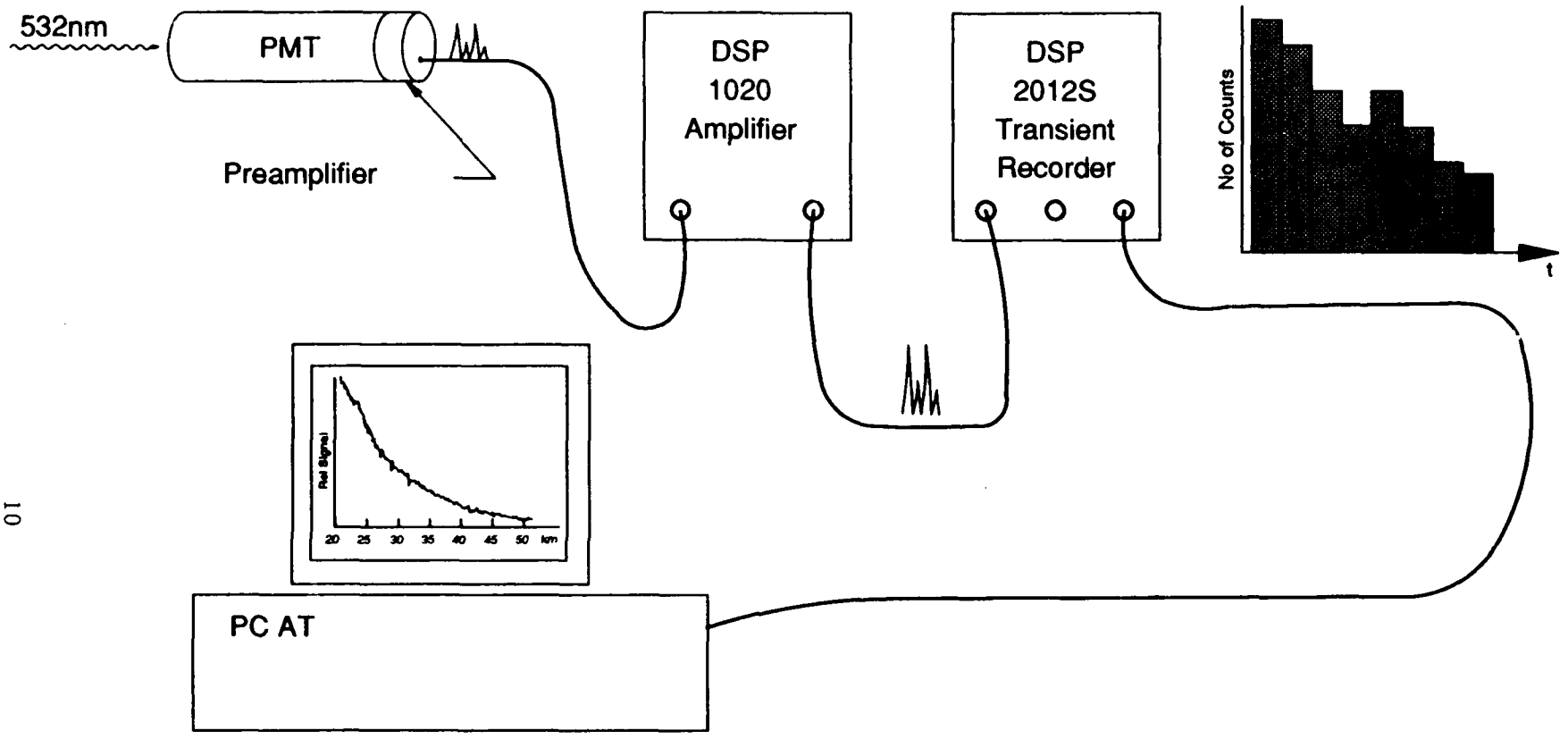

Figure 5. A sketch of the essential parts of the data acquisition subsystem.

4. ADAPTATION OF THE COLLIMATOR FOR LIDAR

Three areas of the collimator building were used in adapting the collimator for lidar. The cross tunnel housed the transmitter, the receiver and data acquisition susbsystem were on the fourth level at the f/6 port of the collimator and the warning radar and observer were on the roof. The operation center for the data collection episodes is the fourth level station which is connected to the other areas by walkie-talkie.

A few additions to the tunnel were needed to accommodate the transmitter so that a mechanically stable optical system was assured. The laser is mounted on a specially constructed platform that rests on the rails on the tunnel floor. A sketch of the laser platform is shown in Figure 6. As shown in Figure 1 the transmitter optical table is fastened to the laser housing so that the transmitter optics are also rigidly supported. The steering mirror is supported over the collimator mirror with a ladder type structure that also rests on the tunnel rail system. This arrangement for the transmitter proved to be very stable so that once the transmitted beam was steered into the field of view of the collimator no further adjustments were needed during a measurement episode and only slight adjustments were required over the entire demonstration period. Figure 7 shows the top view of the arrangement of the transmitter in the tunnel.

The receiver optics, light beam chopper and PMT cooler are held on a specially constructed shelf that was fastened to the bolt circle on the f/6 port. The PMT power supply, chopper driver and chopper laser interface are in a relay rack that rests on the floor next to the receiver shelf. The Camac power crate for the data acquisition subsystem is also fixed to the relay rack and the PC AT is on the operator's desk next to the relay rack. An oscilloscope to monitor the receiver output from the DSP differential amplifier during final adjustment of the steering is also next to the operator's desk along with the joy stick for controlling the mirror.

The radar warning receiver is placed on the roof with a TV camera-VCR system to continuously record. The radar scope screen is located in the elevator at the roof level. The circuitry for the automatic laser kill by the radar is also in the elevator. An interconnection diagram for the roof top subsytem is in Appendix A.

All the interconnections for the three subsytems described above are made of appropriately shielded wire. The cabling for the laser-chopper interface and all the receiver signals use woven wire shields because of the sensitivity of this circuitry to EMI. A diagram showing the interconnections among the three subsystems is shown in Appendix A.

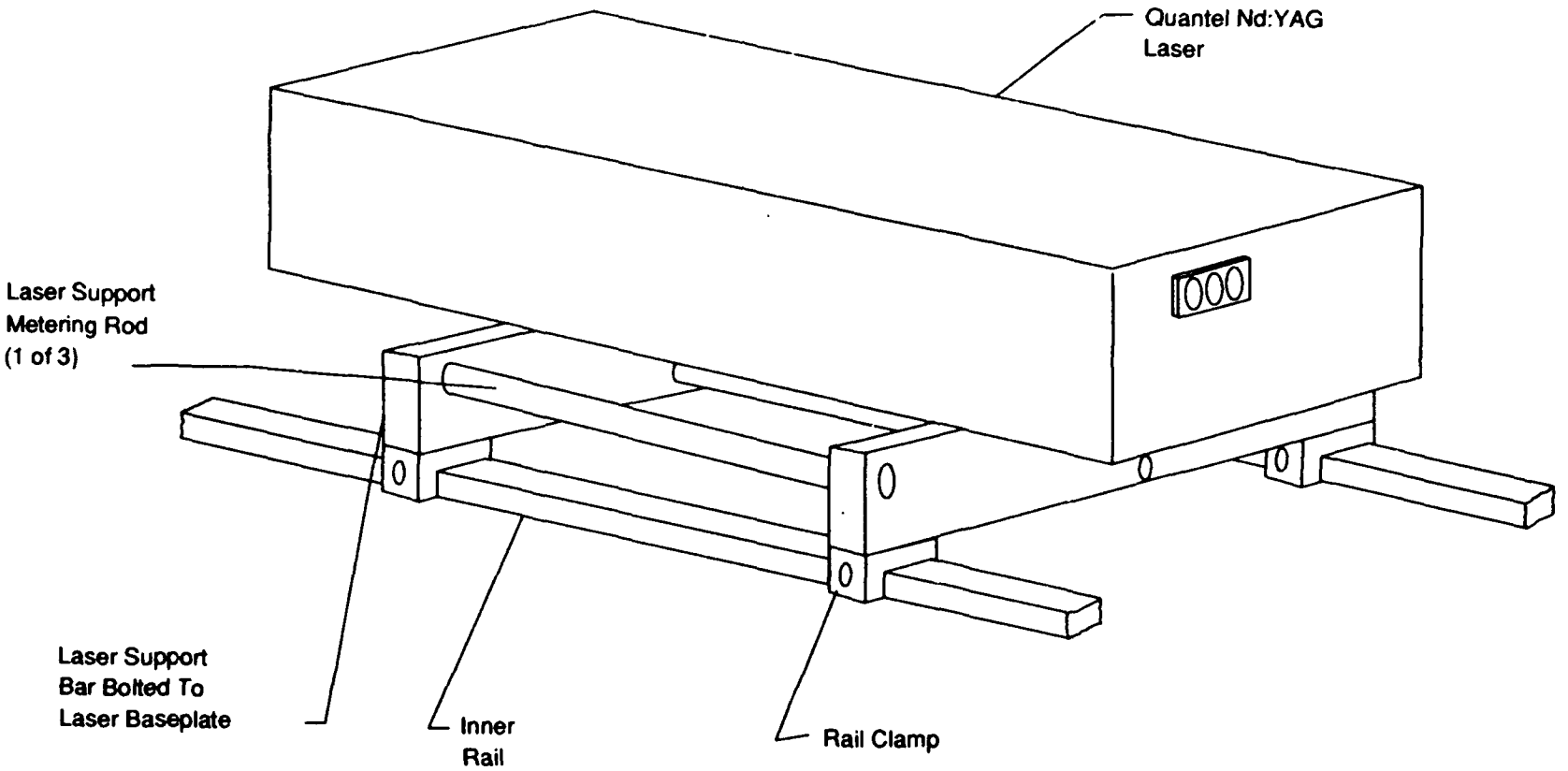

Figure 6. A sketch of the laser platform designed and constructed at Georgia Tech. The rails are those in the collimator cross tunnel floor. The transmitter optical table shown in Figure 1 is omitted for clarity.

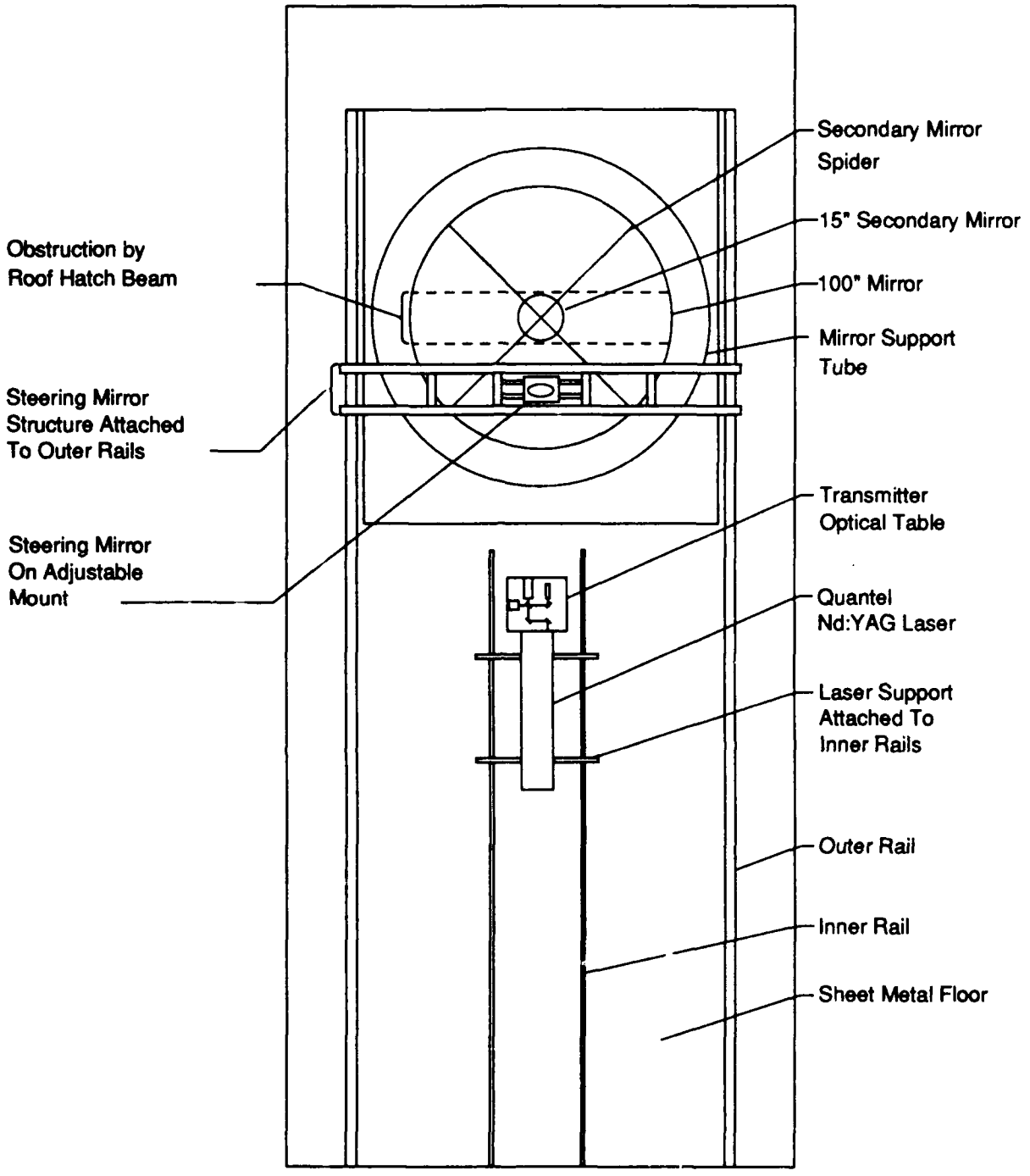

Figure 7. A top view of the transmitter arrangement in the collimator cross tunnel.

5. EVALUATION OF THE COLLIMATOR FACILITY

Beside the exceptionally large mirror, the collimator facility offers an unusually stable environment for the optical systems associated with lidar systems, which was certainly an advantage during the demonstration. Reference 1 gives more details of other advantages of the collimator facility and most of these were also realized during the demonstration. However, there are some recommendations which we wish to make that will improve the facility for operation of permanent lidar systems. The recommendations are given for each area of the collimator facility where subsystems of the demonstration lidar are located.

Rooftop

Roof Hatch

We recommend that the roof hatch be replaced with a motor operated roll-off roof because the current roof hatch is so awkward that a crew of three is required to open and close it, it is susceptible to accidental closing by wind gusts, and the center bar obscures 18 percent of the mirror area.

Observer's Area

We recommend a heated enclosure for the safety observer which provides full view of the sky. Otherwise the operation time of the MEGALIDAR will be determined by the endurance of the observer in the winter. We also recommend railings around the hatch and edge of the building for the safety of all personnel on the roof for MEGALIDAR operation.

Roof Top Instrumentation

We recommend a permanently installed safety radar with an all weather enclosure that would also include weather monitoring instrumentation such as wind speed, air temperature, precipitation indicator and a video sky camera. This installation would eliminate the safety hazard of loose cables strung on the roof top and reduce the preparation time for starting the MEGALIDAR operation.

We recommend that the radar video, sky camera video and the weather instrumentation outputs be hardwired to the level 4 location so that the Test Director can monitor them at all times and so that all data recording occurred on this level. It would also free the observer from all responsibilities except for spotting. We recommend that the walkie-talkies be replaced with an intercom between the roof and level 4 for better communication and less chance for EMI with the lidar circuits.

Level 4

Data and Control Center

We recommend that more room be provided at this location by removing the equipment stored near the f/6 collimator port

Control Center Communications

We recommend the installation of a telephone at the Test Director's desk (the Standard and Emergency Operating Procedure (SEOP) requires the Test Director to use a phone in emergency situations) and the installation of a intercom connecting this location, the tunnel and the roof top.

Tunnel

Hazards

We recommend the installation of railing to prevent personnel from falling into the collimator when it is open and the installation of covers on the rails in the tunnel floor to prevent injuries caused by stepping into the gaps between the rails and the floor.

Temperature

We recommend that the tunnel temperature be set lower to eliminate the problem with the laser power supply mentioned below caused by the high tunnel temperature (78-80°F).

Communications

We recommend a permanent intercom to Level 4 and the roof top.

Other

Shutter Mechanism

We recommend that the mechanism that moves the shutter directly over the mirror be reworked to make it more reliable.

Office Space

We recommend office space, in addition to the Control Center, be assigned to the MEGALIDAR crew for data analysis, planning and coordination tasks, permanent display of data and photographs and for presentations to visitors.

6. MEASUREMENT METHOD

The three subsystems, except for the special fixtures required for attaching them to the collimator, were integrated with a 16-inch telescope and operated as a Rayleigh lidar at Georgia Tech before they were transported to Wright-Patterson AFB. This allowed us to check the reliability and performance of each subsystem including the data acquisition software and to establish a baseline for comparison of the performance of the collimator as a lidar. This was particularly important since the quality of the 100-inch mirror surface was not known.

The tests of the system at Georgia Tech showed that it could consistently obtain data from altitudes up to 60 km. This then, could be used to give an accurate prediction of the maximum altitude we would reach with the MEGALIDAR assuming the only difference between the two systems was the diameter of the mirrors. Using a measured S/N of 11 obtained at Georgia Tech from 50 km altitude, we calculated, assuming that the collimator mirror had the same reflectivity as the one used at Georgia Tech, that data collected by the MEAGLIDAR from 80 km should have a S/N of 3.3 (Reference 2).

Once the lidar system was fitted to the collimator and the subsystems individually tested and then integrated together, the receiver and transmitter optics could be aligned. The transmitter optics were aligned using the HeNe laser so that the transmitter beam would clear the obstructions in the upper part of the collimator. The receiver optics were aligned during the daylight using the real image of the mirror. The receiver electronics were checked using the background from the sun at twilight and watching the background decrease to the amplifier limited value after astronomical twilight. This was the same limiting amplifier noise that was observed at Georgia Tech which was what we expected. The WRDC safety certificate did not authorize daytime operation so no data were obtained during the day.

The first time the transmitter beam went out of the building and returns were obtained, the steering mirror was given a final adjustment while viewing the returns on the oscilloscope and the time delay on the chopper-laser interface was adjusted to avoid saturation of the PMT. These adjustments were checked during subsequent runs, but required very little change. The measurements were taken in 4 minute averages, one right after the other, except for observer or instrumental interruptions. The measurement episodes occurred every night that the weather permitted during the measurement period. The most persistent instrumental interruption was a laser pulse rate instability that was traced to overheating of the laser power supply because of poor cooling ventilation in the cross tunnel.

A copy of the required Standard and Emergency Operation Procedures manual that was developed for the demonstration is included in Appendix B.

7. METHOD OF DATA ANALYSIS

7.1 Quick Look Analysis

The quick look analysis is a set of PC routines that could be run during the data acquisition phase to provide a data quality assessment and zero-th order information on the atmosphere. The routines provide the following functions: (1) display the data without any correction i.e., the "raw data"; (2) display the "raw data" with the background subtracted; (3) compute and display the density versus altitude from the background corrected "raw data"; and (4) compute and display the scattering ratio. The background was computed using the last 300 data values of the return from altitudes where it was assumed that the laser return was below the amplifier noise.

7.2 Analysis at Georgia Tech

The identity of the data obtained from each 4 minute sweep was preserved in the analyses that were done at Georgia Tech so that the average density profile for each sweep period was obtained. The data were processed to reduce the noise by using a sliding rectangular window with a length of 1 km. Several other rectangle lengths were tried, but this one was judged to achieve sufficient noise reduction without severe impact on the data.

The steps in the data processing were: (1) subtract the background from the "raw data"; (2) average the data using the 1 km sliding window; (3) convert the data to density values; (4) compute the ratio of the measured density value to the density value from the U. S. Atmosphere 1976 model. Since the receiver shutter wasn't fully open until 40 km, the averaging in step 2 was started just below the 40 km altitude in order to assure that a full averaging window was used at 40 km. The calculations in steps 3 and 4 used only data from 40 km and above. The effectiveness of the step 2 averaging is shown in Figure 8.

The density values were calculated using the equation 1 for the density, $r(z_i)$, at altitude, z_i, which was given in Reference 3:

$$r(z_i) = r_m(z')F(N(z_i)(z_o - z_i)^2, N(z')(z_o - z')^2)$$

where $N(z_i)$ = the return from altitude z_i in the smoothed data set,

z_o = the altitude of the collimator,

$r_m(z')$ = the density obtained from the U. S. Standard Atmosphere at altitude z',

and $N(z')$ = the return from altitude z' in the smoothed data set.

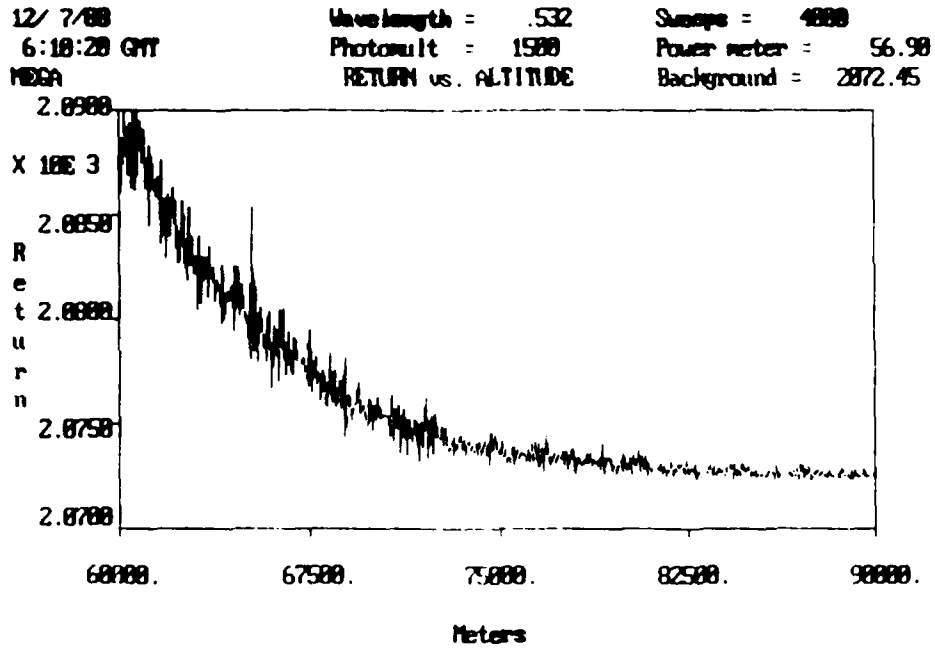

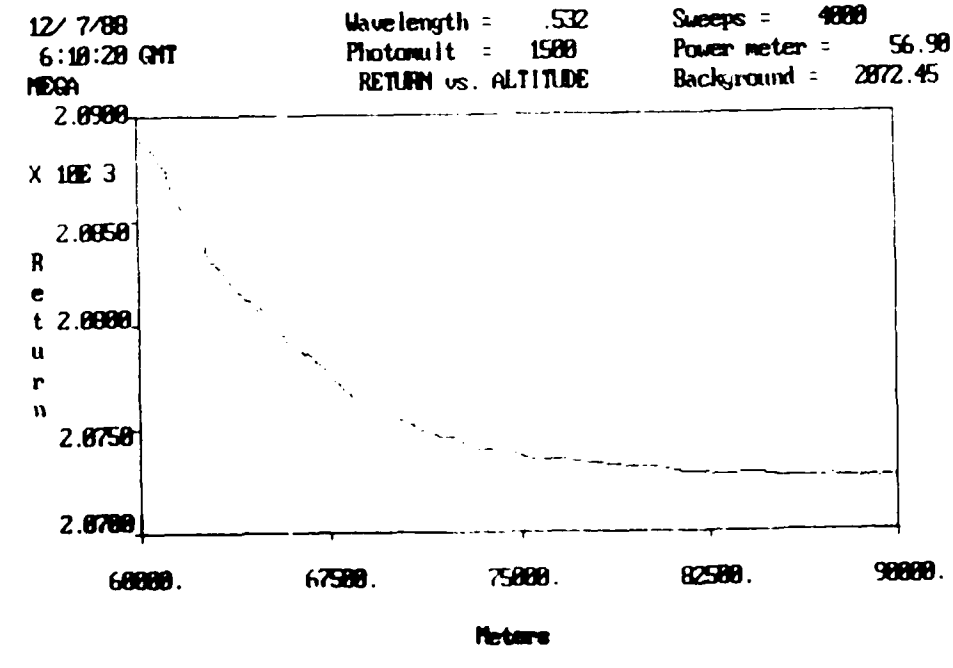

Figure 8. The effect of the spatial averaging using a 1 km filter.
(a) The data from 4000 consecutive sweeps without any corrections.
(b) The data from (a) after the spatial filter.

8. MEASUREMENT RESULTS

Data were acquired during six measurement episodes from December 6 - 19, 1988. During each episode, a sequence of data records was acquired as described above. A data record is the data from a set of consecutive sweeps that was completed, transferred to the PC and stored in the hard disk with its own file name. Each record is identified in this report by the date and start time, in Greenwich Mean Time, of the sweep sequence. Table 3 give the date and the total number of records for each measurement episode.

TABLE 3. Dates and Number of Records for Each Measurement Episode of the MEGALIDAR Proof of Concept Demonstration.

Episode Number	Date GMT	Number of Records
1	12/07	39
2	12/10	25
3	12/11	35
4	12/12	3
5	12/16	16
6	12/19	9

Varying numbers of records were acquired during different episodes for a variety of reasons, including weather conditions, problems with the laser or other electronic equipment, and the type of measurement. The last episode, for example was scheduled during sunrise, in order to measure the effect of sky background on the data.

The figures that follow are plots of the density ratio versus altitude calculated as described in the data analysis section. A plot is included for every data record which was appropriate for this kind of analysis, but in order to ensure that the plots shown are directly comparable, some of the records in Table 3 are not included.

Records were deleted for the following reasons: (1) nonstandard number of sweeps (other than 4000); (2) inconsistent operation of the laser during the measurement; (3) other instrumental problems during the measurement; and (4) measurements for purposes other than atmospheric density profiles, e.g., sky background studies.

Figures 9 through 104 show the plots of the density ratio versus altitude obtained from the measurement records selected. The percent errors shown in Figure 9 at selected altitudes are three standard deviations in the density ratio and hold for all subsequent plots, but are not shown for clarity. The standard deviations in the density ratios were obtained from the root mean square deviations in the smoothed data for 10 data points around the selected altitudes assuming no error in the U.S. Standard Atmosphere, 1976. Table 4 shows the percent error at the selected altitudes.

TABLE 4. Percent Error in the Density Ratios Shown in Figures 9-104 Corresponding to Three Standard Deviations for Selected Altitudes.

Altitude(km)	Percent Error
45	- 2.5
55	- 2.5
65	- 2.5
75	- 4.5
85	- 10.5

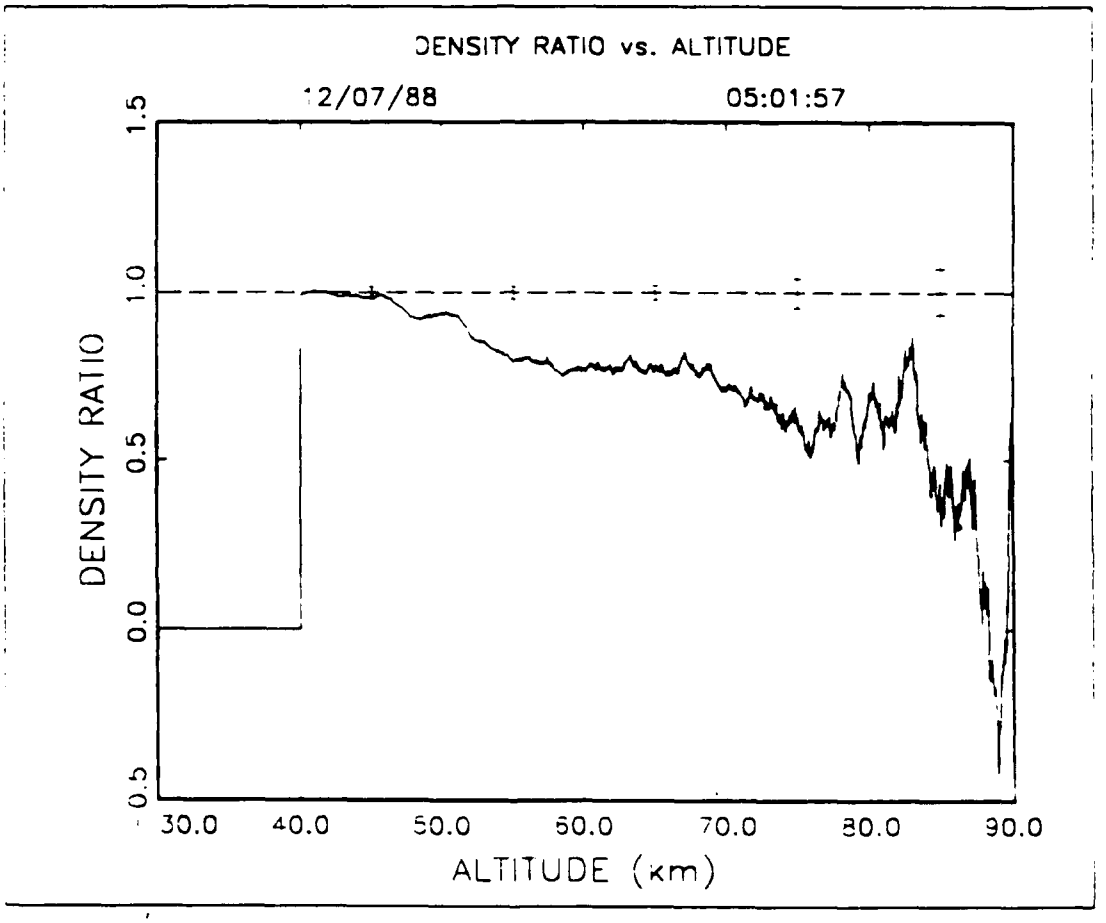

Figure 9. Plot of Density Ratio Versus Altitude for 5:01:57, 12/7/88 GMT. The Error Bars Represent the Percent Error Corresponding to Three Standard Deviations. They Apply to All the Following Data Figures.

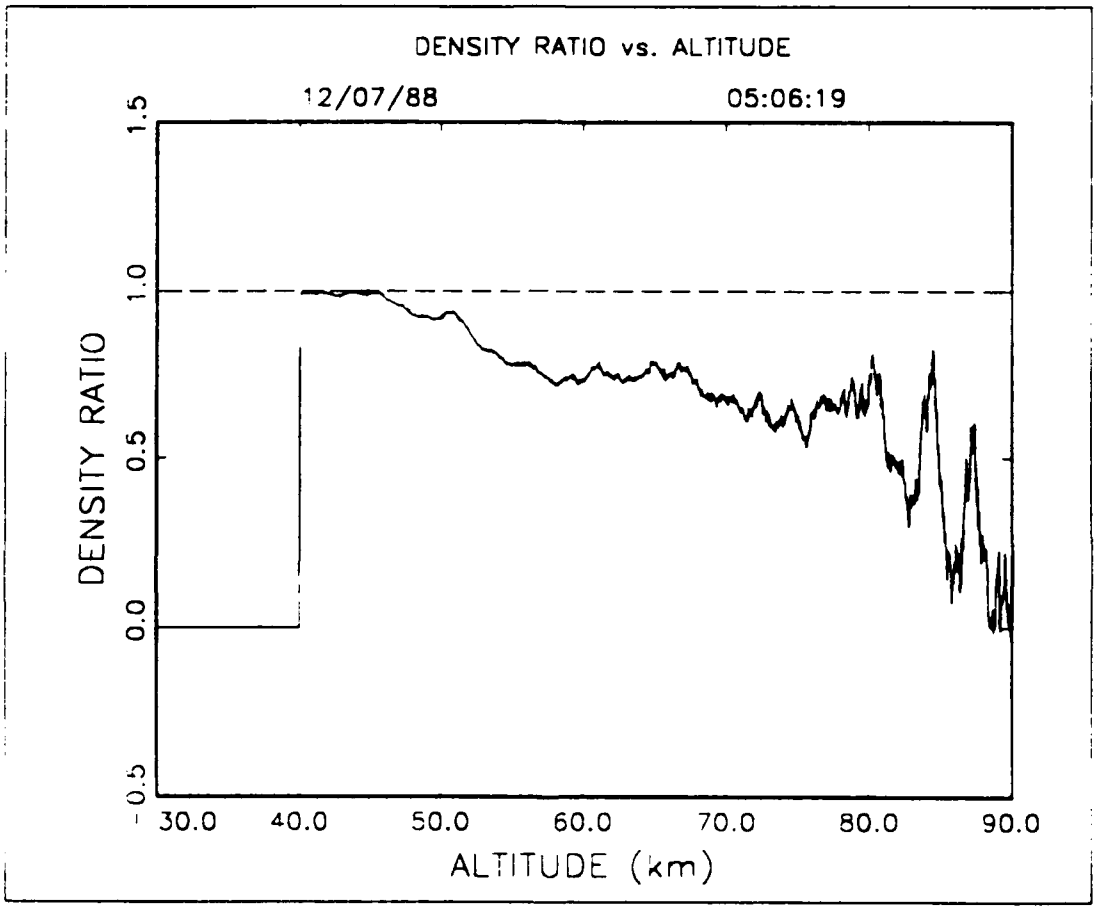

Figure 10. Plot of Density Ratio Versus Altitude for 5:06:19, 12/7/88 GMT.

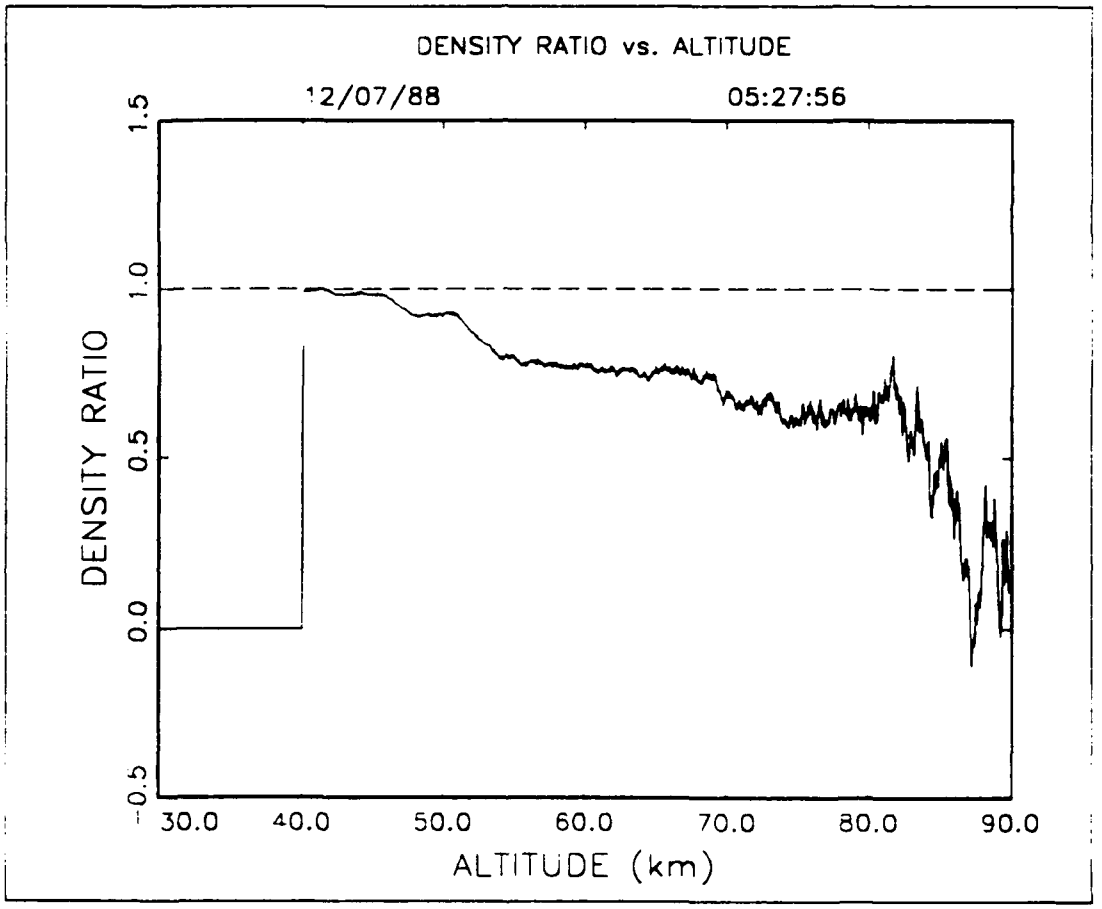

Figure 11. Plot of Density Ratio Versus Altitude for 5:27:56, 12/7/88 GMT.

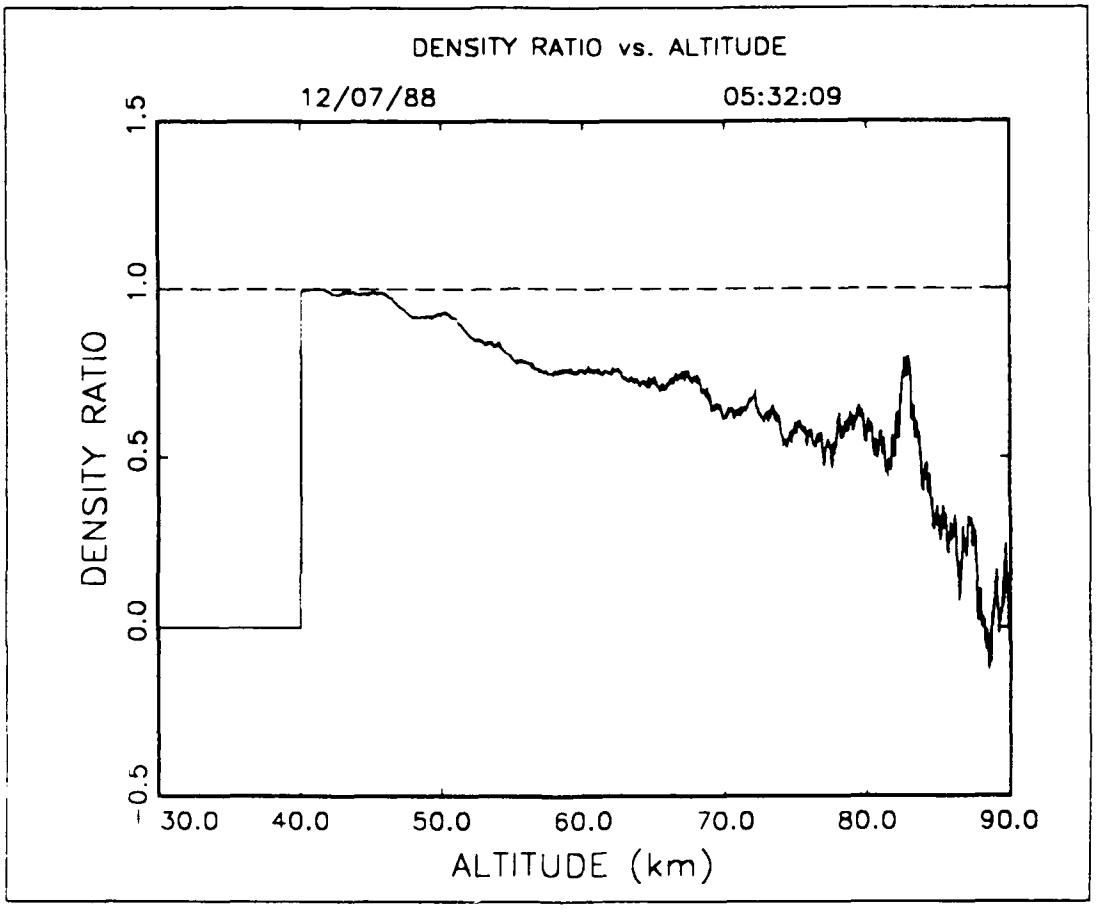

Figure 12. Plot of Density Ratio Versus Altitude for 5:32:09, 12/7/88 GMT.

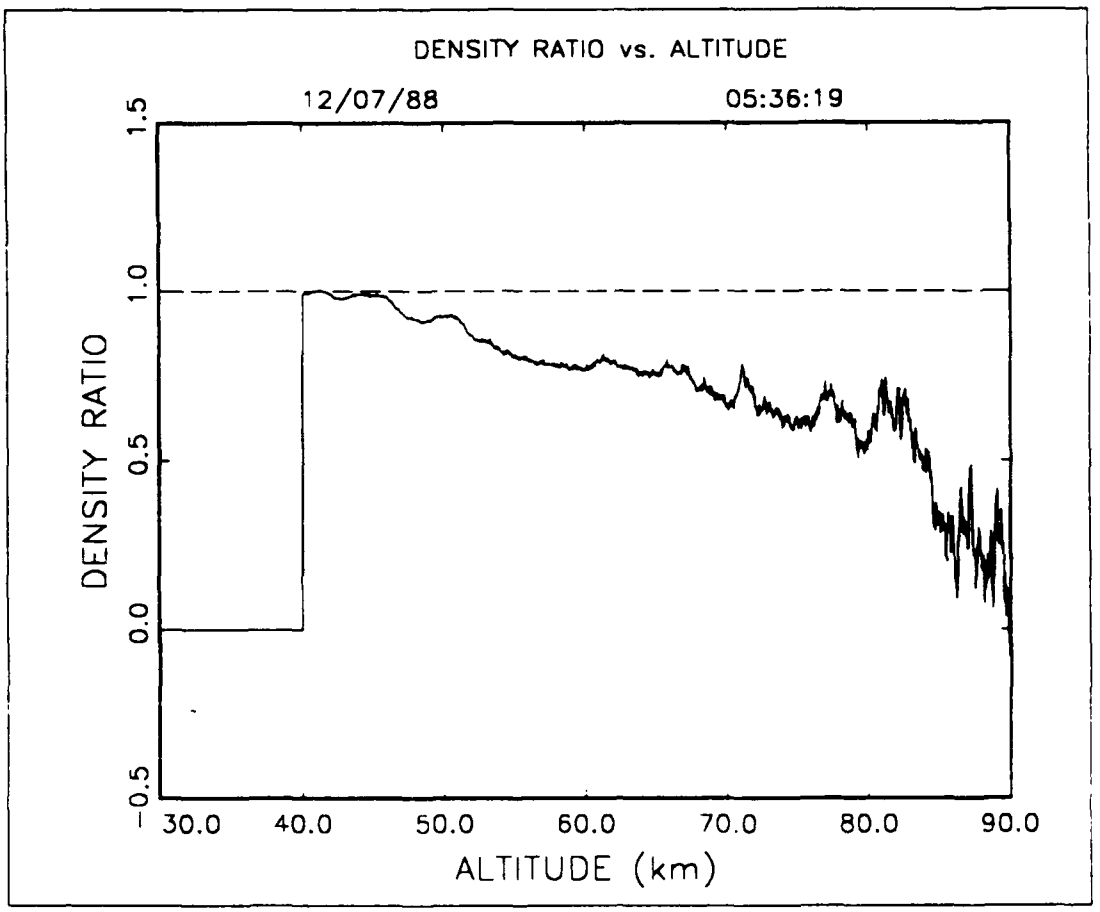

Figure 13. Plot of Density Ratio Versus Altitude for 5:36:19, 12/7/88 GMT.

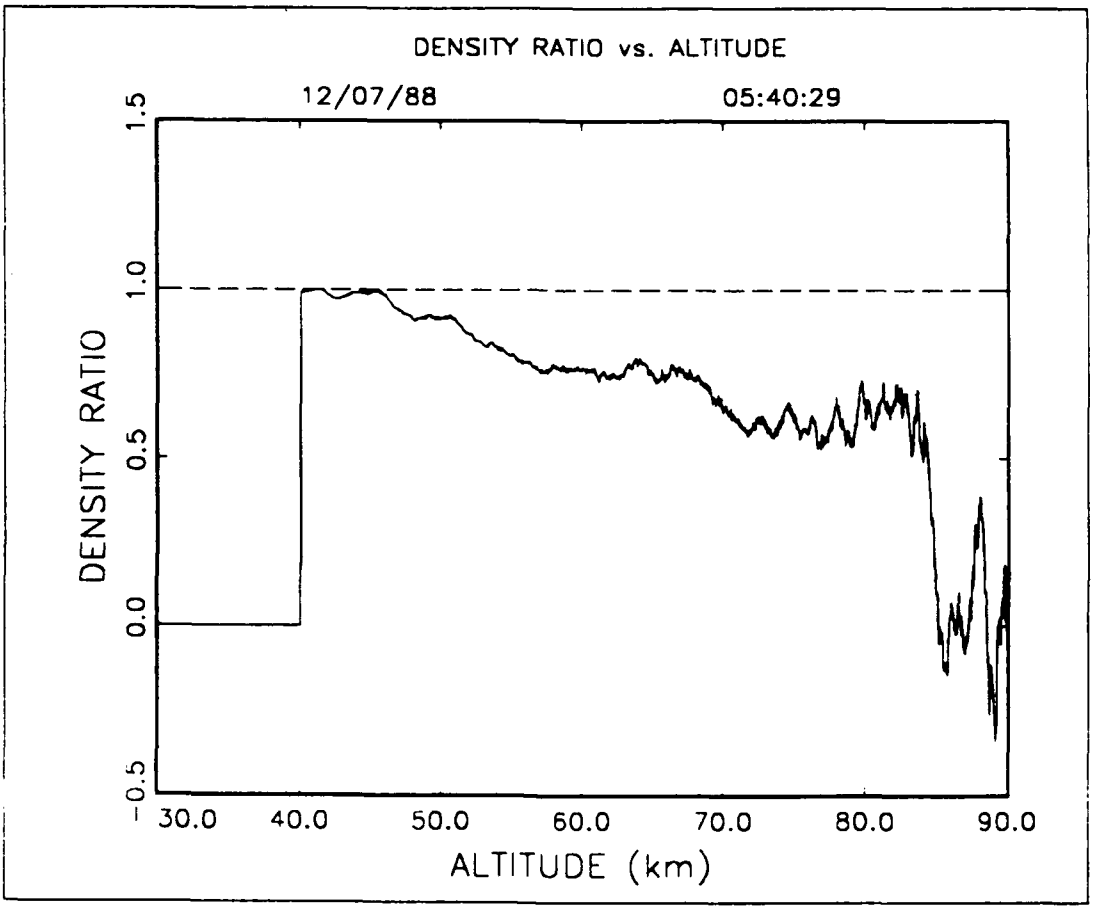

Figure 14. Plot of Density Ratio Versus Altitude for 5:40:29, 12/7/88 GMT.

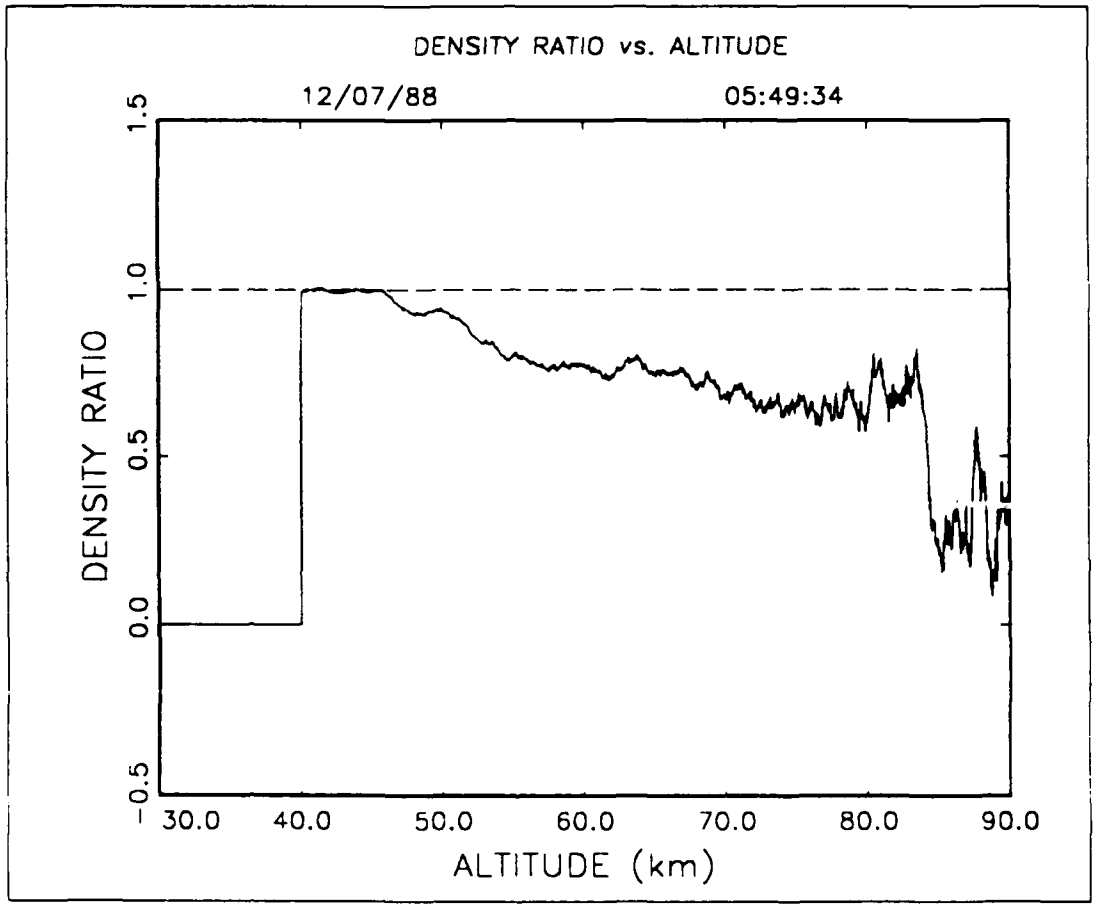

Figure 15. Plot of Density Ratio Versus Altitude for 5:49:34, 12/7/88 GMT.

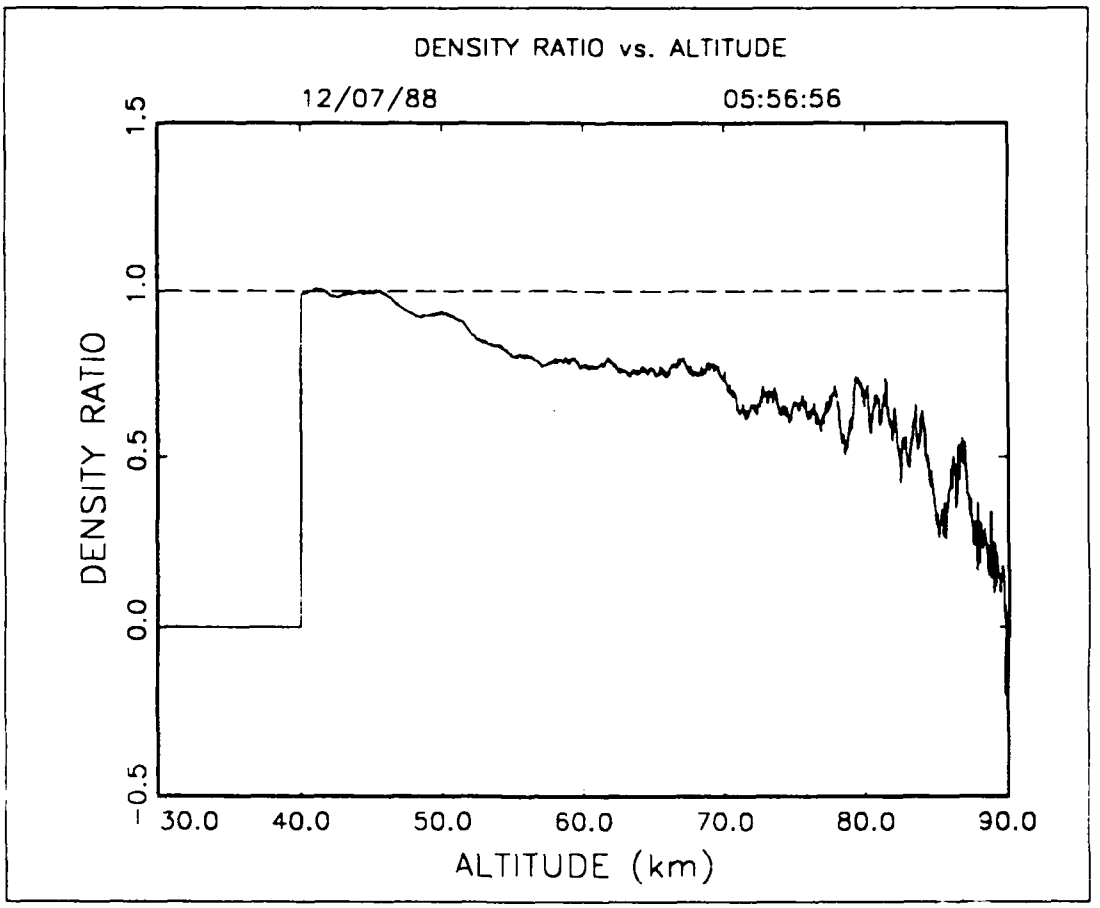

Figure 16. Plot of Density Ratio Versus Altitude for 5:56:56, 12/7/88 GMT.

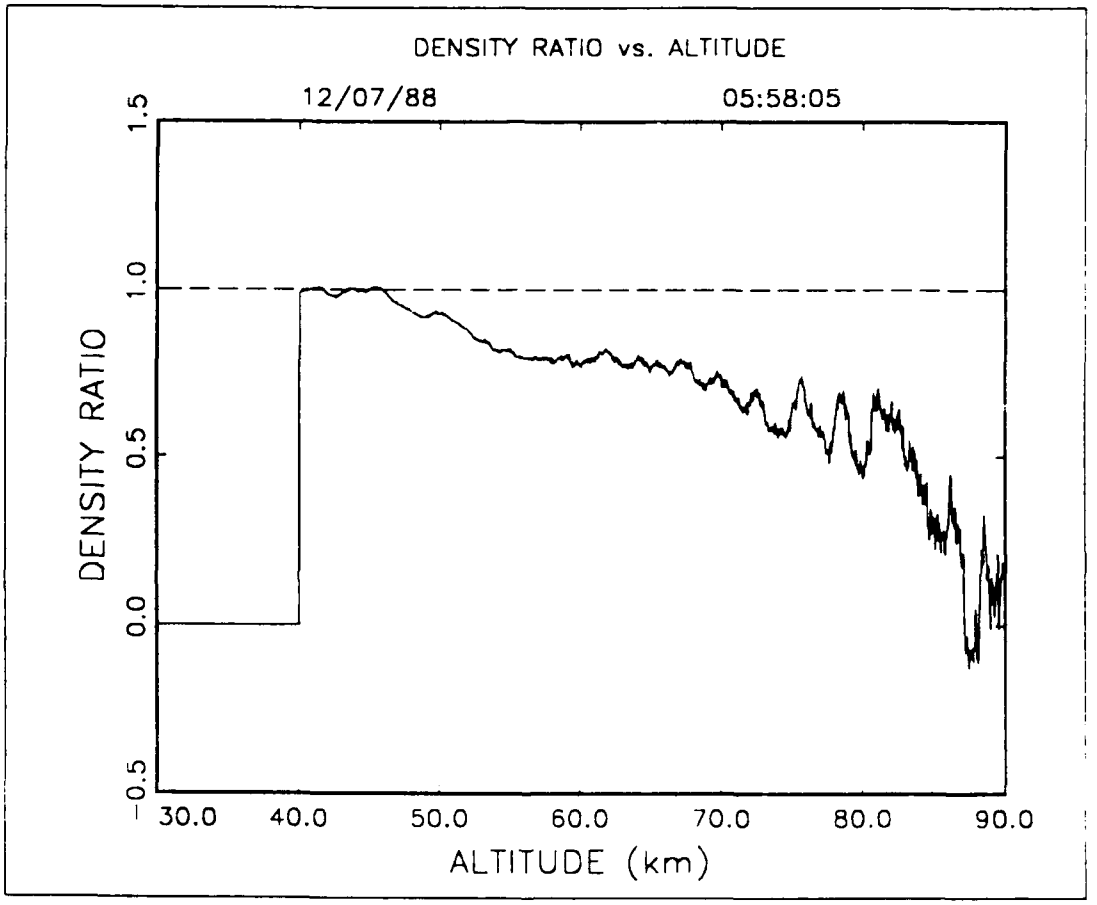

Figure 17. Plot of Density Ratio Versus Altitude for 5:58:05, 12/7/88 GMT.

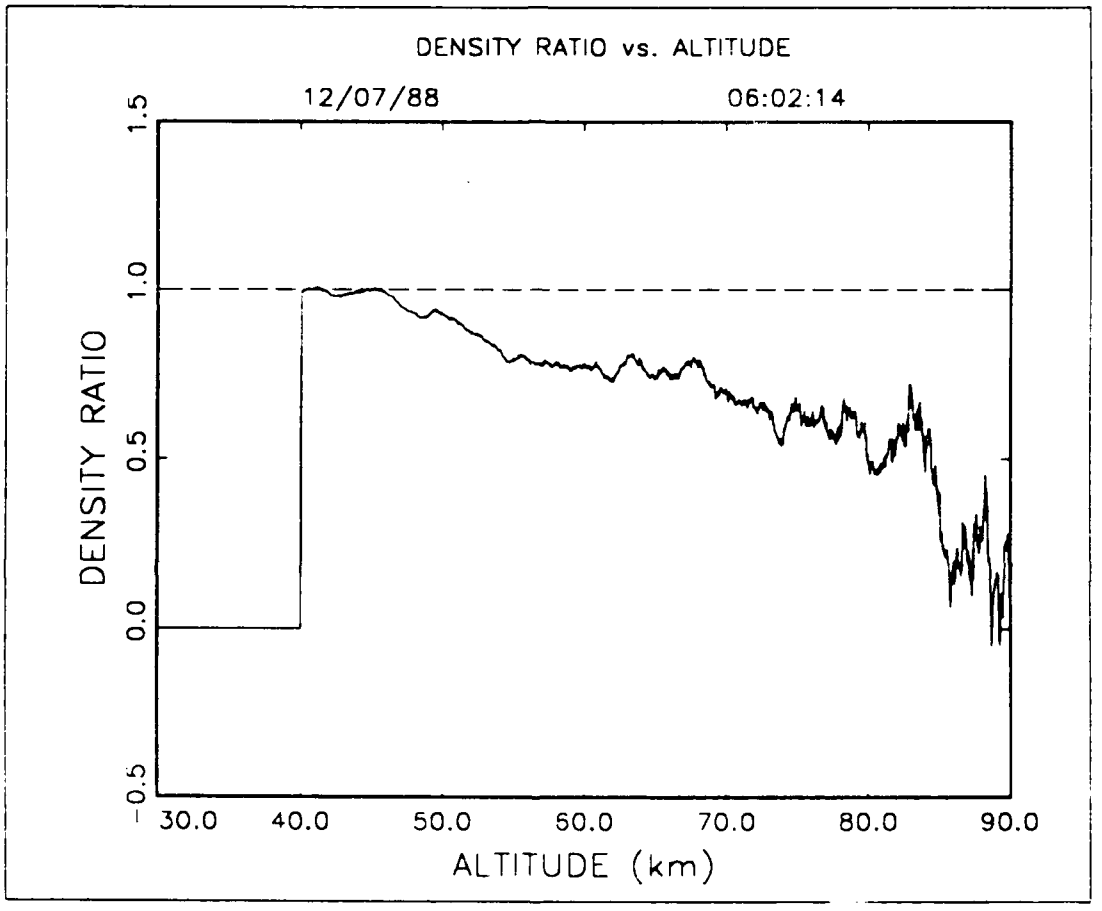

Figure 18. Plot of Density Ratio Versus Altitude for 6:02:14, 12/7/88 GMT.

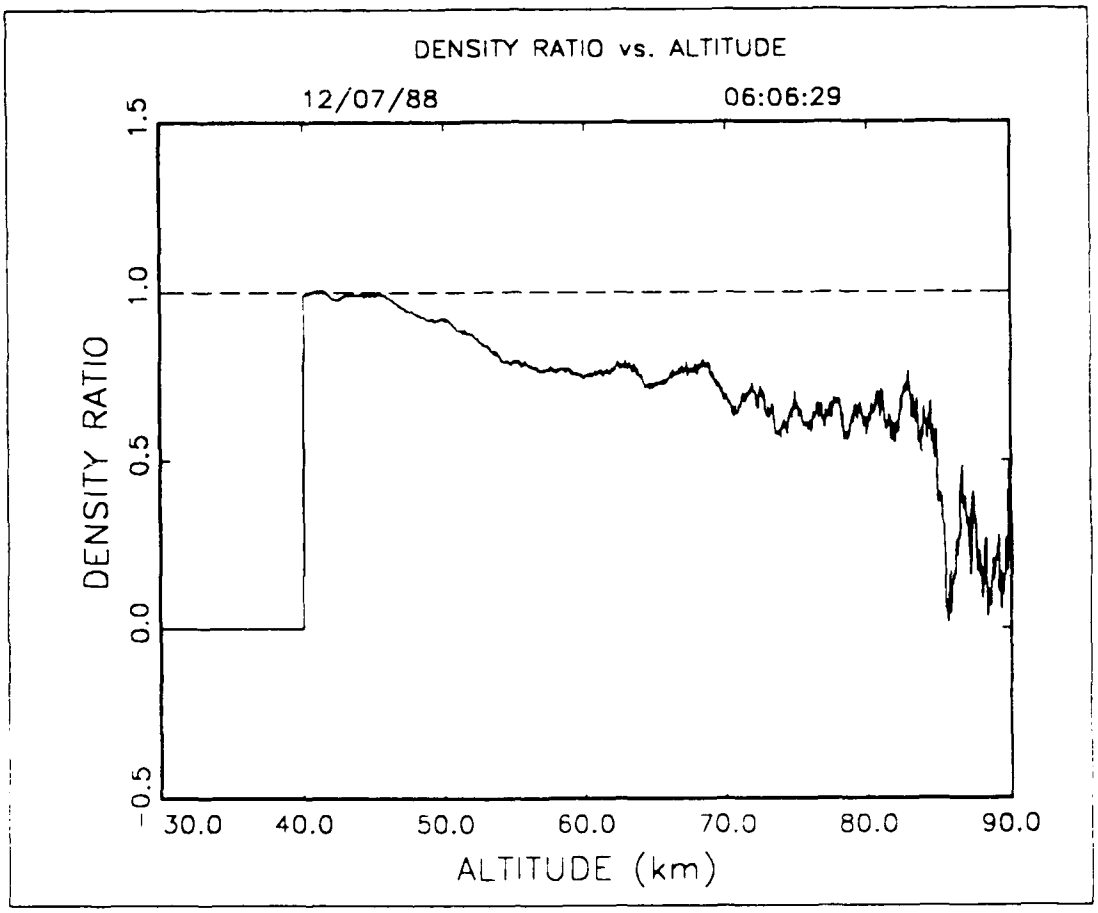

Figure 19. Plot of Density Ratio Versus Altitude for 6:06:29, 12/7/88 GMT.

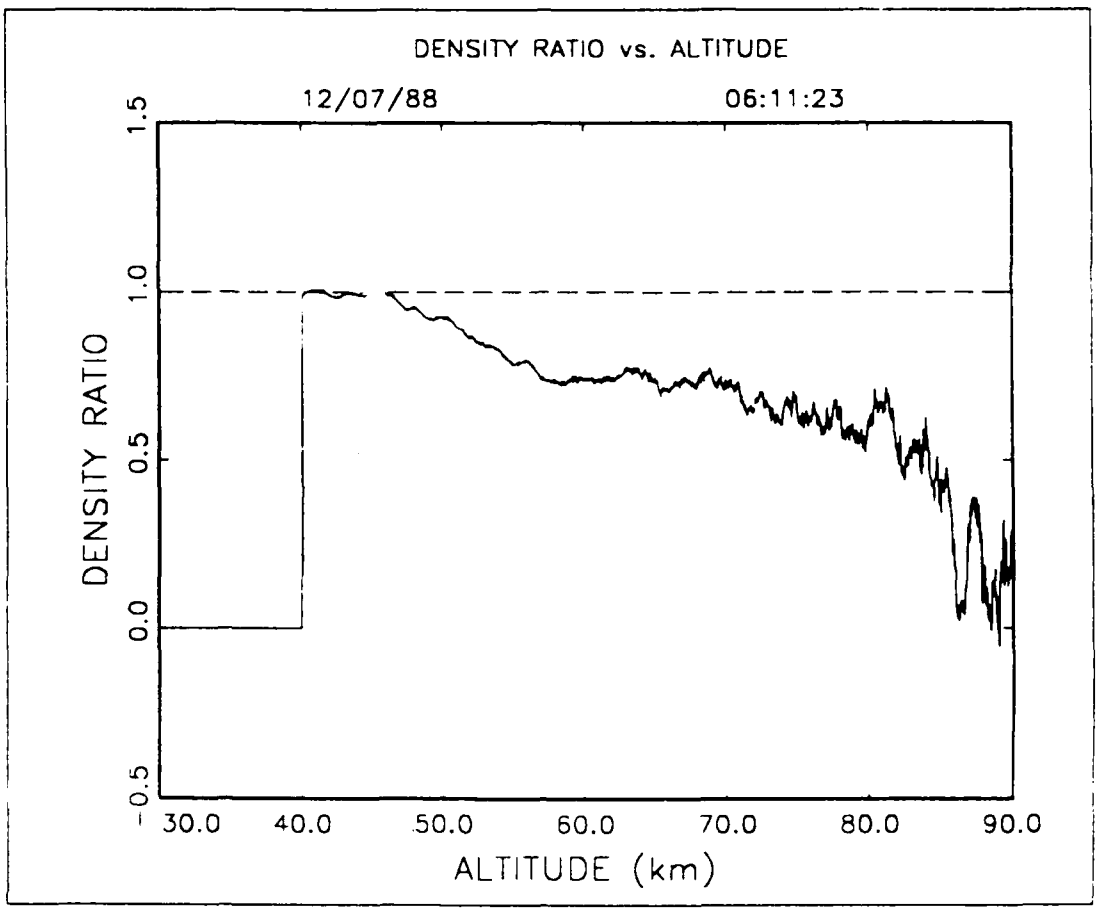

Figure 20. Plot of Density Ratio Versus Altitude for 6:11:23, 12/7/88 GMT.

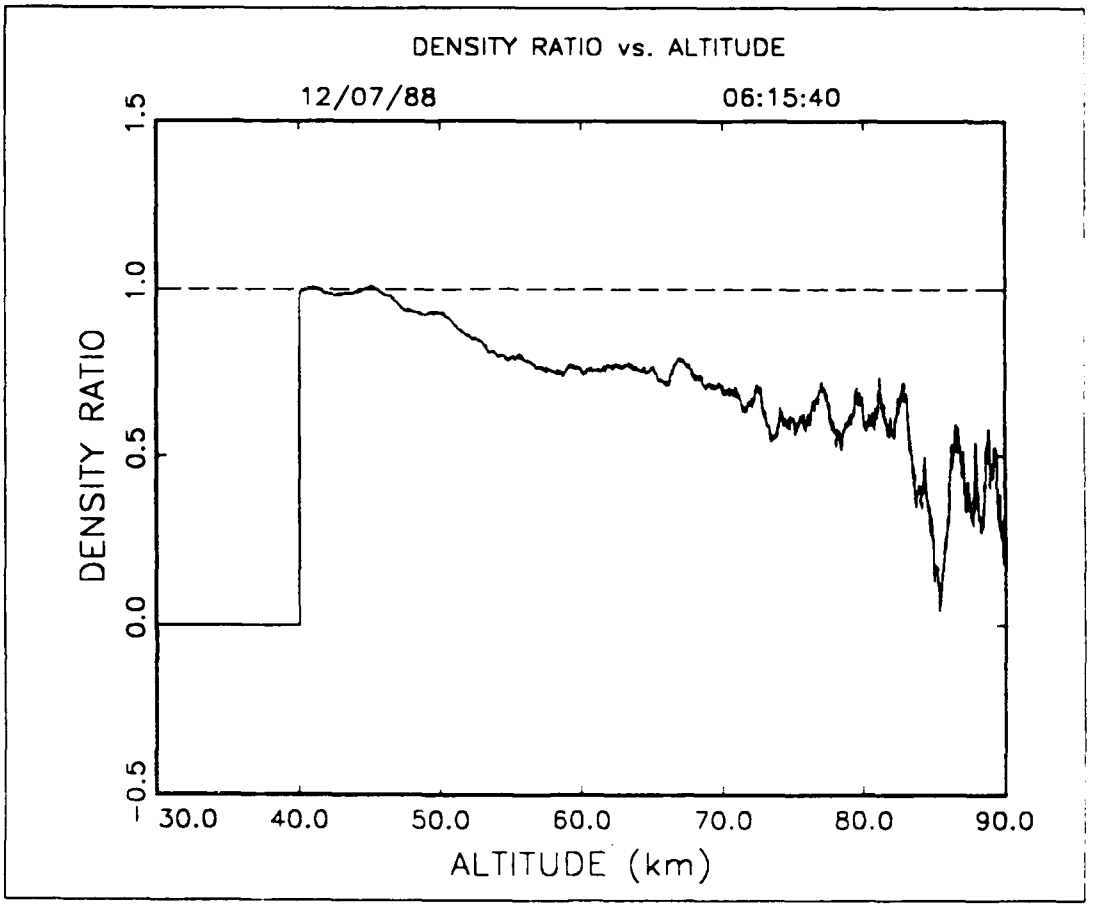

Figure 21. Plot of Density Ratio Versus Altitude for 6:15:40, 12/7/88 GMT.

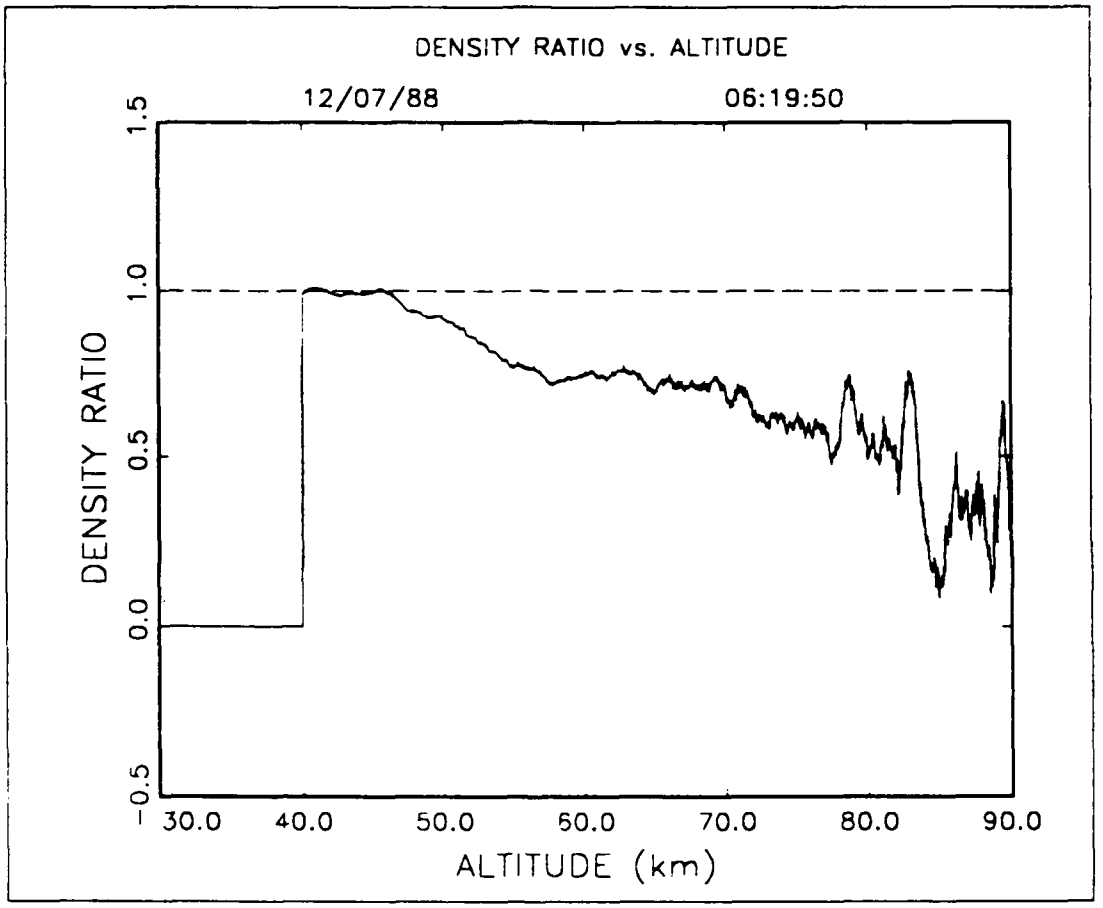

Figure 22. Plot of Density Ratio Versus Altitude for 6:19:50, 12/7/88 GMT.

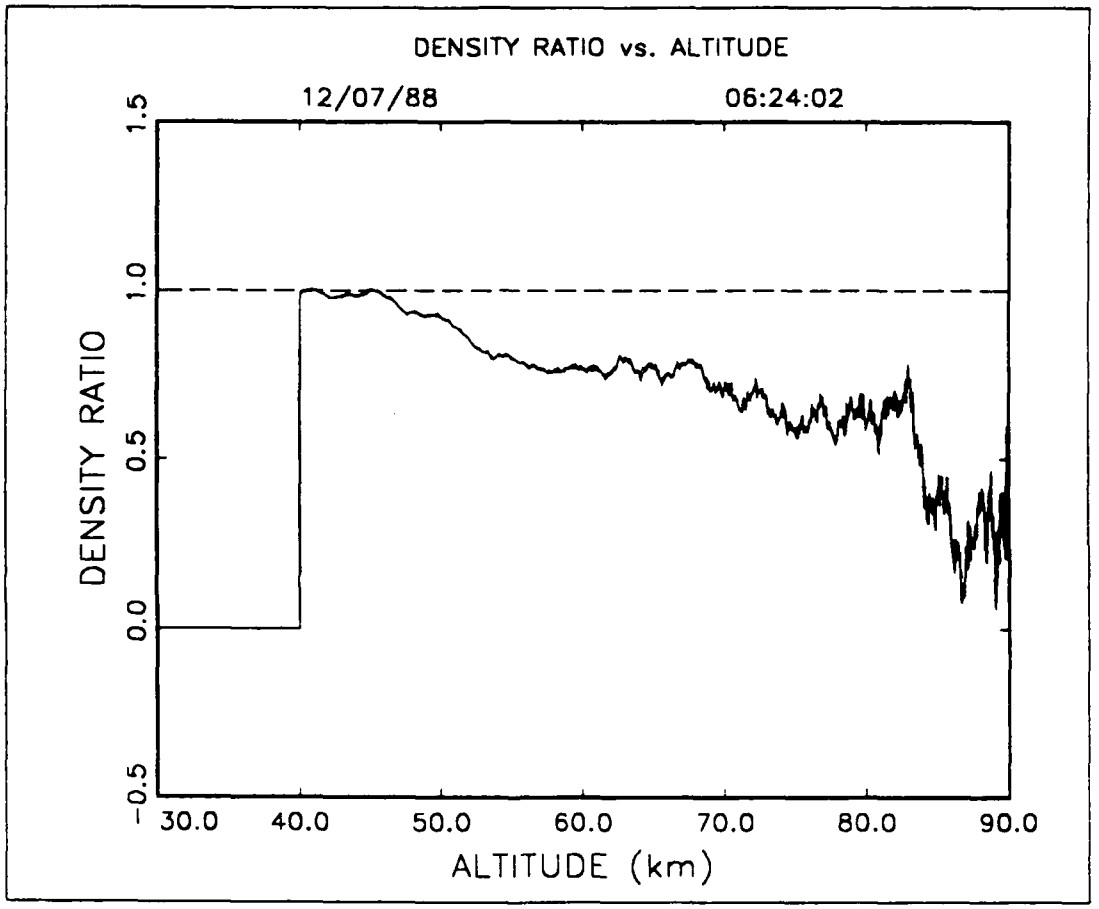

Figure 23. Plot of Density Ratio Versus Altitude for 6:24:02, 12/7/88 GMT.

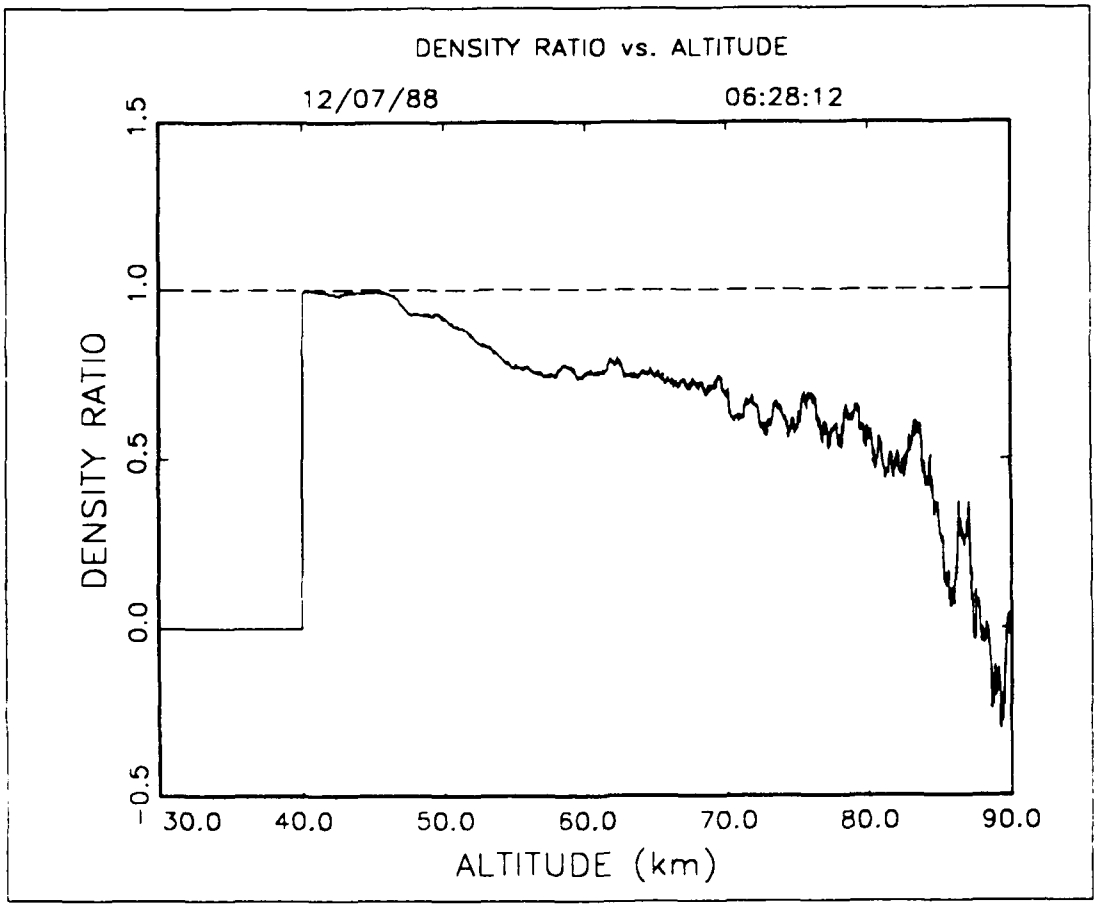

Figure 24. Plot of Density Ratio Versus Altitude for 6:28:12, 12/7/88 GMT.

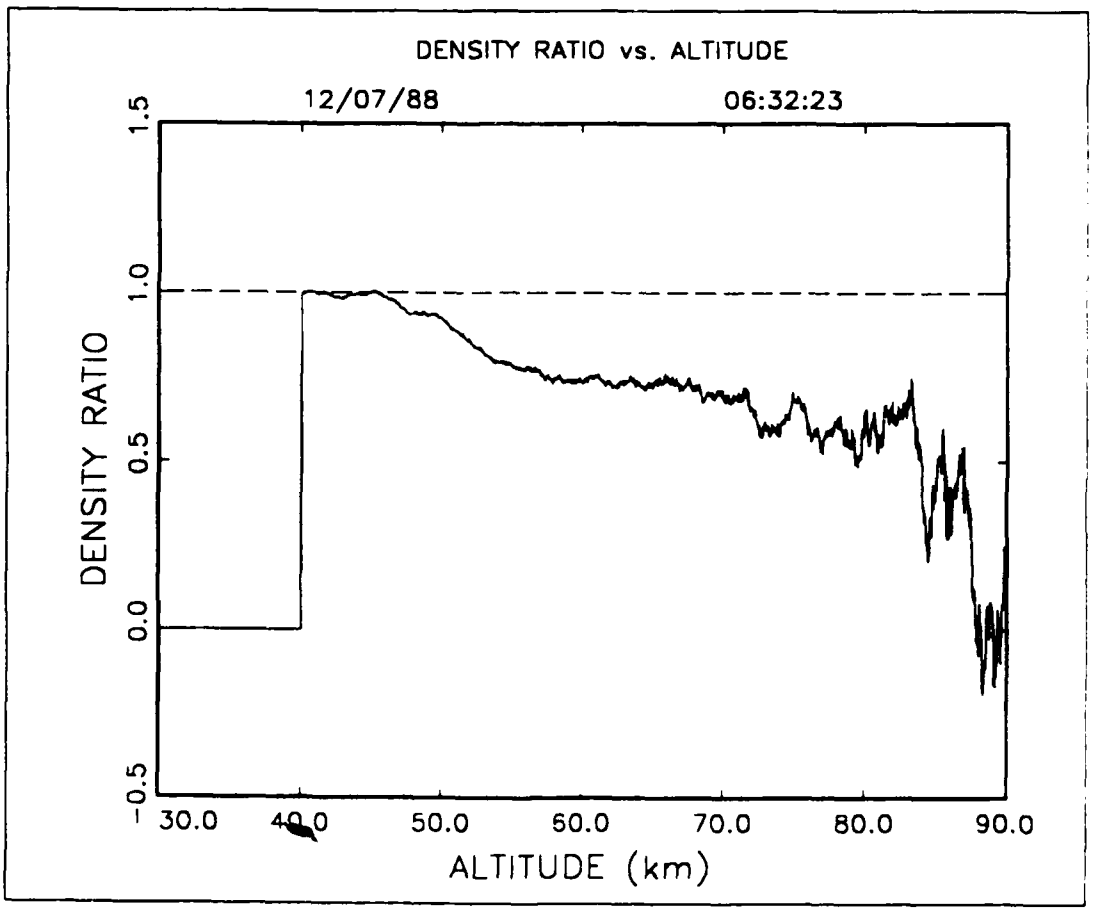

Figure 25. Plot of Density Ratio Versus Altitude for 6:32:23, 12/7/88 GMT.

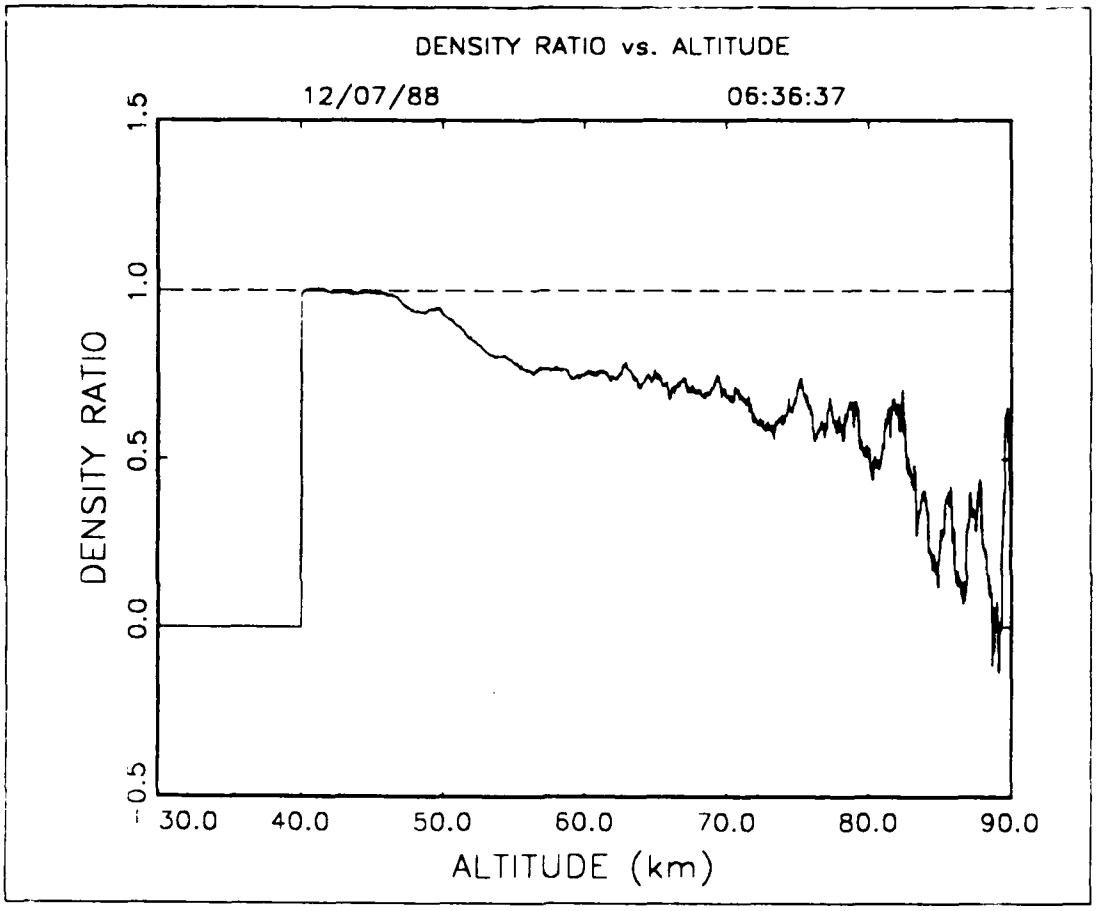

Figure 26. Plot of Density Ratio Versus Altitude for 6:36:37, 12/7/88 GMT.

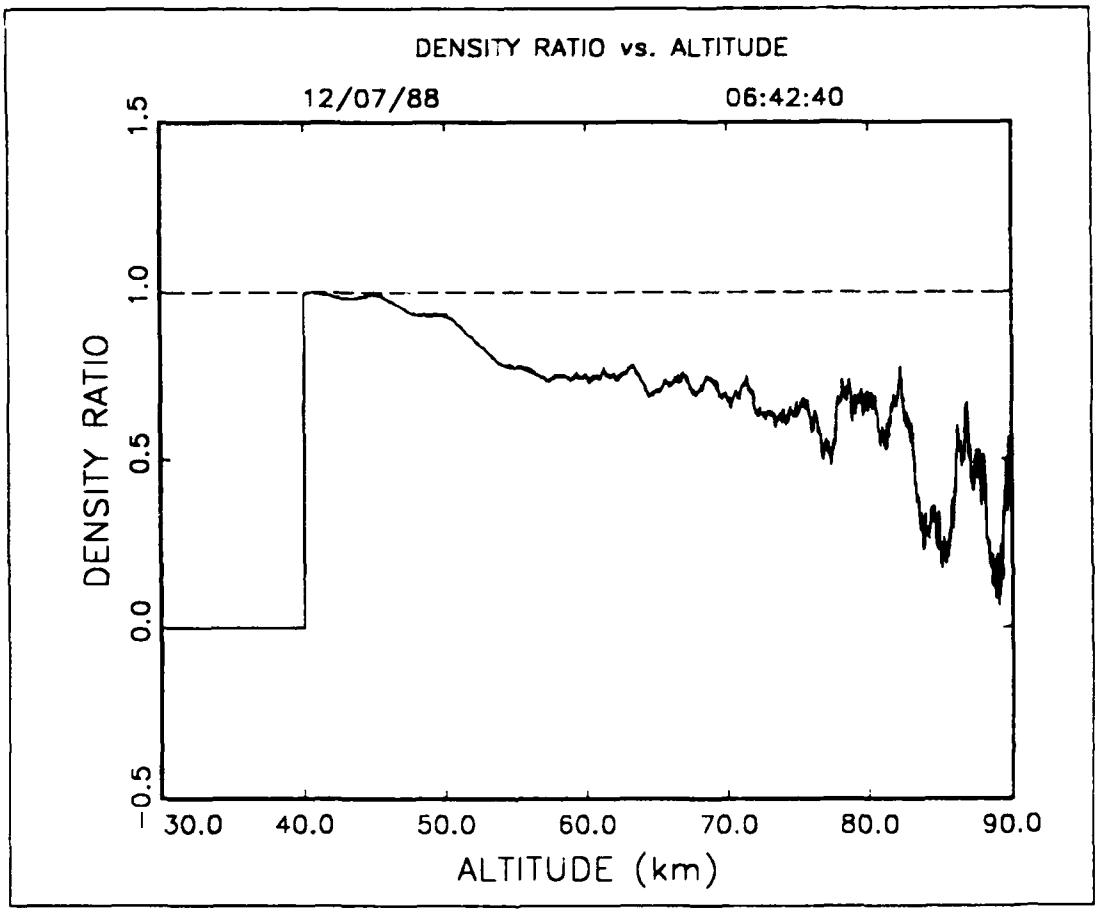

Figure 27. Plot of Density Ratio Versus Altitude for 6:42:40, 12/7/88 GMT.

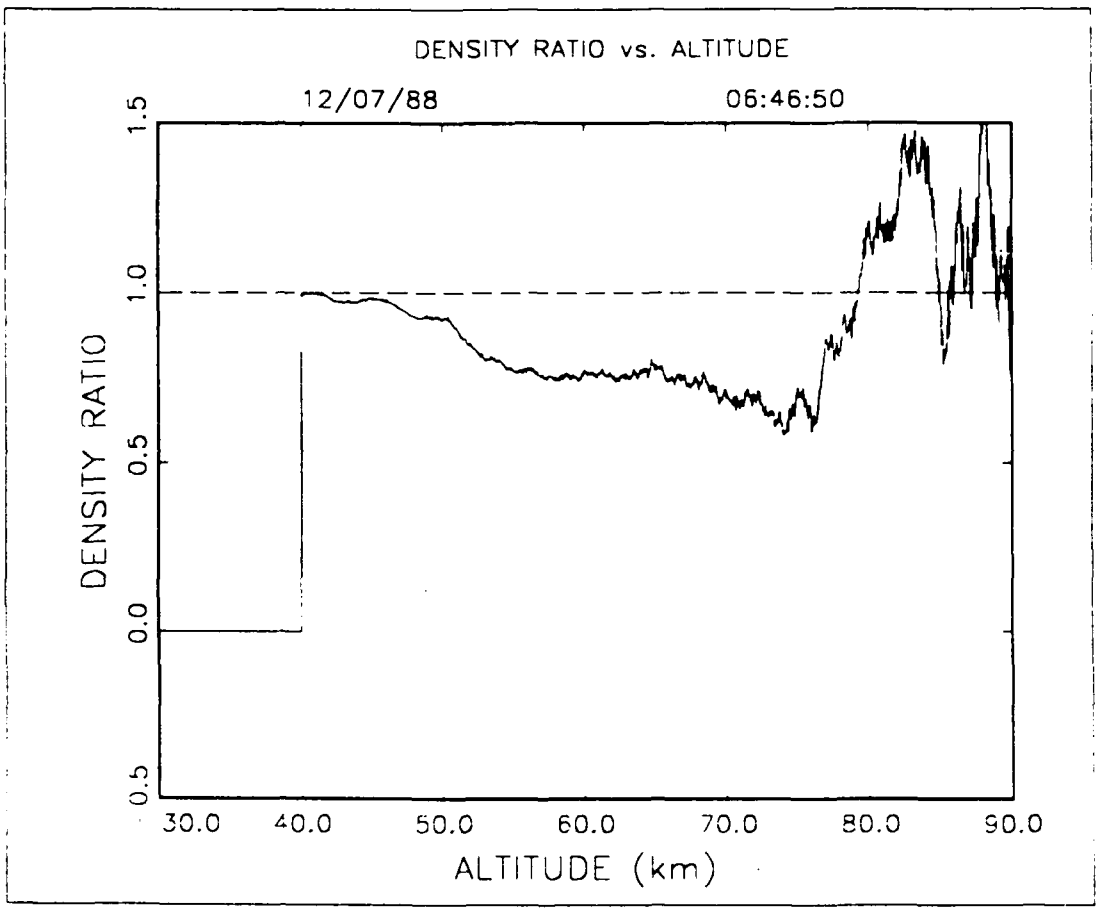

Figure 28. Plot of Density Ratio Versus Altitude for 6:46:50, 12/7/88 GMT.

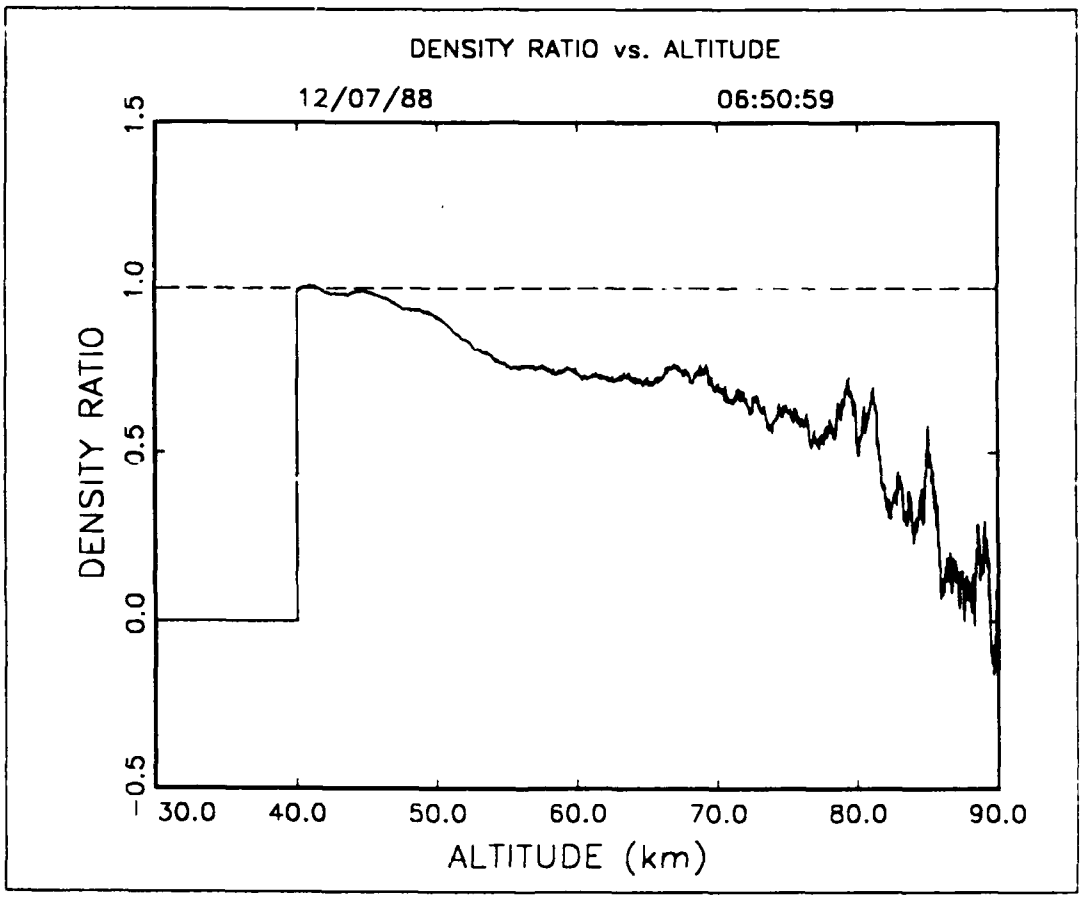

Figure 29. Plot of Density Ratio Versus Altitude for 6:50:59, 12/7/88 GMT.

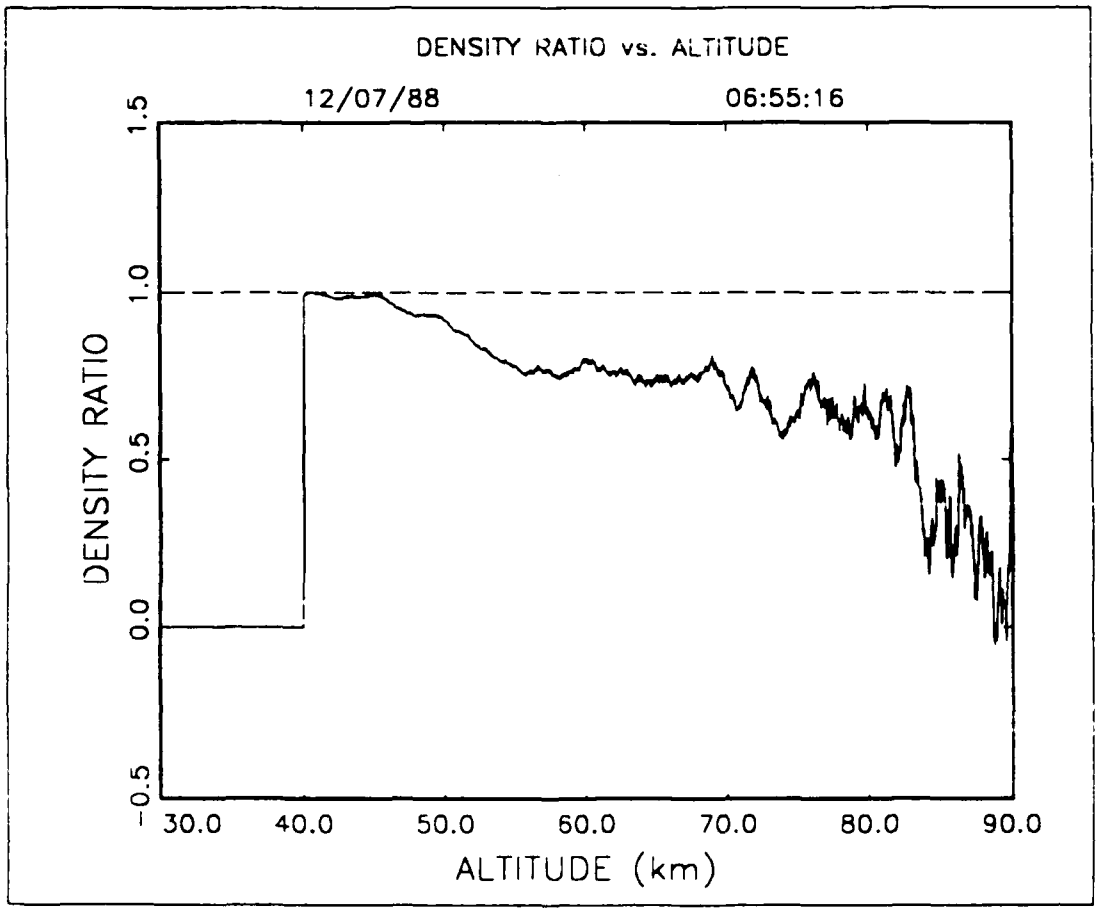

Figure 30. Plot of Density Ratio Versus Altitude for 6:55:16, 12/7/88 GMT.

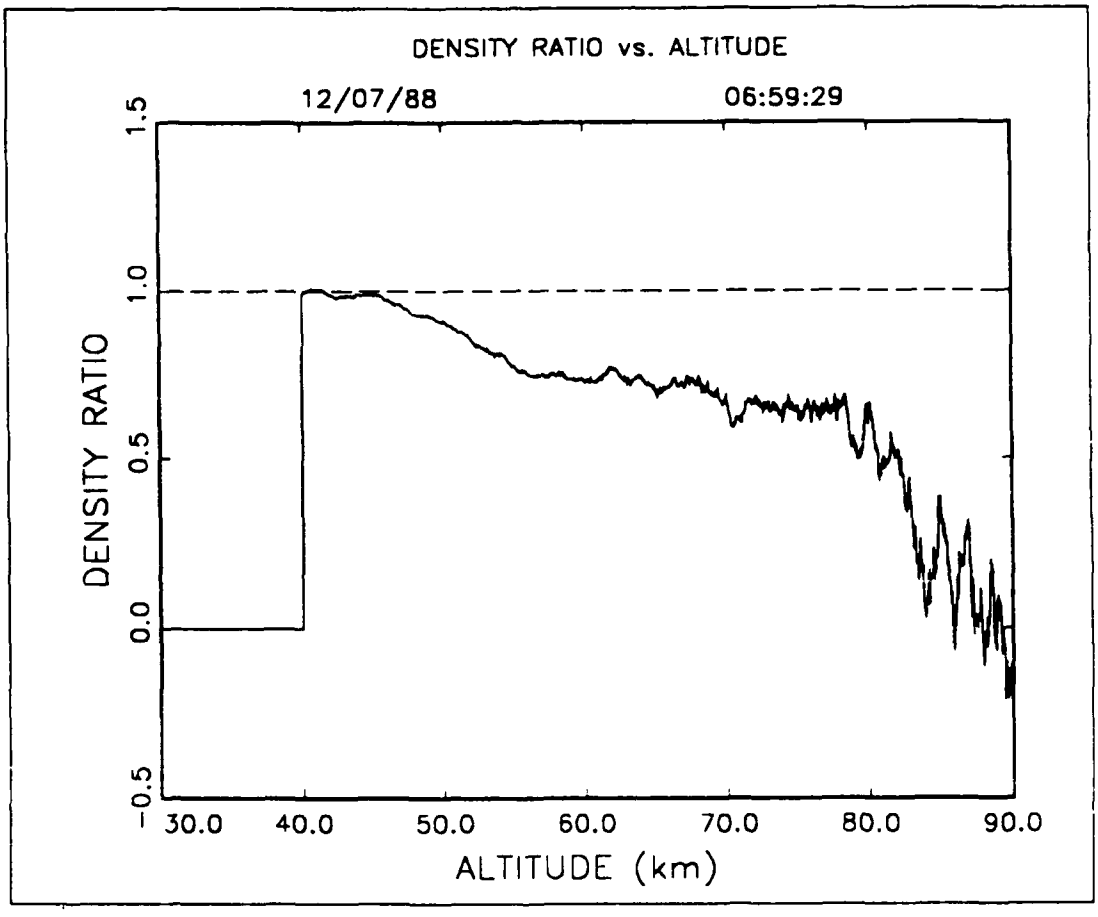

Figure 31. Plot of Density Ratio Versus Altitude for 6:59:29, 12/7/88 GMT.

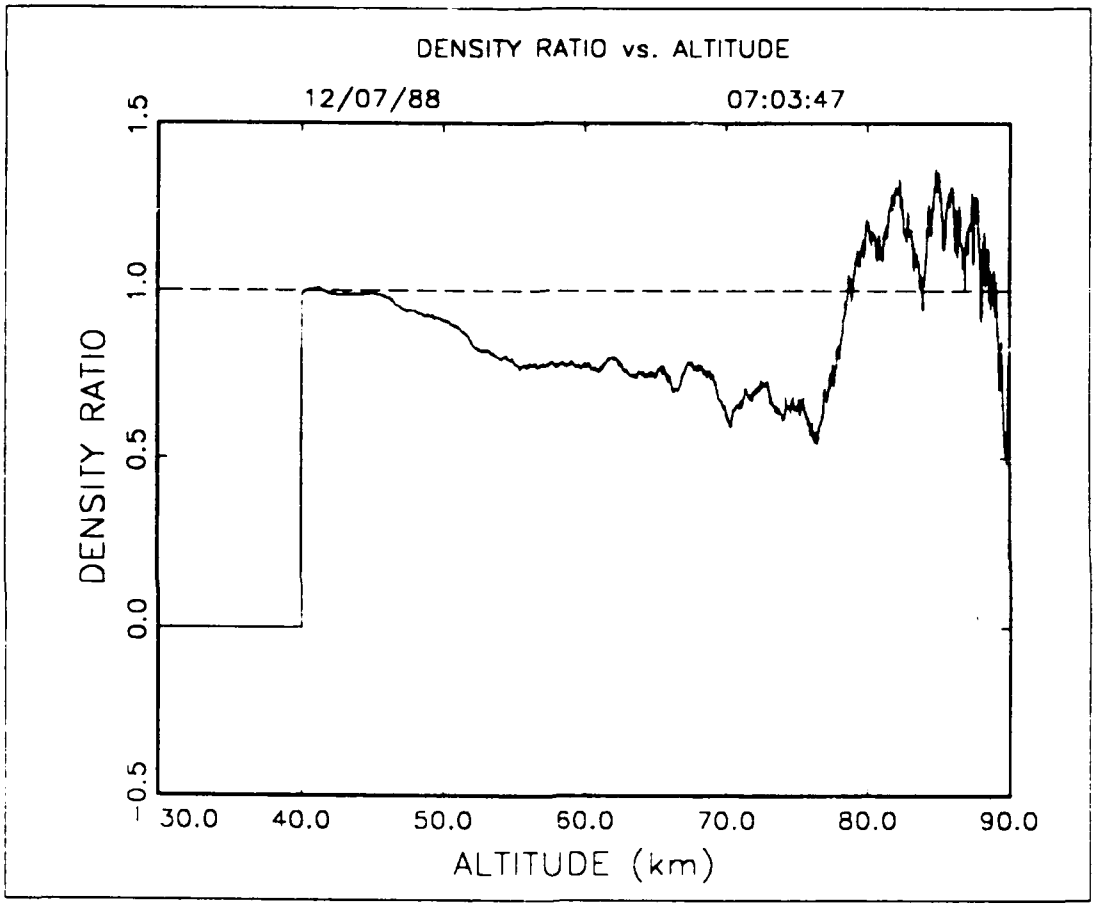

Figure 32. Plot of Density Ratio Versus Altitude for 7:03:47, 12/7/88 GMT.

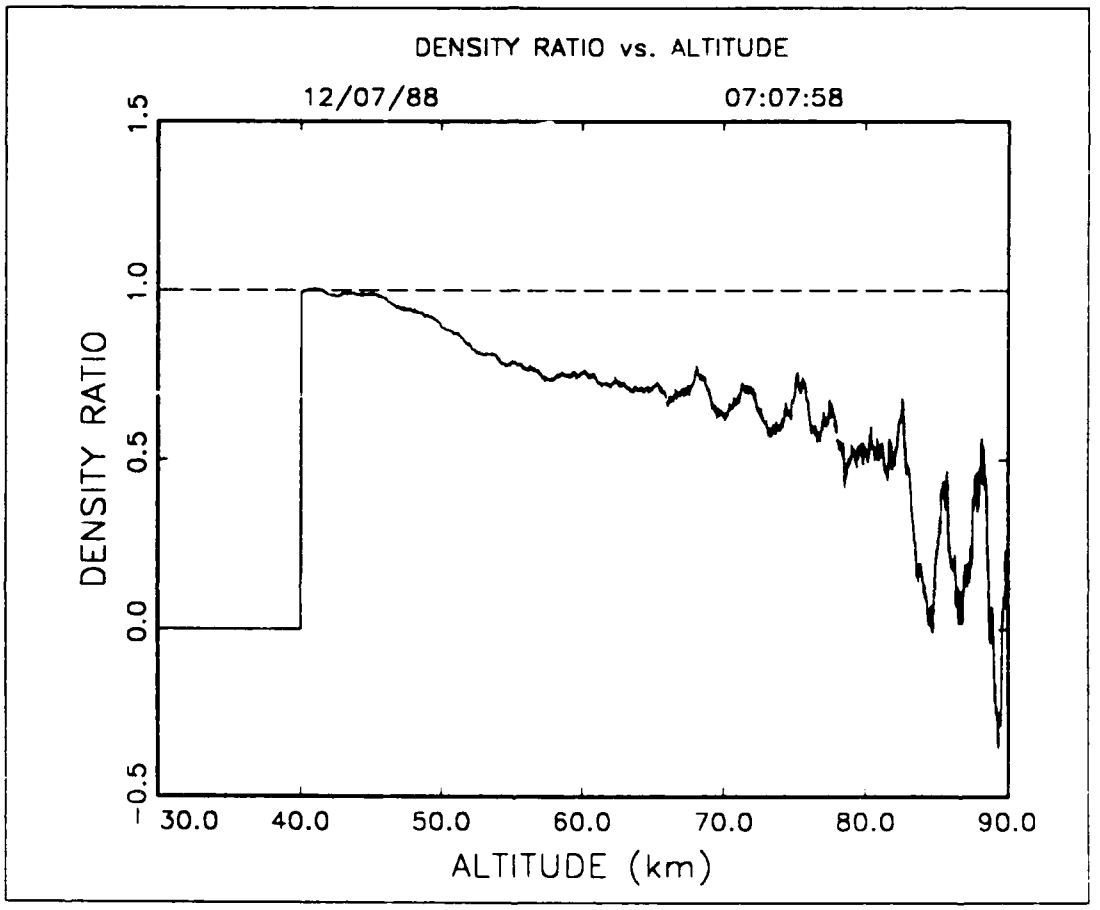

Figure 33. Plot of Density Ratio Versus Altitude for 7:07:58, 12/7/88 GMT

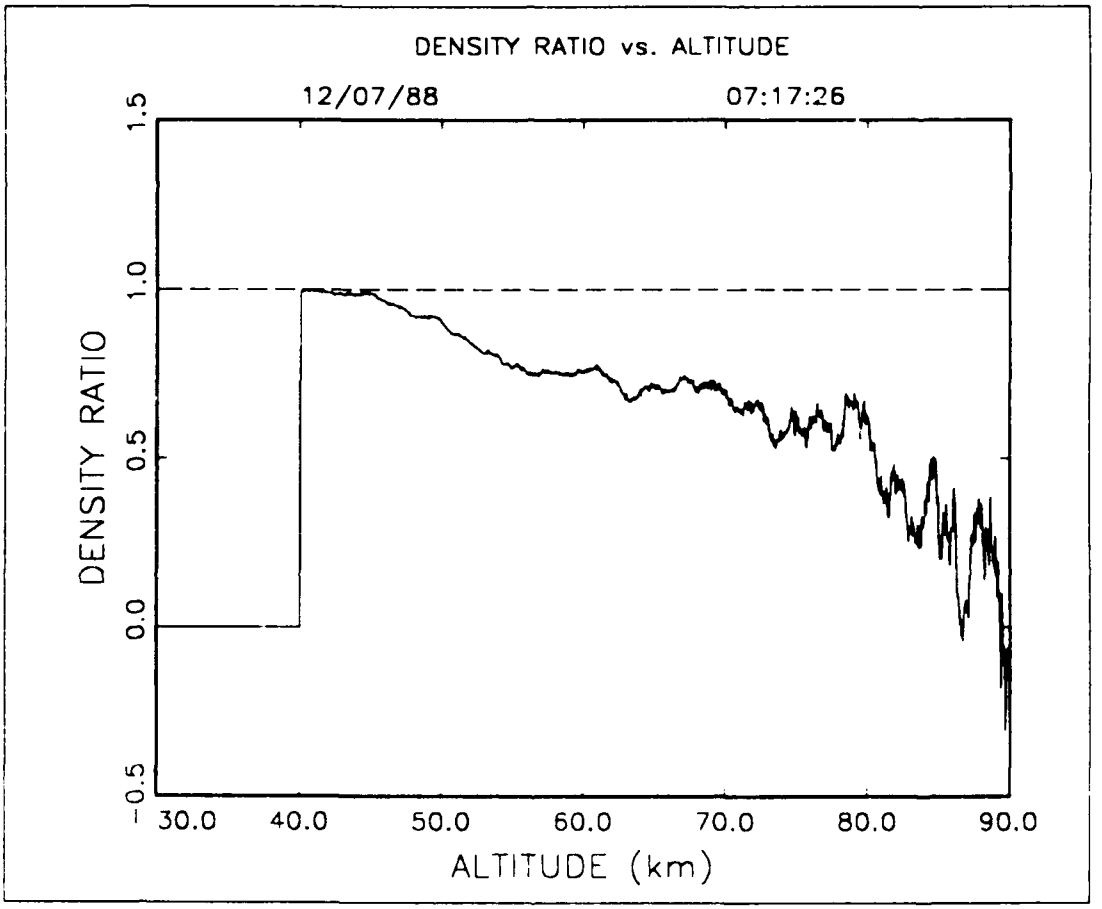

Figure 34. Plot of Density Ratio Versus Altitude for 7:17:26, 12/7/88 GMT.

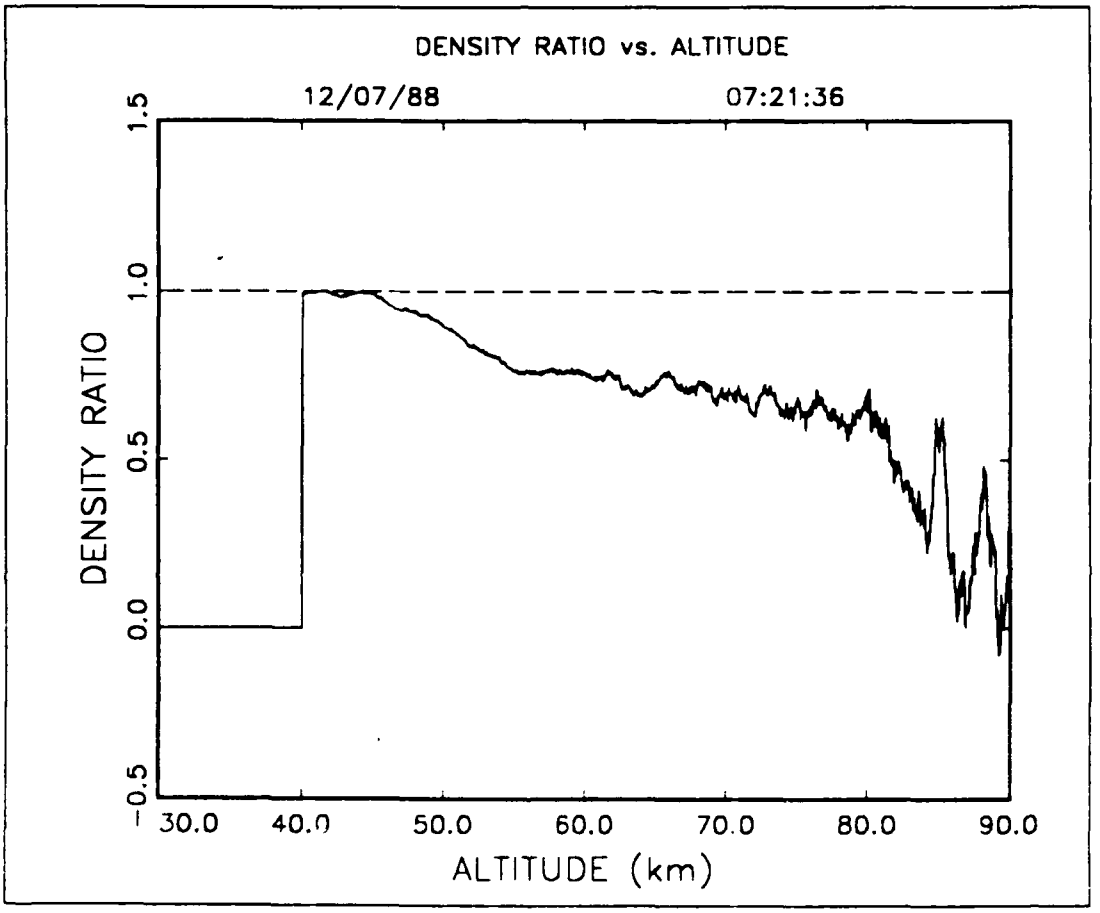

Figure 35. Plot of Density Ratio Versus Altitude for ':21:36, 12/7/88 GMT.

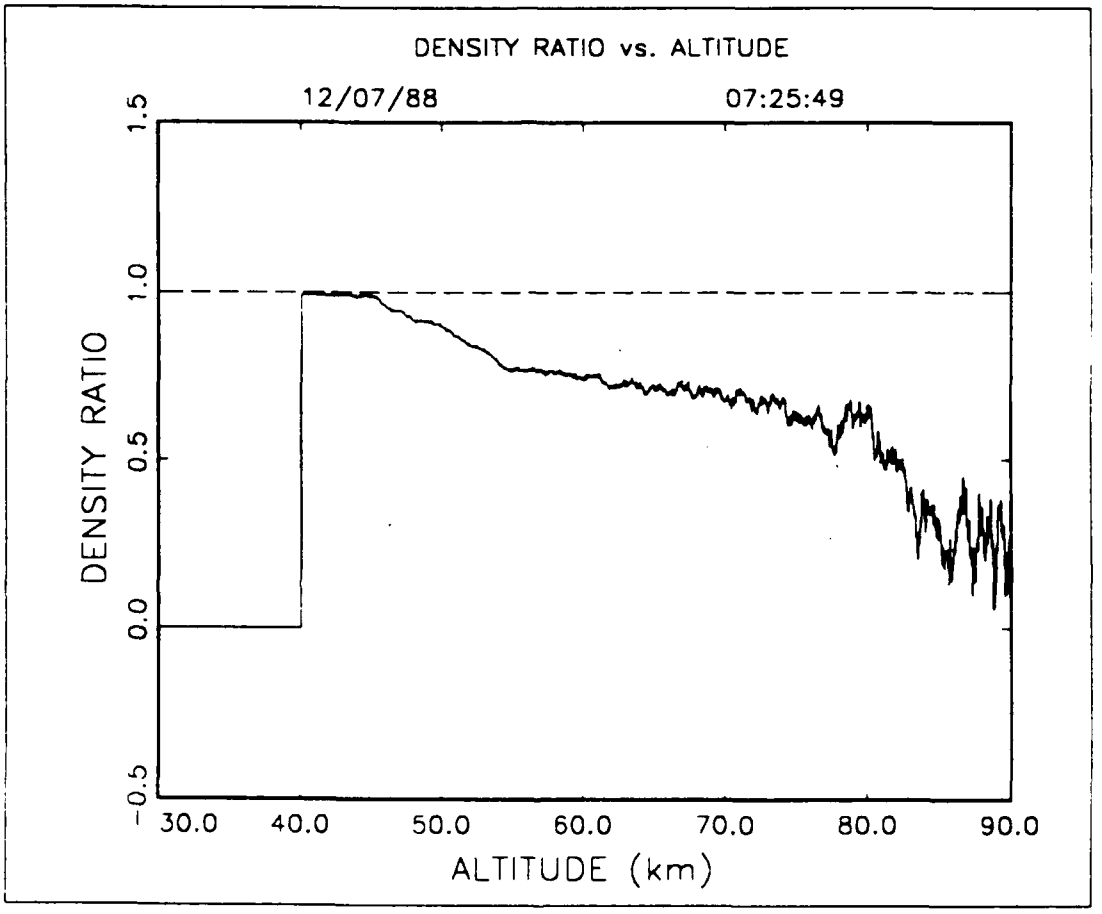

Figure 36. Plot of Density Ratio Versus Altitude for 7:25:49, 12/7/88 GMT.

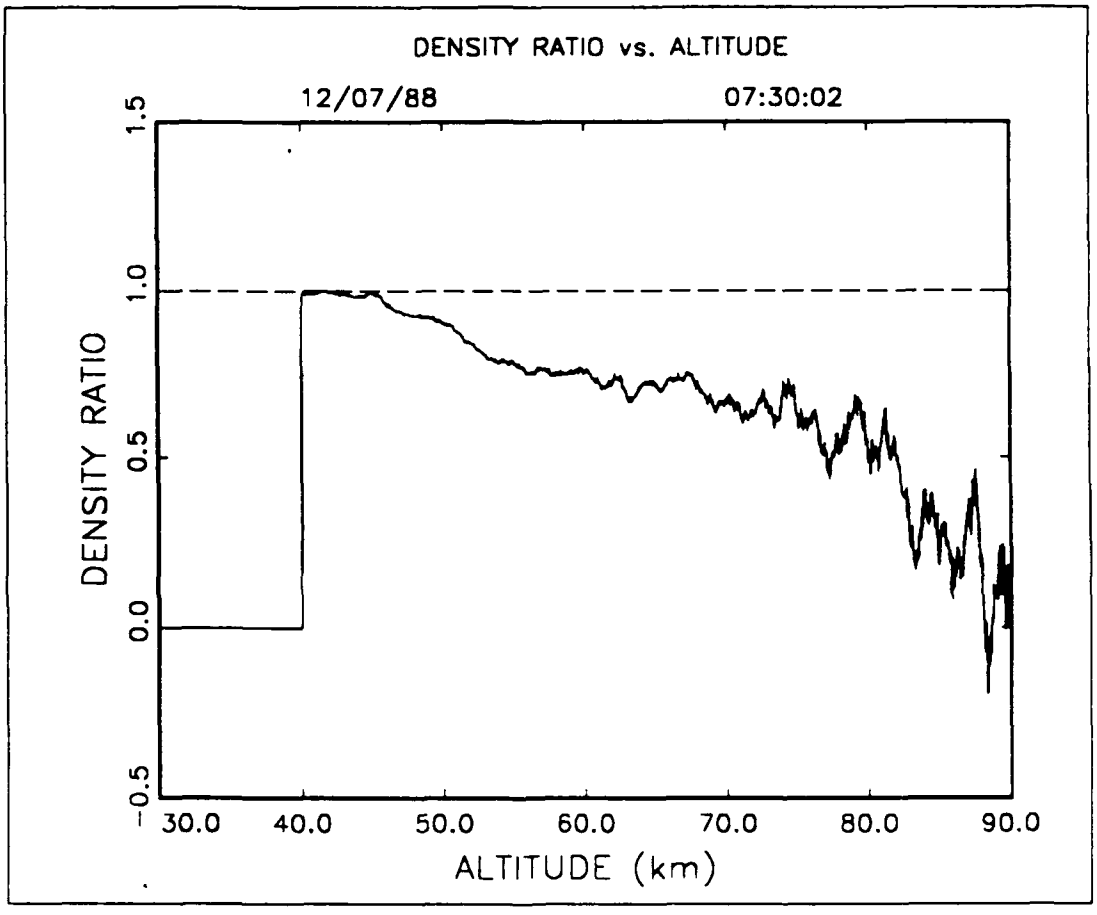

Figure 37. Plot of Density Ratio Versus Altitude for 7:30:02, 12/7/88 GMT.

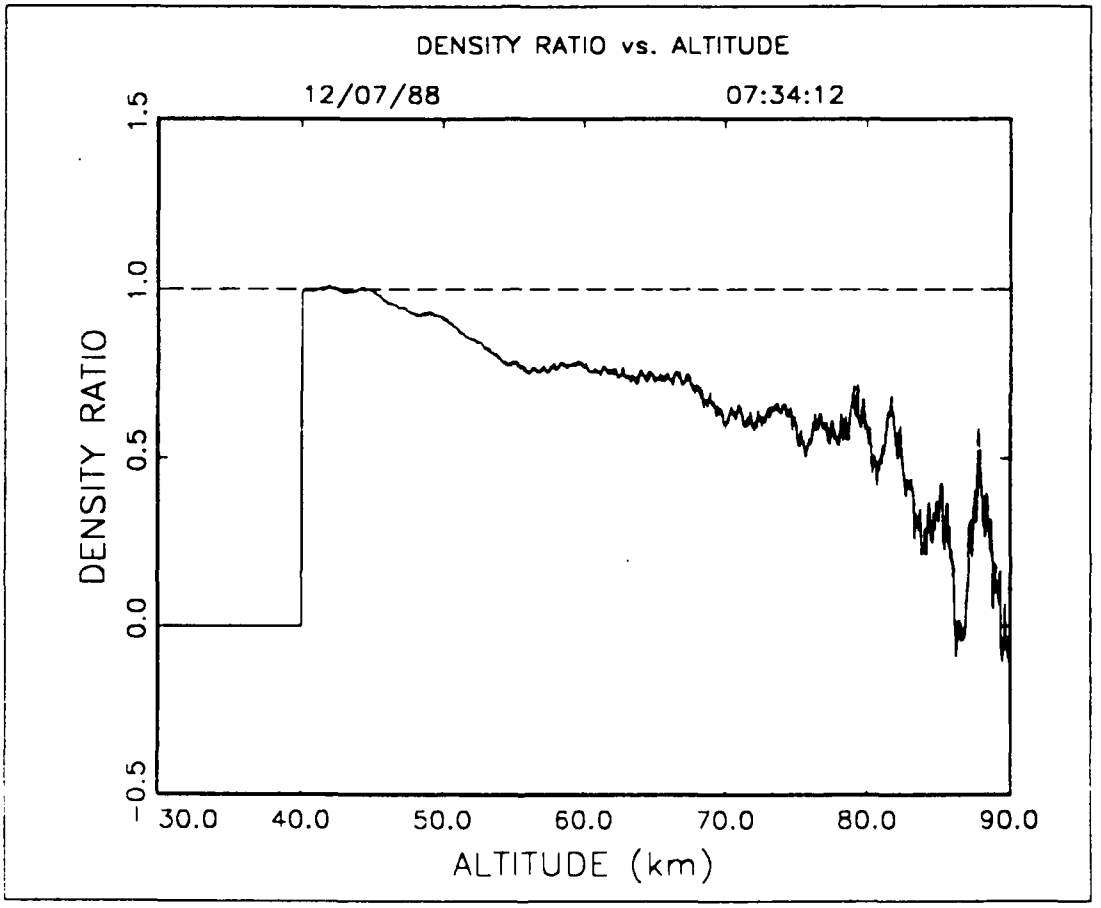

Figure 38. Plot of Density Ratio Versus Altitude for 7:34:12, 12/7/88 GMT.

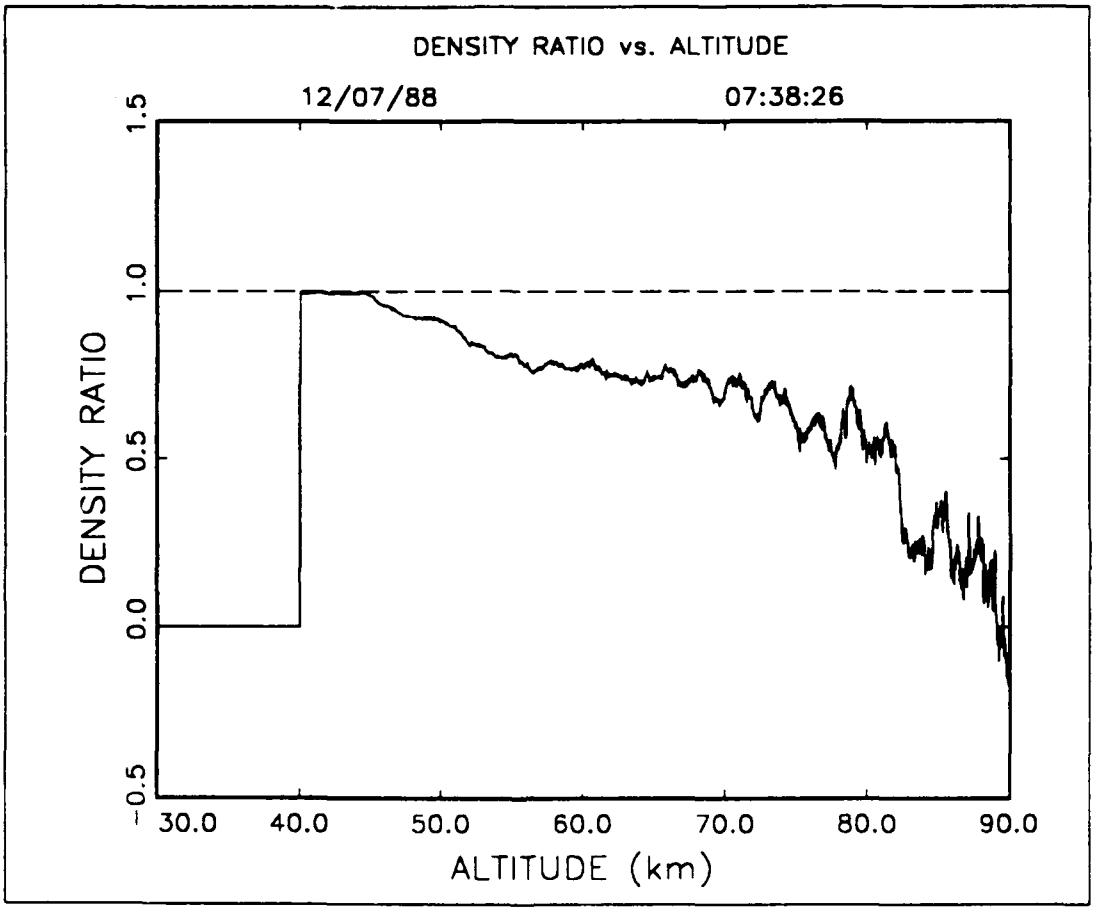

Figure 39. Plot of Density Ratio Versus Altitude for 7:38:26, 12/7/88 GMT.

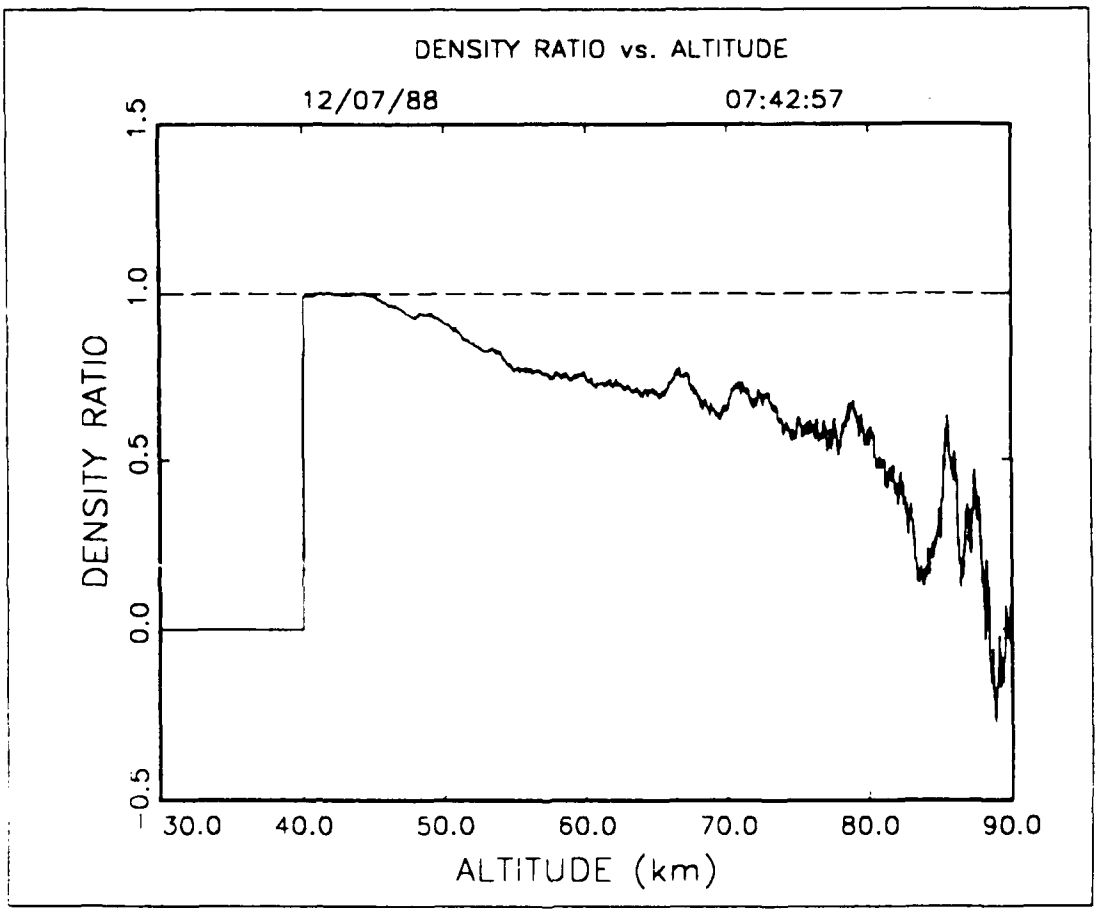

Figure 40. Plot of Density Ratio Versus Altitude for 7:42:57, 12/7/88 GMT.

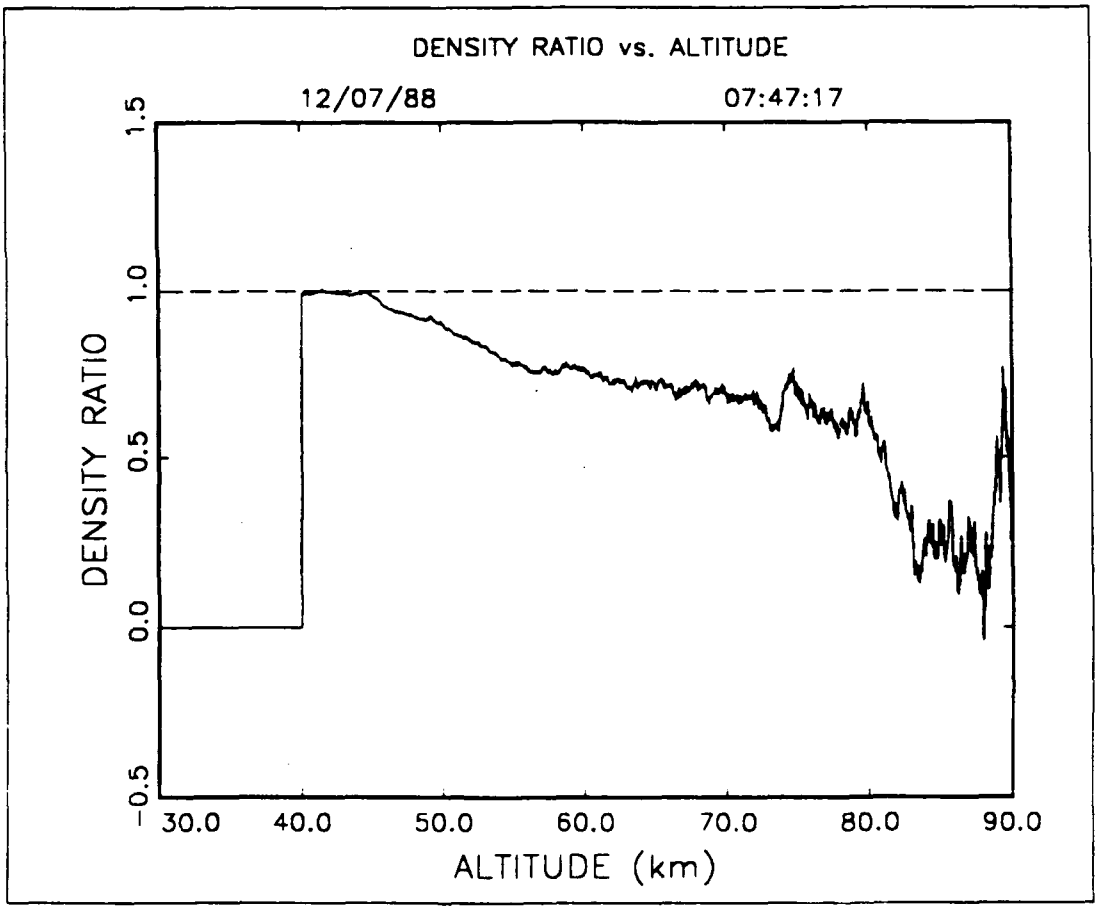

Figure 41. Plot of Density Ratio Versus Altitude for 7:47:17, 12/7/88 GMT.

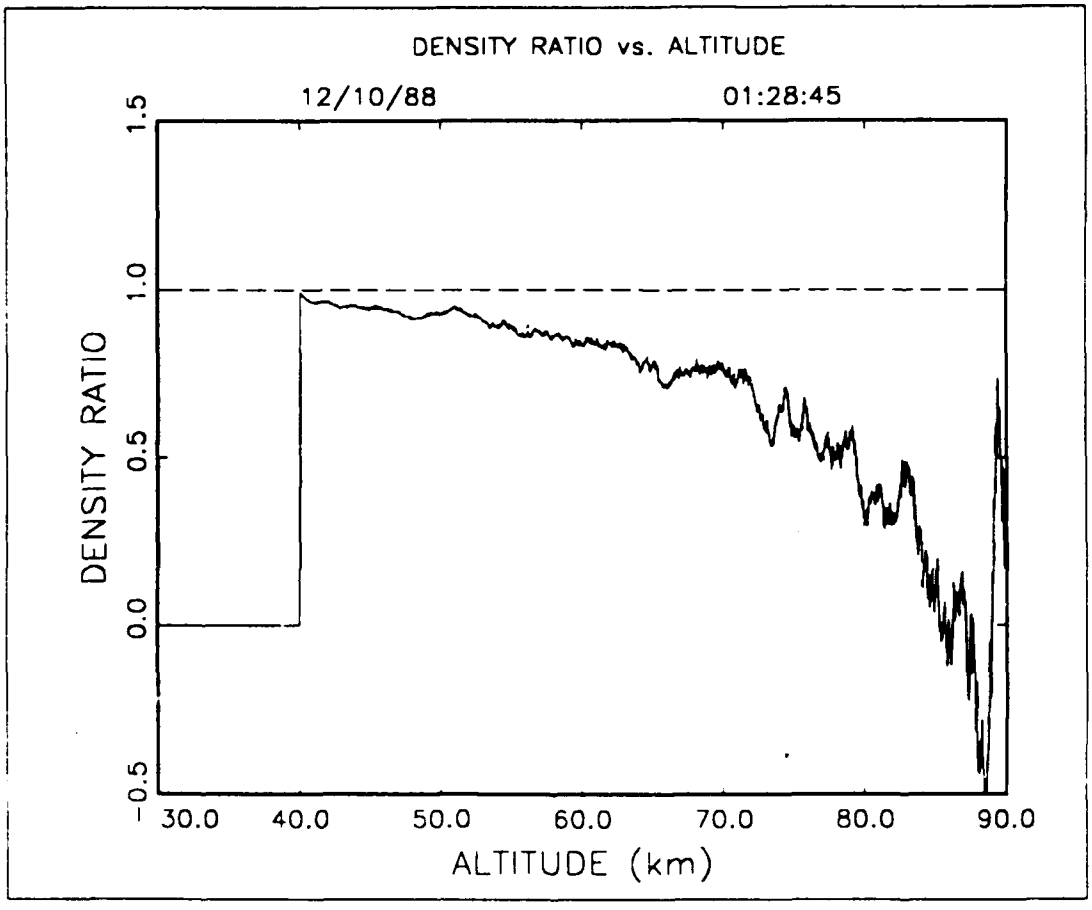

Figure 42. Plot of Density Ratio Versus Altitude for 1:28:45, 12/10/88 GMT.

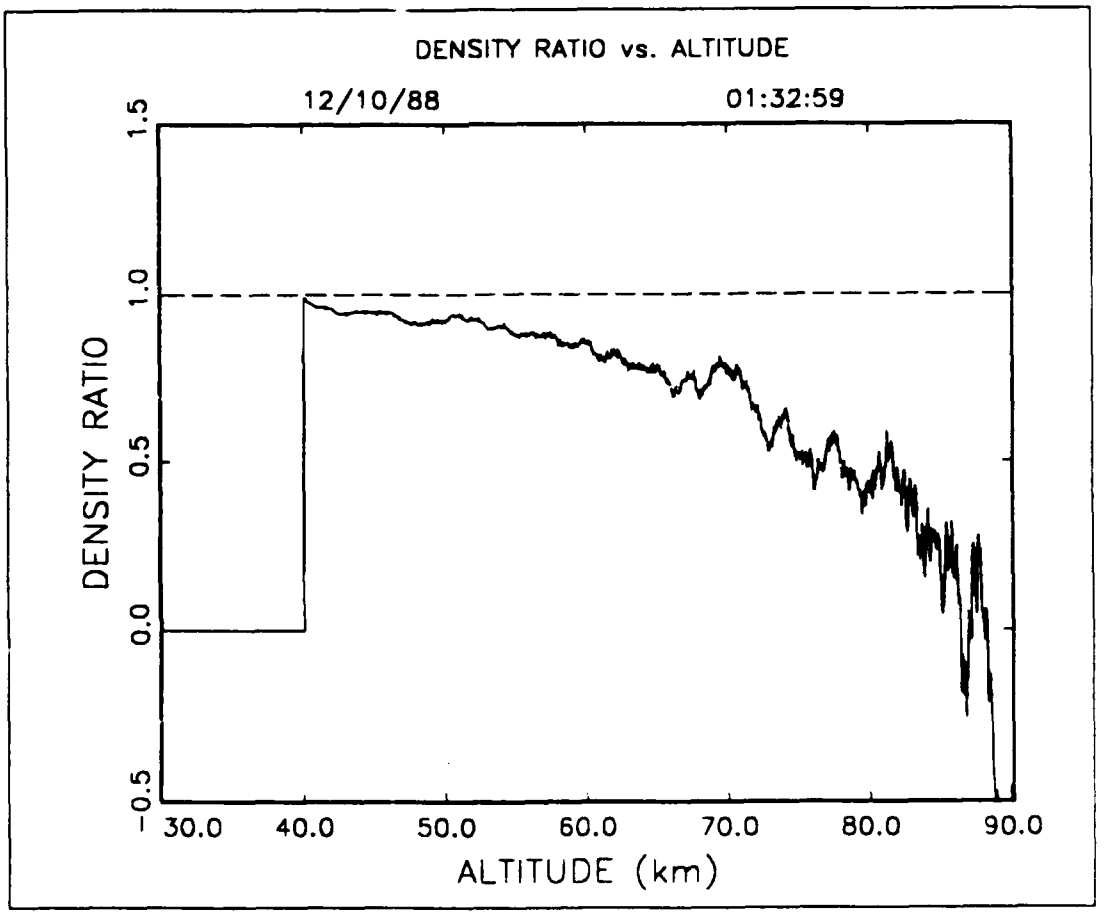

Figure 43. Plot of Density Ratio Versus Altitude for 1:32:59, 12/10/88 GMT.

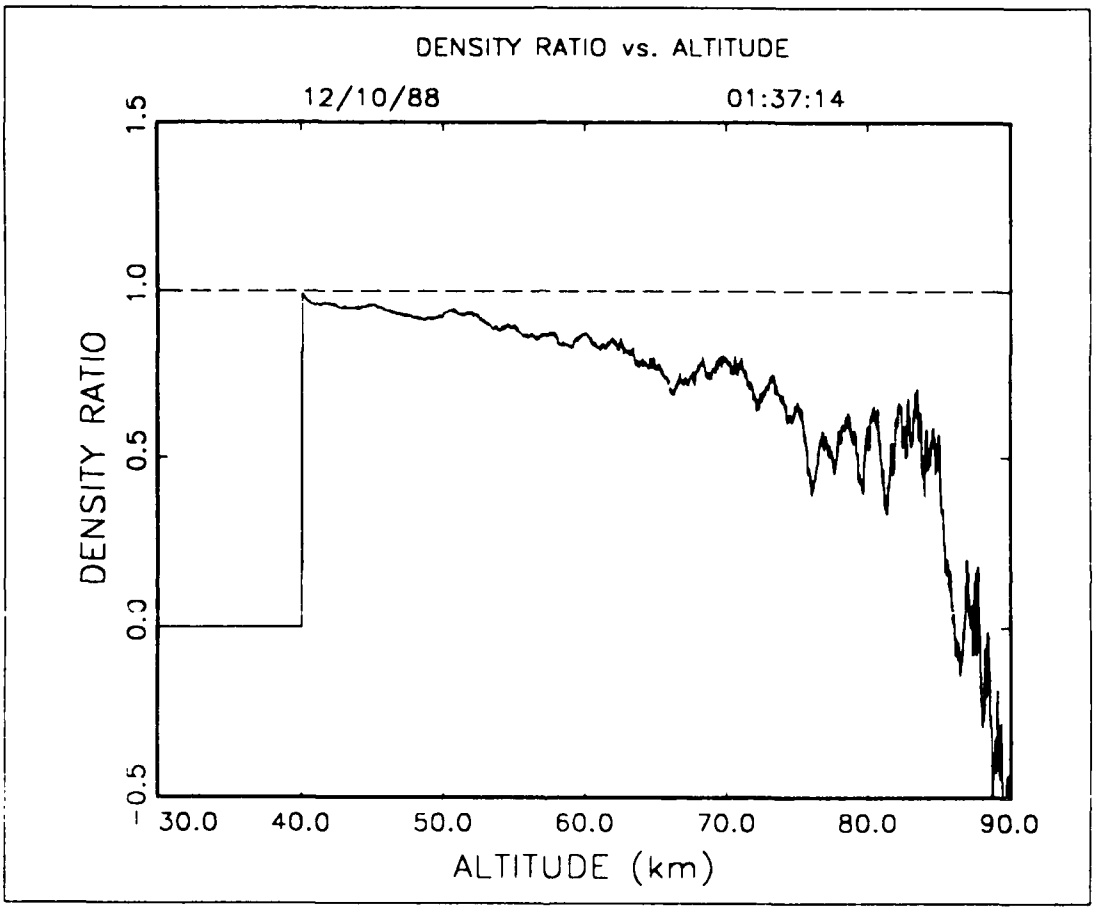

Figure 44. Plot of Density Ratio Versus Altitude for 1:37:14, 12/10/88 GMT.

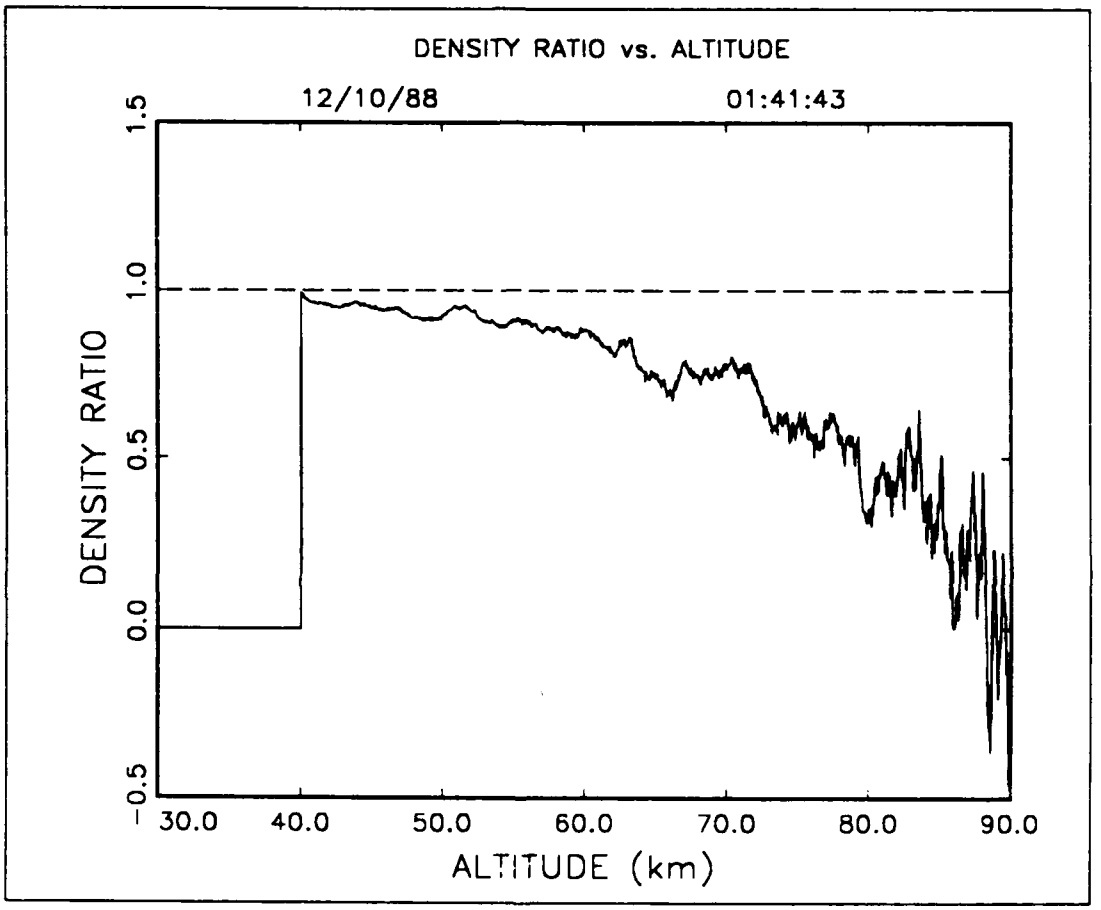

Figure 45. Plot of Density Ratio Versus Altitude for 1:41:43, 12/10/88 GMT.

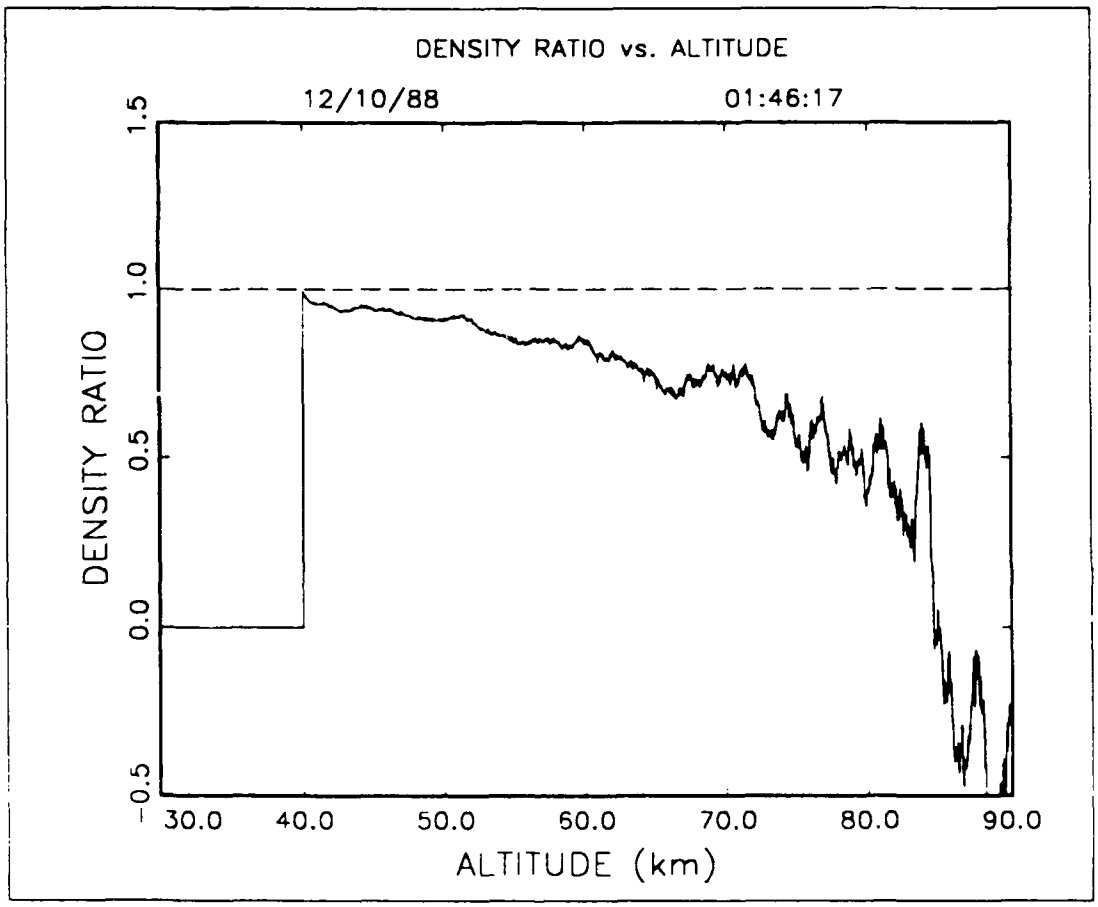

Figure 46. Plot of Density Ratio Versus Altitude for 1:46:17, 12/10/88 GMT.

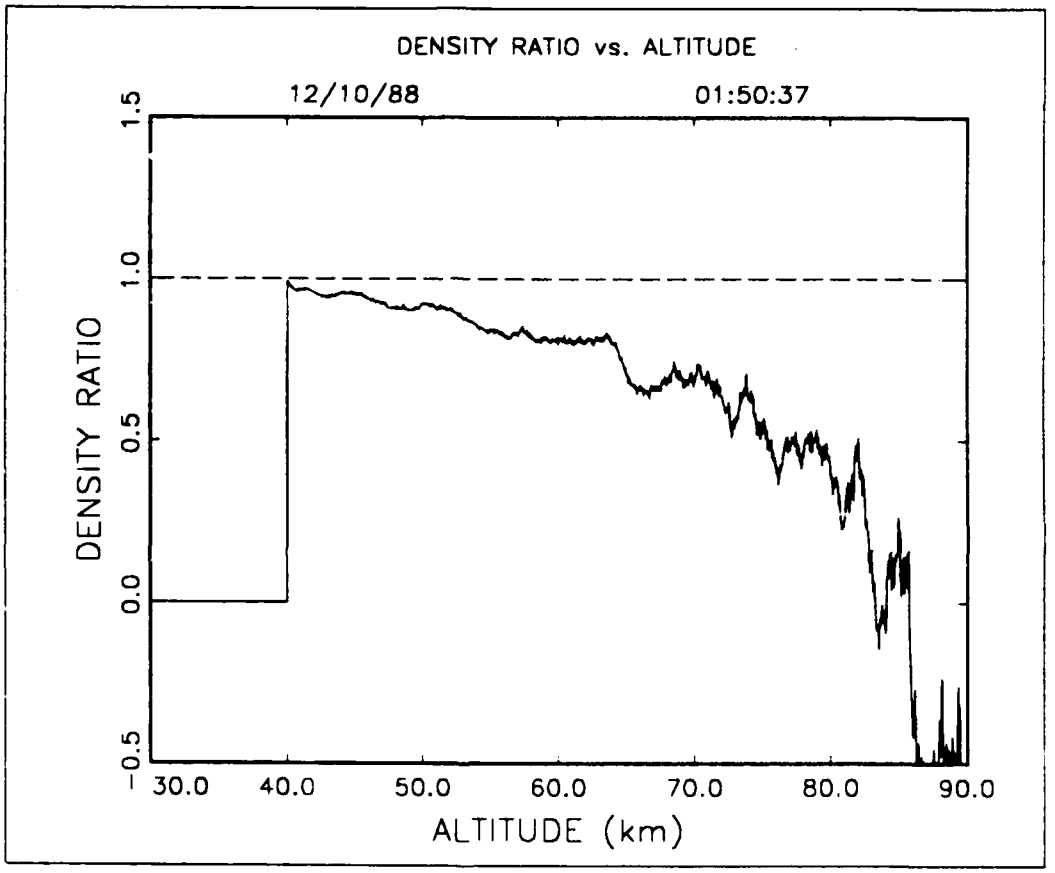

Figure 47. Plot of Density Ratio Versus Altitude for 1:50:37, 12/10/88 GMT.

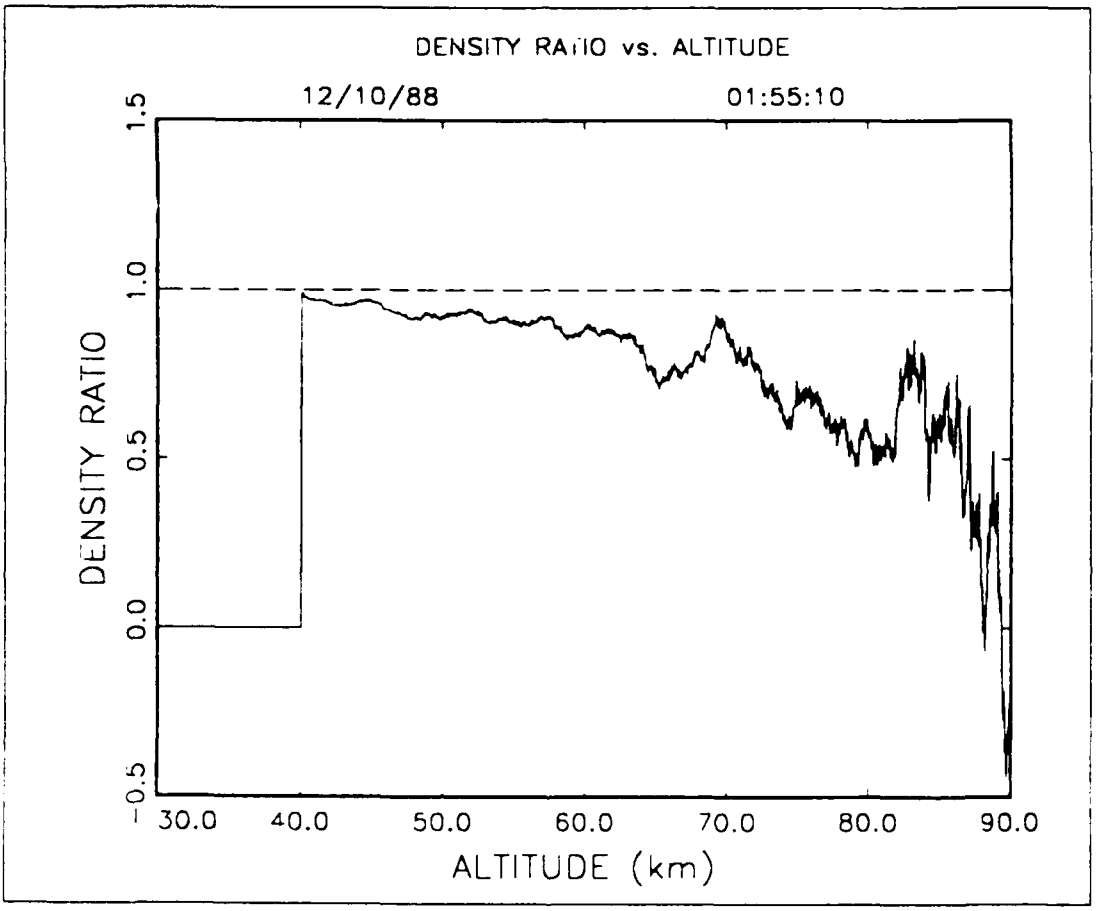

Figure 48. Plot of Density Ratio Versus Altitude for 1:55:10, 12/10/88 GMT.

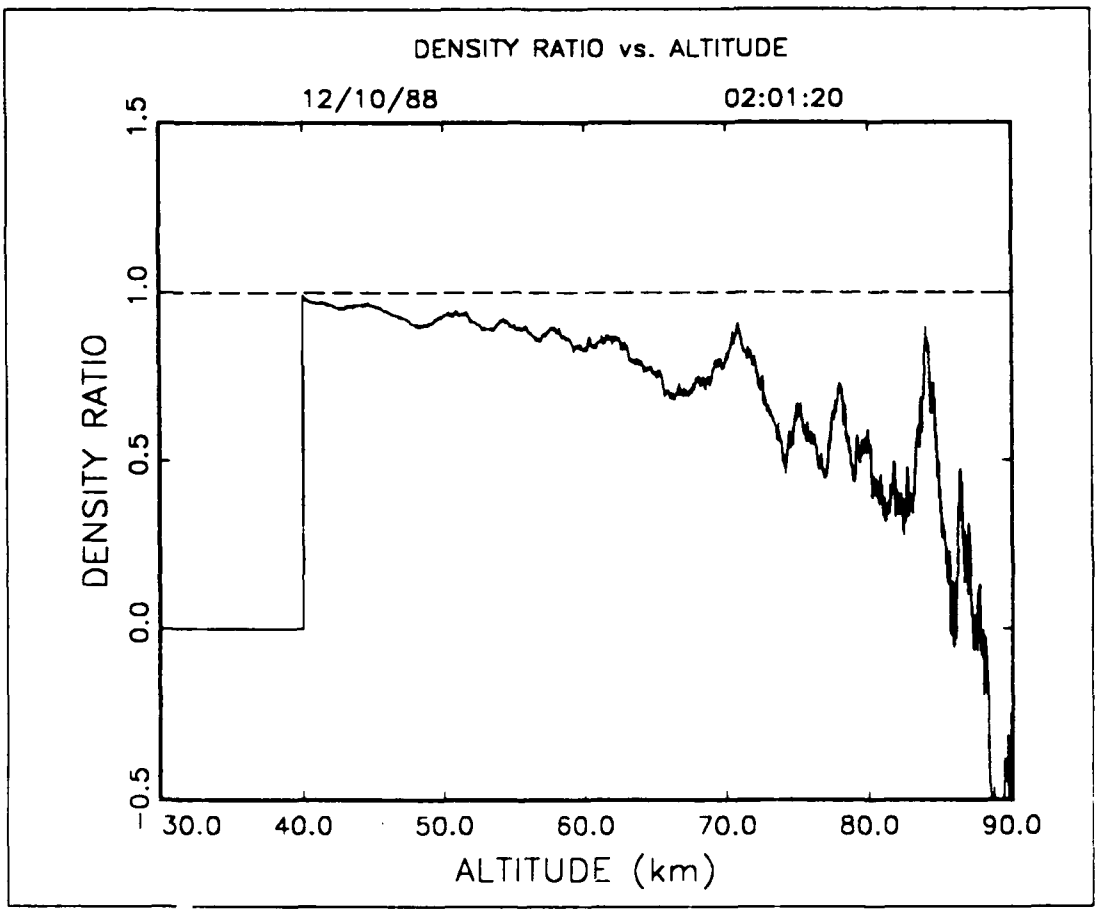

Figure 49. Plot of Density Ratio Versus Altitude for 2:01:20, 12/10/88 GMT.

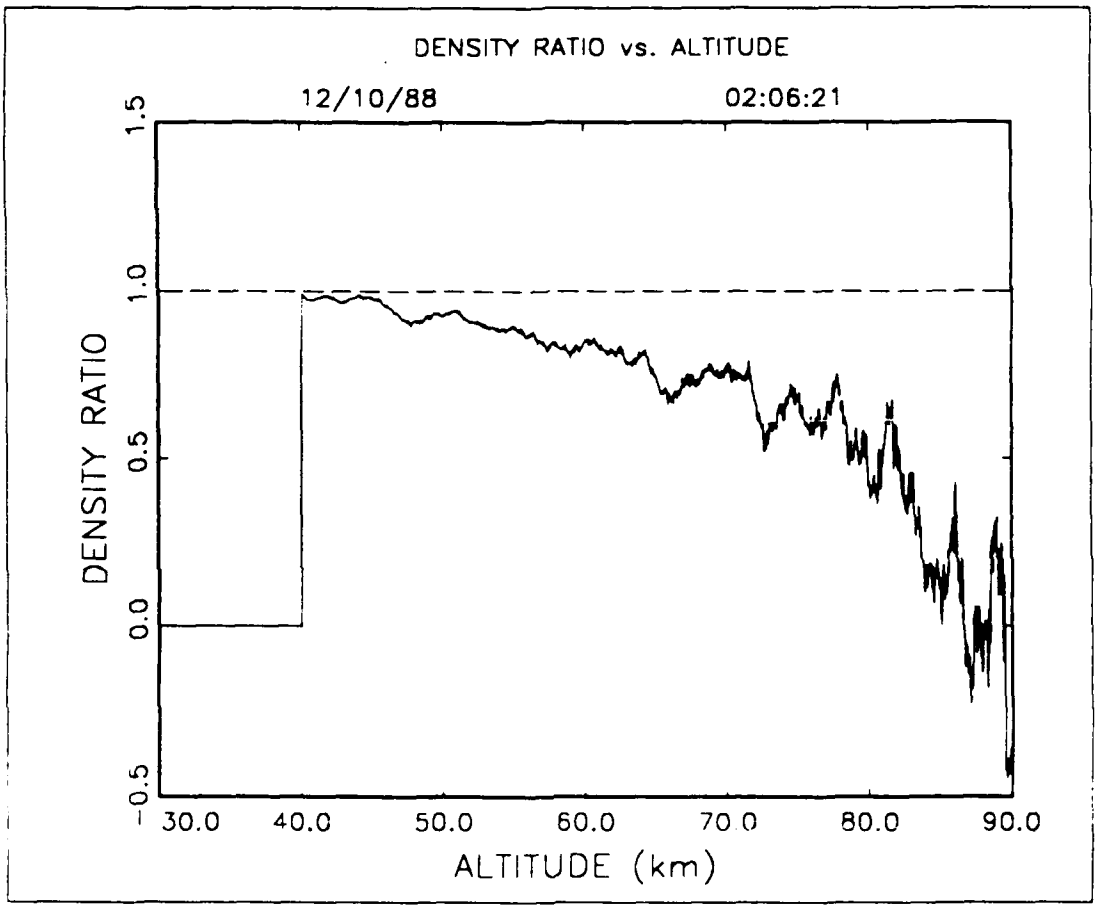

Figure 50. Plot of Density Ratio Versus Altitude for 2:06:21, 12/10/88 GMT.

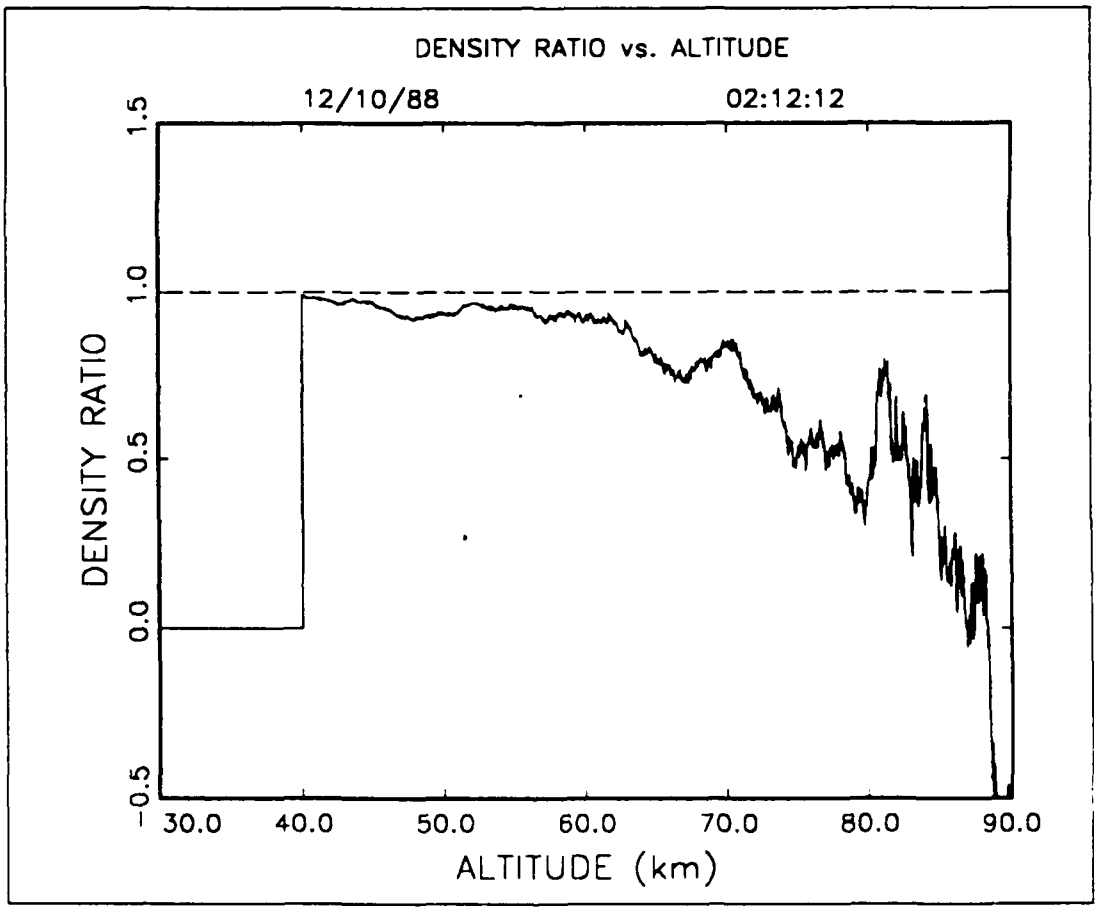

Figure 51. Plot of Density Ratio Versus Altitude for 2:12:12, 12/10/88 GMT.

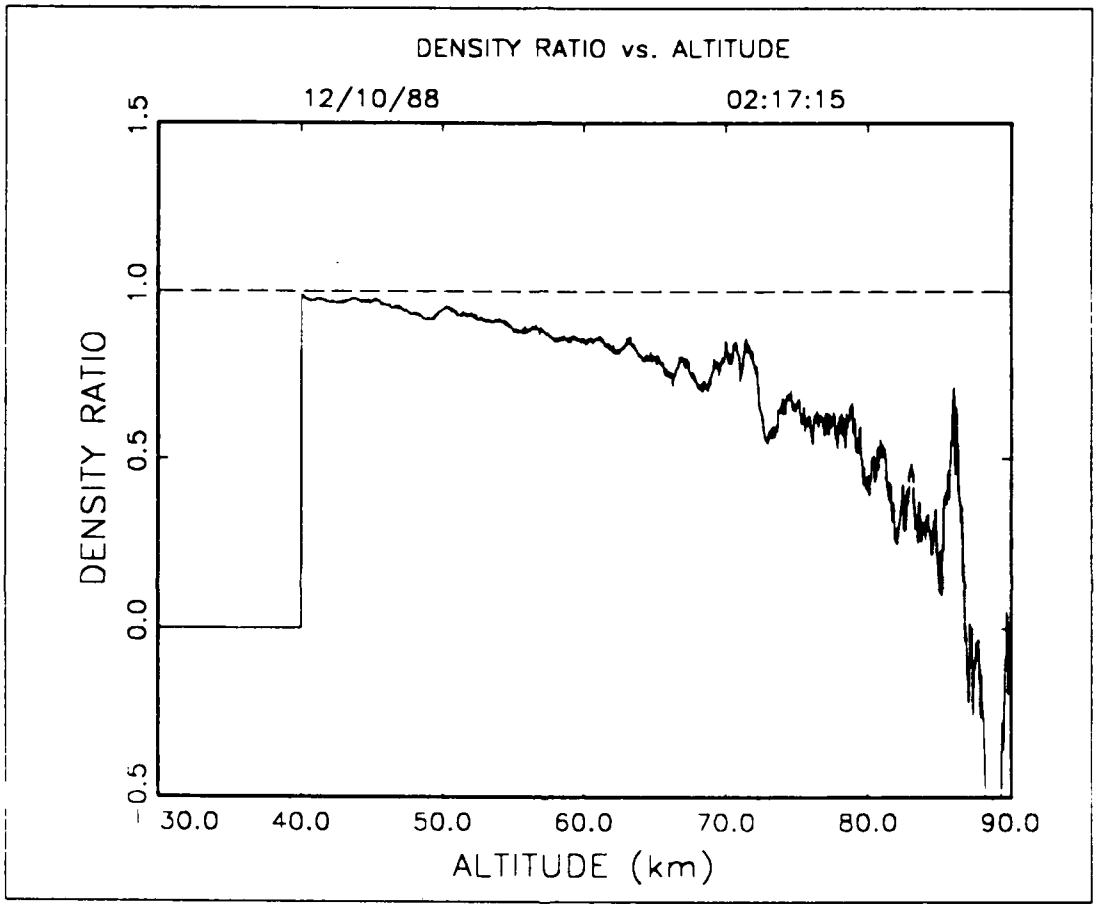

Figure 52. Plot of Density Ratio Versus Altitude for 2:17:15, 12/10/88 GMT.

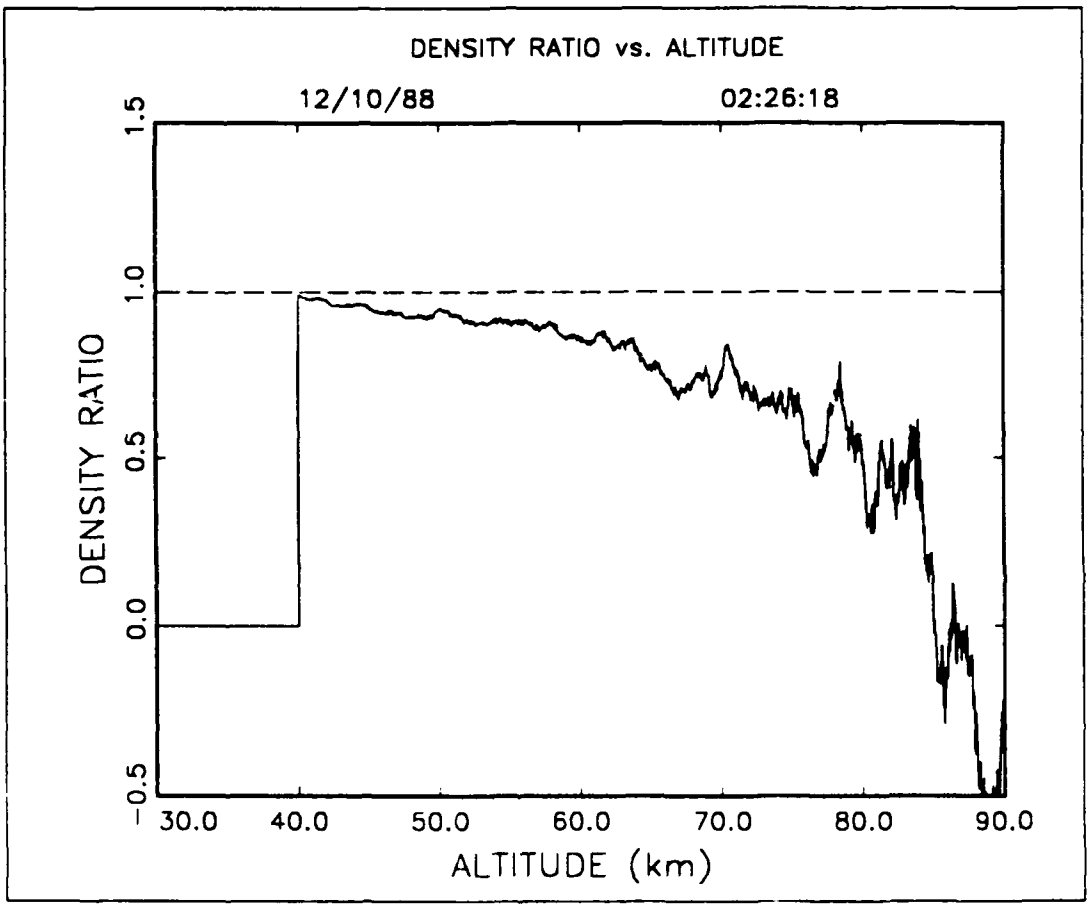

Figure 53. Plot of Density Ratio Versus Altitude for 2:26:18, 12/10/88 GMT.

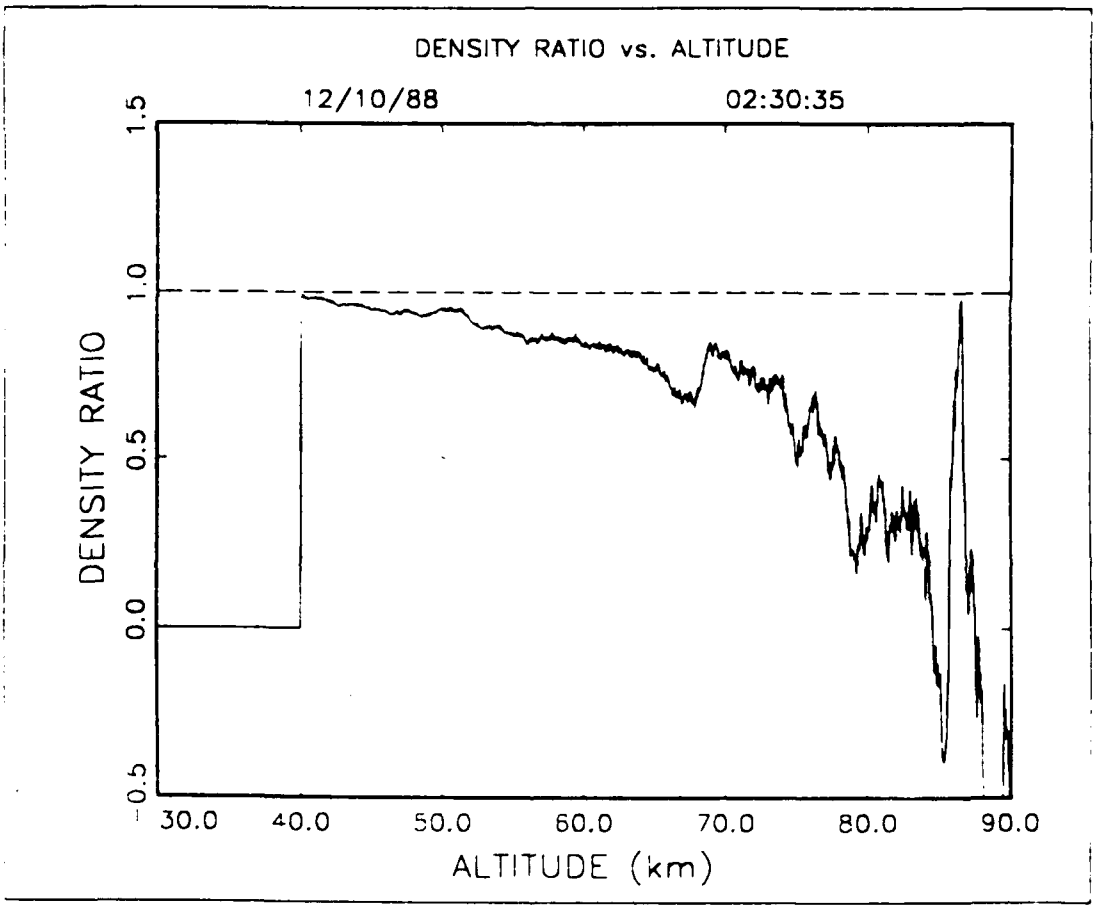

Figure 54. Plot of Density Ratio Versus Altitude for 2:30:35, 12/10/88 GMT.

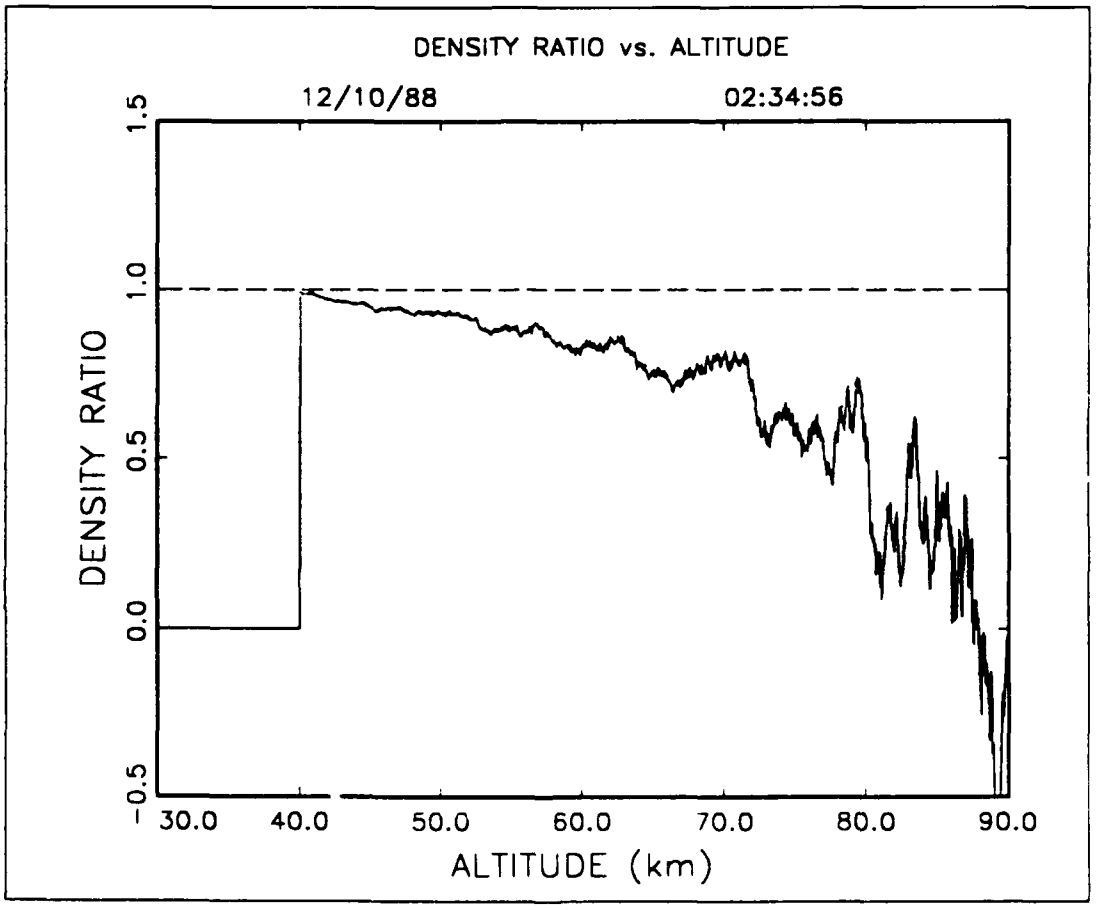

Figure 55. Plot of Density Ratio Versus Altitude for 2:34:56, 12/10/88 GMT.

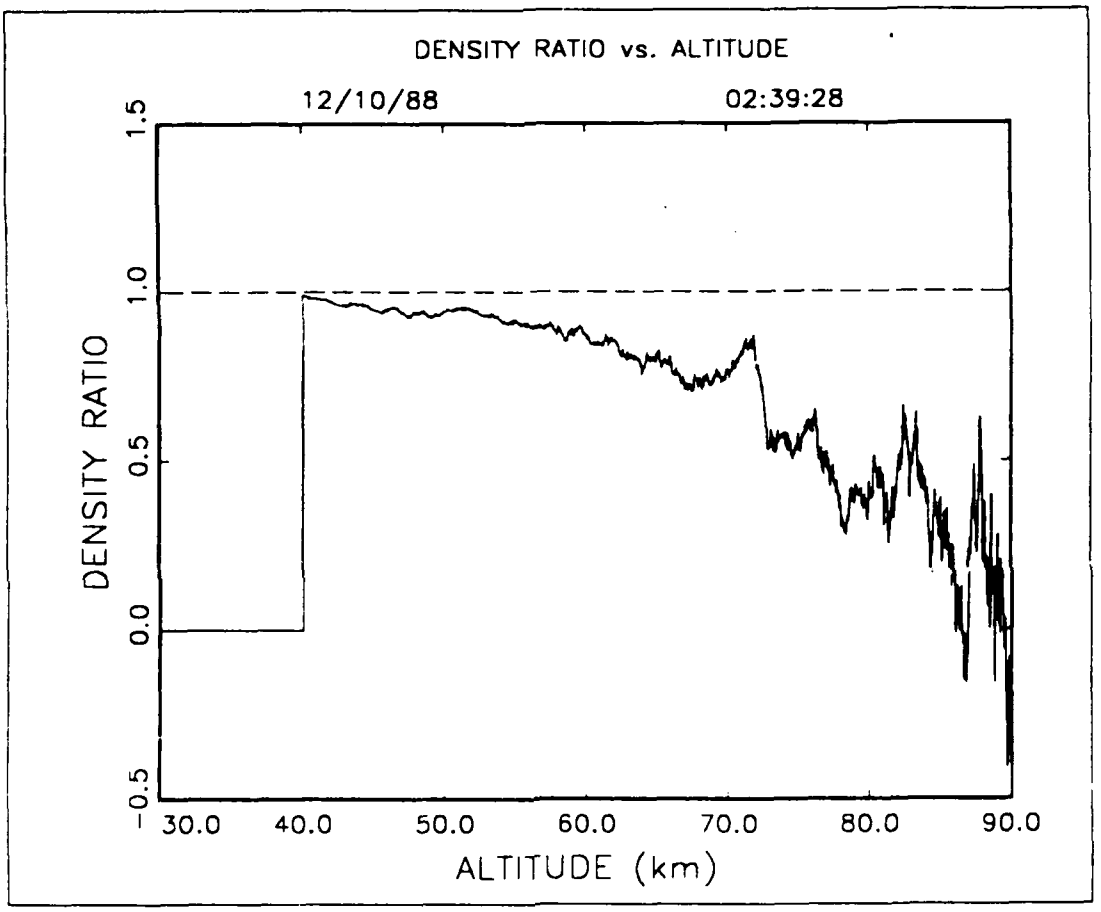

Figure 56. Plot of Density Ratio Versus Altitude for 2:39:28, 12/10/88 GMT.

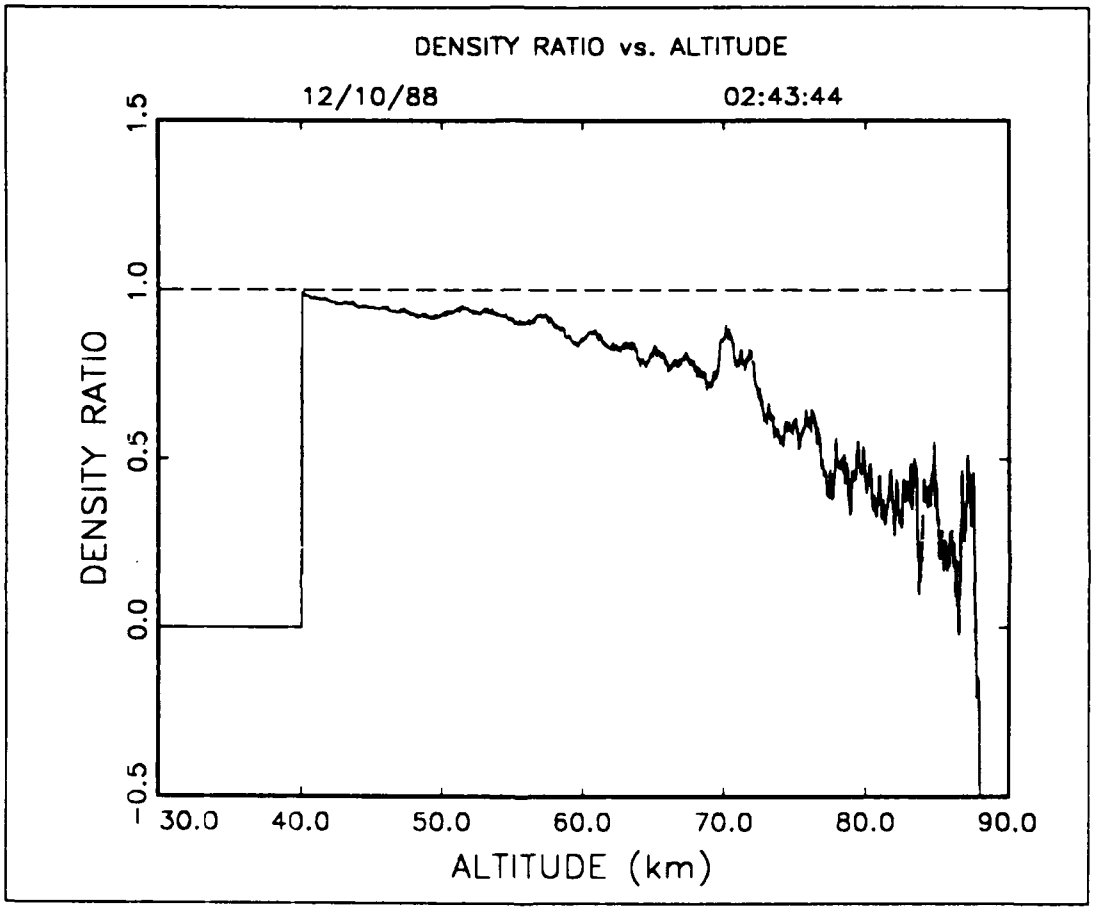

Figure 57. Plot of Density Ratio Versus Altitude for 2:43:44, 12/10/88 GMT.

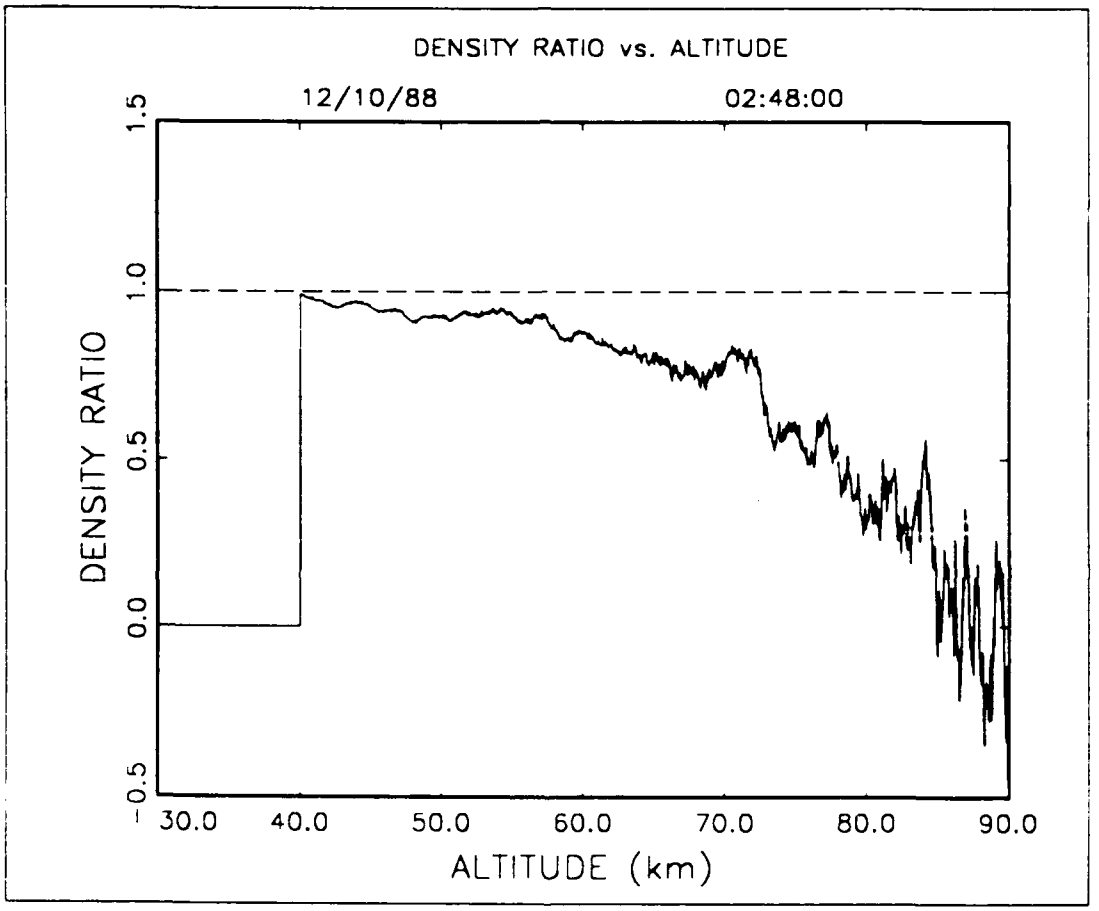

Figure 58. Plot of Density Ratio Versus Altitude for 2:48:00, 12/10/88 GMT.

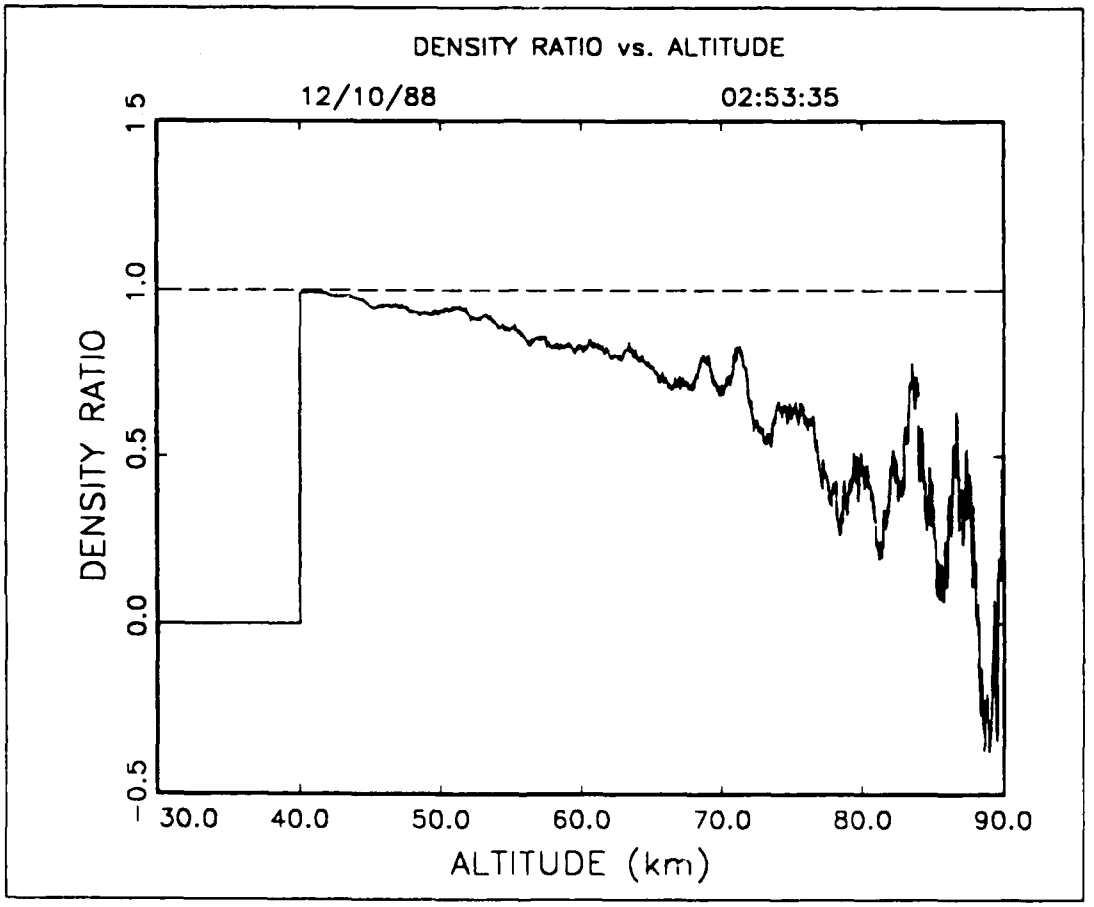

Figure 59. Plot of Density Ratio Versus Altitude for 2:53:35, 12/10/88 GMT.

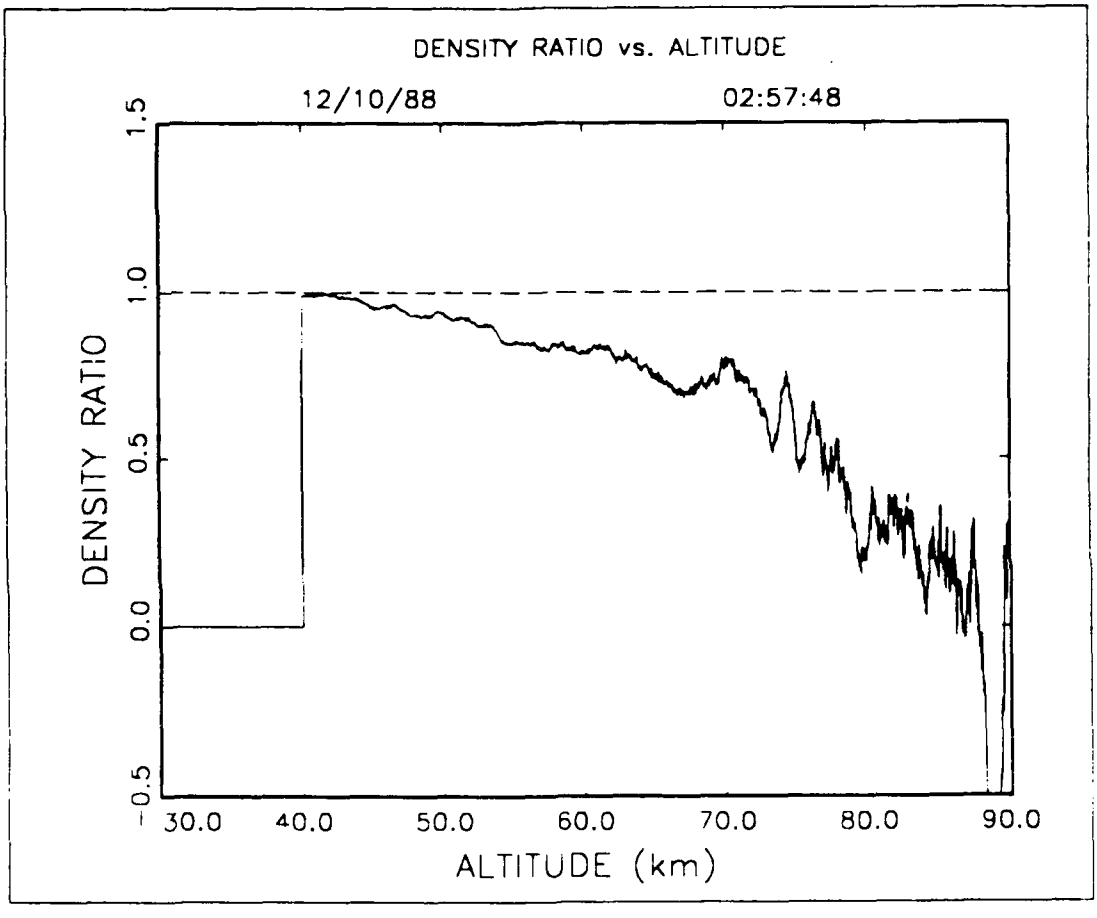

Figure 60. Plot of Density Ratio Versus Altitude for 2:57:48, 12/10/88 GMT.

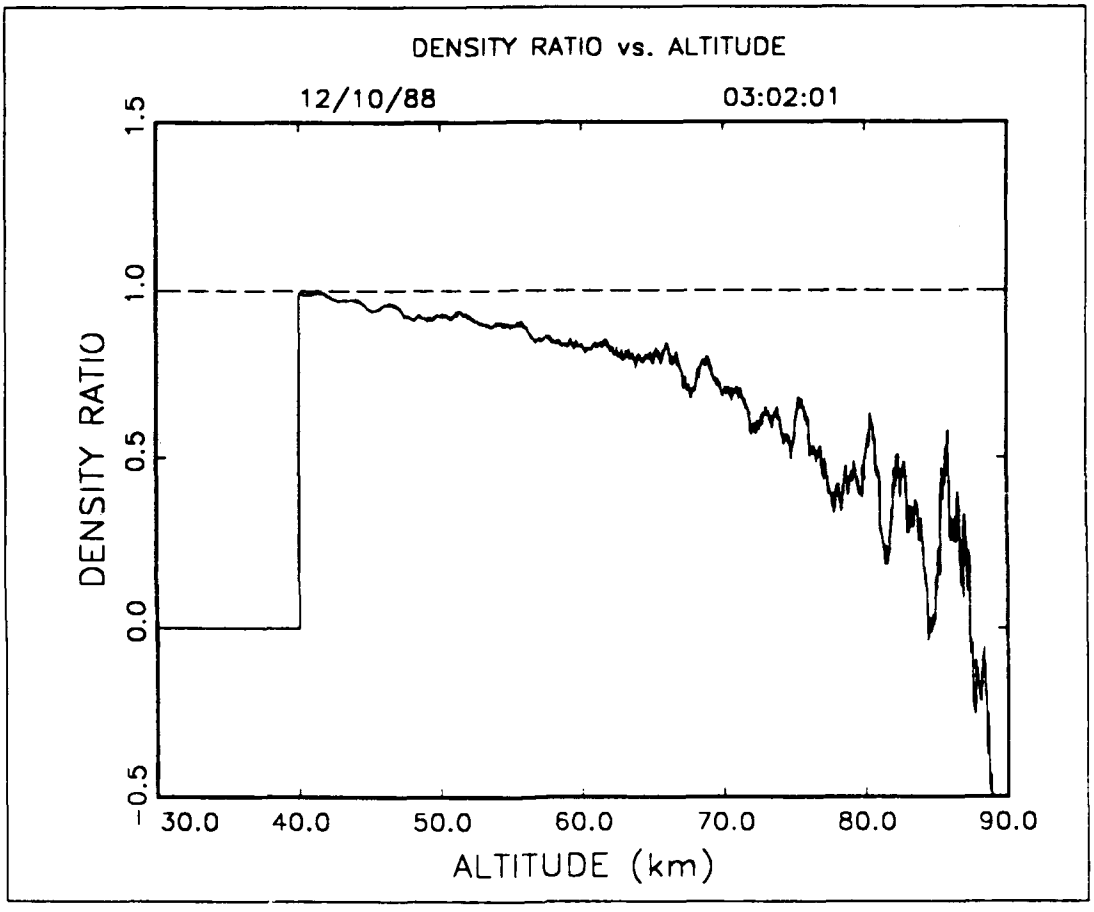

Figure 61. Plot of Density Ratio Versus Altitude for 3:02:01, 12/10/88 GMT.

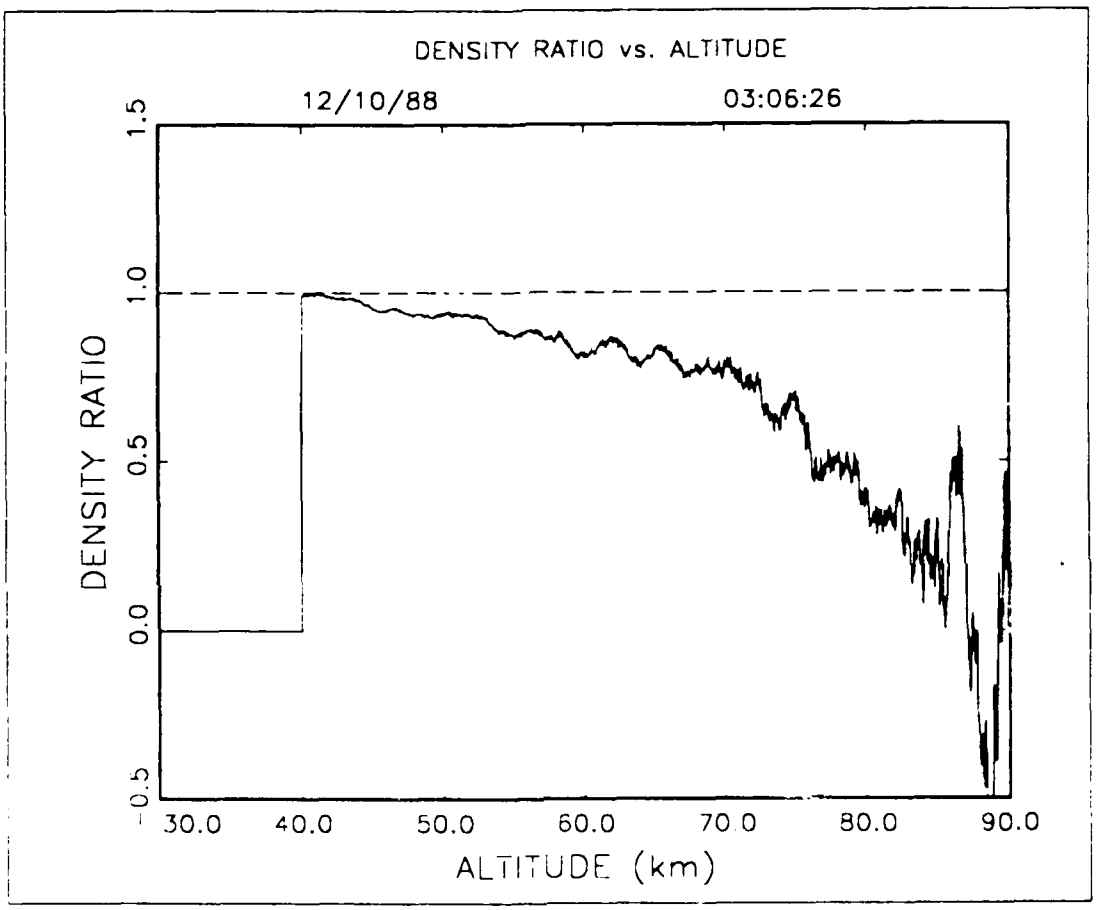

Figure 62 Plot of Density Ratio Versus Altitude for 3:06:26, 12/10/88 GMT.

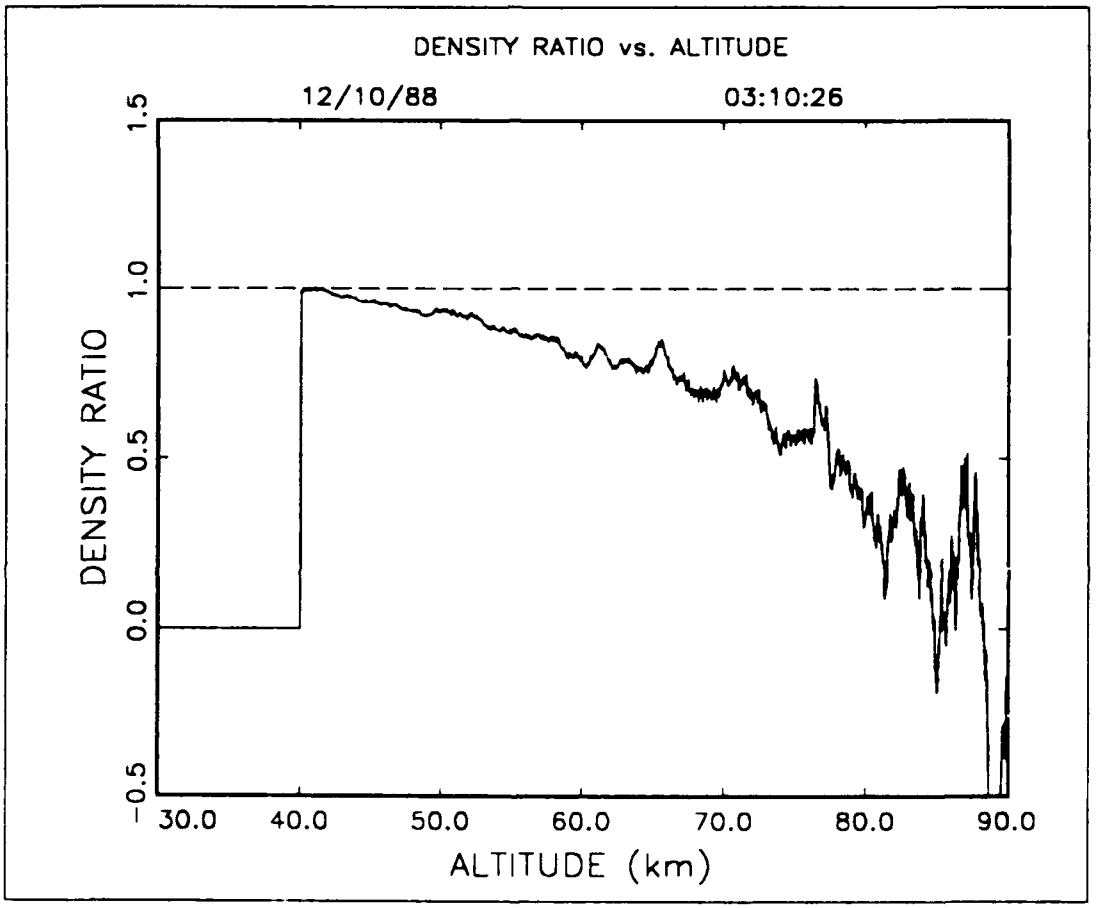

Figure 63. Plot of Density Ratio Versus Altitude for 3:10:26, 12/10/88 GMT.

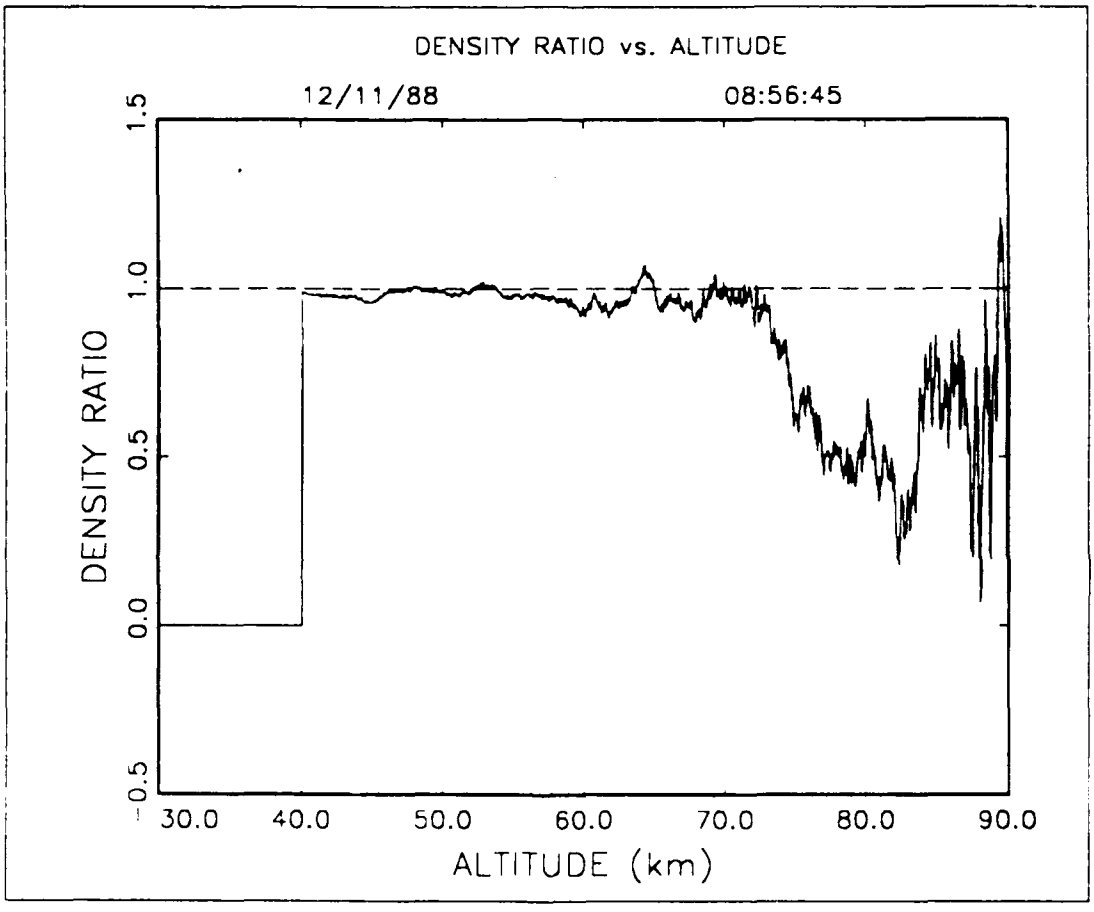

Figure 64. Plot of Density Ratio Versus Altitude for 8:56:45, 12/11/88 GMT.

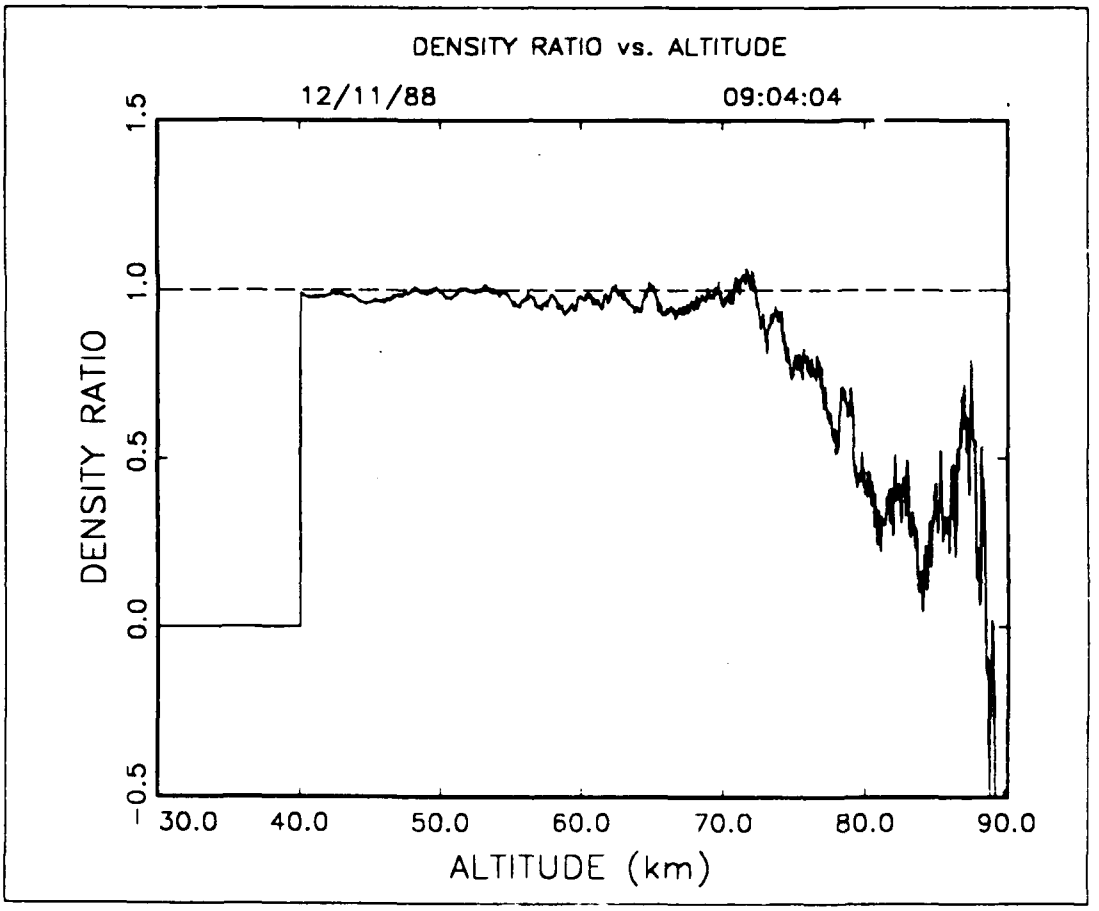

Figure 65. Plot of Density Ratio Versus Altitude for 9:04:04, 12/11/88 GMT.

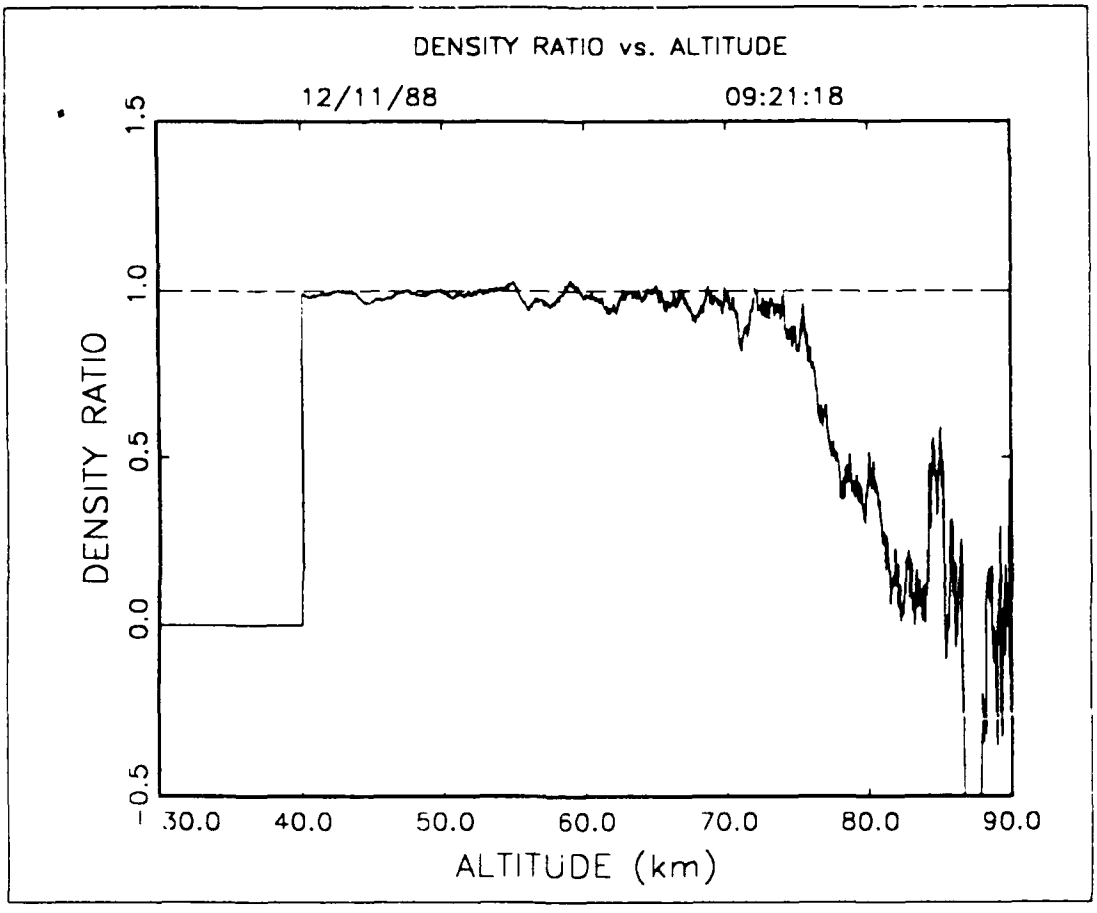

Figure 66. Plot of Density Ratio Versus Altitude for 9:21:18, 12/11/88 GMT.

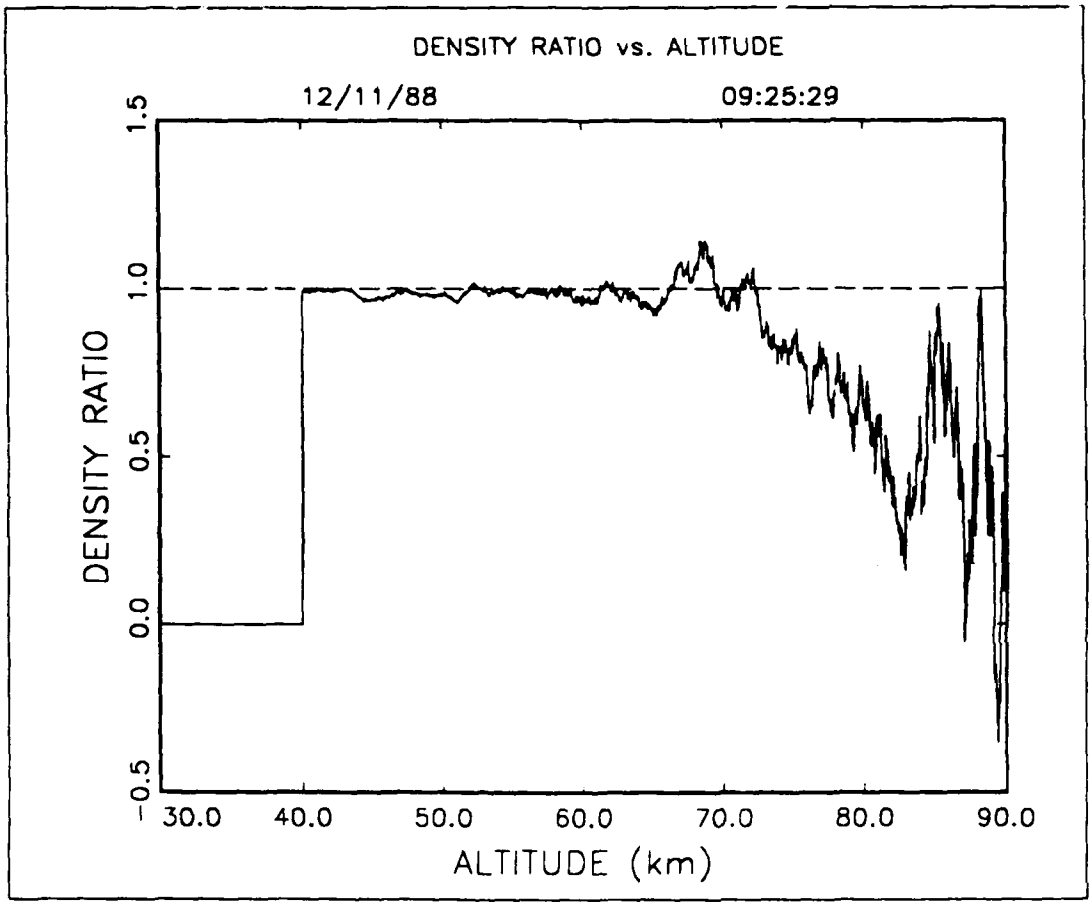

Figure 67. Plot of Density Ratio Versus Altitude for 9:25:29, 12/11/88 GMT.

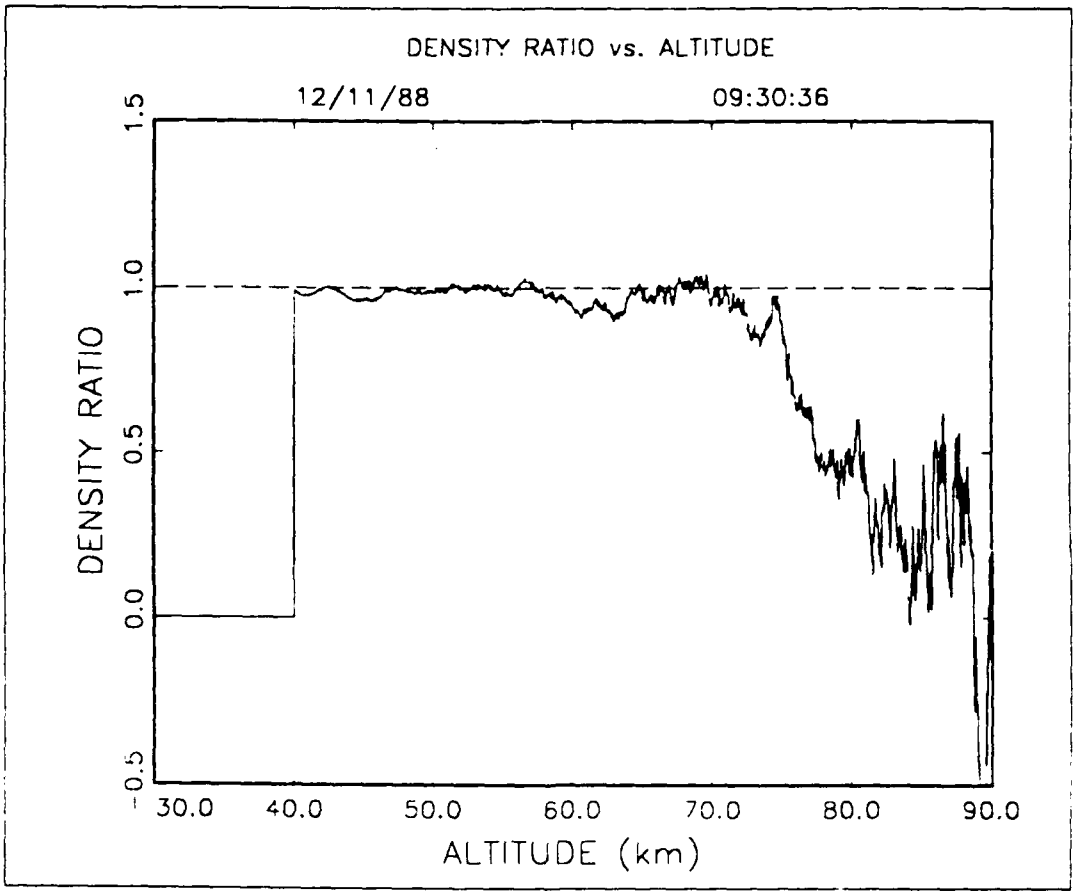

Figure 68. Plot of Density Ratio Versus Altitude for 9:30:36, 12/11/88 GMT.

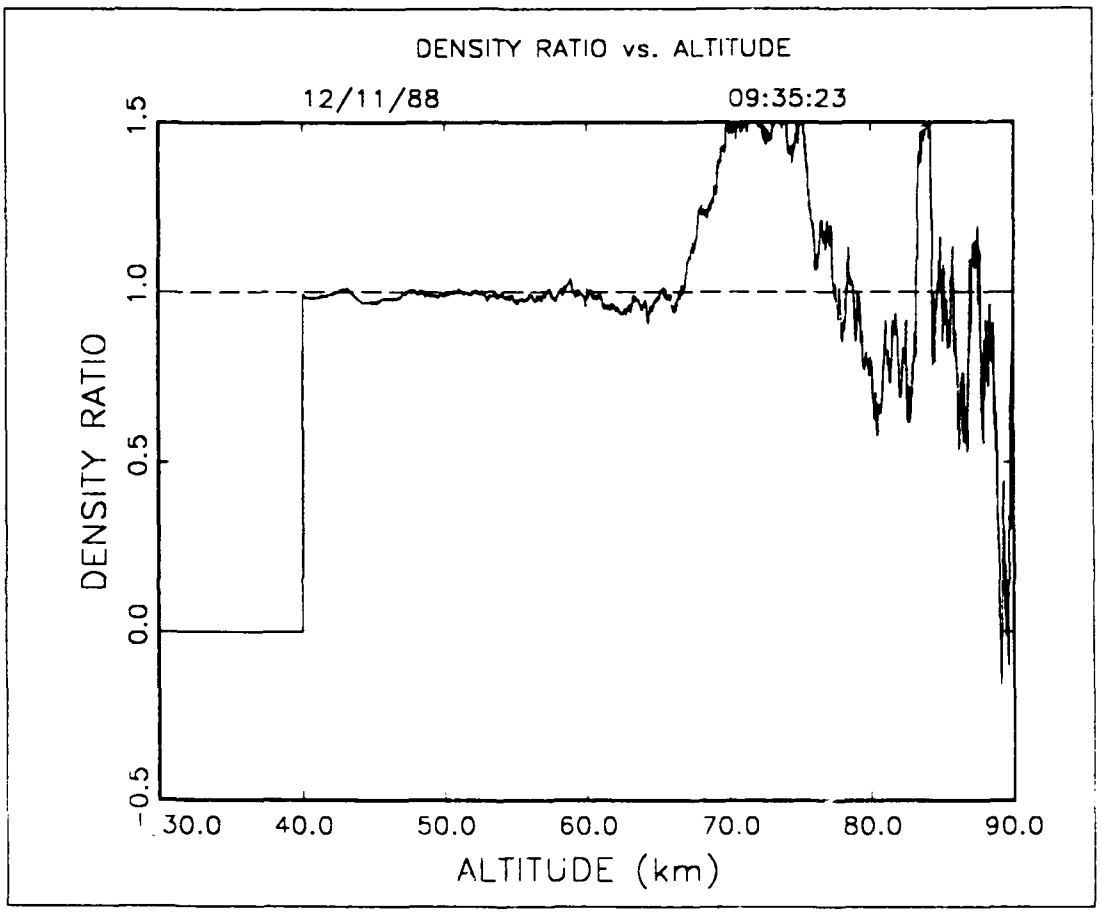

Figure 69. Plot of Density Ratio Versus Altitude for 9:35:23, 12/11/88 GMT.

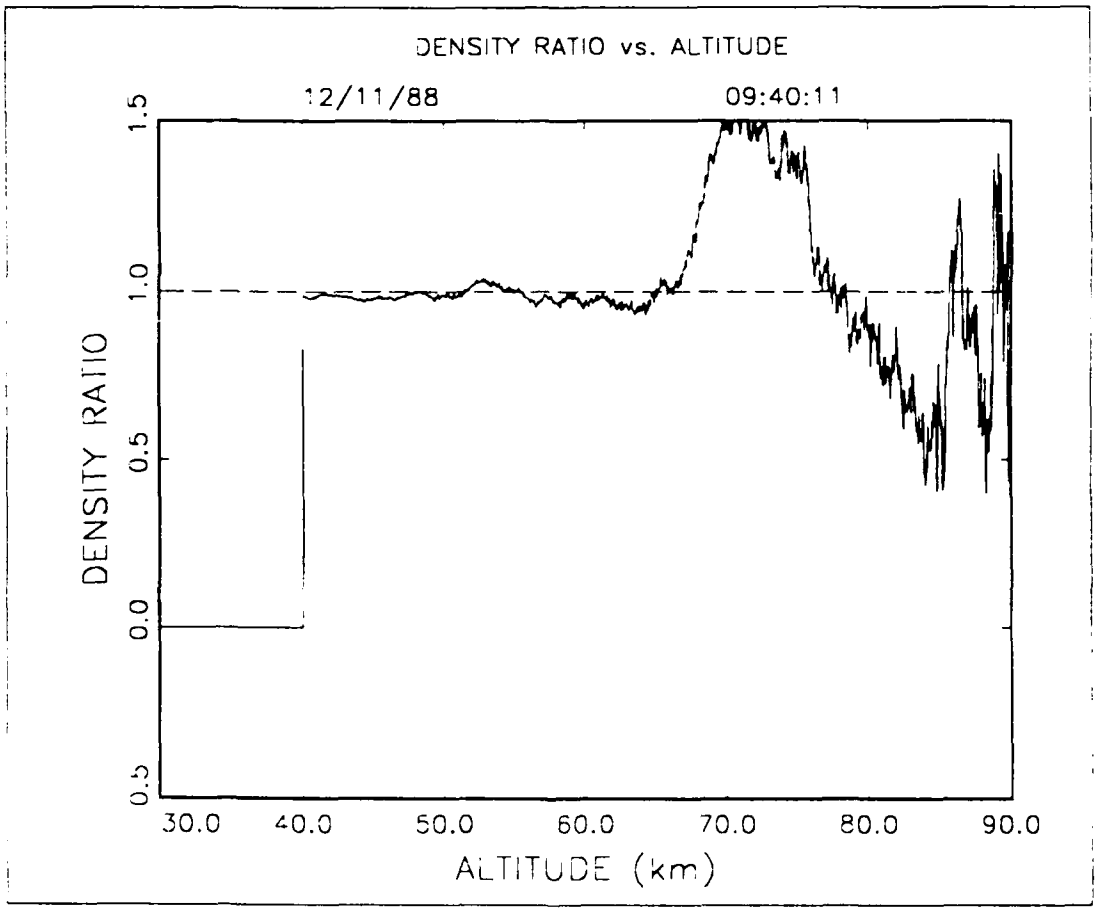

Figure 70. Plot of Density Ratio Versus Altitude for 9:40:11, 12/11/88 GMT.

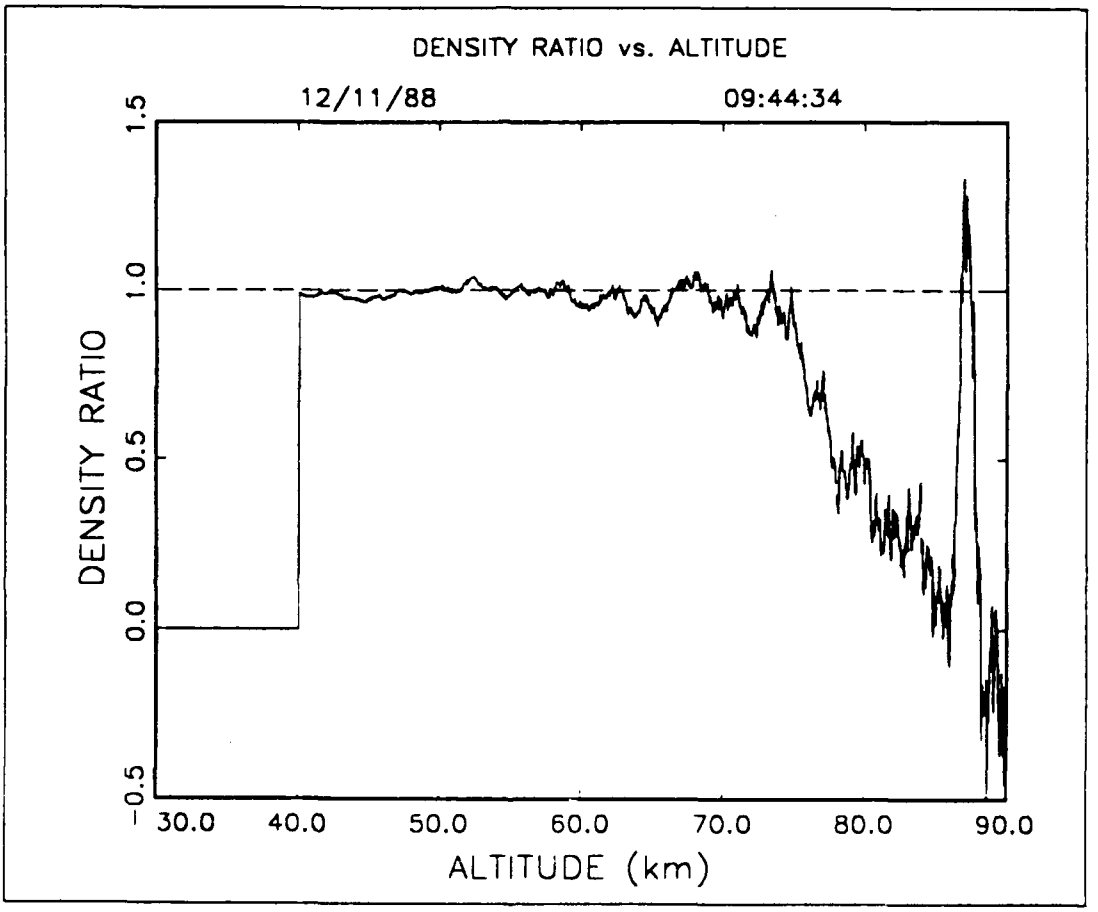

Figure 71. Plot of Density Ratio Versus Altitude for 9:44:34, 12/11/88 GMT.

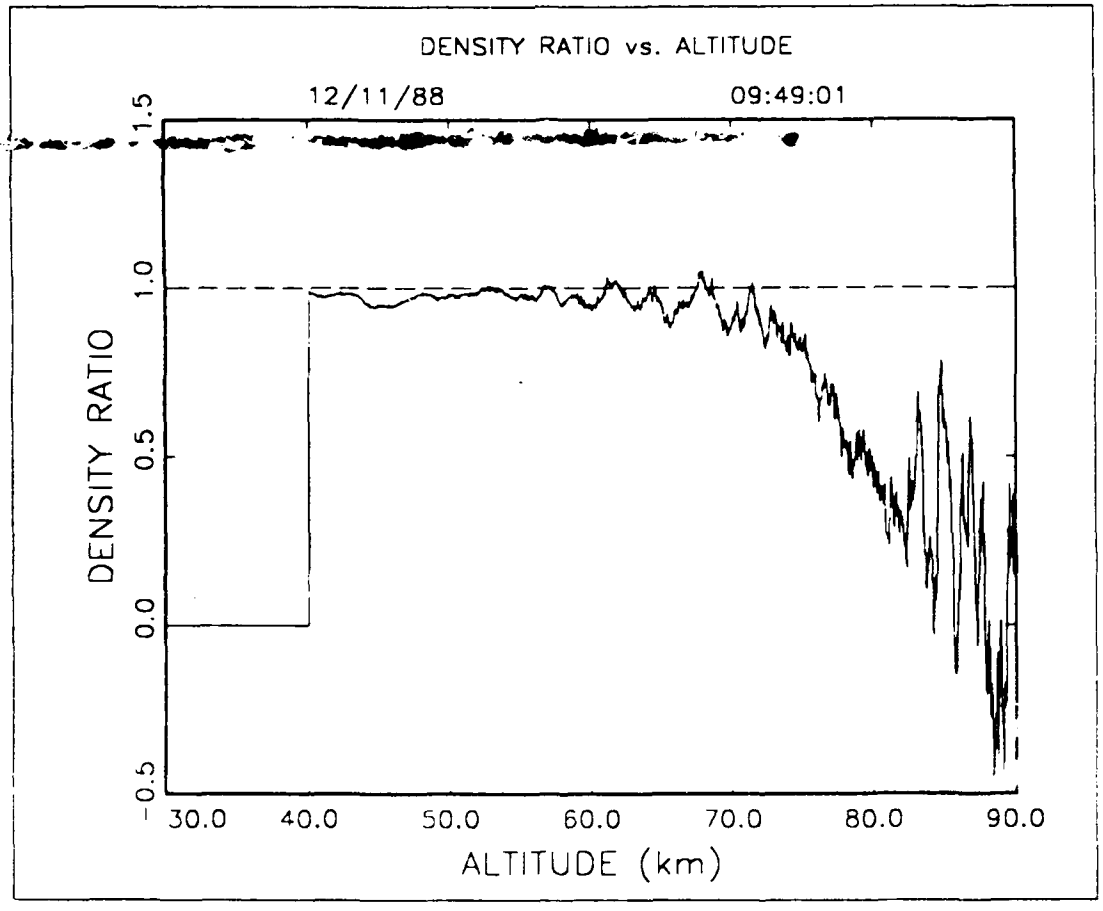

Figure 72. Plot of Density Ratio Versus Altitude for 9:49:01, 12/11/88 GMT.

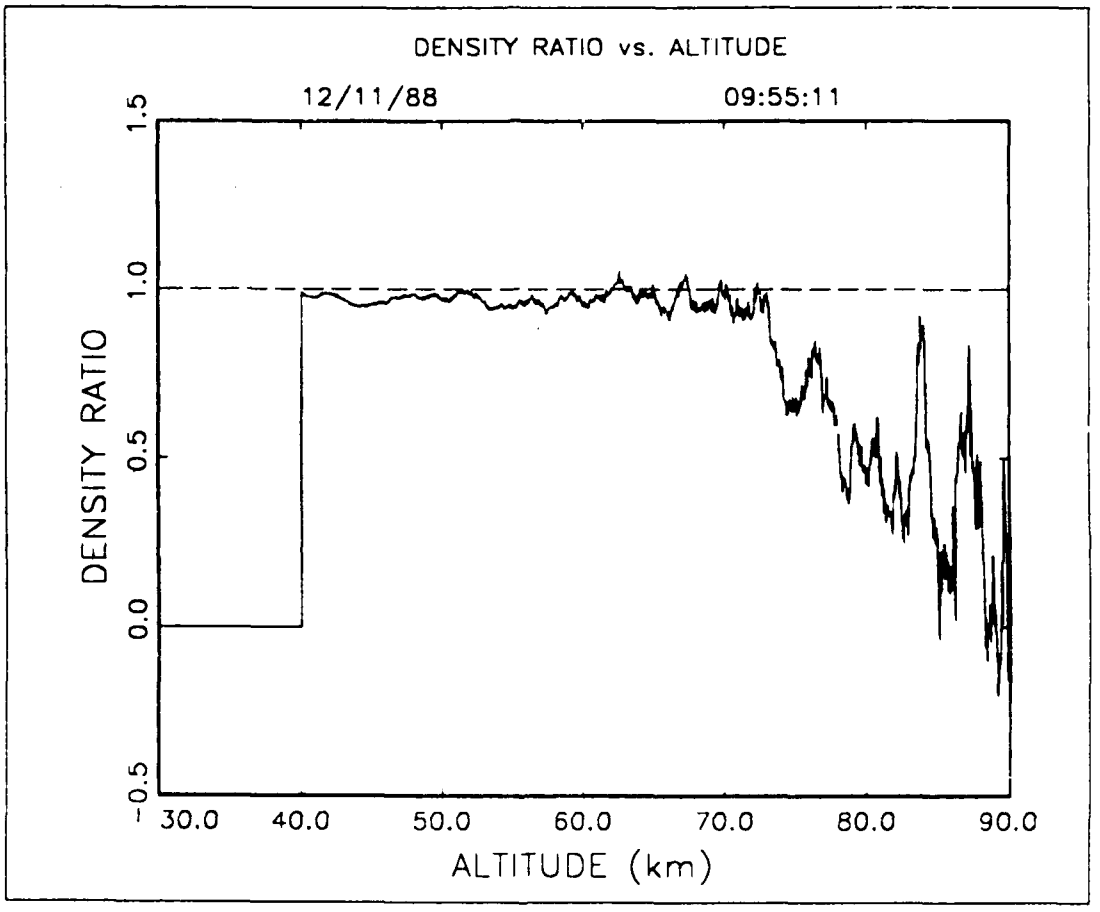

Figure 73. Plot of Density Ratio Versus Altitude for 9:55:11, 12/11/88 GMT.

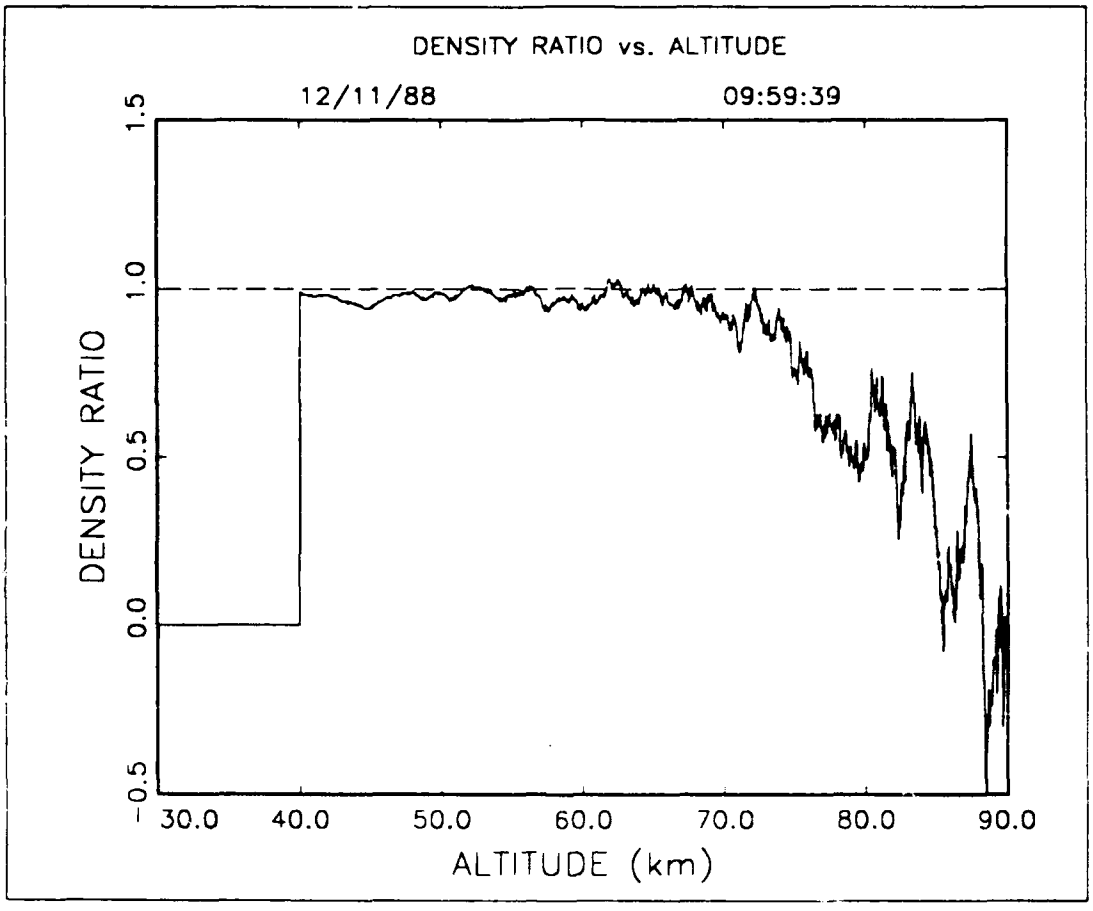

Figure 74. Ploit of Density Ratio Versus Altitude for 9:59:39, 12/11/88 GMT.

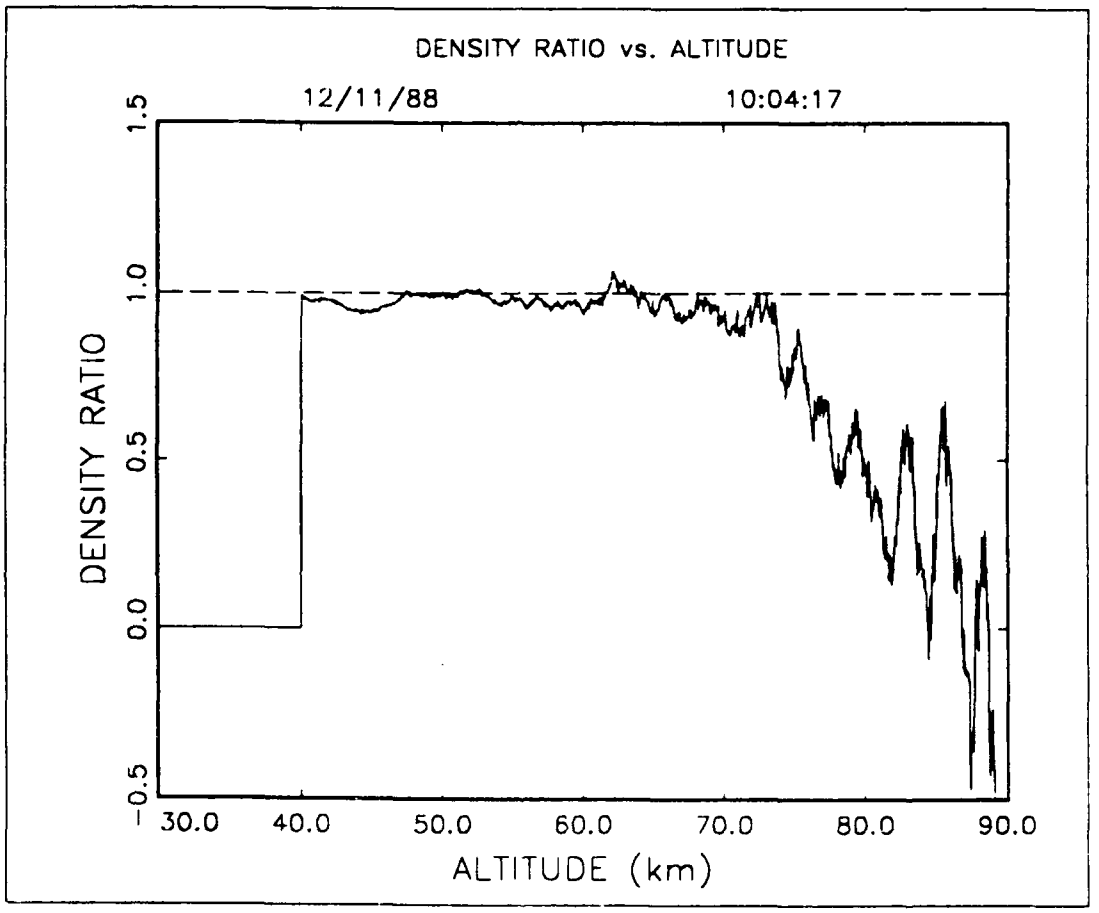

Figure 75. Plot of Density Ratio Versus Altitude for 10:04:17, 12/11/88 GMT.

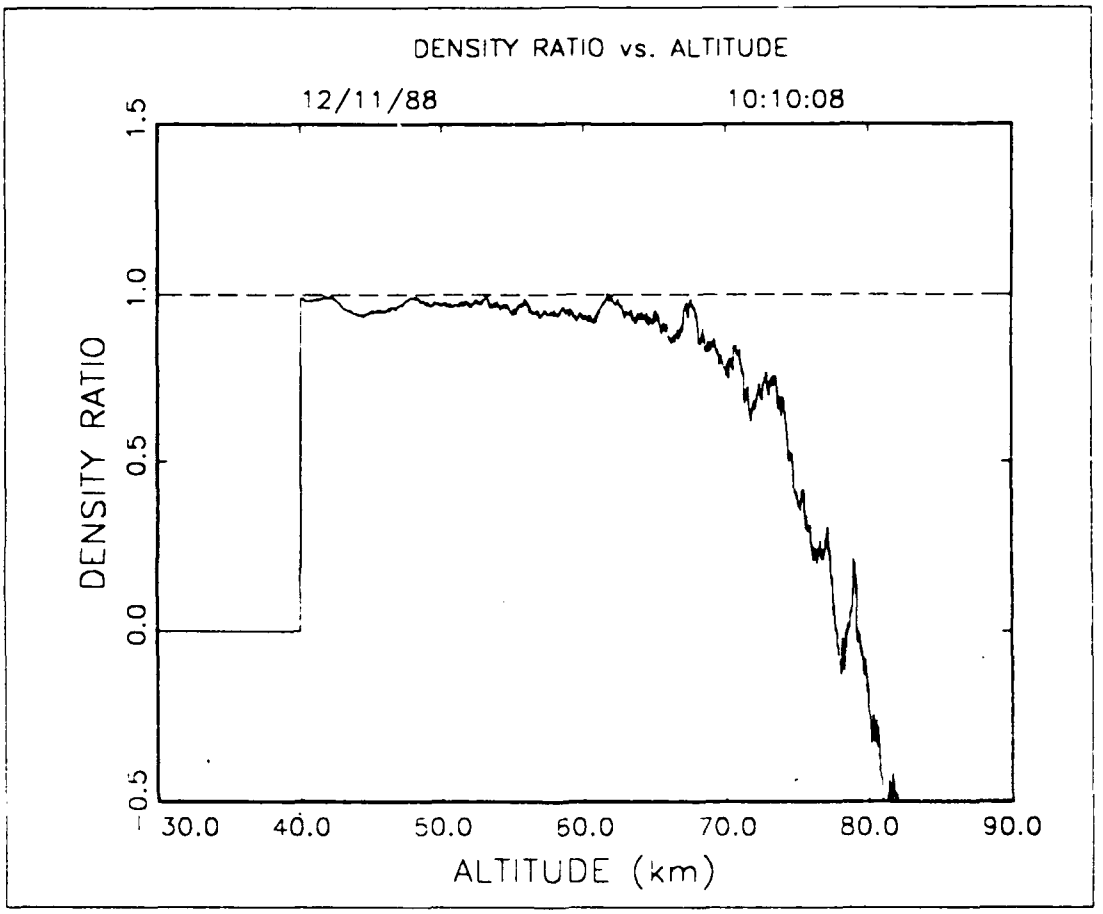

Figure 76. Plot of Density Ratio Versus Altitude for 10:10:08, 12/11/88 GMT.

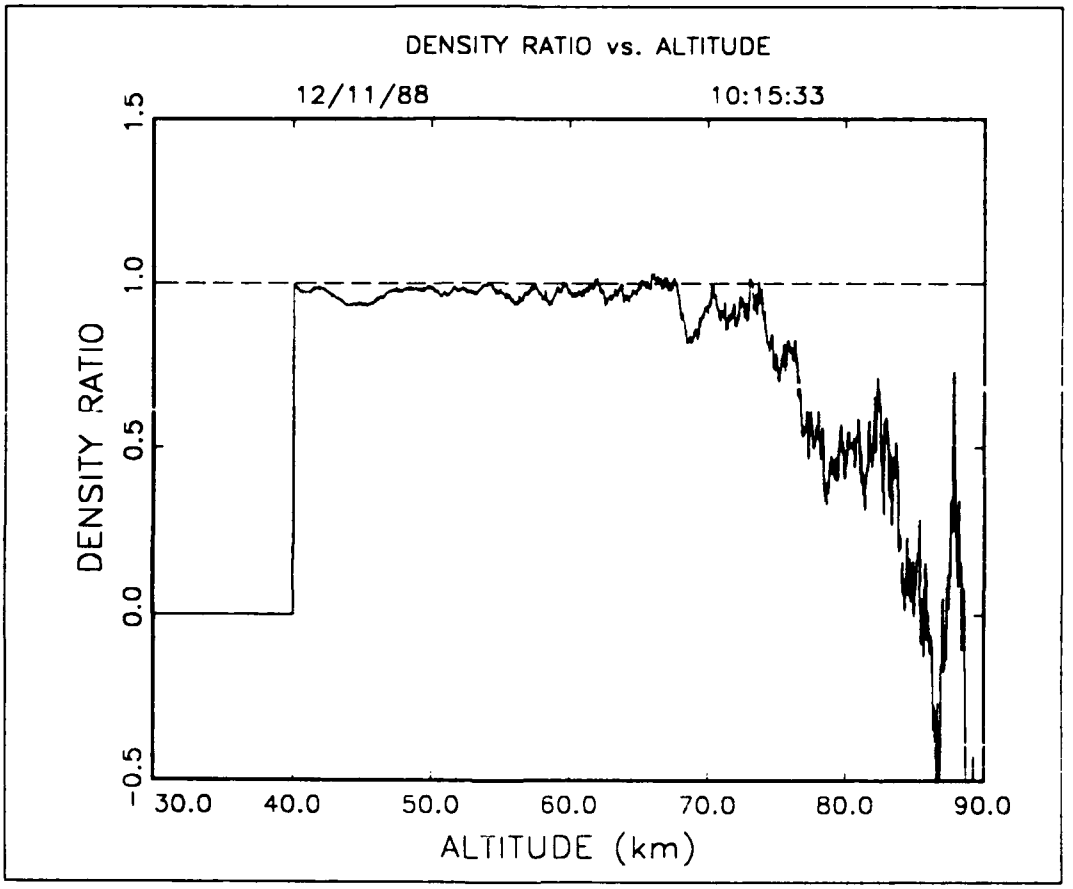

Figure 77. Plot of Density Ratio Versus Altitude for 10:15:33, 12/11/88 GMT.

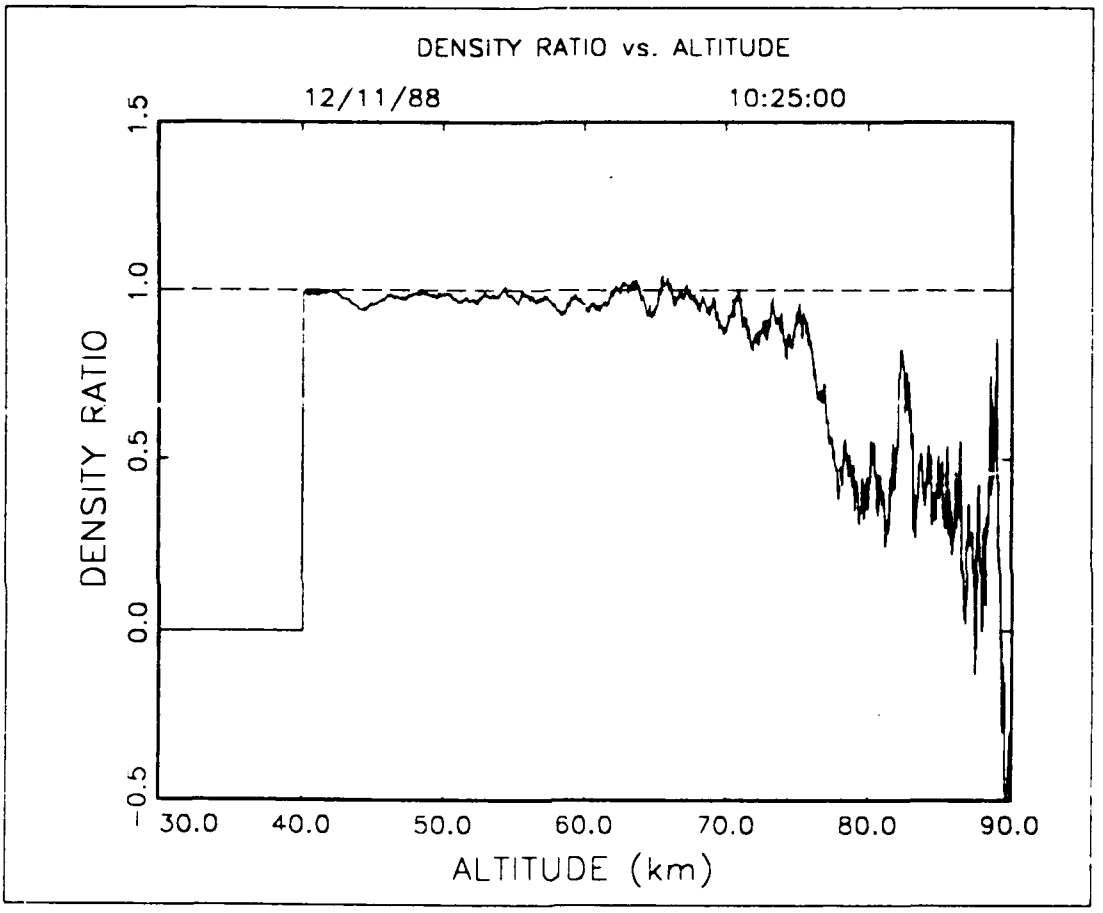

Figure 78. Plot of Density Ratio Versus Altitude for 10:25:00, 12/11/88 GMT.

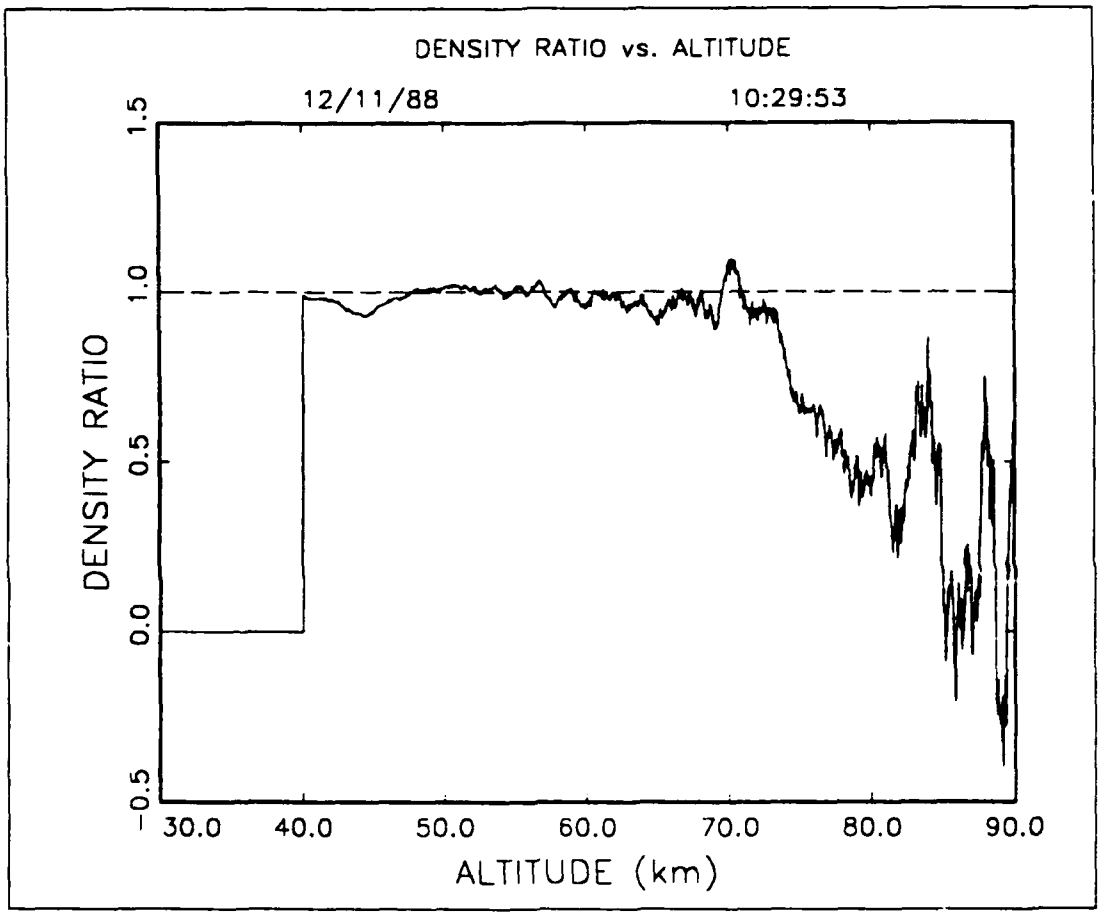

Figure 79. Plot of Density Ratio Versus Altitude for 10:29:53, 12/11/88 GMT.

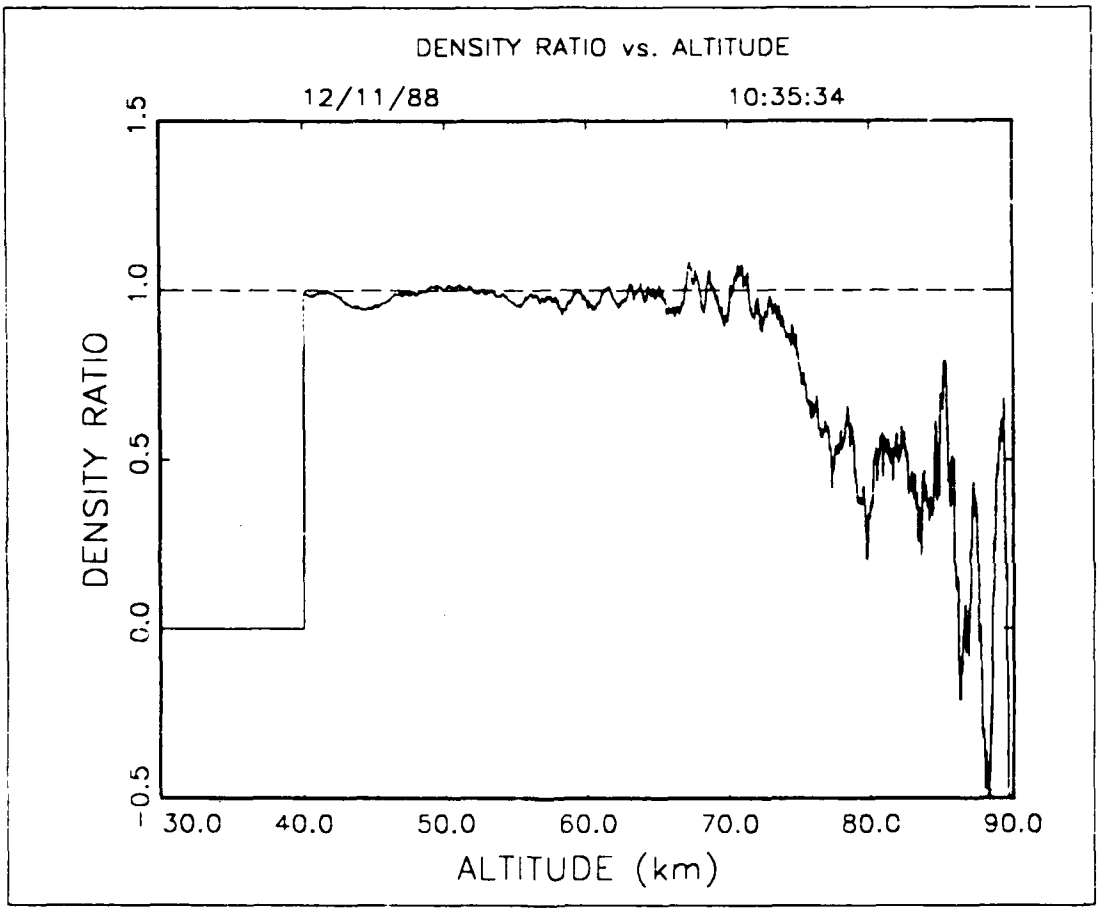

Figure 80. Plot of Density Ratio Versus Altitude for 10:35:34, 12/11/88 GMT.

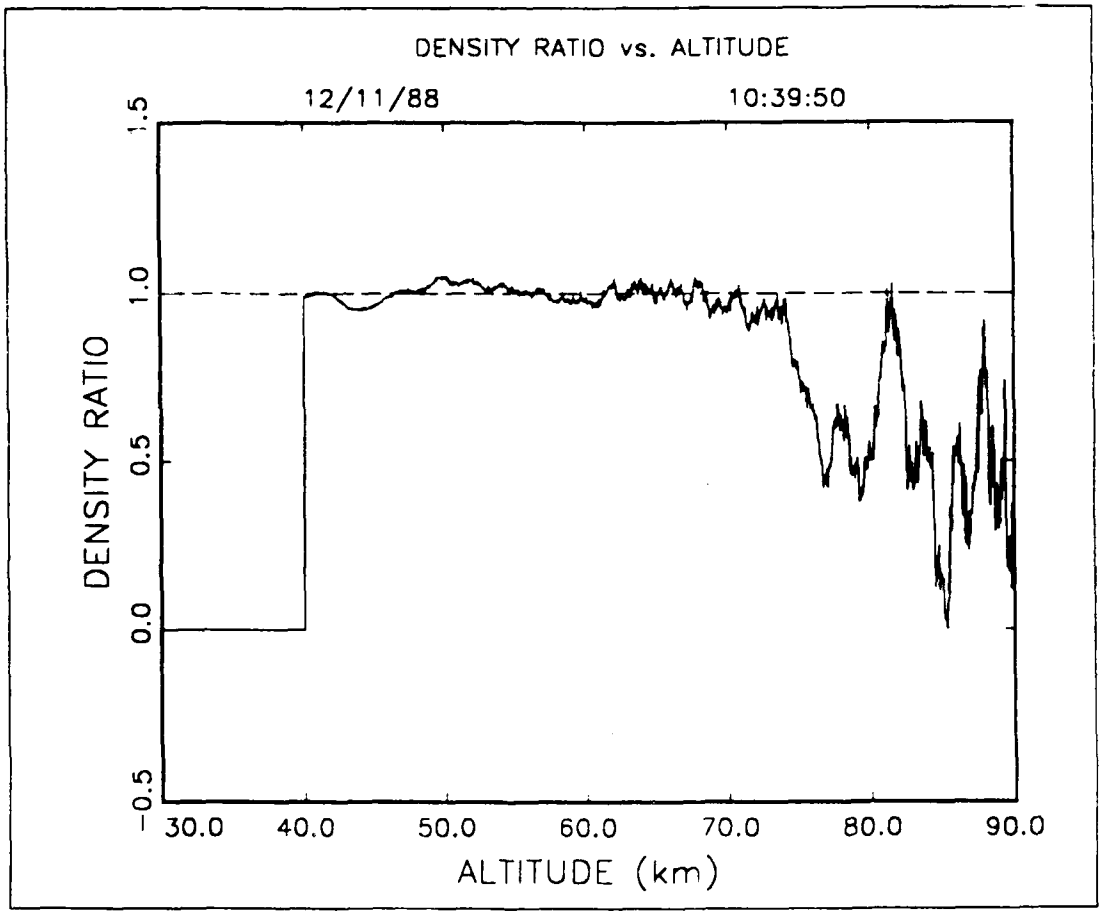

Figure 81. Plot of Density Ratio Versus Altitude for 10:39:50, 12/11/88 GMT.

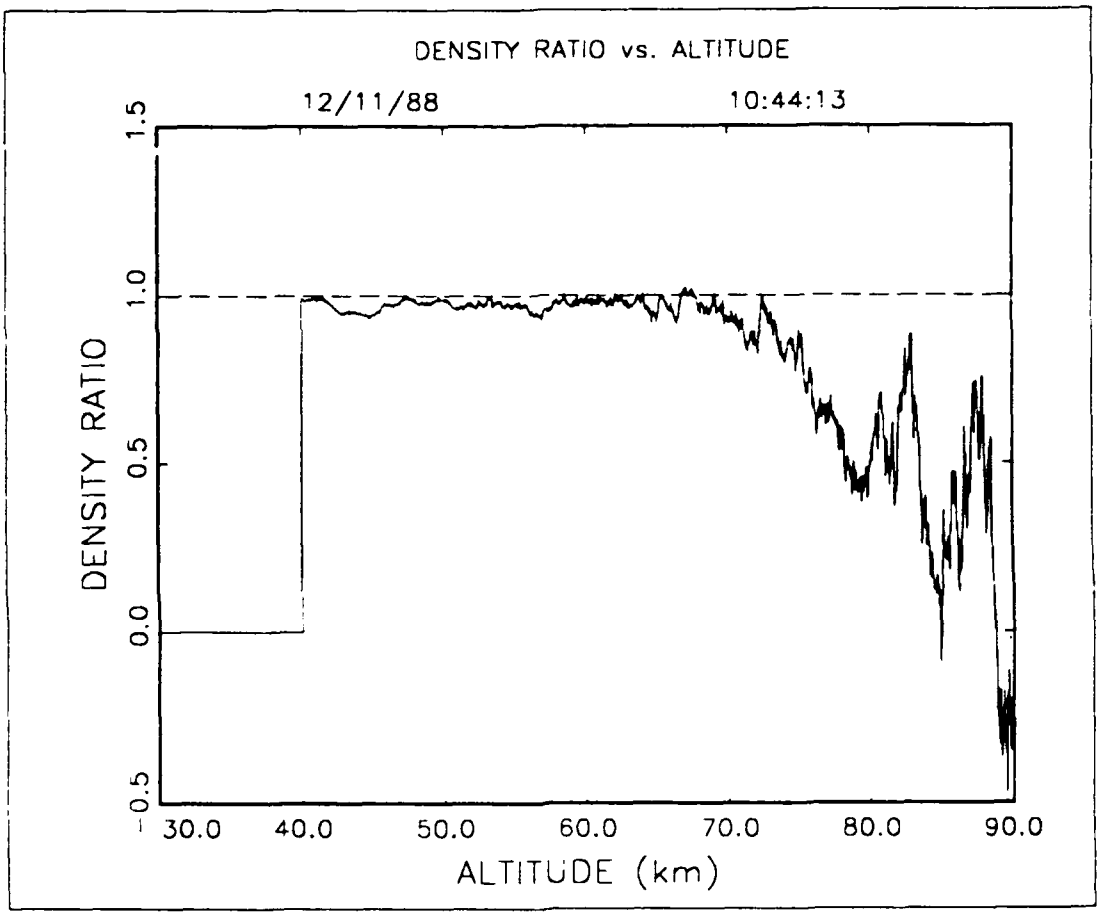

Figure 82. Plot of Density Ratio Versus Altitude for 10:44:13, 12/11/88 GMT.

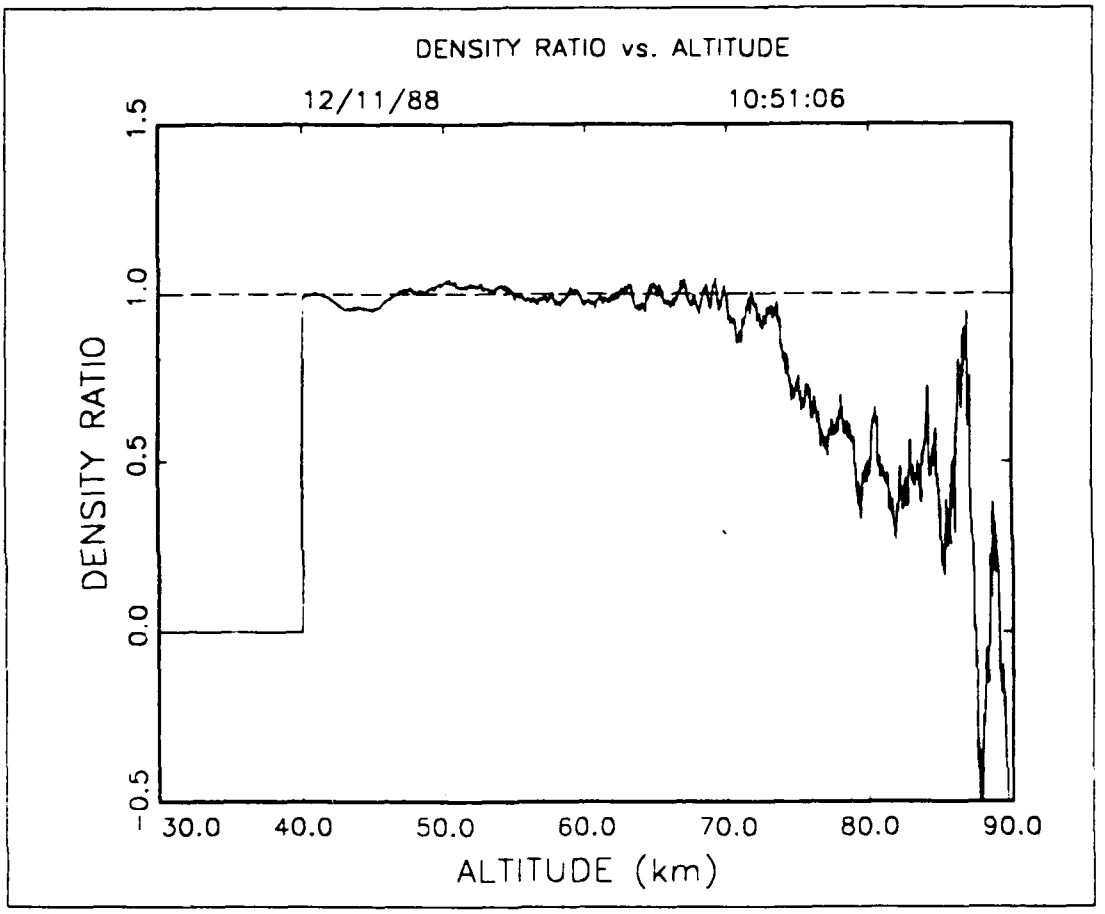

Figure 83. Plot of Density Ratio Versus Altitude for 10:51:06, 12/11/88 GMT.

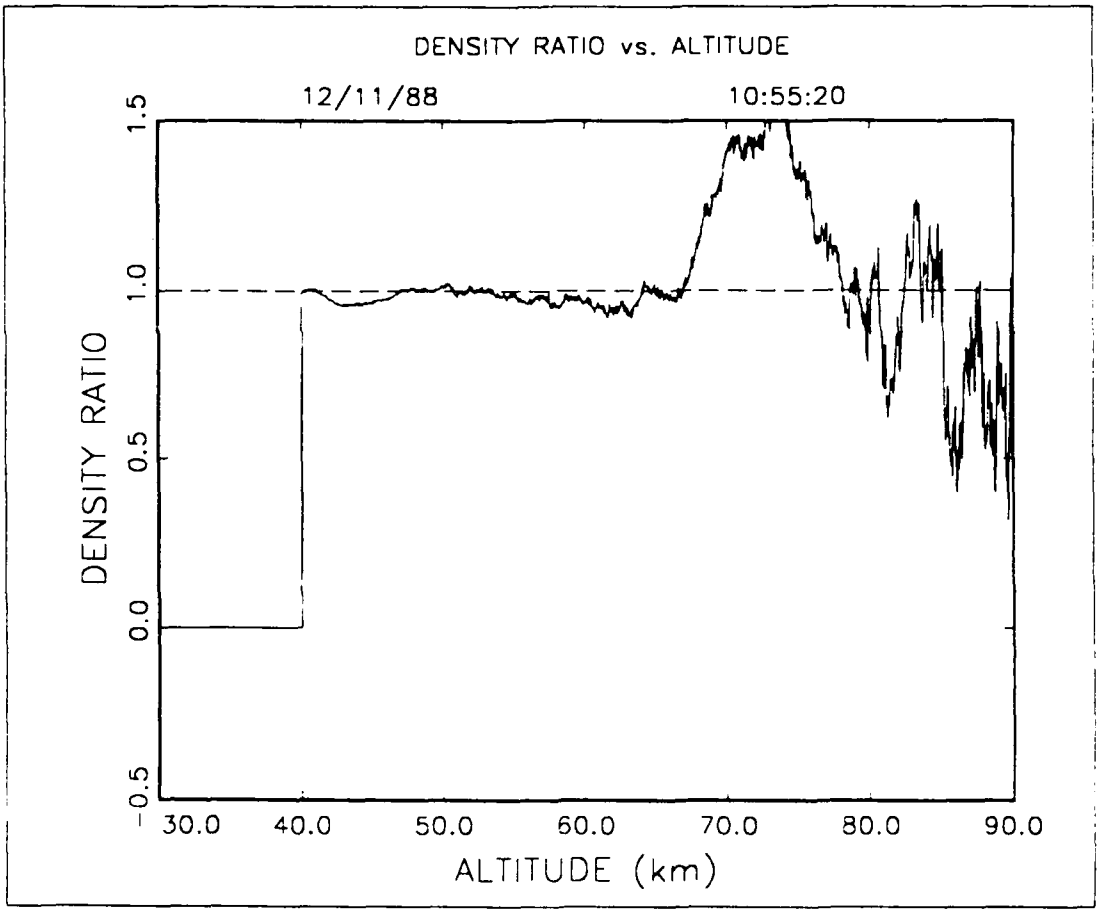

Figure 84. Plot of Density Ratio Versus Altitude for 10:55:20, 12/11/88 GMT.

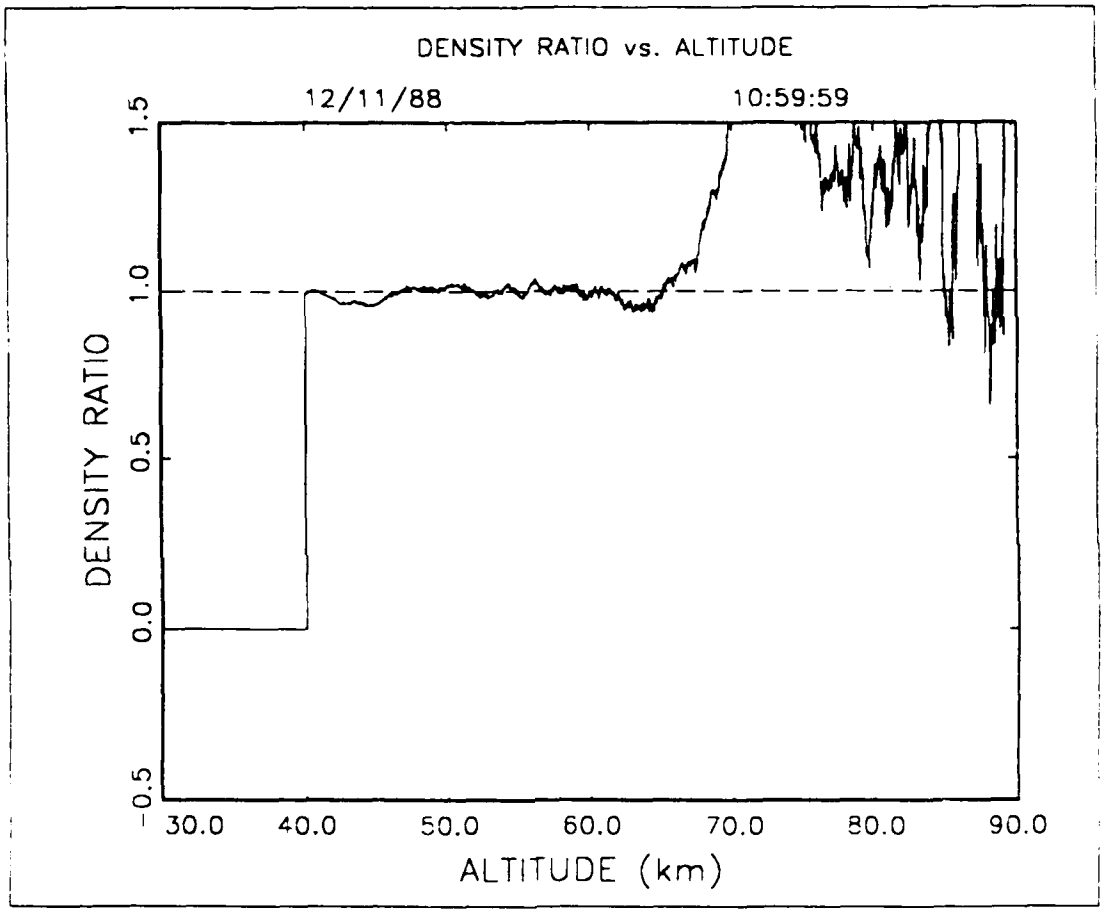

Figure 85. Plot of Density Ratio Versus Altitude for 10:59:58, 12/11/88 GMT.

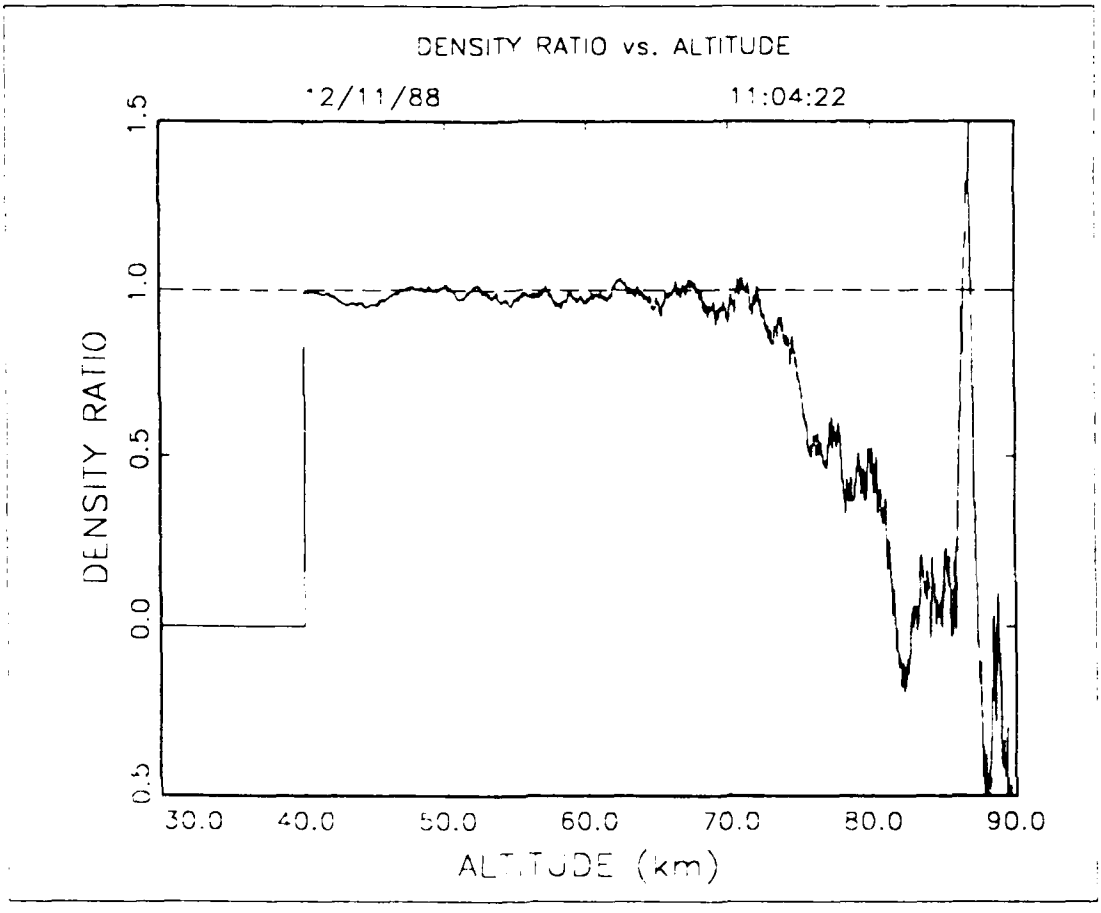

Figure 86. Plot of Density Ratio Versus Altitude for 11:04:22, 12/11/88 GMT.

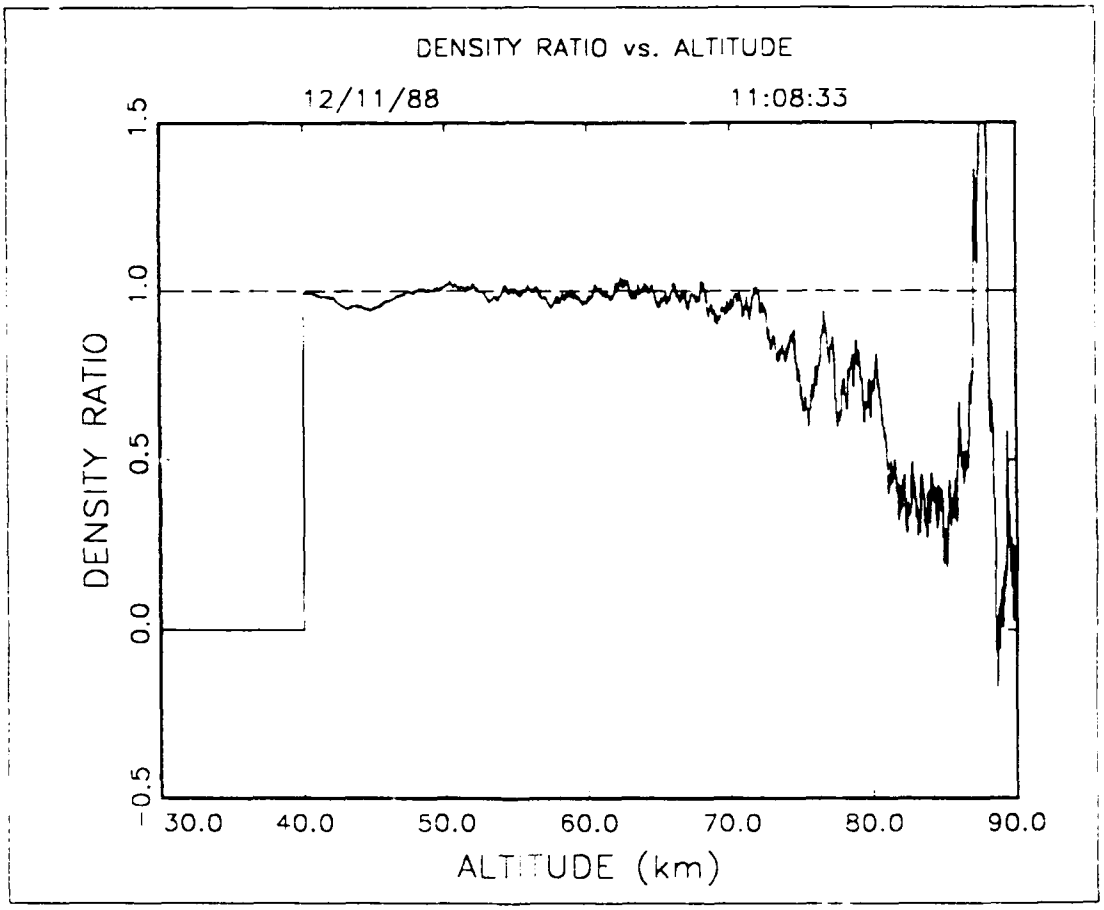

Figure 87. Plot of Density Ratio Versus Altitude for 11:08:33, 12/11/88 GMT.

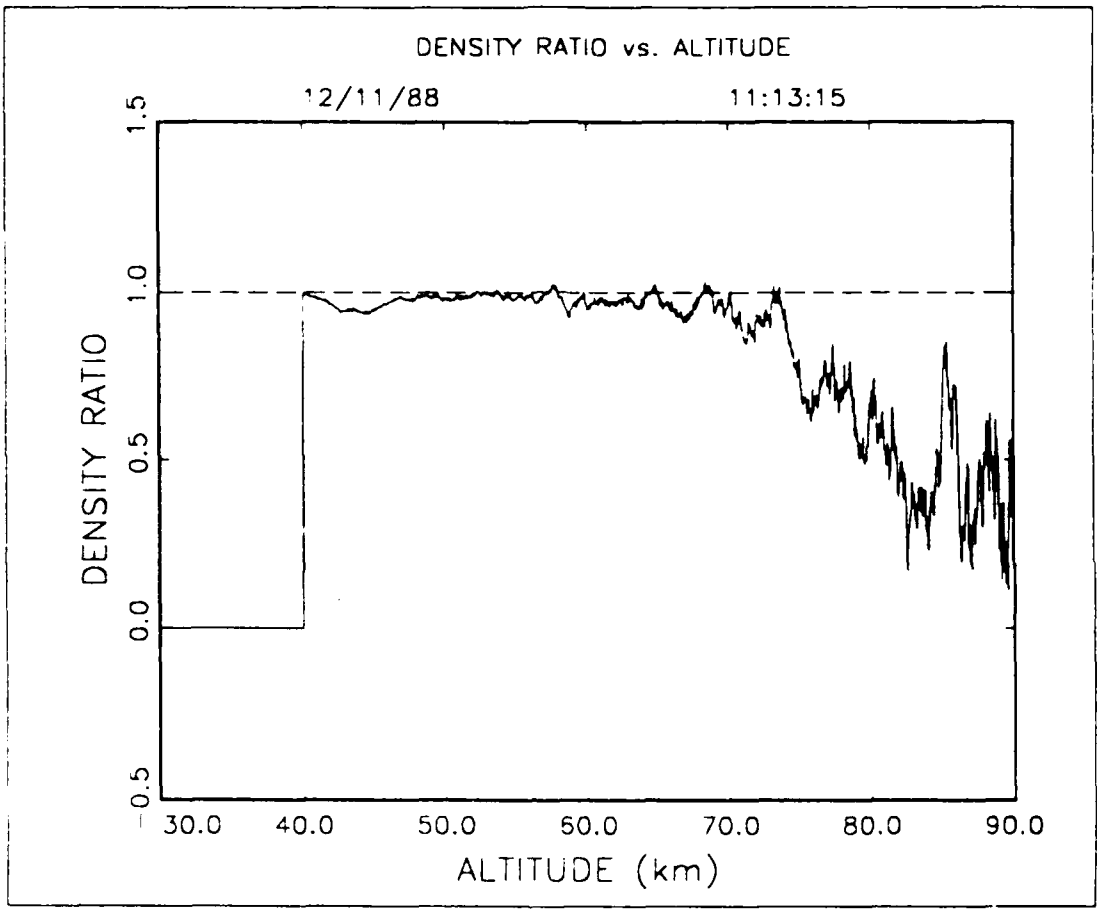

Figure 88. Plot of Density Ratio Versus Altitude for 11:13:15, 12/11/88 GMT.

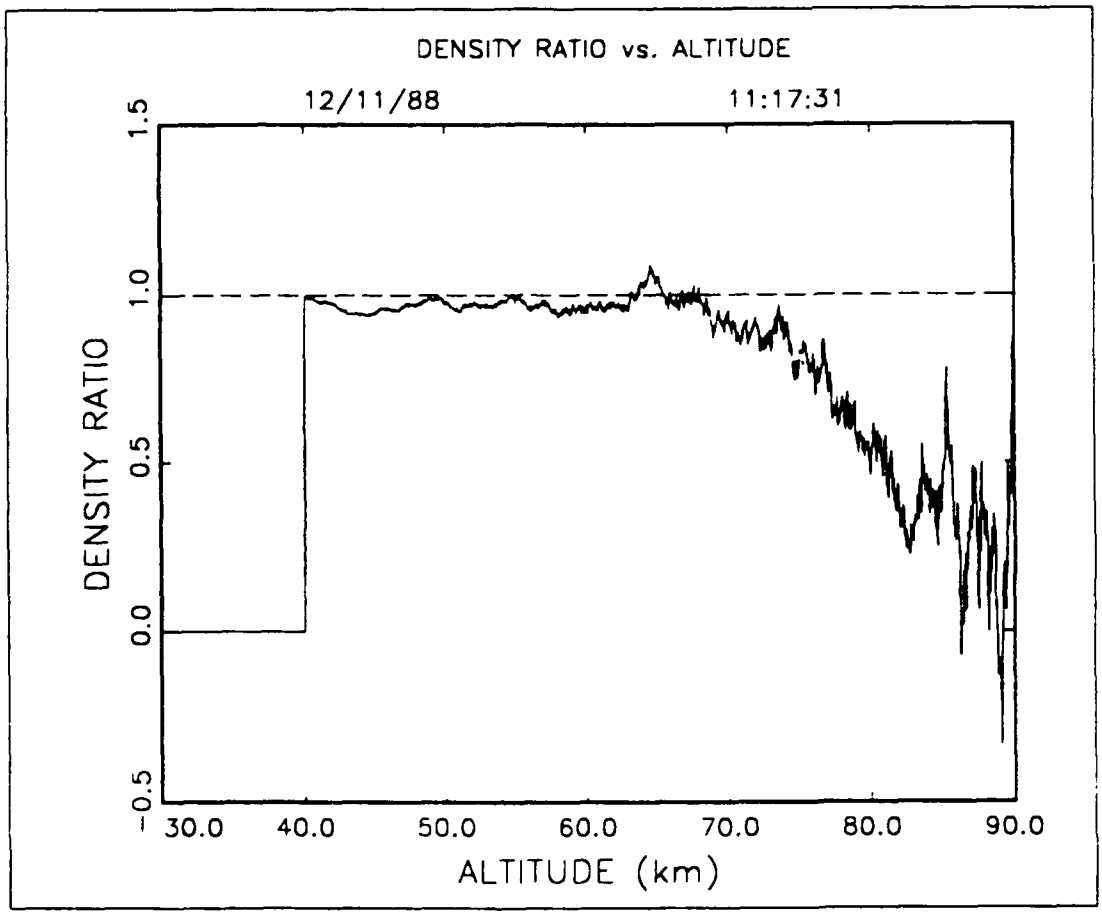

Figure 89. Plot of Density Ratio Versus Altitude for 11:17:31, 12/11/88 GMT.

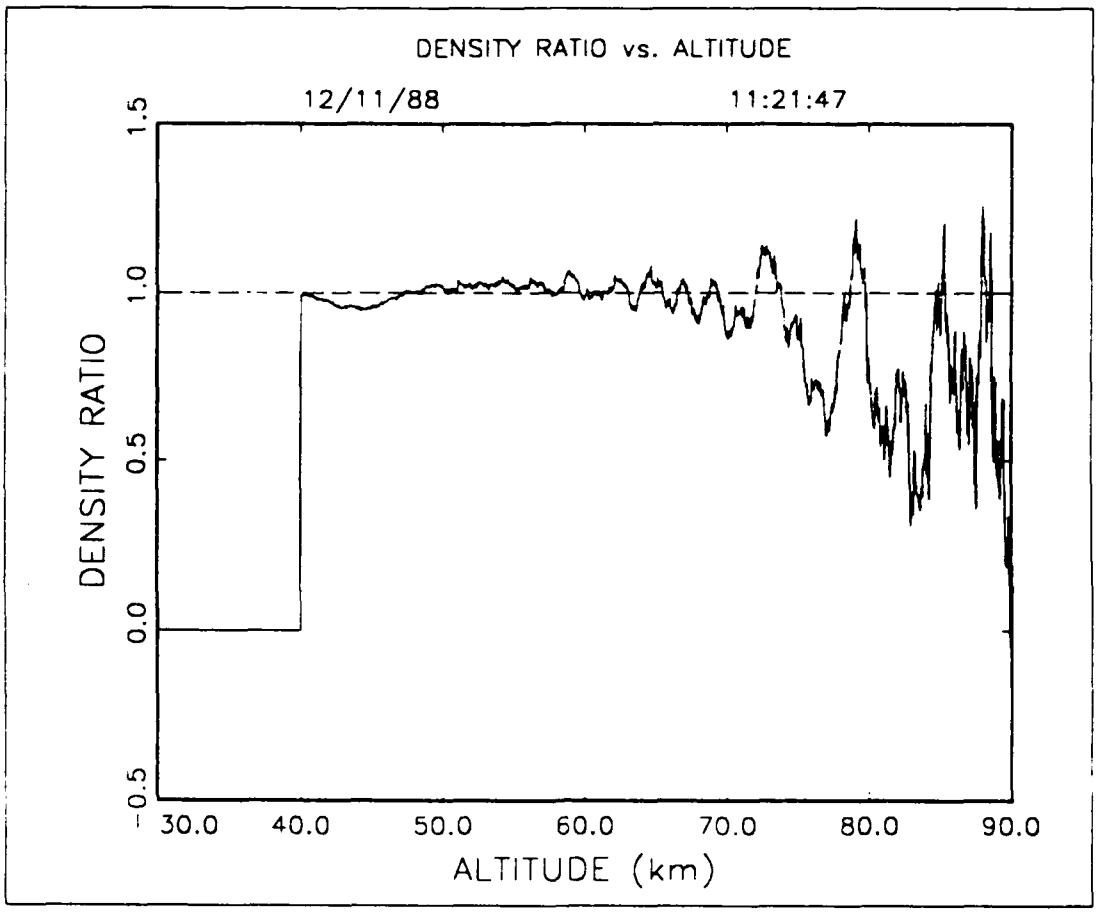

Figure 90. Plot of Density Ratio Versus Altitude for 11:21:47, 12/11/88 GMT.

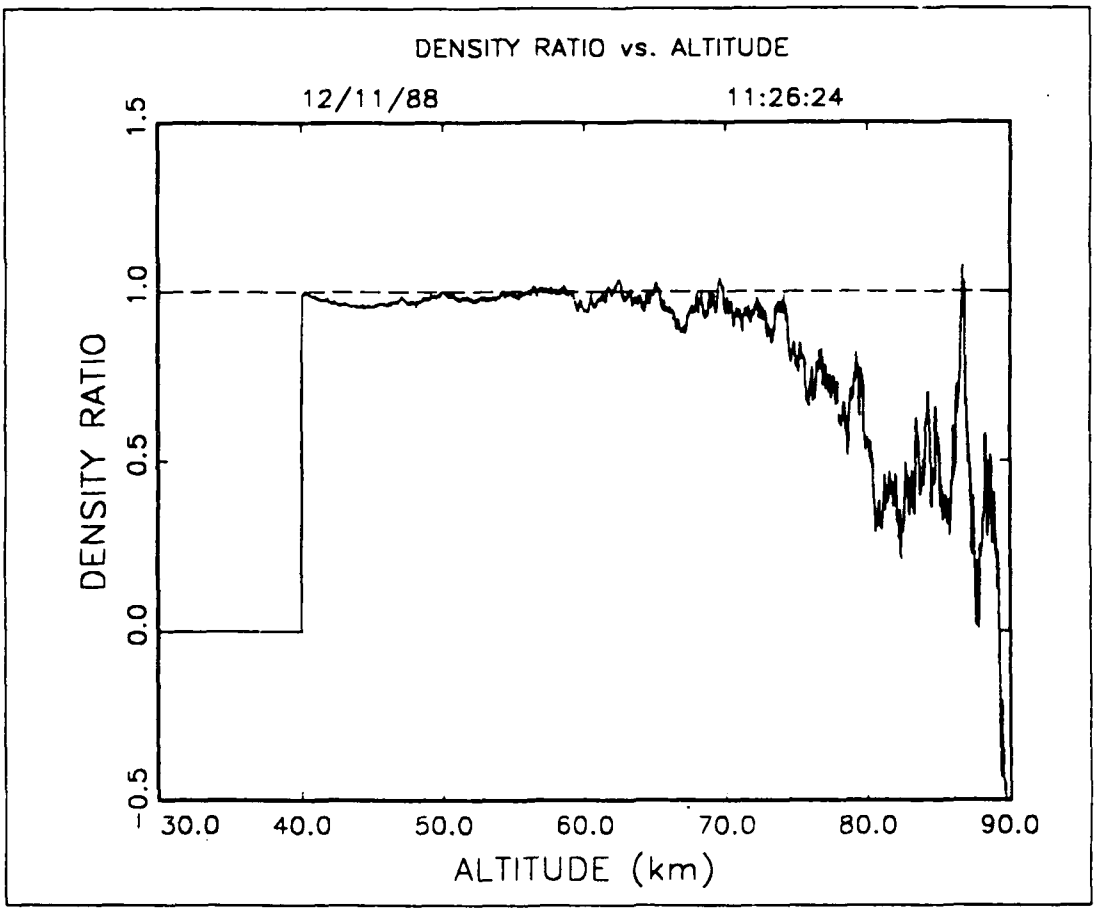

Figure 91. Plot of Density Ratio Versus Altitude for 11:26:24, 12/11/88 GMT.

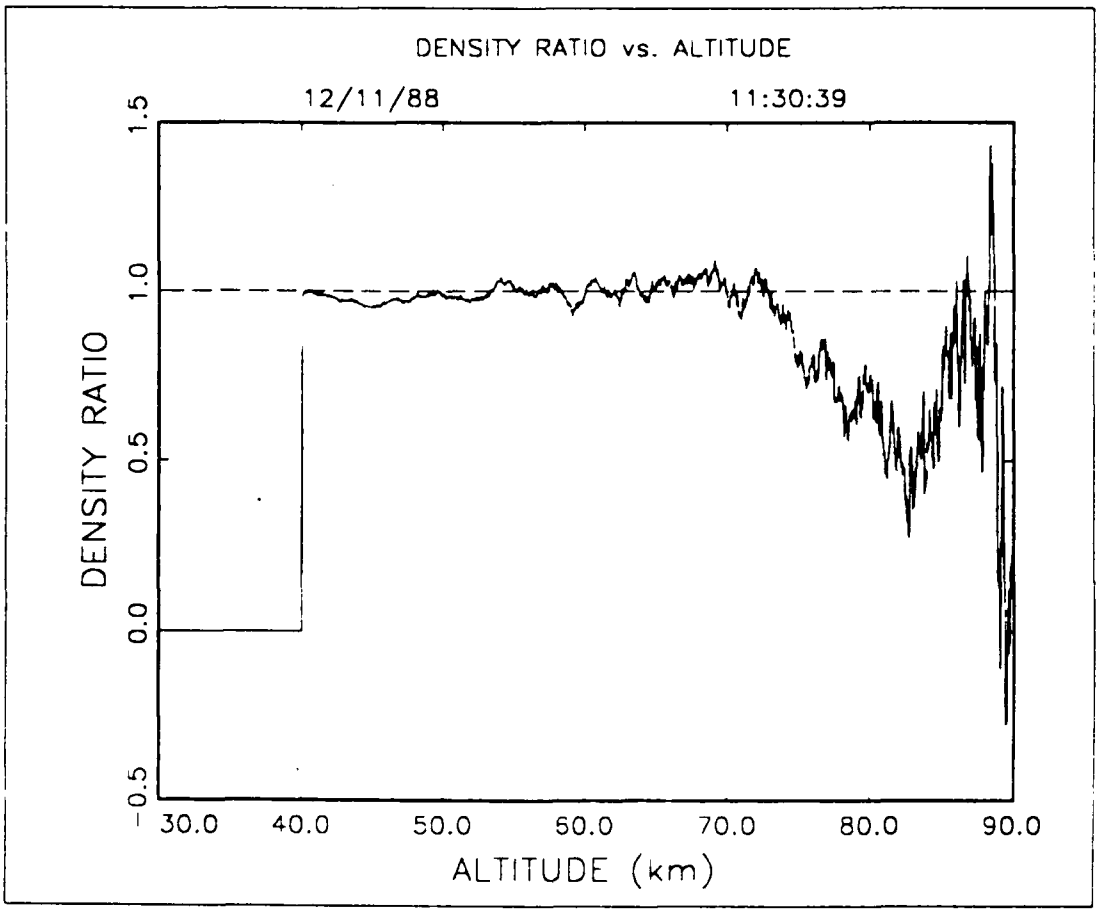

Figure 92. Plot of Density Ratio Versus Altitude for 11:30:39, 12/11/88 GMT.

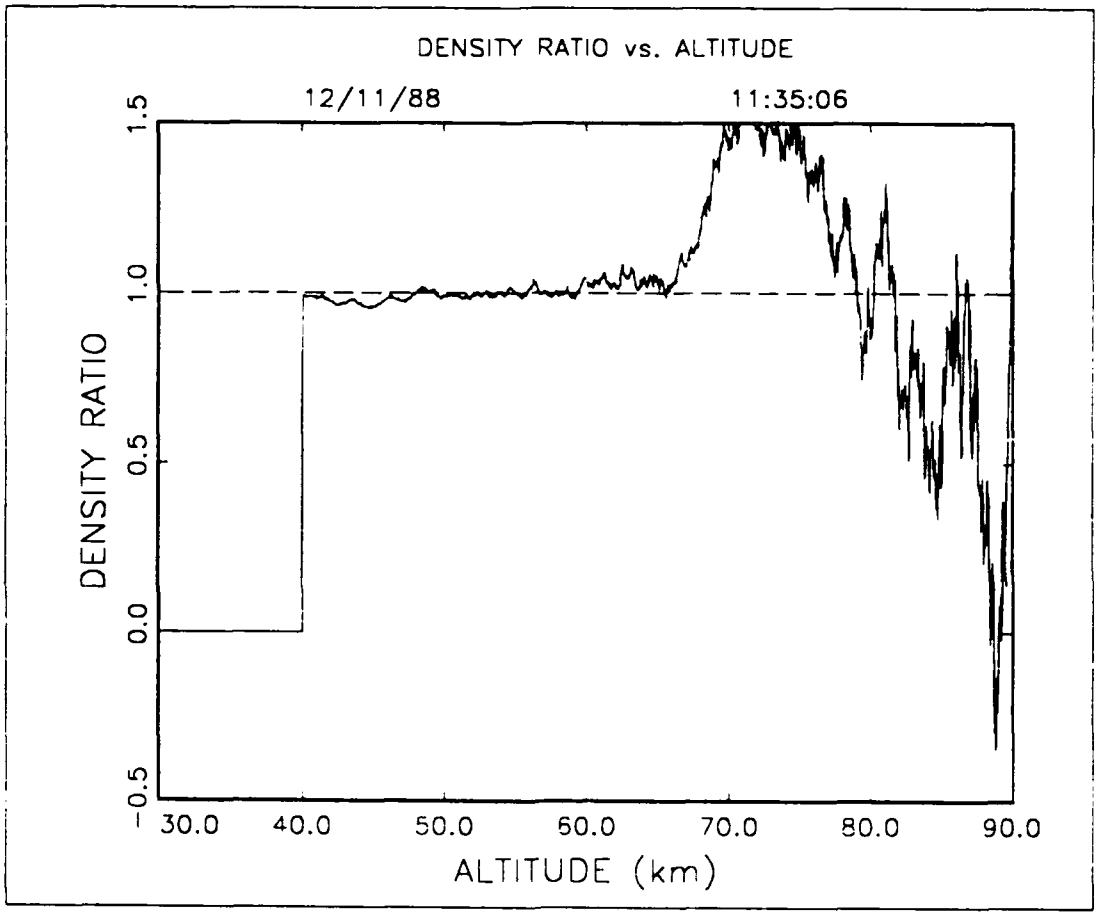

Figure 93. Plot of Density Ratio Versus Altitude for 11:35:06, 12/11/88 GMT.

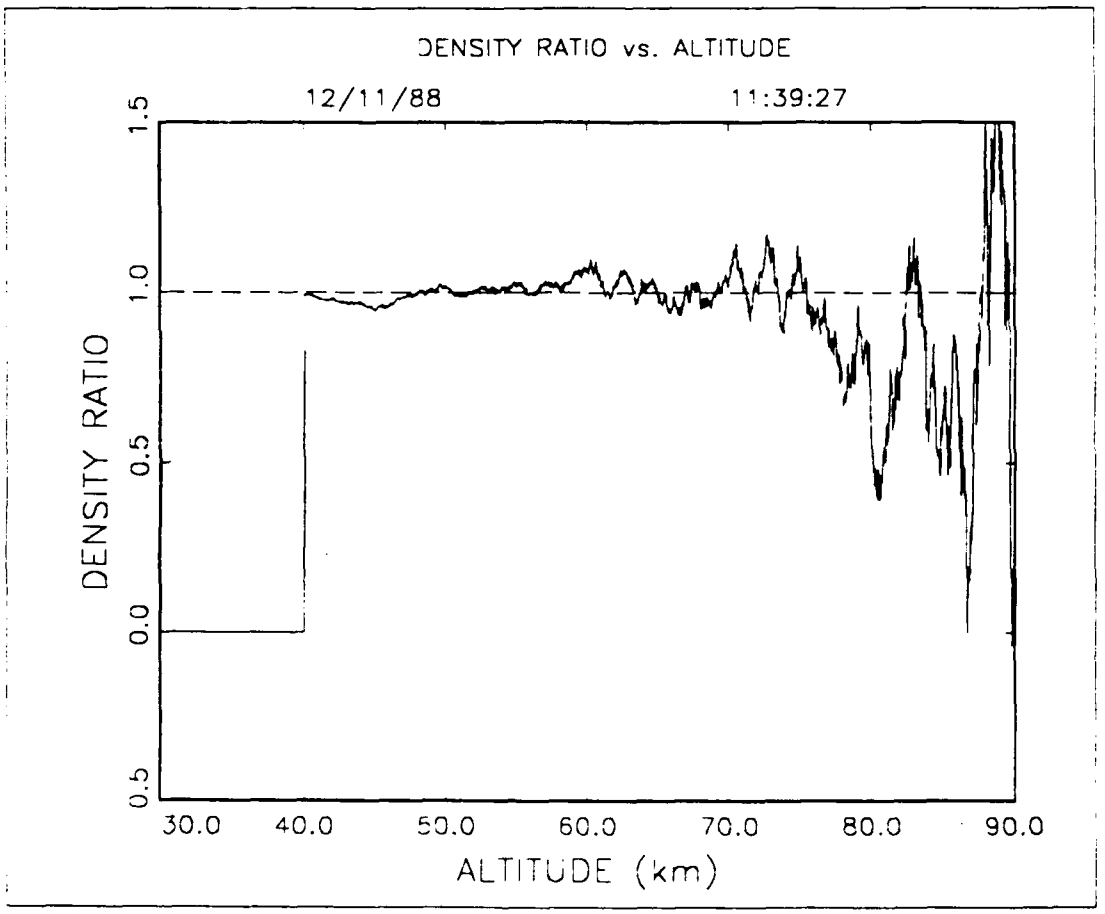

Figure 94. Plot of Density Ratio Versus Altitude for 11:39:27, 12/11/88 GMT.

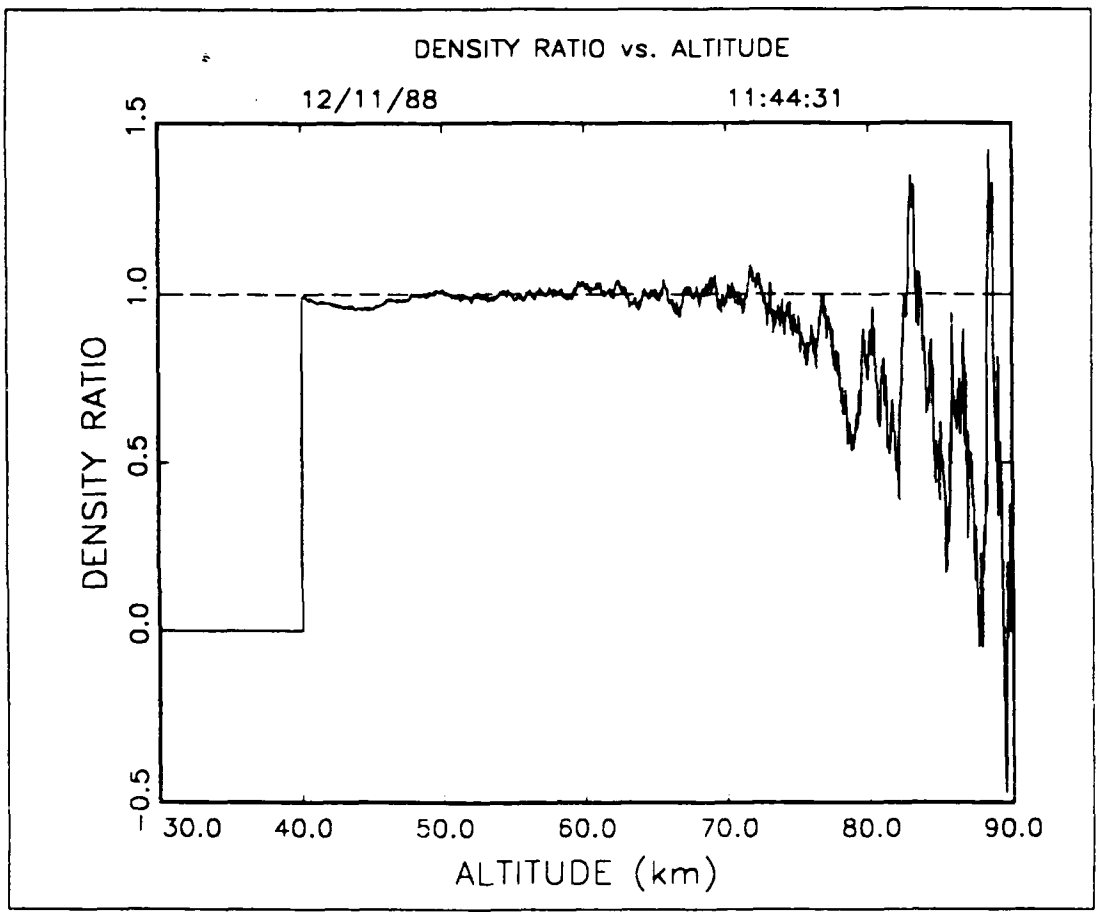

Figure 95. Plot of Density Ratio Versus Altitude for 11:44:31, 12/11/88 GMT.

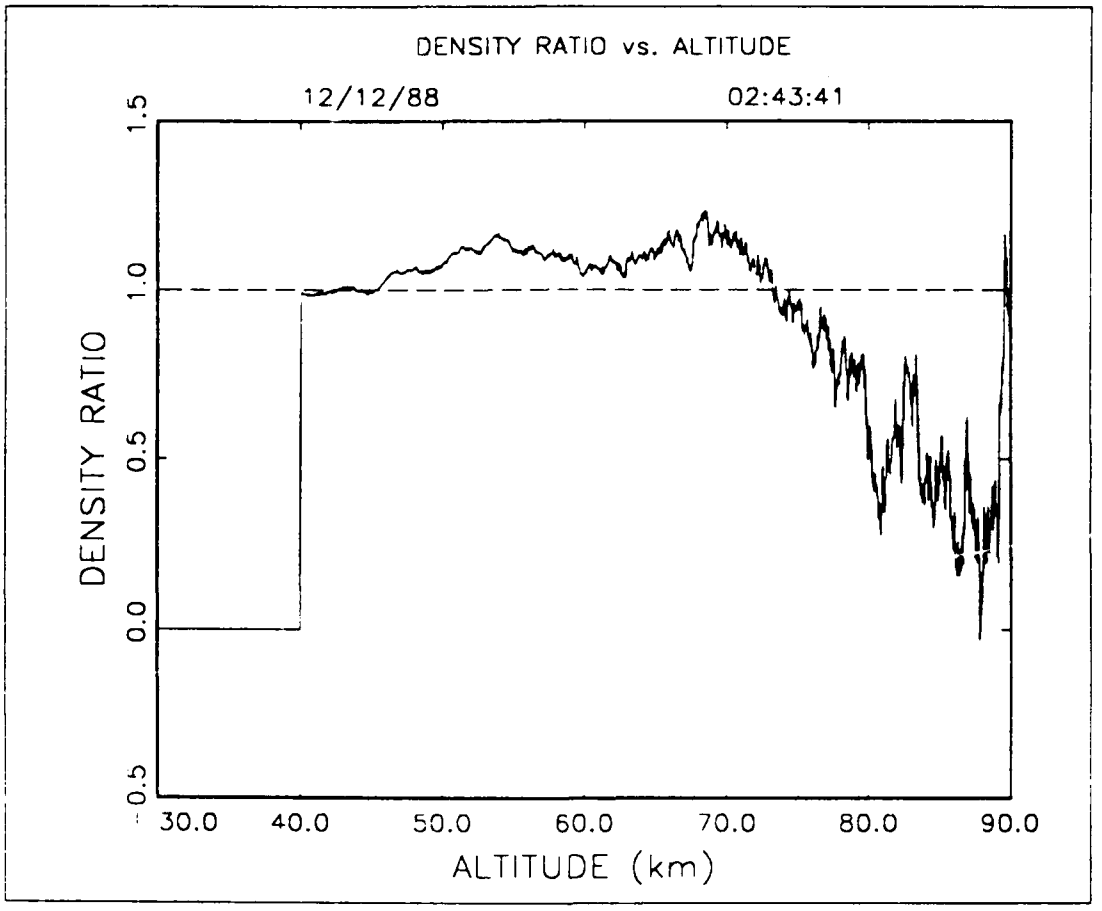

Figure 96. Plot of Density Ratio Versus Altitude for 2:43:41, 12/12/88 GMT.

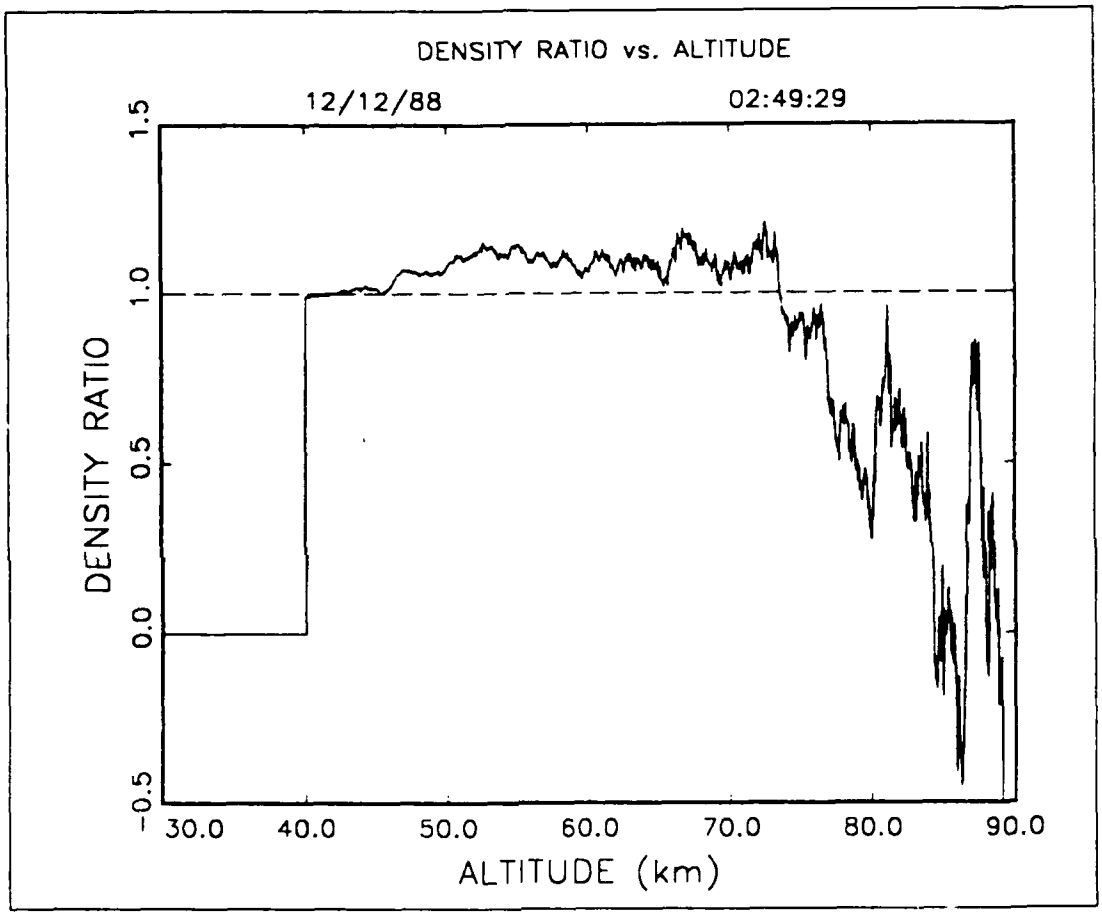

Figure 97. Plot of Density Ratio Versus Altitude for 2:49:29, 12/12/88 GMT.

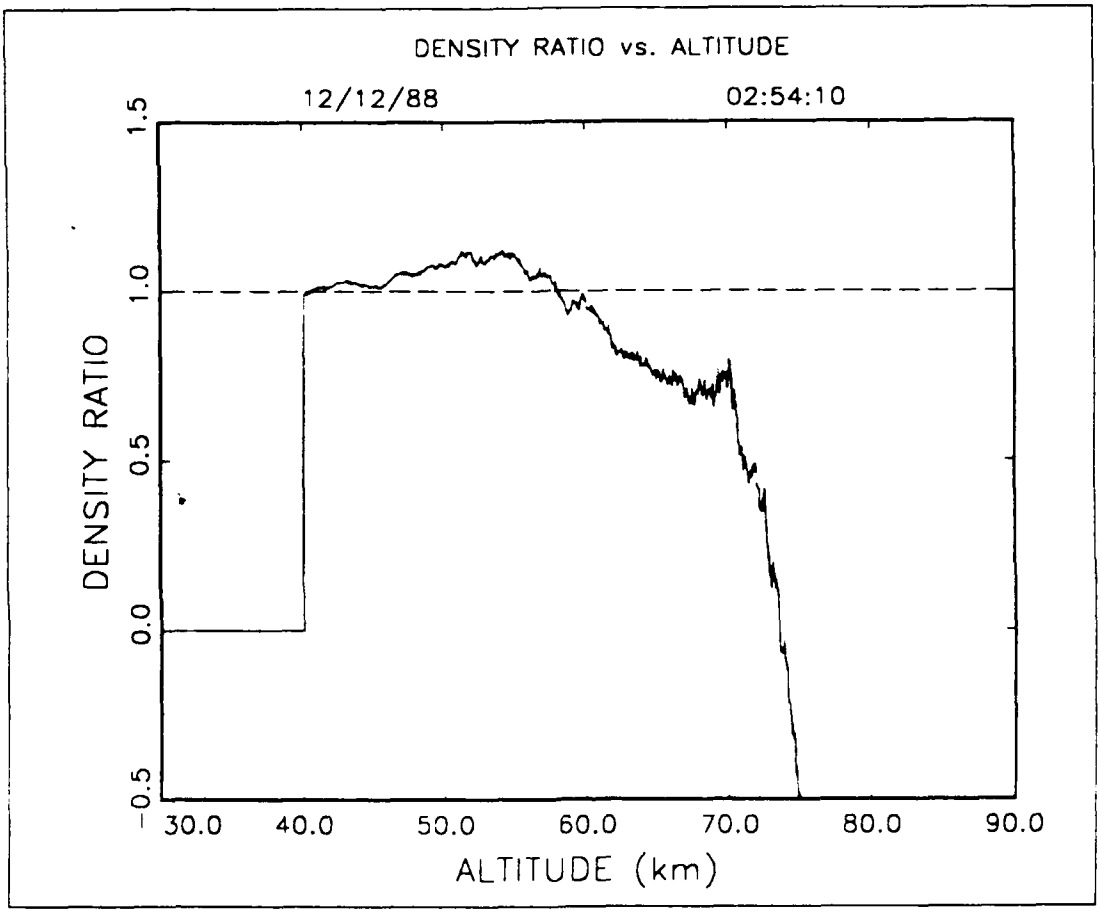

Figure 98. Plot of Density Ratio Versus Altitude for 2:54:10, 12/12/88 GMT.

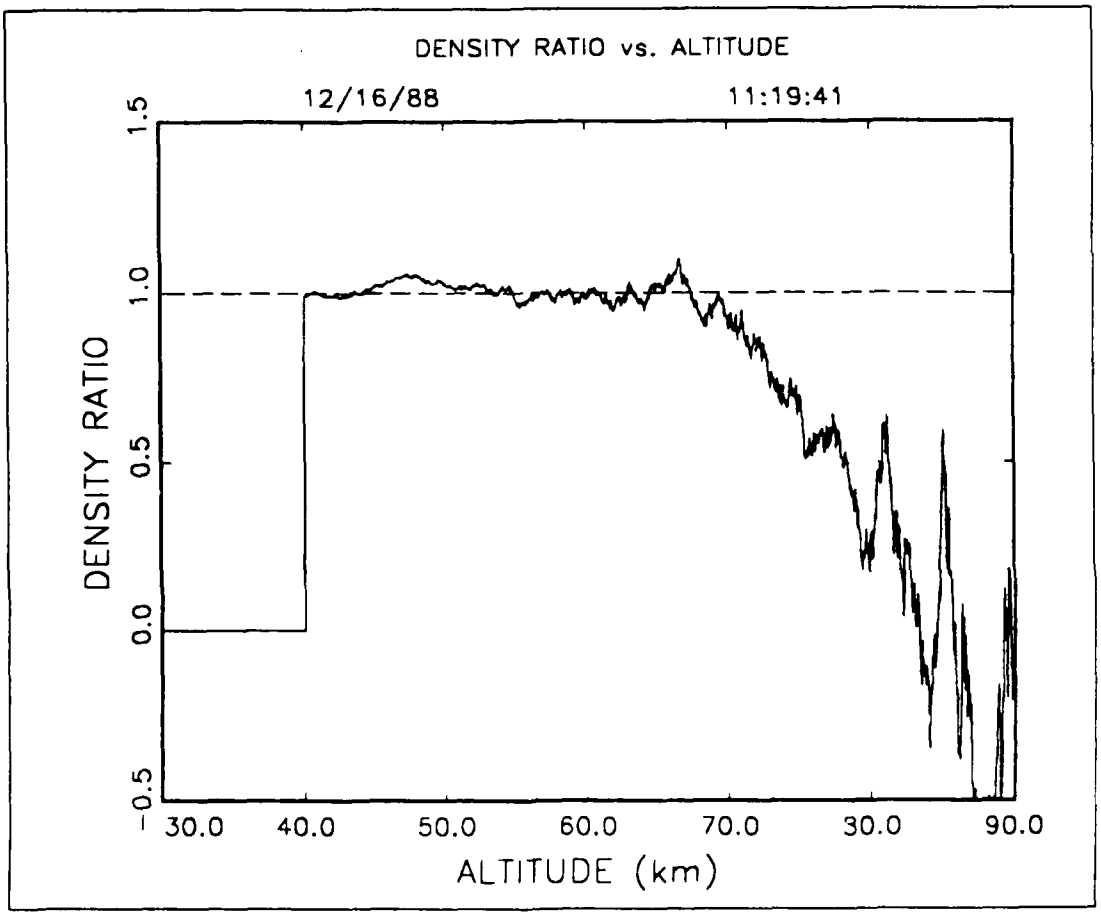

Figure 99. Plot of Density Ratio Versus Altitude for 11:19:41, 12/16/88 GMT.

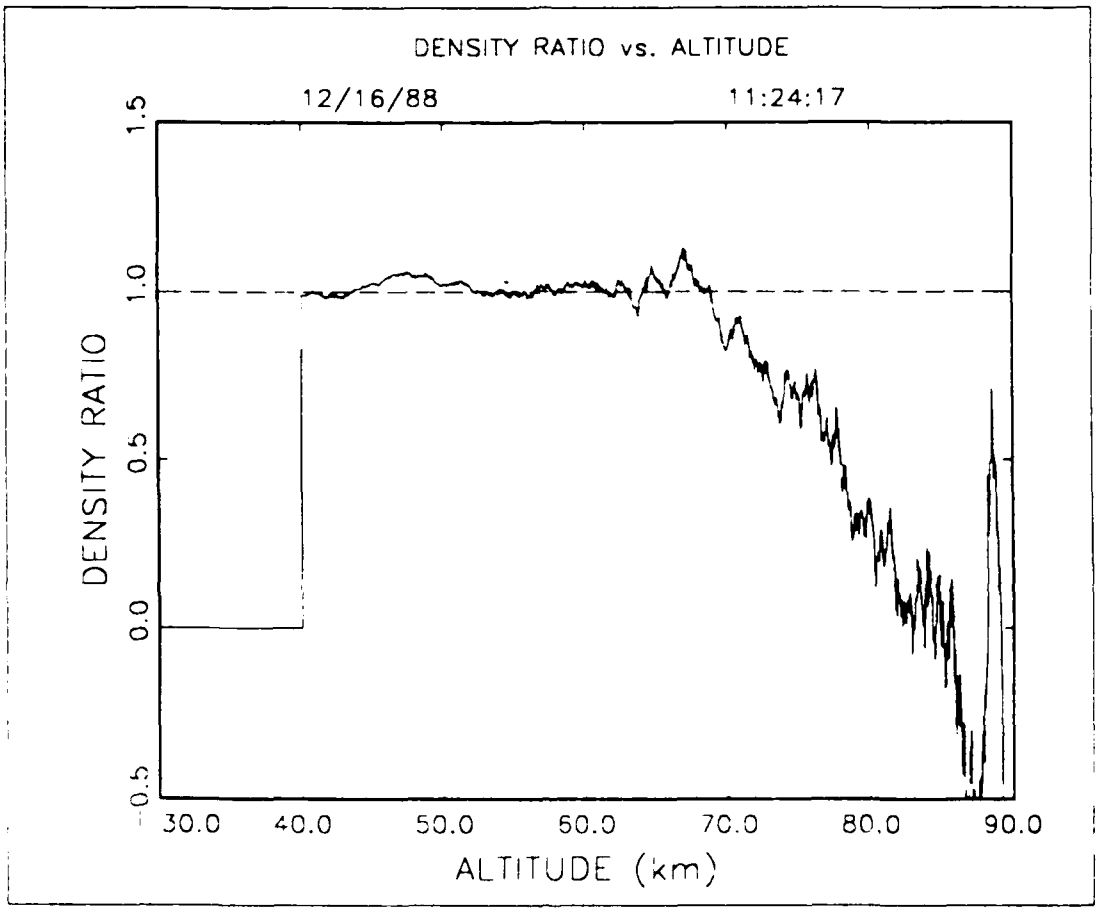

Figure 100. Plot of Density Ratio Versus Altitude for 11:24:17, 12/16/88 GMT

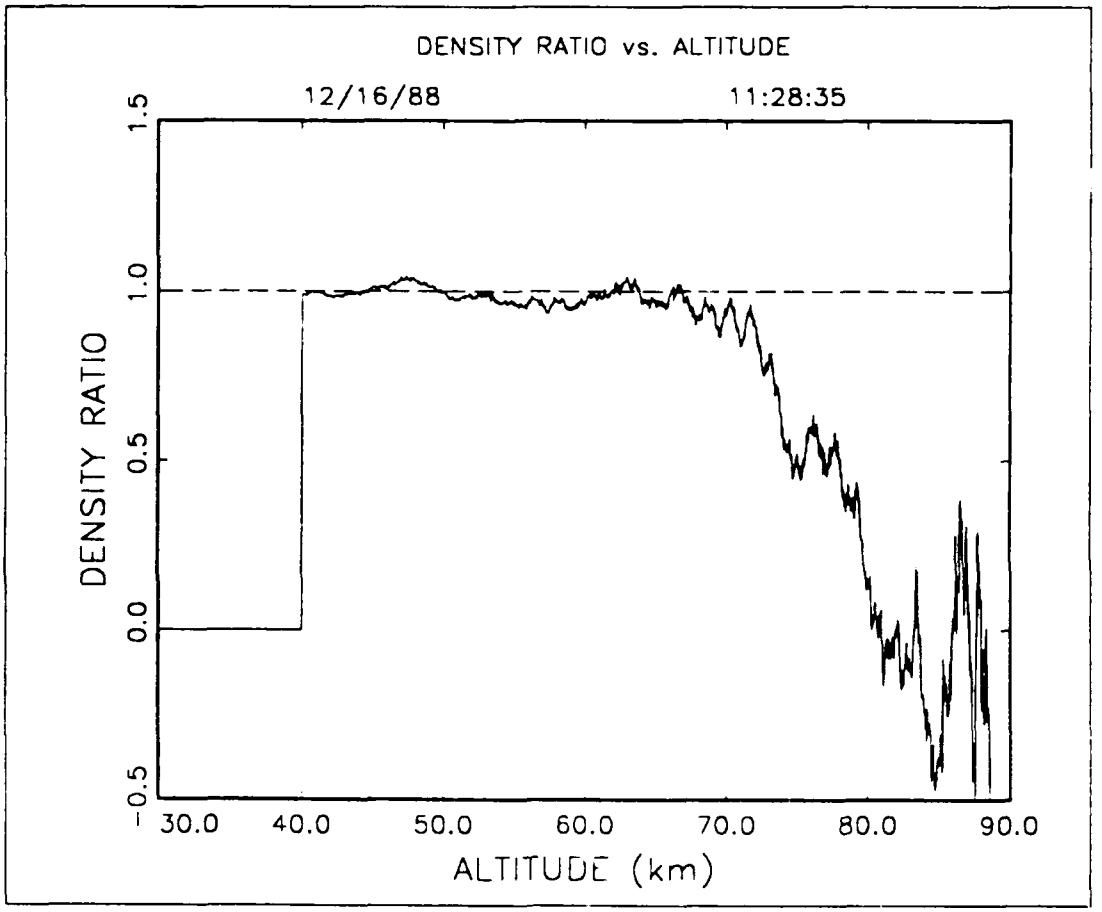

Figure 101. Plot of Density Ratio Versus Altitude for 11:28:35, 12/16/88 GMT.

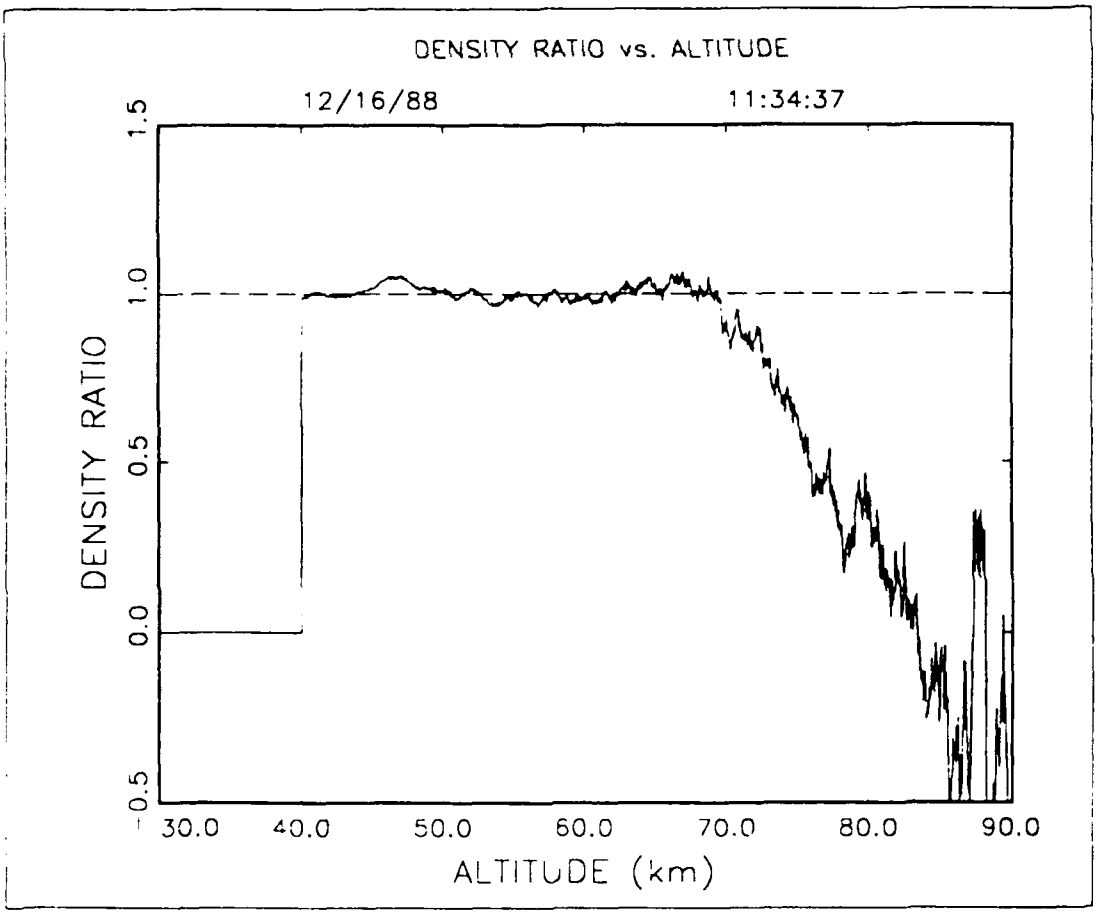

Figure 102. Plot of Density Ratio Versus Altitude for 11:34:37, 12/16/88 GMT.

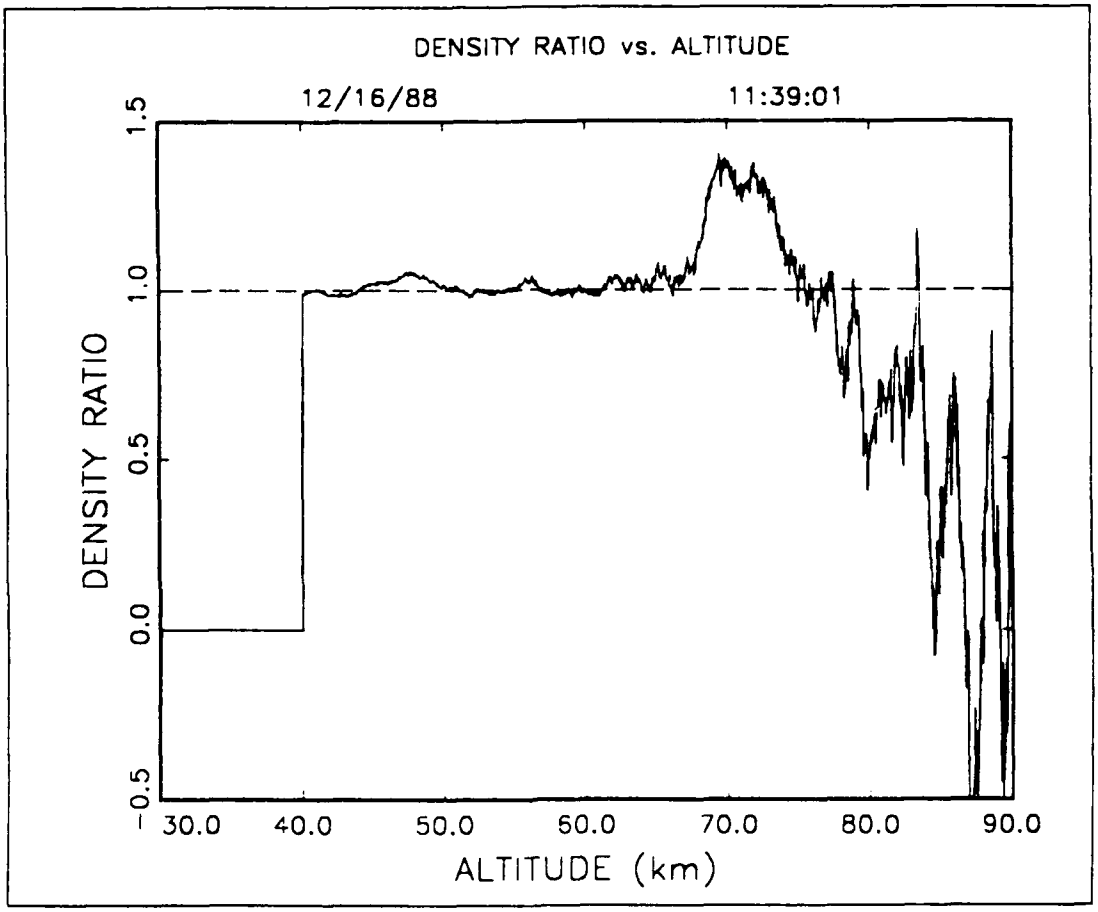

Figure 103. Plot of Density Ratio Versus Altitude for 11:39:01, 12/16/88 GMT.

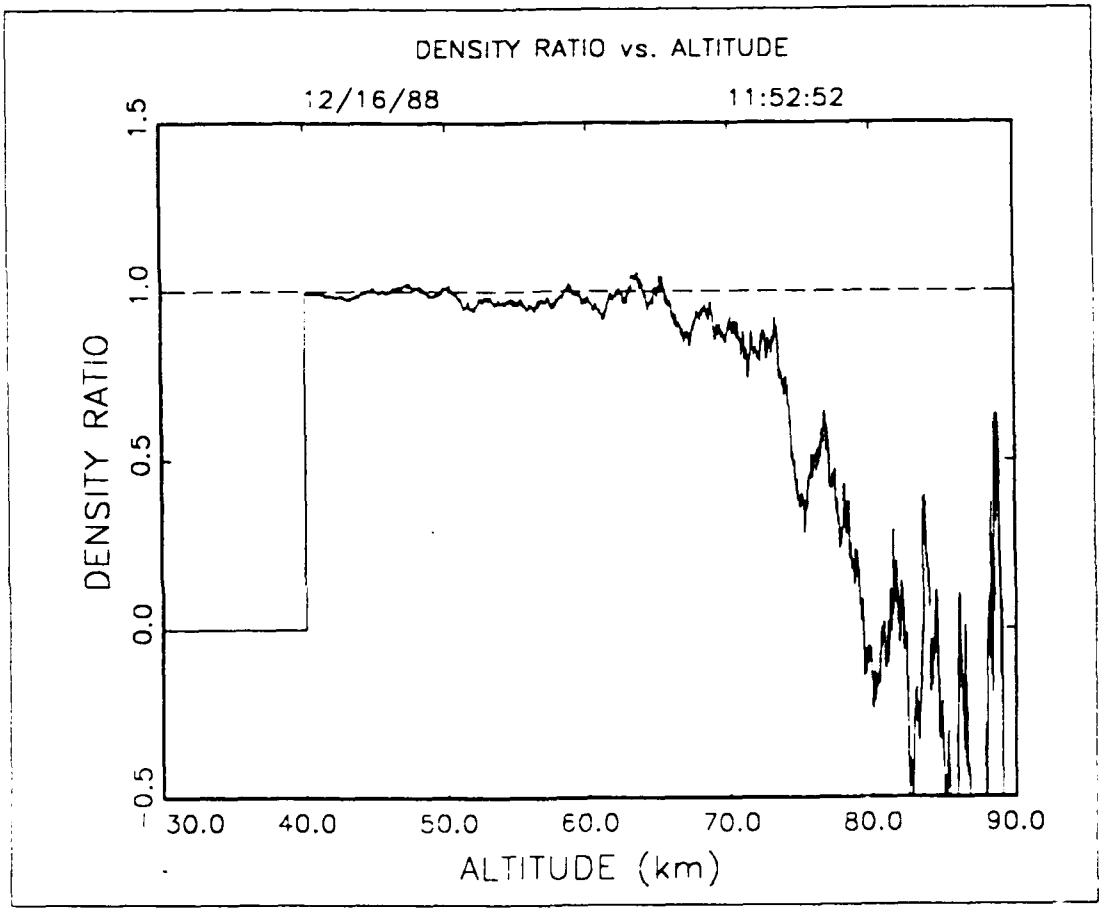

Figure 104. Plot of Density Ratio Versus Altitude for 11:52:52, 12/16/88 GMT.

9. DISCUSSION OF RESULTS AND SUMMARY

Figures 9 through 104 show that the MEGALIDAR using the lidar described in this report can measure atmospheric densities to an altitude of 85 km. Furthermore, the errors in the density ratios indicate that the deviations from a density ratio of 1.0 as the altitude increases are real up to an altitude of 85 km. The variations in the ratios for altitudes above about 75 km appear to be outside the error limits but a definite conclusion requires more detailed analyses. The consistency of the variation of the ratios with altitude up to about 75 km from record to record during a particular episode supports the accuracy of the error analysis. Also,this consistency within an episode shows clearly that the difference in the variations with altitude that occurs in episode 3 is an atmospheric phenomenon rather than an instrumental artifact. The variation in the ratios in a single plot above 85 km are shown because returns were received from these altitude, but they are thought not to be significant. The S/N of the returns received with the 100-inch mirror were well within those predicted using the Georgia Tech lidar as the baseline. Hence it is concluded that the reflectivity and general condition of the mirror are not in question.

Thus, the proof-of-concept demonstration showed that the 100-inch collimator can be used successfully as a Rayleigh lidar and that it can consistently and accurately collect data from altitudes that are difficult if not impossible to get with a smaller collector. Not only can the MEGALIDAR reach higher altitudes, it can get useable data in shorter averaging times than most receivers and hence can be used to observe atmospheric phenomenon that have a short time scale. The demonstration also showed that the facilities around the collimator are adequate for lidar measurements, but could be made much more convenient and efficient for lidar operation with a few modifications.

REFERENCES

1. Garrison, A. K., G. W. Grams, E. M. Patterson, and D. W. Roberts, 1989,"MEGALIDAR," AFWAL-TR-88-1128, Air Force Wright Aeronautical Laboratories, Wright-Patterson Air Force Base, Ohio.

2. Garrison, A.K. "MEGALIDAR SENSITIVITY," Memo to Jan Servaites, 11/5//88.

3. Garrison, A.K., J. M. Cathcart, G. G. Gimmestad, D. W. Roberts, "MEGALIDAR Proof of Concept Demonstration Test Plan," AFWAL Briefing, August, 1988.

APPENDIX A: INTERCONNECTION AND CIRCUIT DIAGRAMS

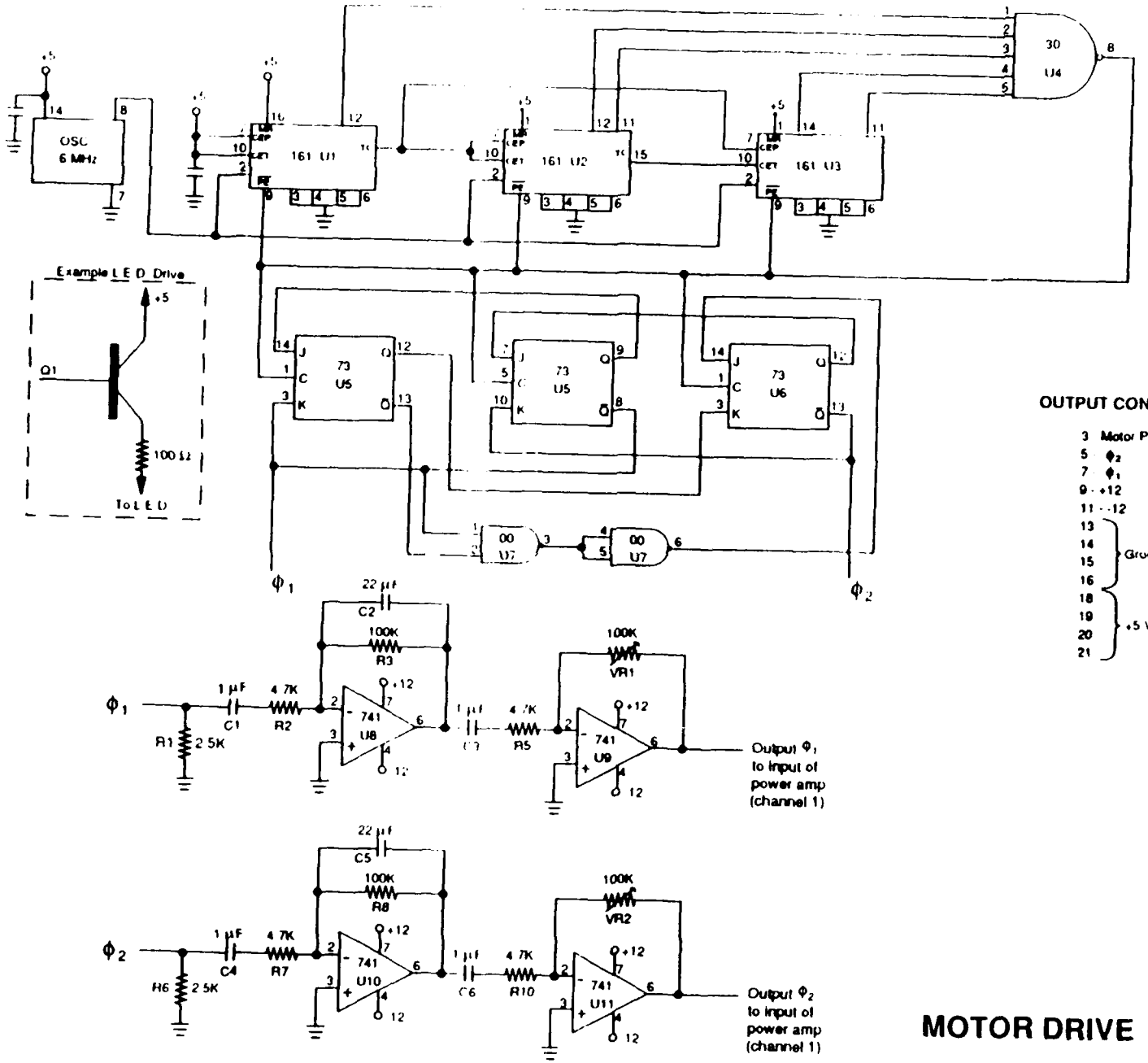

OUTPUT CONNECTIONS

3	Motor Pickup
5	ϕ_2
7	ϕ_1
9	+12
11	-12
13, 14, 15, 16	Ground
18, 19, 20, 21	+5 Volts

MOTOR DRIVE

R C. Du Varney
W Brittain 1988

MOTOR CONNECTION DIAGRAM

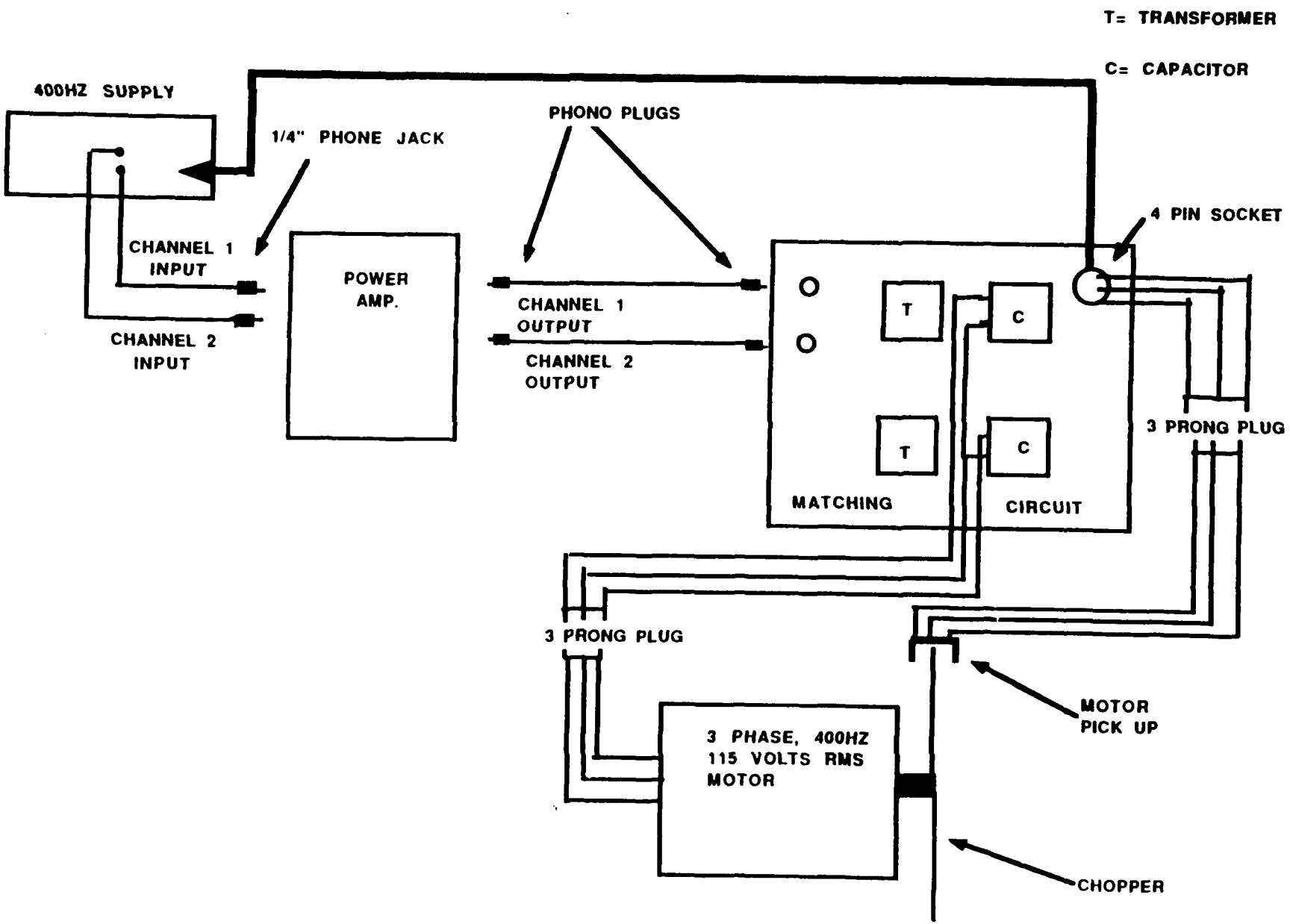

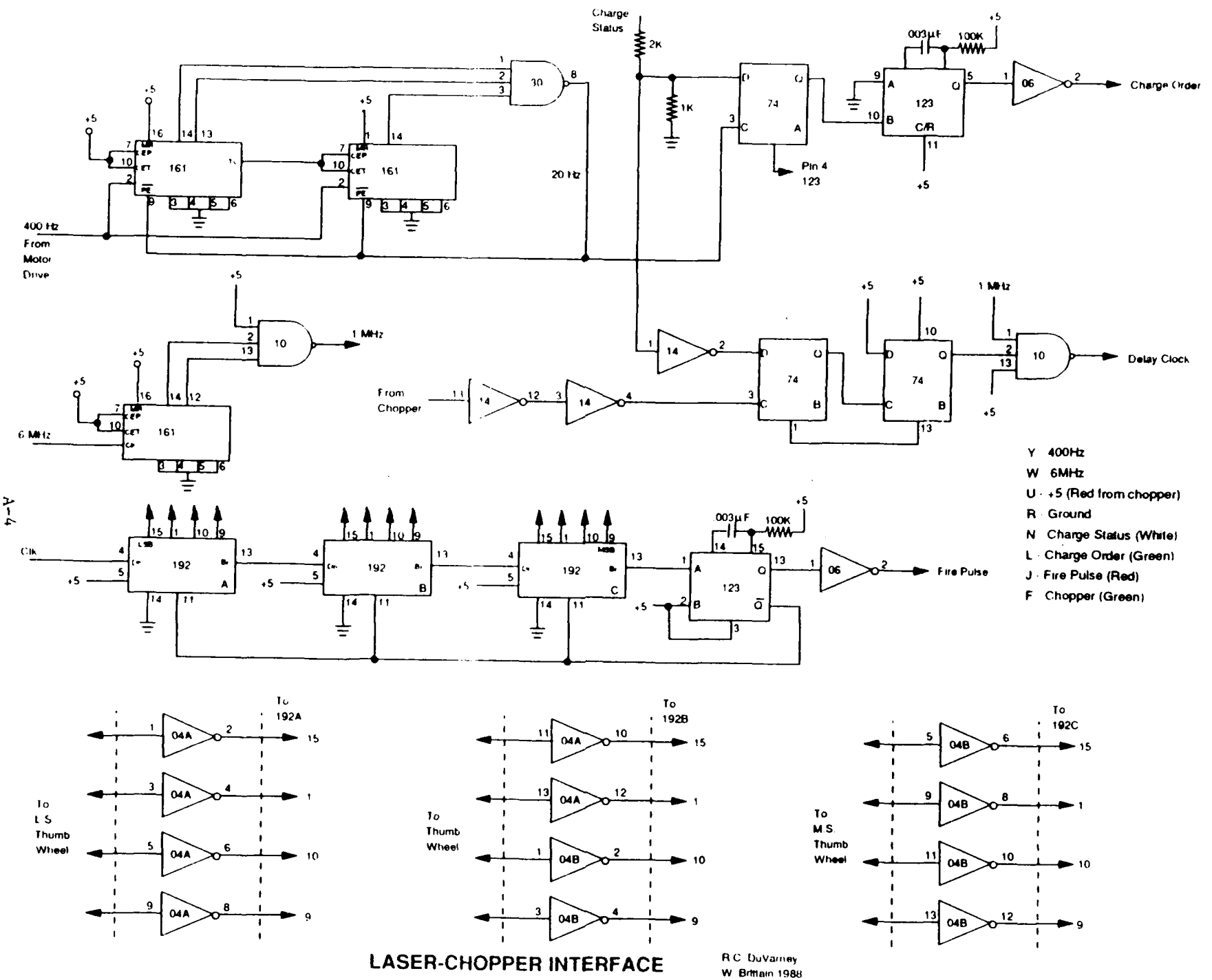

A-4

LASER-CHOPPER INTERFACE

R C DuVarney
W Britain 1988

LIDAR SYSTEM CABLING DIAGRAM

GGG 5/18/89

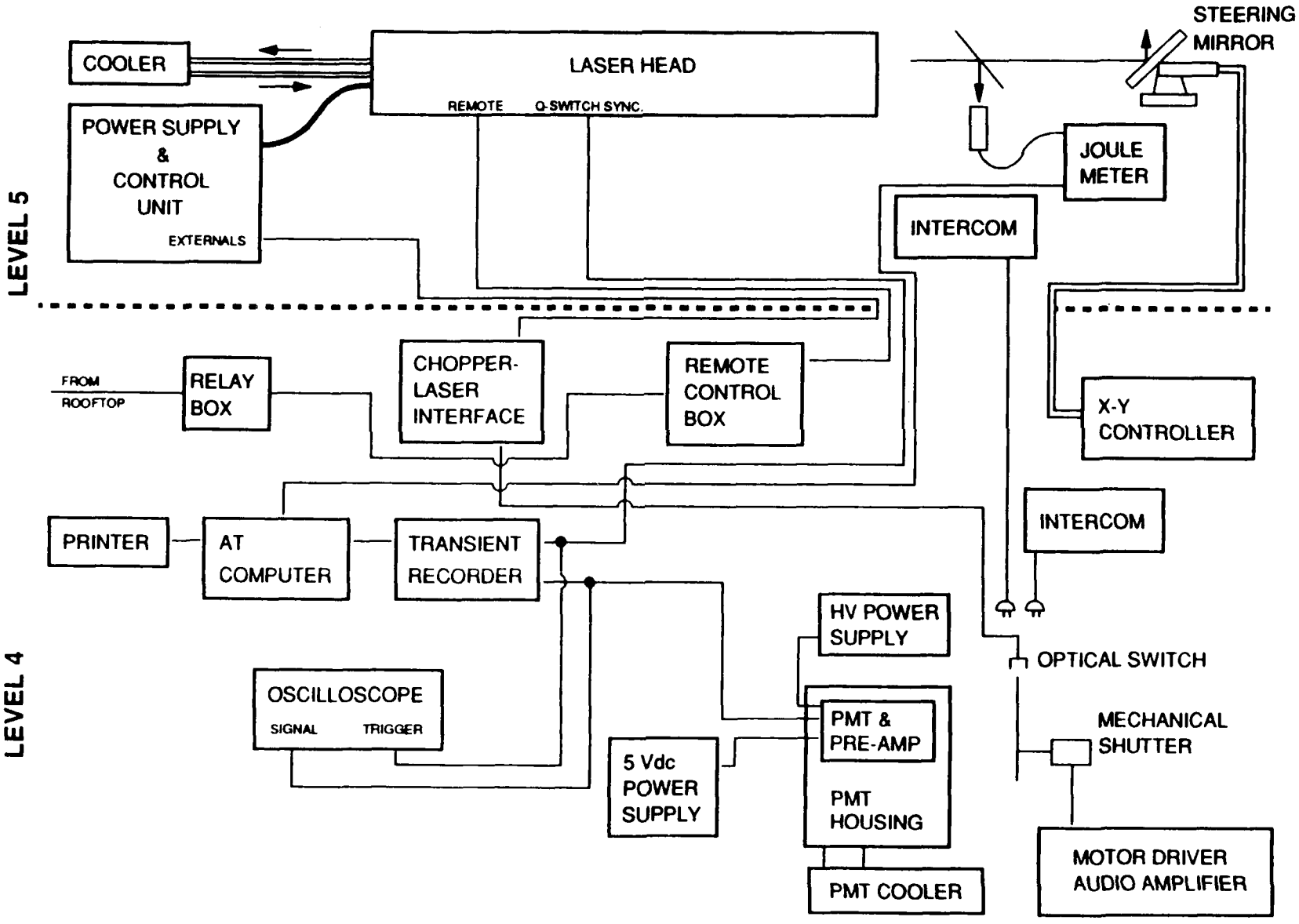

RADAR SAFETY SYSTEM CABLING DIAGRAM

GGG 5/18/89

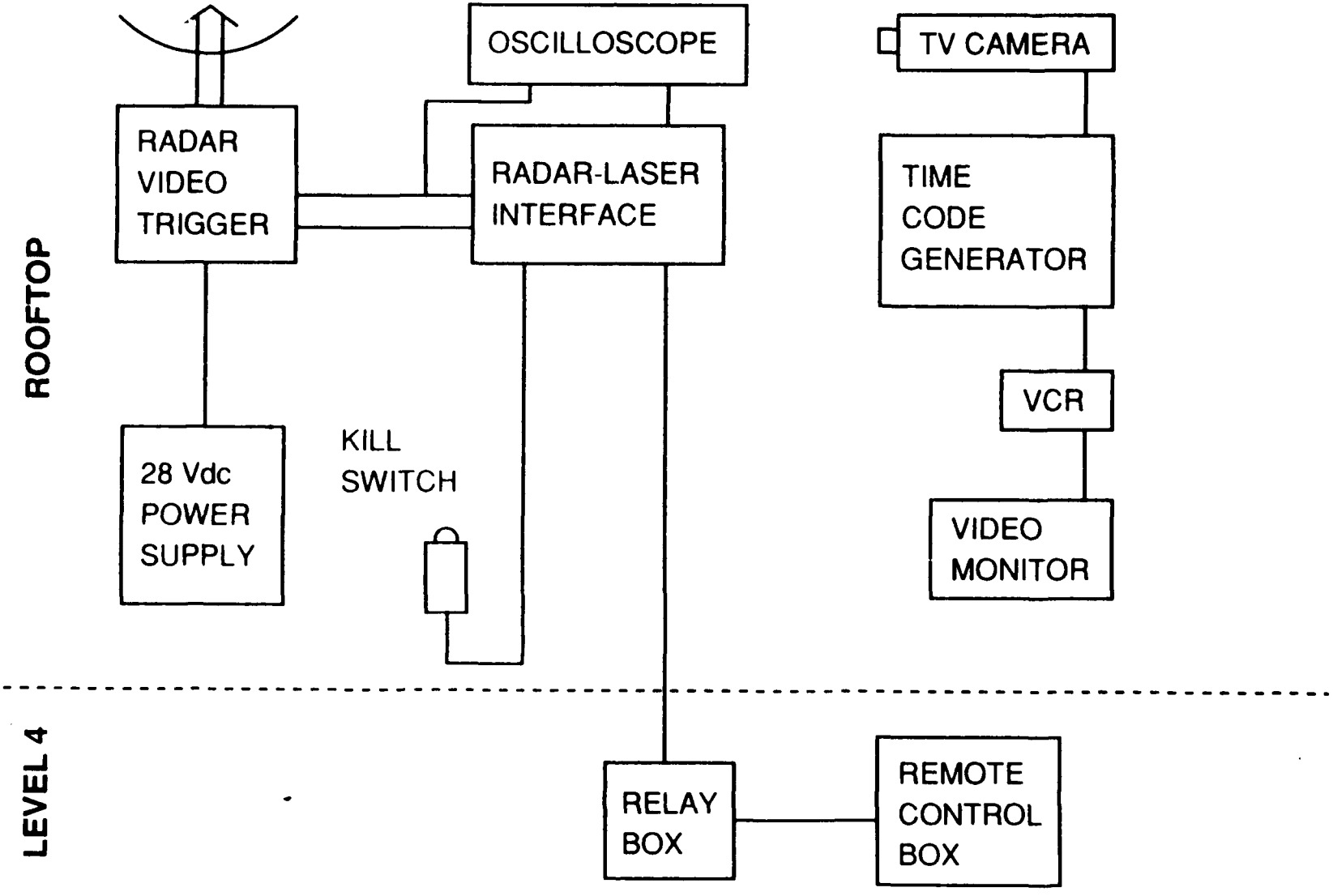

APPENDIX B: STANDARD AND EMERGENCY OPERATIONS PROCEDURES MANUAL

MEGALIDAR PROOF-OF-CONCEPT DEMONSTRATION
· Standard and Emergency Operating Procedures

Revised 16 November 1988

EO SENSOR/ATMOSPHERIC SCIENCE GROUP
Electro-Optics Branch
Mission Avionics Division
Avionics Laboratory
Air Force Wright Aeronautical Laboratories

in conjunction with

Electro-Optics Division
Electromagnetics Laboratory
Georgia Tech Research Institute
Georgia Institute of Technology
Atlanta, GA 30332

TABLE OF CONTENTS

1. **EXPERIMENT DESCRIPTION** B-5
   - 1.1 Experimental Set up B-5
     - 1.1.1 Lidar System B-5
     - 1.1.2 Safety Systems B-7
   - 1.2 Dates of Tests B-7
   - 1.3 Times of Operation B-8
   - 1.4 Weather Conditions Required B-8
2. **STANDARD OPERATING PROCEDURES** B-9
   - 2.1 Duties of Test Crew B-9
     - 2.1.1 Duties of the Test Director B-9
     - 2.1.2 Duties of the Laser Operator B-9
     - 2.1.3 Duties of the Observer B-9
   - 2.2 Turn on Procedure B-10
     - 2.2.1 Opening the Roof Hatch B-10
     - 2.2.2 Laser System Turn On B-10
     - 2.2.3 Data System Turn On B-11
     - 2.2.4 Surveillance System Turn On B-11
   - 2.3 Normal Operation B-11
     - 2.3.1 Test Director B-11
     - 2.3.2 Observer B-12
     - 2.3.3 Laser Operator B-12
   - 2.4 Turn Off Procedure B-12
   - 2.5 Visitor Control B-13
3. **HAZARD ANALYSIS** B-13
   - 3.1 Safe Eye Exposure Distance (SEED) Analysis B-13
   - 3.2 Radar Hazard Zone B-14
   - 3.3 Collimator Facility in Building 622 . . . . . B-14
   - 3.4 Airspace B-14
4. **ENVIRONMENTAL IMPACT ANALYSIS** B-14
   - 4.1 Description of Laser B-14
   - 4.2 Summary of Hazards B-14
     - 4.2.1 To Materials B-15
     - 4.2.2 To Living Organisms B-15
   - 4.3 Previous Experience B-16
     - 4.3.1 At Other Sites B-16
     - 4.3.2 At Building 622 . . . . . B-16
   - 4.4 Effects on Environment B-16
5. **EMERGENCY OPERATING PROCEDURES** B-16
   - 5.1 Exposure B-16
   - 5.2 Building 622 . . . . . B-17

LIST OF TABLES

Table No.	Title	Page
B-1	Laser Parameters	B-6

1. EXPERIMENT DESCRIPTION

The experiment described here will be carried out under contract No. F 33615-86-C-1051, Task No. 88-5-3, "MEGALIDAR Proof-of-Concept Demonstration," by personnel from the Georgia Tech Research Institute (GTRI), in conjunction with personnel from the Avionics Laboratory.

The 100-inch collimator in building 622 will be modified to serve as a large lidar system (known as the MEGALIDAR) by installing a laser transmitter, an optical receiver, and a data system. A safety radar system will be installed on the roof of building 622. The system configuration is illustrated in the attachment entitled "MEGALIDAR System Configuration."

This system will be unique because it will have the largest receiving aperture of any lidar in the USA. This means that the collimator can potentially be the basis for very sensitive lidar systems. The collimator has other notable features [rigid mechanical construction, temperature control system, etc.] which may also contribute to making a first-class lidar facility.

The collimator was constructed in 1963 at a cost of $5 million. Estimated cost to duplicate it today is $25 million. The lower half of the collimator is embedded in solid rock. It cannot, of course, be moved to another location.

The experiment described here is a short-term demonstration. The objective is to demonstrate the usefulness of the MEGALIDAR to programs concerned with middle-atmosphere flight dynamics by measuring atmospheric density at altitudes up to 80 km. The measurements were planned to extend over a period of four weeks; because of delays they are now planned for one week.

1.1 Experimental Set up

1.1.1 Lidar System

The laser transmitter will be installed in the 20-foot diameter cross tunnel on level 5. It includes a laser, its power supply and cooler, and associated electro-optical components to expand and steer the laser beam and to measure the energy of each laser pluse. The laser itself is not unusual - it is a standard model YG581C doubled-YAG laser purchased from Quantel. Laser parameters are listed in Table B-1.

TABLE B-1 Laser Parameters

Wavelength:	532 nm
Energy per pulse (max.):	500 mJ
Pulse repetition rate:	16.7/sec.
Beam diameter	
raw beam:	9 mm
expanded beam:	30 mm
Beam divergence ($1/e^2$)	
raw beam:	0.6 mr
expanded beam:	0.1 - 0.2 mr

The optical receiver is a module attached to the f/6 port of the collimator, on level 4. It consists of several lenses, a narrow-band filter centered at 532-nm wavelength, a photomultiplier tube (PMT), and a mechanical shutter which shields the PMT from near-by lidar returns.

The data system is also on level 4, adjacent to the receiver. It is based on a transient digitizer and an IBM AT microcomputer, and it is also includes the control circuitry for the mechanical shutter as well as various power supplies.

In normal operation, the entire system will be controlled by a test director on level four, at the data system. A laser operator will be required in the cross tunnel on level 5, however, in the following circumstances:

- during turn on.
- periodically during the measurements, to retune the laser (because of thermal drift).
- in the event of Laser system failure.
- during turn off.

1.1.2 Safety Systems

Safety Systems are shown schematically in the attachment entitled "Aircraft Warning and Documentation System." An Observer will be stationed on top of building 622. His primary responsibility is to ensure that the laser beam is off at all times when aircraft are present in the airspace around building 622. The Observer will carry a laser kill switch in his hand at all times, and he has the following means to detect aircraft:

- acoustic surveillance. The Observer will be able to hear low-flying aircraft. Previous experience at this site shows that the Observer will often hear aircraft before he sees them.

- visual surveillance. The Observer will constantly scan the entire airspace, looking for aircraft flying too high to be easily heard.

- radar surveillance. A radar will be installed on the roof of building 622, pointing in the same direction as the laser beam. It will have an interlock to automatically shut off the laser if it detects an aircraft.

A document entitled "Radar Safety System" is attached.

A log will be kept of all events during which the laser was shut off because of the presence of aircraft (see attached sample copy of log sheet entitled MEGALIDAR Operation Log).

As described below, this demonstration will be conducted during hours of darkness in clear weather conditions only. This makes visual detection of aircraft easy, because their lights are easily visible. The combination of acoustic, visual, and radar detection with hardware interlock with complete record keeping is considered to be more than adequate to ensure that no airborne personnel are endangered by the laser beam, and to document that fact.

ANSI Class IV laser warning signs will be placed across the only door to the collimator cross tunnel containing the laser, and at both the elevator and stairwell entrances to the roof.

1.2 Times of Operation

In the Proof-of-Concept Demonstration, the MEGALIDAR will be used in its most sensitive configuration and will therefore be adversely affected by background light. Operation will only be possible during darkness, roughly 1 hour after sunset to 1 hour before sunrise.

1.3 Weather Conditions Required

Clear air is required for this demonstration, for two reasons:

- The collimator cannot be opened to the atmosphere during periods when there is any chance of precipitation, because of possible damage to the primary mirror.

- Clouds would attenuate the laser beam, and significantly limit the system's ability to measure at high altitudes.

2. STANDARD OPERATING PROCEDURES

2.1 Duties of Test Crew

The test crew will have three members: the Test Director, who will always be at the data control center on level 4; the Laser Operator, who will be in the cross tunnel on level 5 during turn on, turn off, and occasionally as needed during the course of the measurements; and the Observer, who will always be on the roof of building 622 when measurements are in progress.

Both the Test Director and the Laser Operator will be GTRI personnel, and both will be familiar with the laser and able to carry out any emergency procedures if required

2.1.1 Duties of the Test Director:

- to ensure safe and proper operation of the MEGALIDAR
- to provide overall test direction and coordination
- to maintain communication with the Laser Operator (when he is in the cross tunnel) and the Observer
- to ensure that all other personnel comply with the procedures in this document

2.1.2 Duties of the Laser Operator:

- to ensure safe and proper operation of the laser
- to maintain communication with the Test Director when in the cross tunnel
- to control access to the cross tunnel when the laser is in operation

2.1.3 Duties of the Observer:

- to ensure that no aircraft enter the laser beam, by maintaining acoustic, visual and radar surveillance of the airspace around building 622.
- to carry a laser kill switch at all times
- to maintain constant communication with the Test Director during measurements
- to control access to the roof of building 622 during measurement periods
- to maintain a written log of all times and dates when the laser beam was turned off because of the presence of aircraft, and to video tape the oscilloscope display of radar data [with date and time information].

NOTE

Nothing in these procedures shall preclude any member of the crew from issuing a stop transmitting directive to the Test Director should that crewmember detect the development of any condition that he/she feels may be unsafe.

2.2 Turn on Procedure

A crew of three persons is required for these procedures.

2.2.1 Opening the Roof Hatch

Before the hatch is opened, the Test Director will determine that rooftop winds are not so strong as to pose a hazard to personnel. At level 9, with the collimator end cap closed, one person will stand on the end cap and release the chains which hold the roof hatch closed. Two persons on the roof will open the hatch doors and pull the chains up onto the roof.

Rooftop personnel will remain in the immediate vicinity of the roof hatch during this procedure.

The crew will then remove the collimator end cap. The Observer will return to the roof, while the other personnel proceed to levels 4 and 5.

2.2.2 Laser System Turn On

The laser operator will turn on the lights in the cross tunnel and conduct a visual inspection of the laser system, to ensure that all electrical wiring is properly installed; to ensure that the cooling system is not leaking; to ensure that no foreign objects are in the laser beam path or blocking walk ways; and to ensure that no unauthorized personnel are in the cross tunnel.

The laser operator will then turn on the Molectron Joule meter (2 switches) and the intercom. He will verify that he is in communication with the Test Director on level 4.

The laser operator will then turn on the flashing laser warning light affixed to the tunnel door, and will put on his laser safety goggles.

The laser operator will install the beam stop so that no laser radiation can exit from the tunnel, attach the remote control box, and then bring the laser into normal operation, firing in the AUTO mode at 20 pulses per second.

The laser operator will open the sliding door at the tunnel level and the shutters over the primary mirror.

After the system has stabilized, the Laser Operator will switch the control unit to EXTERNAL mode, and install the remote control box at the data and control station on level 4. He will return to the tunnel, and notify that Test Director that the laser system is ready, by intercom. The Test Director will attempt to fire the laser for a few seconds, to verify that the system is operating properly.

The Test Director will then contact the Observer and request that he operate the laser kill switch, to verify that it is operational.

The laser operator will then remove the beam stop, turn off the lights, exit the tunnel, and lock the door and retain the key in his possession. He may then remove his safety goggles.

2.2.3 Data System Turn On

The Test Director will conduct a visual inspection of the data system to verify that all electrical connections are proper and that no hazardous conditions exist.

The Test Director will turn on all data system power switches.

The Test Director will verify that he is in communication with both the Observer and the Laser Operator.

The Test Director will coordinate checkout of the laser kill switch, as described above.

2.2.4 Surveillance System Turn On

The Observer will see that the radar is installed in its proper rooftop location. He will see that the oscilloscope, TV camera and video recorder are installed properly. He will visually check all cables to ensure that they are safe and properly connected.

The Observer will turn on the safety system, and verify that it is operational. He will load a blank tape into the VCR.

The Observer will verify that he is in radio contact with the Test Director.

The Observer will participate in a check of the laser kill switch, as described above.

When notified that tests are about to begin, the Observer will start recording video tape. He will record the date and time on the audio track.

2.3 Normal Operation

2.3.1 Test Director

In normal data acquisition, the Test Director will first verify that the laser system is operating properly and that the data system is ready. Then he will request a status update from the Observer. When the Observer givers an All Clear report, the Test Director will begin firing the laser.

If the Observer (or any other crewmember) notifies the Test Director of a hazardous condition, he will immediately cease firing the laser. The laser will not be restarted until the hazardous condition no longer exists.

The Test Director will communicate with the Observer periodically throughout the test to insure that communication lines are open.

NOTE

AVOID THE WORDS LASER, BEAM, AND FIRE OR COMBINATIONS OF THESE WORDS IN RADIO COMMUNICATIONS

2.3.2 Observer

The Observer will remain inside a designated area on the roof at all times, away from the edge of the roof and also away from the hatch. He will never look down into the hatch.

The Observer will maintain acoustic and visual surveillance of the airspace around building 622 at all times while the laser beam is on. He will carry the laser kill switch in his hand at all times, and will use it to shut off the laser if necessary.

The Observer must ensure that the laser is off at all times when he is writing, changing video tapes, etc. These activities will not be allowed to interfere with his primary duty of maintaining airspace surveillance.

2.3.3 Laser Operator

Because of thermal instabilities in the laser head, it will occasionally be necessary to adjust the doubler to maximize output power. This must be done while the laser is operating, in accordance with the following procedure.

When the Test Director determines that laser adjustment is necessary he will dispatch the laser operator to the cross tunnel.

The laser operator will carry a flashlight and laser safety goggles. He will put on the goggles, unlock the tunnel door, enter the tunnel, and proceed to the intercom. He will immediately notify the test director that he is in the tunnel. He will then tune the laser for maximum output power. He will contact the Test Director and report the power reading. He will leave the tunnel, lock the door, and remove his safety goggles.

During all times of operation ANSI CLASS IV laser warning signs will be placed across the only access door to the tunnel containing the laser and the elevator and stairwell entrance doors to the roof.

2.4 Turn Off Procedure

The Test Director will determine when to turn off the system. He will then cease firing the laser, dispatch the Laser Operator to the tunnel, and notify the Observer that the measurement series has ended. The Test Director will turn off all of the instrumentation of level 4.

The Observer will turn off the surveillance radar system, secure all equipment, and retrieve all video tapes and his written log.

The Laser Operator will turn off all instrumentation in the tunnel, following normal shut down procedures. He will also close the shutters over the primary mirror and the sliding door in the tunnel.

The Laser Operator will remove the key to the laser and keep it in his possession. He will then leave the tunnel and turn off the laser warning light on the tunnel door.

The Test Director and the Laser operator will then proceed to level 9 and the roof top. They will replace the collimator end cap. Two personnel will then proceed to the roof. They will close the roof hatches, while the third crew member secures the hatches with the chains on level 9.

The crew will then exit the building, making sure the doors are secured.

2.5 Visitor Control

Visitors are defined as WRDC or GTRI personnel who are not part of the crew described above.

Visitors will be verbally briefed on the operation of the MEGALIDAR and all potential dangers.

Visitors will be subject to the same regulations and SOPs as test personnel, where applicable.

Visitors will not be allowed in the tunnel while the laser is firing.

Visitors will not be allowed on the roof top during normal operation.

3. HAZARD ANALYSIS

3.1 Safe Eye Exposure Distance (SEED) Analysis

The SEED for the MEGALIDAR laser was computed by 2750 AABW/EMB, using the parameters listed in TABLE B-1 and an exposure duration of 1/4 second. Assuming no atmospheric attenuation the SEED is 179 km; using values for clear air transmittance listed in AFOSH 161-10 the SEED is 128 km. This clearly shows that this laser is potentially hazardous. However, these calculations are for direct exposure to the beam or specular reflection. These will be prevented by controlling access to the tunnel and by keeping foreign objects out of the beam path. Because the atmosphere does not contain specular reflectors, laser safety goggles will not be required when observing the beam as it propagates vertically above the collimator facility. The Laser Operator will, however, wear goggles when he is in the tunnel and the laser system is turned on.

3.2 Radar Hazard Zone

The radar hazard zone has been calculated by MED CEN/SGB based on the radar parameters listed in the attachment entitled "Radar Safety System." The hazard zone extends from the dish to a distance of about 6 feet in front of it. Personnel will not be able to enter this zone because the radar will be mounted so that it points vertically, with the dish at or above head height.

3.3 Collimator Facility in Building 622

After hours access to Building 622 is controlled by key and monitored by a door interlock system. This will prevent unauthorized personnel from gaining access to the MEGALIDAR.

The laser power supply is key controlled and the Laser Operator will keep the key in his possession at all times. This will prevent anyone else from firing the laser.

3.4 Airspace

The Observer will be responsible for ensuring that the laser is not firing when aircraft are in the vicinity of the MEGALIDAR. See procedures described in Sections 1.1.2, 2.1.3, and 2.3.2.

The experiment described here has been coordinated with the FAA dated 3 November 88.

The experiment has also been coordinated with the Space Command. See attached letter dated 15 September 88.

4. ENVIRONMENTAL IMPACT ANALYSIS

4.1 Description of Laser

The laser to be used in this experiment is a commercially available doubled YAG laser, model YG581C purchased from Quantel.

As shown in Table B-1, its output is pulses of green light [532-nm wavelength] with a maximum energy per pulse of 500 milliJoules. The beam will be expanded so that it is about 30 mm in diameter as it leaves the collimator, and it has a very small divergence, about 0.2 milliradians. In normal operation, the pulse repetition rate will be 16.7 per second. Each pulse is very short, about 10 nanoseconds.

4.2 Summary of Hazards

The average power of this laser is

0.5 J/pulse X 16.7 pulses/s = 8.4 J/s = 8.4 Watts

so the heating effect of the laser beam is negligible. Compared to the carbon-arc searchlights commonly used for sales promotions, the average power of this system is miniscule.

The reason the laser beam presents a hazard is that each pulse delivers a large amount of energy in a short amount of time. The peak power is

$$0.5\ J/10^{-8}s = 50\ Megawatts$$

There are several damage mechanisms to living organisms from such pulses, and the primary injury of concern here is eye damage by retinal scarring. This can occur because the cornea can focus green light onto a tiny spot on the retina.

This concentrates the light into a small area, and if it is intense enough, it will cause damage to the tissue of the retina.

A laser beam of short pulse length is considered an eye hazard if its intensity, measured in Joules/cm^2, is above a certain limit. For example, the ANSI standard for the type of laser described here is 5×10^{-7} J/cm_2. Because of its very small beam divergence, the beam must travel a very long distance before it has expanded enough to get down to a safe level, as shown in Section 3.1.

4.2.1 To Materials

Hazards to solid material objects, where the primary effect of the laser beam is heating, are minimal. For example, the laser beam pattern is routinely measured by using heat sensitive paper as is used in certain chart recorders. An exposure of several seconds at 20 pulses per second is required to record the pattern. A block of wood is often used as a beam stop, with no noticeable effect on the wood after minutes of exposure.

This means that the laser would have no effect on the skin of an aircraft should it fly through the beam.

4.2.2 To Living Organisms

Because the beam will exit Building 622 at rooftop level, an organism in the beam must be a flying organism. This would include personnel in aircraft, birds, and insects. Hazards to personnel in aircraft have been eliminated by a set of safety procedures, as described above.

There is one known endangered species of bird in this area, the Upland Sandpiper which nests the marshes near Area C. However, this bird is not nocturnal, and because the Megalidar will be operated only during hours of darkness, it will not present a hazard to any threatened or endangered species.

In any event, a bird or insect would not be expected to remain in the beam for a long period of time, because airborne animals are in motion. This means that the effects of heating will be negligible. The only hazard to airborne animals is therefore possible eye damage.

4.3 Previous Experience

4.3.1 At Other Sites

It is important to realize that similar lidar systems have been operated at sites over the world, including airports, for a number of years. Some of these systems used safety radars, many relied solely on an Observer. We know of no incidents where lidar systems caused injury to personnel or damage to aircraft. One would not expect operation in Dayton, Ohio to be especially hazardous.

4.3.2 At Building 622

A similar lidar system was operated from a trailer parked outside Building 622 for a period of weeks in September, 1988. This system also used a doubled-YAG laser, but with no power and a larger beam divergence so the eye safe distance was much less, and aircraft safety was ensured by an Observer only. This experience showed that an Observer can be very effective, and that detection for low flying aircraft is done by a combination of acoustic and visual observations.

4.4 Effects on Environment

As mentioned earlier, clear skies are required for this demonstration. The system will not be in operation when there are clouds or particulates in the air.

The laser beam will have no effect on the molecular constituents of the atmosphere.

5. EMERGENCY OPERATING PROCEDURES

5.1 Exposure

If human exposure to laser energies greater than the maximum permissible limits should occur,

- obtain medical treatment immediately
- contact 2750 ABW/EMB, extension 72010
- obtain information about the accident

5.2 Building 622

Electric power circuit breakers for the laser system are located inside the collimator cross tunnel.

A Fire Use Telephone is in Building 622. Phone extension 117.

An Injury Use Telephone is in Building 622. Phone extension 7333.

In case of fire, accident, or injury, use the communications network to notify the Test Director.

OTHER IMPORTANT PHONE NUMBERS

WRDC SAFETY OFFICE (CARL JOHNSON)	52101/54782
BASE POLICE	74000
EO SENSOR/ATMOSPHERIC SCIENCE GROUP	56361

APPENDIX C: PICTURES OF THE MEGALIDAR

LIST OF FIGURES

Figure No.	Title	Page
C-1	A Schematic Showing Parts of Collimator.	C-4
C-2	A View of the Door to the Cross-Tunnel and the Upper Part of the Collimator.	C-6
C-3	A View of the Upper Part of the Collimator and the Top of the Cross-Tunnel.	C-8
C-4	A View of the MEGALIDAR Transmitter, Laser, Laser Beam and Steering Mirror Inside the Cross-Tunnel.	C-10
C-5	A View of the MEGALIDAR Receiver System at the Collimator Prime Focus Level.	C-12
C-6	The MEGALIDAR Transmitter Beam Leaving the Collimator Building Roof-Top Hatch.	C-14
C-7	The MEGALIDAR Transmitter Beam as Seen Outside the Collimator Building.	C-16
C-8	The MEGALIDAR Transmitter with Parts of Wright-Patterson AFB and Dayton in the Background.	C-18

Figure C-1. A Schematic Showing Parts of Collimator.

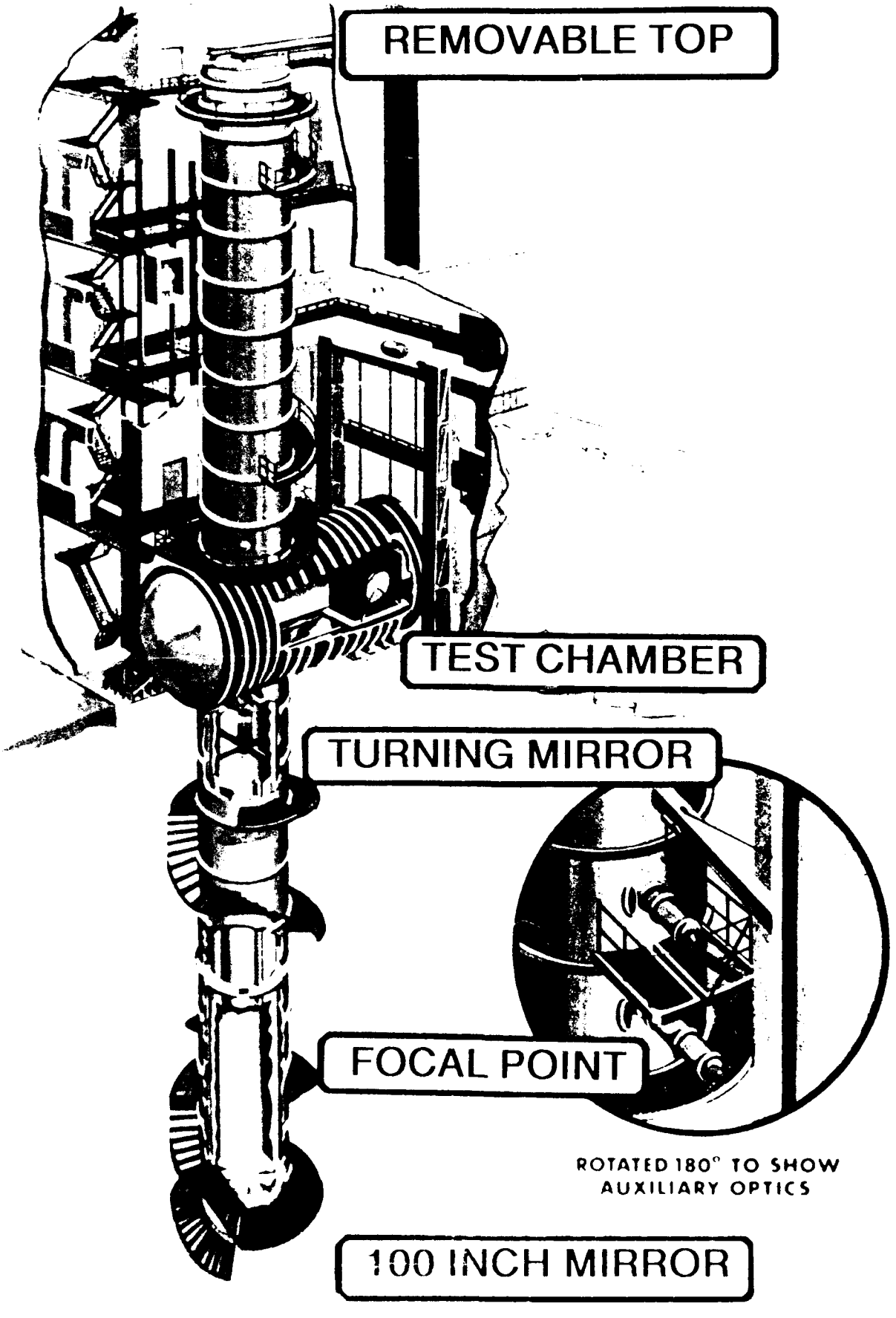
REMOVABLE TOP
TEST CHAMBER
TURNING MIRROR
FOCAL POINT
ROTATED 180° TO SHOW
AUXILIARY OPTICS
100 INCH MIRROR

Figure C-2. A View of the Door to the Cross-Tunnel and the Upper Part of the Collimator.

Figure C-3. A View of the Upper Part of the Collimator and the Top of the Cross-Tunnel.

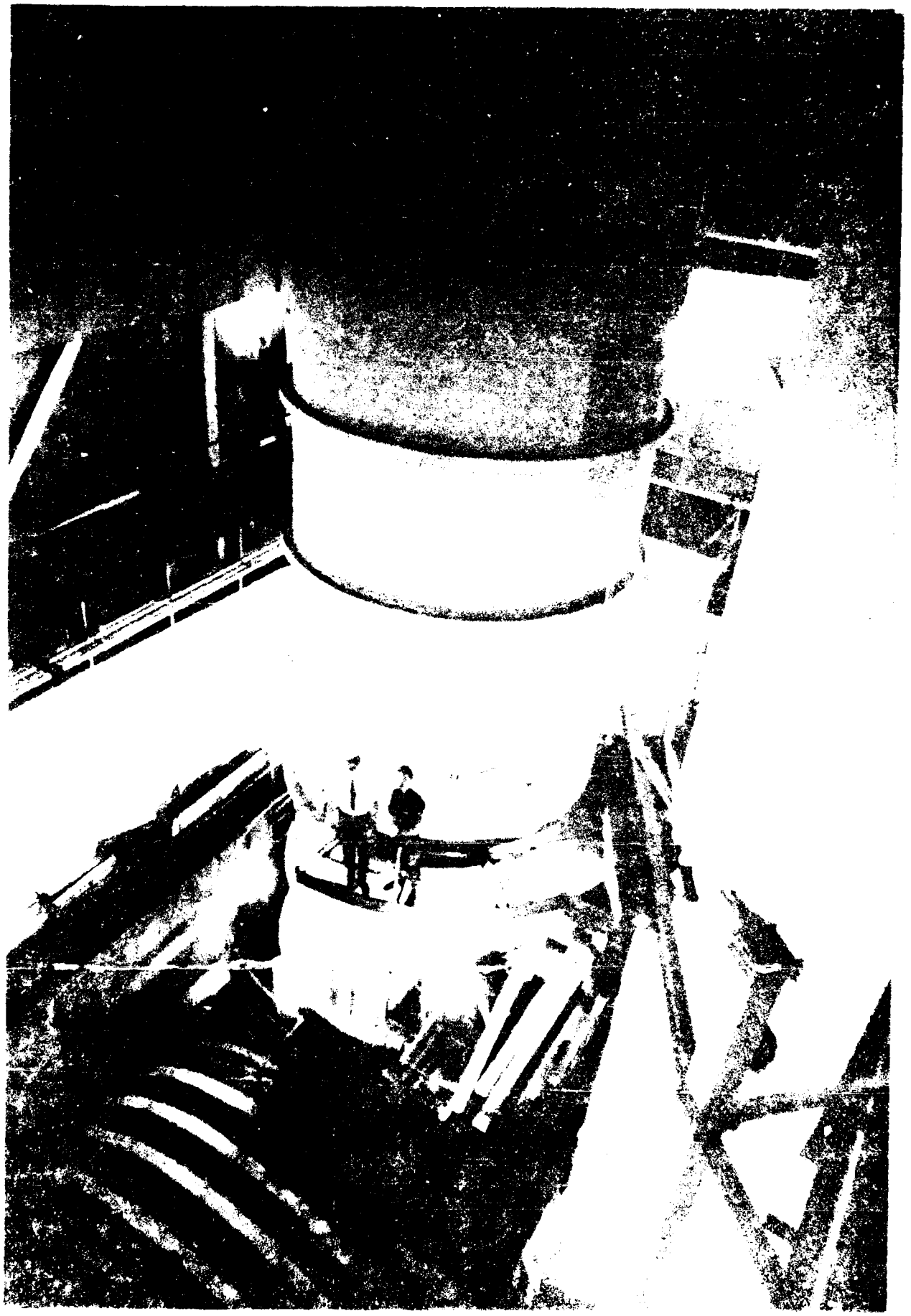

Figure C-4. A View of the MEGALIDAR Transmitter, Laser, Laser Beam and Steering Mirror Inside the Cross-Tunnel.

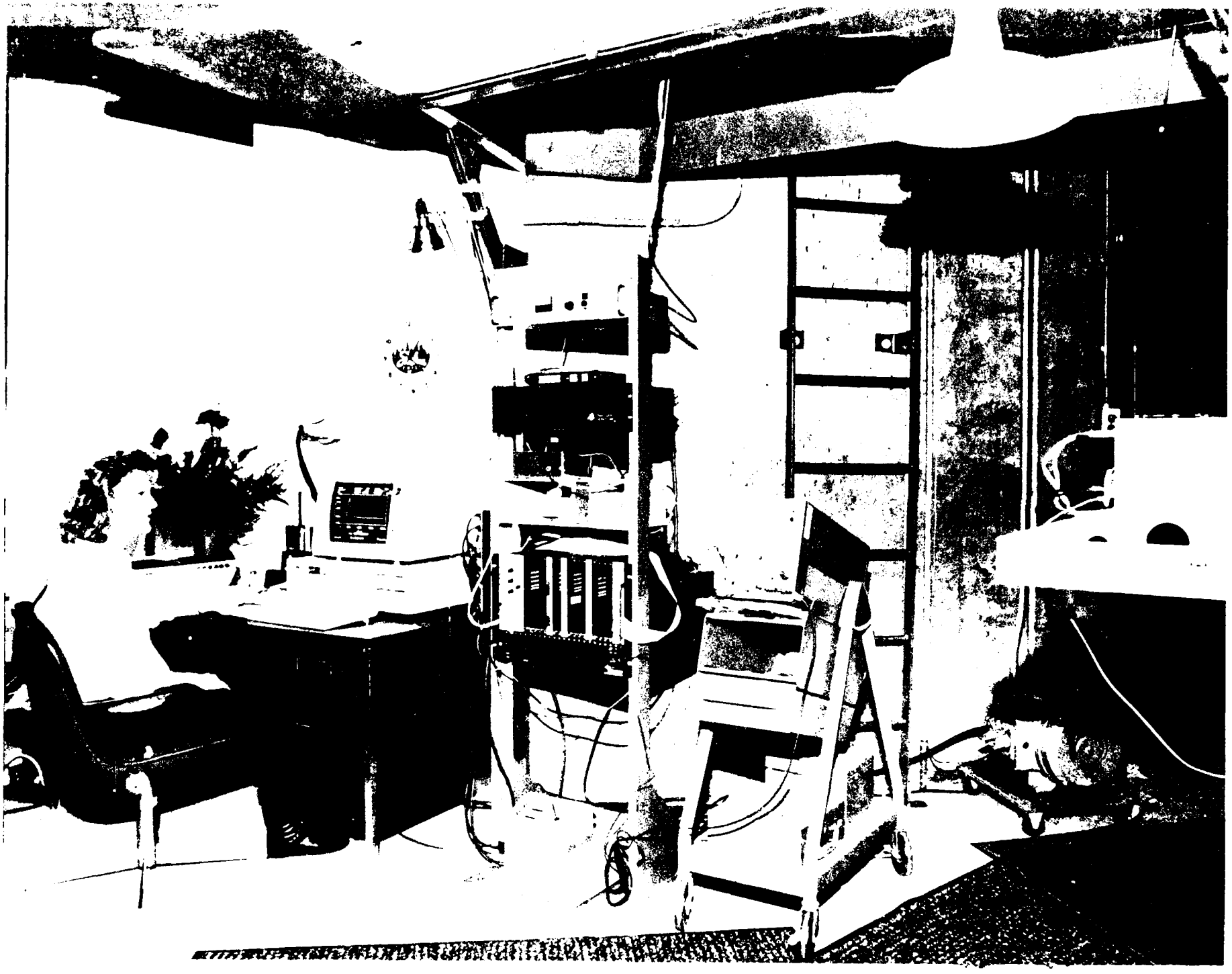

Figure C-5. A View of the MEGALIDAR Receiver System at the Collimator Prime Focus Level.

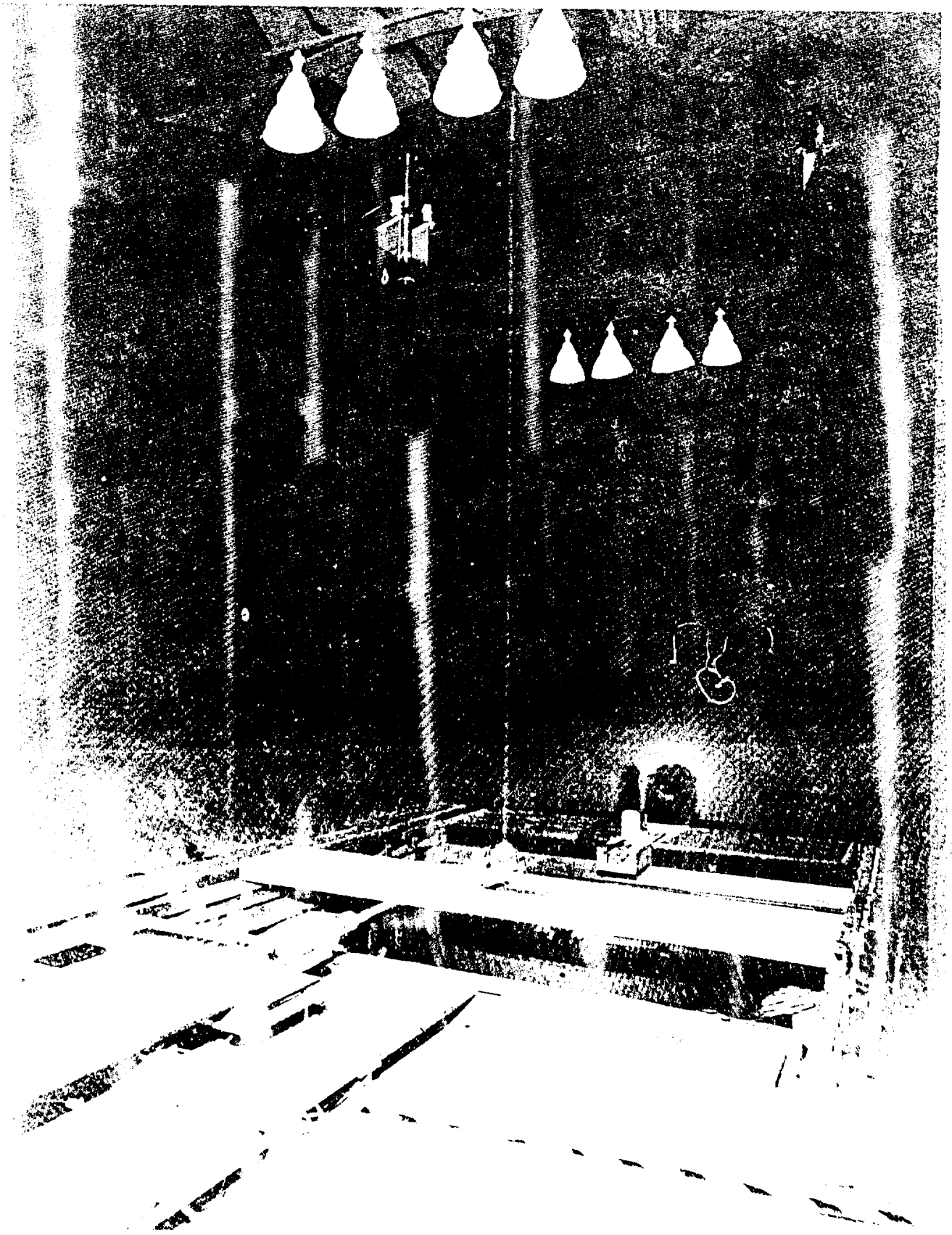

Figure C-6. The MEGALIDAR Transmitter Beam Leaving the Collimator Building Roof-Top Hatch.

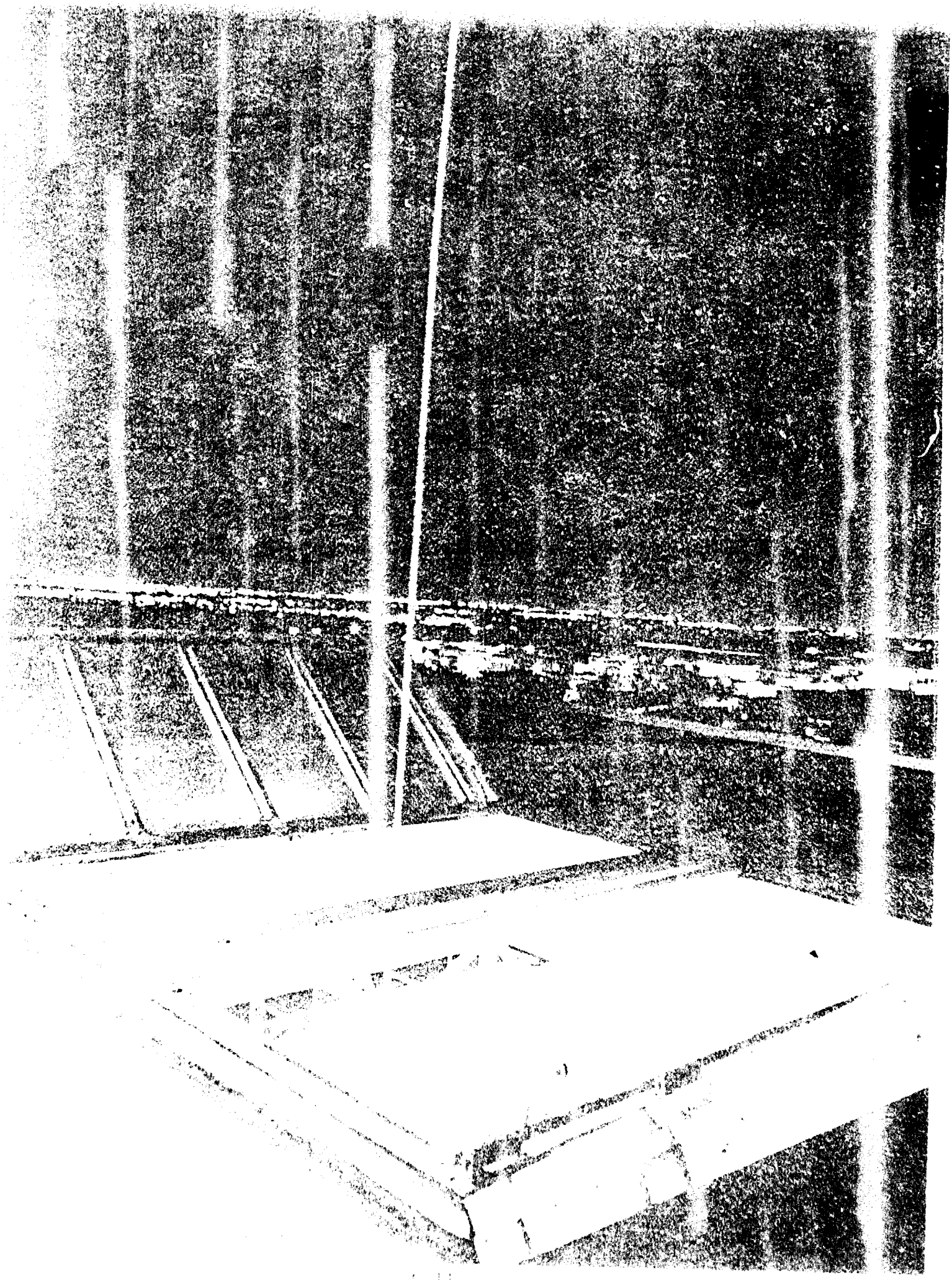

Figure C-7. The MEGALIDAR Transmitter Beam as seem Outside the Collimator Building.

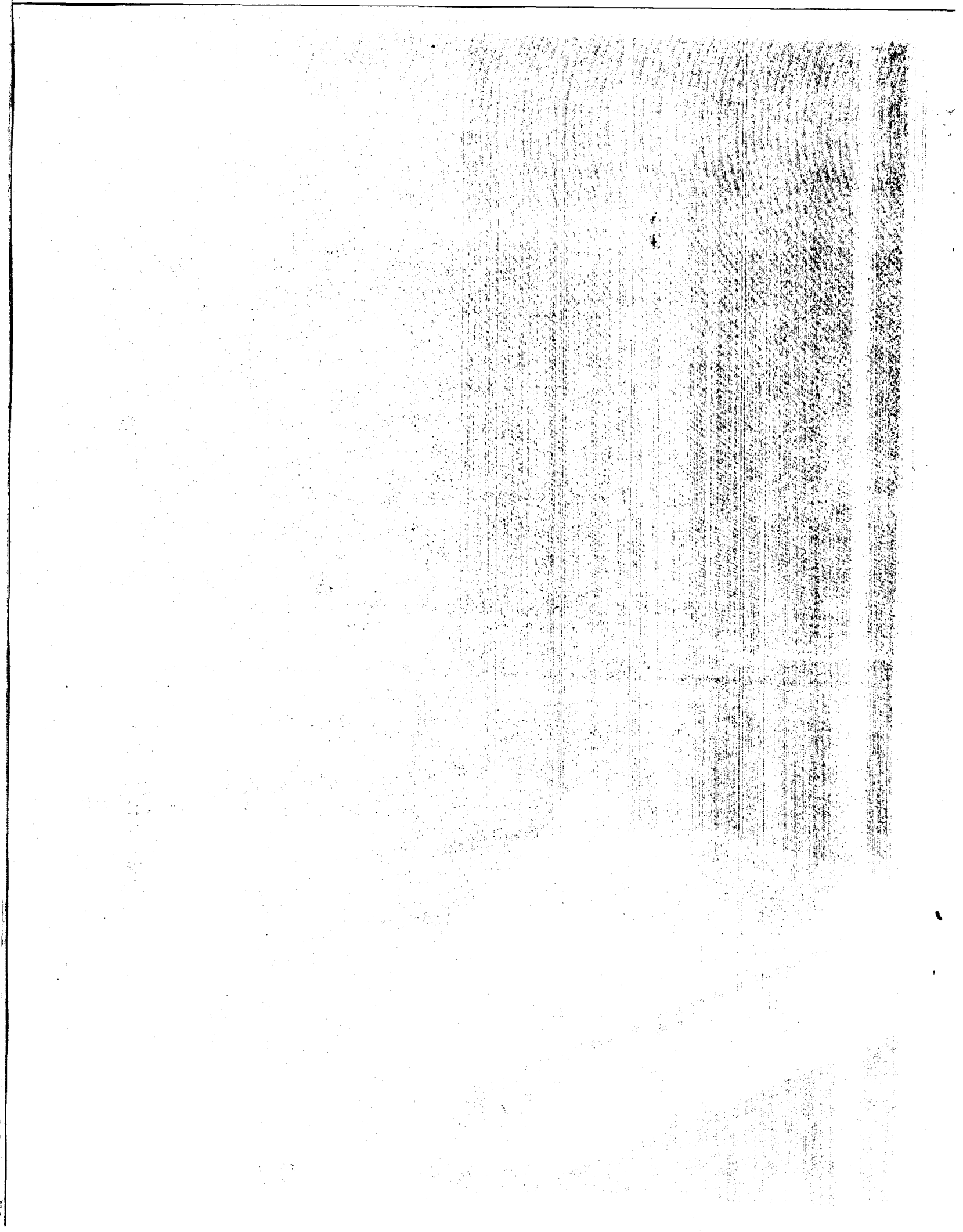

Figure C-8. The MEGALIDAR Transmitter with Parts of Wright-Patterson AFB and Dayton in the Background.